A multi-omic analysis of the photosynthetic endosymbioses of *Paramecium bursaria*

A DISSERTATION PRESENTED
BY
FINLAY MAGUIRE

IN PARTIAL FULFILLMENT OF THE REQUIREMENTS
FOR THE DEGREE OF
DOCTOR OF PHILOSOPHY

UNIVERSITY COLLEGE LONDON
LONDON, UNITED KINGDOM
DECEMBER 2015

I, Finlay Maguire, confirm that the work presented in this thesis is my own. Where information has been derived from other sources, I confirm that this has been indicated in the thesis.

Author List

The following authors contributed to Chapter 1: David Milner, Katie Jones
The following authors contributed to Chapter 2: David Milner, Karen Moore/ESS, Ines Yang
The following authors contributed to Chapter 3: David Milner, Scott Campbell
The following authors contributed to Chapter 4: David Milner, Chloe Ormorod

A multi-omic analysis of the photosynthetic endosymbioses of Paramecium bursaria

Abstract

ABSTRACT TEXT

Contents

List of Figures

List of Tables

Acknowledgements

I'd like to thank Thomas Richards for extensive guidance and support during and before this research, particularly in allowing me the freedom to pursue diverse avenues of learning and research.

Gavin Gray for a constant end-to-end encrypted presence, chip-tunes and machine learning side-projects.

Aurelie Chambouvet and Adam Monier for frequent "Auld Alliance" coffee trips.

Guy Leonard for advice and guidance in my first forays into bioinformatics.

David Milner for his considerable contributions to the lab work in this thesis. Theresa Hudson and Ines Yang for help in the culturing and maintenance of *Paramecium bursaria* cultures.

Karen Moore and Konrad Paskiwicz for sequencing.

Hofstadter's Law: It always takes longer than you expect, even when you take into account Hofstadter's law

- Douglas Hofstadter: *Gödel, Escher, Bach: An Eternal Golden Braid, 1979*

1 Introduction

1.1 Endosymbiosis

1.1.1 What is endosymbiosis?

Endosymbiosis has proven one of the most fundamental processes in the evolution of the eukaryotic cell (Timmis et al., 2004; Lane, 2007; Martin and Herrmann, 1998; Archibald, 2015). It has both shaped the global climate and created the cellular context in which specialised multicellular organisms have evolved.

Endosymbiosis is a special case of symbiosis, which results in a long-term stable interdependent living together ("sym/σύν" – together, "bios/βίωσις" – living) of two or more organisms to a point of mutual benefit (de Bary, 1869; Pound, 1893) (although many now expand this definition beyond mutualism to include other categories of biological interactions (Leung and Poulin, 2008; O'Malley, 2015)). What differentiates endosymbiosis from symbiosis in general is that one partner (the endosymbiont) lives wholly inside ("endo/ἔνδον" - inside) of another (the host). This "inside" can refer to symbionts either living intracellularly or within the tissues of multicellular organisms. However, it excludes niches such as the digestive tract of metazoa as as this can be considered as an external surface of the host. These latter symbionts are occasionally termed ectosymbionts.

There is a considerable diversity of endosymbiotic relationships in nature. These relationships can encompass many different degrees of host-symbiont integration, interdependence and ecological interaction types (see

Interaction Name	Interaction Outcome
Mutualism	$(+,+)$
Antagonism	$(+,-)$
Competition	$(-,-)$
Commensalism	$(+,0)$
Amensalism	$(-,0)$
Neutralism	$(0,0)$

Table 1.1.1: An overview of the categories of biological interaction and the effect they have on the two interacting biological units, which may be anything from individual species to whole populations. The outcome column contains a tuple relating the effect an interaction has on a pair of interacting biological units. This "effect" is often assessed in terms of metrics such as individual fitness, population size and/or growth rate. Note: parasitism and predation are mechanisms by which an antagonistic interaction may take place (Abrams, 1987) in the same sense that endosymbiosis is a mechanism by which a mutualistic interaction can take place. In reality most interactions will not fall neatly into one of these categories and throughout it's duration will often display characteristics of multiple categories (Leung and Poulin, 2008)
.

table 1.1.1). Even if we restrict ourselves to endosymbioses that are largely "mutualistic" (noting that the exact nature of a certain endosymbiosis is highly dependent on the specific ecological context at a particular point of time and doesn't always neatly quantise (Leung and Poulin, 2008))[1]) there is broad range of characteristics.

For example, in terms of interdependence of host and endosymbiont you could construct a spectrum with "incidental" endosymbioses such as bacterial escape of digestion in macrophages at one extreme and at the other obligate systems such as the mitochondria or chloroplast where host and symbiont are essentially a unified unit of selection. In the middle of such a spectrum you could find facultative endosymbioses where each partner is capable of, and does, live aposymbiotically for extended life phases e.g. Rhizobia soil bacteria and legume (Fabaceaea) plants (reduction of atmospheric N_2 to ammonia (Hirsch, 1992) in exchange for host-derived carbon sources such as malate and succinate (Prell and Poole, 2006)).

An endosymbiosis may be highly integrated in terms of metabolism, genome and life history while still only being moderately interdependent (such as the facultative Rhizobia nitrogen fixation which takes place in carefully controlled specialised root nodule structures (Crespi and Frugier, 2008)). However, generally interdependence and integration correlate reasonably well due to the increased selective pressure to minimise lethal aberrant interactions that comes with interdependence. This can be seen in the extreme of host-symbiont integration: that of the endosymbiotic organelles, which are so highly integrated they were considered part of the cell by mainstream scientific establishment until only relatively recently.

Intracellular endosymbionts can be found inhabiting multiple host-compartments from nakedly in the cytoplasm, to host-derived vacuolar compartments (often from secretory and endocytic systems) (e.g. (Kodama and Fujishima, 2009)) along with a range of host oraganelles including the endoplasmic reticulum (Vogt, 1992), Golgi body (Cho et al., 2011), mitochondria Sassera et al. (2006), chloroplast (Wilcox, 1986) as well as the nucleus

[1]It is worth briefly addressing a common motif of biology: the application of discrete schemas to continuous distributions. These biological quantisations are prone to error (fuzzy delineations) and are constantly challenged by novel discoveries which exhibit a mosaic of category features. There are many examples of this such as the classification of mitochondria-related organelles (Maguire and Richards, 2014), types of biological interactions (see table 1.1.1), and the numerous species concepts (De Queiroz, 2007; Boenigk et al., 2012). That is not to say biological quantisation is without utility or is a futile task. Indeed, as long as there is a clarity to the application, basis and limitations of these schema then they form a critical (epistemological) framework upon which further research and communication can build (Boenigk et al., 2012). However, care must be taken not to forget that they do not reflect reality and can inadvertently obscure the grey areas (Leung and Poulin, 2008).

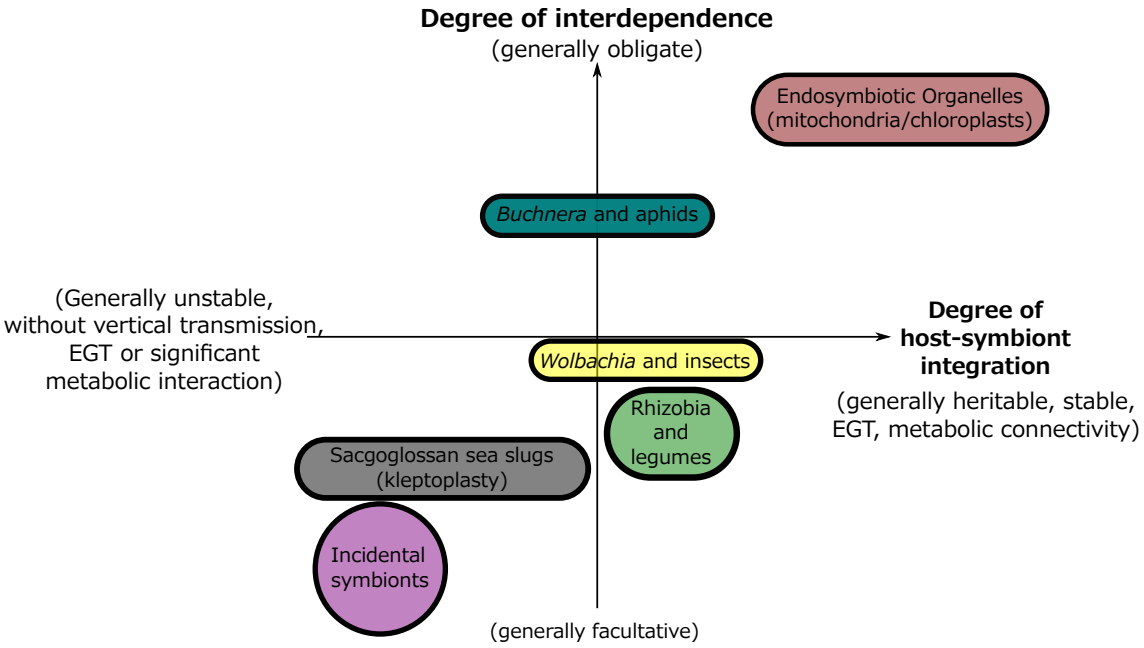

Figure 1.1.1: Plot demonstrating a fragment of the diversity of endosymbioses and specifically hi-lighting the possibility of a well integrated by facultative endosymbiosis. Host-symbiont integration is a rough measure of how connected the host and symbiont have become genomically, metabolomically and in terms of life history. Whereas, interdependence is a approximate measure of the degree to which the relationship is necessary for life of organisms involved. It should be noted that both axes can be highly reliant on specific ecological and environmental context.

(first discovered in *Paramecium* (Schulz and Horn, 2015)). Owing to the endosymbiotic origin of the chloroplast and mitochondria it becomes apparent that there can be multiple "layers" of endosymbiosis. A primary endosymbiont is an endosymbiont that is the direct endosymbiont of the host (e.g. the mitochondria to eukaryotes) whereas a secondary endosymbiont is the endosymbiont of an endosymbiont. The layers of endosymbioses can get impressively deep, for example, bacterial endosymbionts have been identified within the chloroplast stroma (cyanobacterial endosymbiont) of dinoflagellates (e.g. *Woloszynskia pascheri* (Wilcox, 1986)) In turn, dinoflagellate plastids have been discovered that are likely the product of tertiary endosymbioses (Gabrielsen et al., 2011) with higher-order events hypothesised in related groups (Stiller et al., 2014). Therefore, bacteria like this could be the endosymbiont of an endosymbiont of an endosymbiont of an endosymbiont (quaternary) or higher.

With this considerable diversity it is perhaps not surprising that endosymbioses have been discovered featuring partners from all 3 domains of cellular life. However, with the exception of one extant Bacteria-Bacteria endosymbiosis (von Dohlen et al., 2001), typically the majority of known endosymbioses feature a eukaryotic host[2] but can include endosymbionts from all 3 domains. For example:[3]

[2]There are however many examples of mutualistic symbioses which are Bacteria-Bacteria (e.g. biofilms (Watnick and Kolter, 2000)), Bacteria-Archaea (e.g. anaerobic methanotrophic archaea and sulphate-reducing bacteria likely responsible for a large proportion of global methane consumption (Boetius et al., 2000; Knittel and Boetius, 2009) and SM1 euryarchaea/*Thiothrix* sp. sulphide-oxidising bacteria (Henneberger et al., 2006; Wrede et al., 2012)), and at least one example of Archaea-Archaea (*Igniococcus hospitalis/Nanoarchaeum equitans* (Huber et al., 2002). Interestingly *Igniococcus* is the first identified case of an energised outer-membrane in double-membrane bound archaea or bacteria, a significant finding for the development of theories of eukaryogenesis (Küper et al., 2010))

[3]Although with all these example, it is important not to consider an endosymbiotic relationship in isolation from other endosymbionts present in the same host. There are examples where facultative "secondary endosymbionts" are able to compensate for the loss of an obligate endosymbiont (Koga et al., 2003). Symbiont-symbiont interactions have been found to play a role in determining which endosymbionts are capable of establishing themselves in a certain host and can even be capable of generating additional phenotypes e.g. the R-bodies of "killer" *Paramecium* species which may be a product of an interaction between the *Paramecium* host, *Caedibacter* and a bacteriophage (Schrallhammer and Schweikert, 2009).

- Eukaryote-Archaea (Moissl-Eichinger and Huber, 2011)
  - Methanogenic archaea within various ciliates species (e.g. *Plagioplya frontata*) (Fenchel and Finlay, 1992; Lange et al., 2005)
  - *Cenarchaeaum symbiosum* within the tissues of marine sponges (Preston et al., 1996; Wrede et al., 2012)
- Eukaryote-Bacteria
  - *Hartmannella* and it's intranuclear endosymbiont *Candidatus Nucleicultrix amoebiphilia* (Schulz et al., 2014)
  - the most famous pairing of mitochondria and plastids
- Eukaryote-Eukaryote
  - The fungi *Diplodia mutila* which aids herbivory resistance in the palm *Iriartea deltoidea* in lowlight conditions but becomes pathogenic if host is well lit (Álvarez Loayza et al., 2011)
  - Red alga derived plastids in brown algae (Dorrell and Smith, 2011)
  - Numerous examples of algal mediated acquired phototrophy in ciliates (Johnson, 2011)

Endosymbiosis is the one of the most significant evolutionary processes in eukaryotic cell. It offers a means for eukaryotes to benefit from the extensive metabolic diversity present in the bacterial and archael pangenome, especially the only known forms of primary energy production - photosynthesis and chemosynthesis (Wernegreen, 2012).

1.1.2 Plastid Endosymbioses

Most molecular evidence currently points towards a single primary endosymbiotic event between a phagotrophic ancestral eukaryote (with mitochondria and developed endomembrane system (Rockwell et al., 2014)) and a cyanobacteria (blue-green algae) as giving rise to the archaeplastida (that is the green algae, red algae, glaucophytes and land plants (Green, 2011)) and their double membrane bound plastids (Keeling, 2013). While, this event is one of the must fundamental events in the evolution of life in and of itself it is only capable of explaining a small proportion of the diversity of plastids across the eTOL (Keeling, 2013) Apart from one other putative primary endosymbiosis in *Paulinella chromatophora* (a euglyphid amoeba with photosynthetic chromatophores that are vertically inherited, synchronised to host and bear a much stronger molecular and morphological resemblance to reduced cyanobacteria than the chloroplast of the archaeplastida (Kies and Kremer, 1979; McFadden, 2014)) all other oxygenic phototrophs (as well as several non-photosynthetic but plastid bearing pathogens (Sato, 2011)) have arisen by secondary or higher order endosymbioses (Hoshina and Imamura, 2009). Secondary endosymbioses are those in which another eukaryotic lineage has engulfed a primary plastid bearing algae and reduced and integrated them in a simulacrum of primary endosymbiosis, occasionally serially (Keeling, 2010). This and subsequent loss of membranes leads to the range of membrane layer numbers around plastids in various eukaryote

lineages (Keeling, 2013). This secondary order plastid endosymbioses have occurred independently in divergent eukaryote lineages e.g. chloroarachniophytes and euglenids, and an unresolved number of times in the the set of cryptomonads, haptophytes, stramenopiles, dinoflagellates and apicomplexans (Keeling, 2013). As well as an uncertain number of higher order endosymbioses in the dinoflagellates (Keeling, 2013).

Therefore, understanding the mechanisms and evolution of secondary photosynthetic endosymbioses would provide important insight into the evolution of a considerable number of eukaryotic lineages. Unfortunately, most extant examples feature endosymbioses within which metabolic co-dependence has already become fixed masking the potential mechanisms through the endosymbiosis may have originated. Facultative systems such as the *Chlorella* endosymbionts of *Paramecium bursaria* offer a potential avenue to investigate secondary photosynthetic endosymbioses at an earlier stage before metabolic co-dependence has become fixed (while acknowledging the impossibility of interrogating events that have already occurred within the correct ecological context. Furthermore, as the ancestral protist involved in the primary plastid endosymbiosis likely exhibited a similar life style to serially phagotrophic *Paramecium* and would initially at least have been mixotrophic (combining phagotrophy with phototrophy via the newly acquired plastid (Rockwell et al., 2014) in the same manner as *Paramecium bursaria* (and other mixotrophic ciliates (Johnson, 2011)) the study of the *Paramecium bursaria-Chlorella* system offers potential insight into this early and fundamental stage of eukaryote evolution.

1.2 *Paramecium bursaria*

Paramecium are large ($50 - 330\mu m$) phagotrophic single-celled eukaryotes belonging to a genetically diverse (Prescott, 1994) sub-grouping of the alveolates known as the ciliates (see 1.3.1). They have been studied since the invention of microscopy (Görtz and Fokin, 2009) (first recorded by a contemporary of van Leeuwenhoek see 1.2.1) and are some of the longest-standing model unicellular eukaryotes. They have been used to study everything from mutagenisis and developmental genetics, to genomics rearrangement and epigenetics (McGrath et al., 2014). As such have a well-developed methodological (Sonneborn, 1970) and theoretical literature along with several available genomes (see 1.2.2 for genomes and their relative relationship to *P. buraria*).

Paramecium bursaria "the green *Paramecium*" is distinguished from most[4]other *Paramecium* by the distinctive stable, heritable secondary photosynthetic endosymbiosis it maintains with several species of the green algae *Chlorella*. Each *P. bursaria* $100 - 160\mu m$ (Jennings, 1939) cell contains $\sim$ 300 endosymbiotic algae maintained in individual perialgal vacuoles (PV) around the cell cortex (Hoshina and Imamura, 2009).

Much like other ciliates, *Paramecium* are covered by cilia. These are minute hairlike biochemically heterogeneous organelles capable of sensing the environment and by beating in co-ordinated metachronal waves of power strokes and recovery strokes (Funfak et al., 2015) provide cellular locomotion and, in the case of phagotrophic ciliates like *Paramecium*, forcing food bacteria towards the oral groove (cytopharynx) where they can be phago-

[4]There is at least one other species, *Paramecium chlorelligerum*, that harbours a different green algae (*Meyerella*) (Kreutz et al., 2012) and owing to the multiple origins of algal symbionts in *P. bursaria* (Hoshina and Imamura, 2009) and the general prevalence of mixotrophy in ciliates (Johnson, 2011) there are likely others yet to be discovered.

Figure 1.2.1: **A**: Carving of Christiaan Huygens (1629-1695), the prominent Dutch Golden Age mathematician and scientist and contemporary of Antoni van Leeuwenhoek, from a medallion by Jean-Jacques Clérion 1679 (reproduced from (Huygens, 1899)). **B**: Likely the first sketch of the micro-organism that we now know as *Parameciu*m by Christiaan Huygens in a letter (No. 2133, 11th of August 1678) to his father Constantijn Huygens. An approximate translation of the accompanying text goes as follows "I have twice seen in this water an animal 10 times as large as the others and with feet all over its body and a narrow form. 4 or 5 feet stirred even when the animal was at rest. It moves as fast as the others, turning and spinning in the water. Hartfoecker thinks he may have discovered the same species in 'semine corrupto' (as a dried out husk?)." (reproduced from (Huygens, 1899)). **C**: 8 of the 10 volumes of the collected correspondences of Christian Huygens as prepared for the Dutch Society of Sciences and published from 1888-1905)

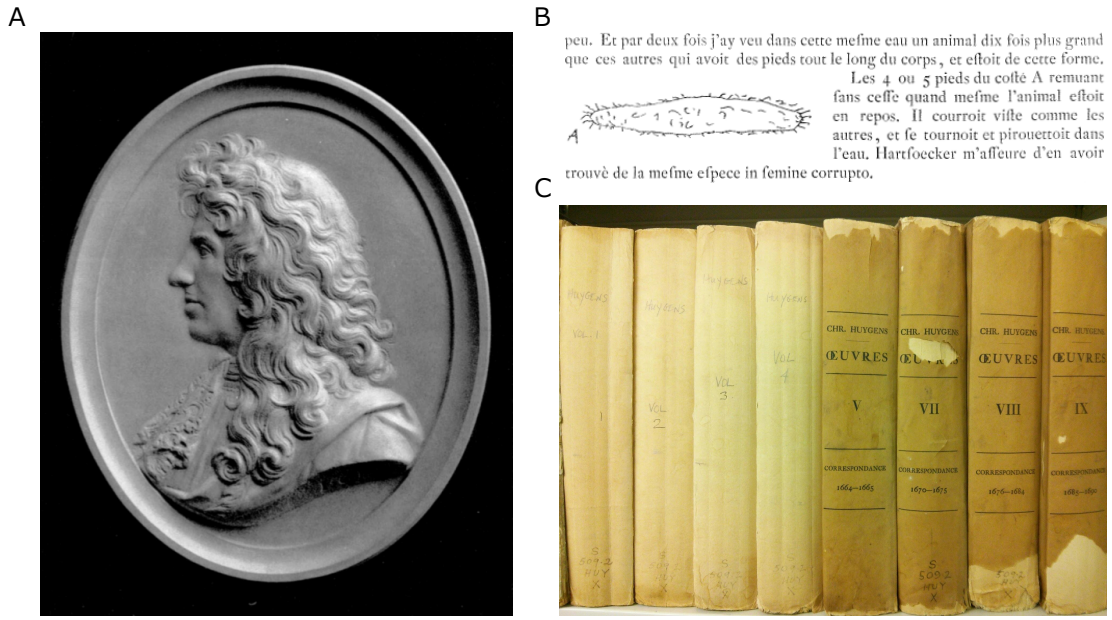

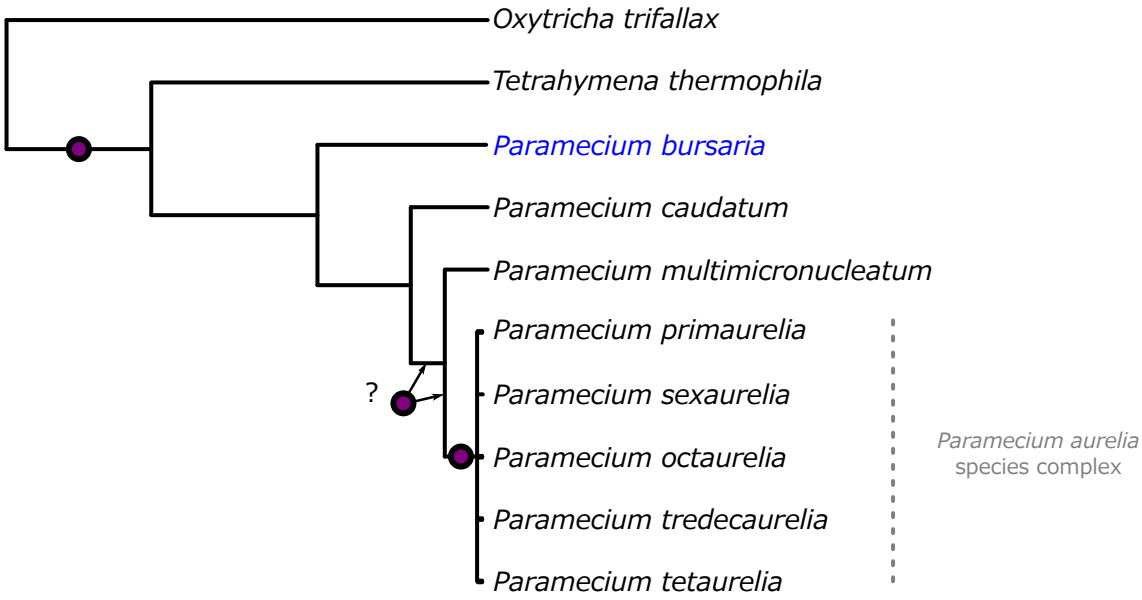

Figure 1.2.2: Modified phylogeny redrawn from (Fokin et al., 2004; Aury et al., 2006; McGrath et al., 2014) Showing the relative relations of ciliate species with genomic/transcriptomic resources and hypothesised WGD event locations with a purple dot. Specifically 2 strains of *Paramecium tetaurelia* (Aury et al., 2006), assemblies for *P. caudatum*, *P. multimicronucleatum*, and *P. aurelia* complex species *P. sexaurelia*, *P. primaurelia*, *P. octaurelia* and *P. tredecaurelia* on ParameciumDB (as of 05/03/2015) (Arnaiz and Sperling, 2011). As well as *Tetrahymena thermophila* (Eisen et al., 2006) and *Oxytricha trifallax* (Swart et al., 2013).

cytosed (Hamel et al., 2011; Aubusson-Fleury et al., 2015). *Paramecium* is also capable of rapid locomotion via the expulsion of trichocysts. These are defensive membrane-bound organelles known as trichocysts containing a

crystalline spike which can be rapidly ejected into the environment on fusion of trichocyst membrane with plasma membrane (Hamel et al., 2011).

Like other ciliates, including *Tetrahymena*, *Paramecium* deviates from the universal genetic code. Canonical stop codons TAA and TAG have been reassigned to produce glutamine therefore there is only one stop codon (TGA) but 4 glutamine codons (Salim et al., 2008).

Another defining feature of *Paramecium*, and ciliates in general, is a unique means of germline sequestration from somatic function in the form of "nuclear dimorphism" (Jahn and Klobutcher, 2002). Specifically, they have two types of nuclei, expression optimised highly polyploid somatic macronuclei (MAC) and largely silent diploid germline micronuclei (MIC) (Prescott, 1994).

During normal vegetative growth the MIC is densely packed with chromatin, is transcriptionally silent and undergoes mitosis as standard. Meanwhile, the MAC reproduces by a non-standard pinching process termed "amitosis". This process appears to lack any mechanism to ensure equal segregation of chromosomes such as spindle fibres (Chalker et al., 2013). On the other hand, during sexual reproduction (in which two compatible *P. bursaria* exchange haploid MIC gametes generated by meosis) the MAC degrades and must be reconstituted entirely from the newly formed heterozygous MIC (Jahn and Klobutcher, 2002) (see 1.2.3). The exact number of MIC and MAC varies widely by species and genus however, *P. bursaria* contains a single large MIC which consists of 80 to several hundred chromosomes depending on the exact subspecies (Chen, 1940).

P. bursaria reaches sexual maturity after 50-100 fissions (Siegel and Larison, 1960) and will conjugate with another *Paramecium bursaria* cell of compatible mating type and exchange haploid MIC gametes. Most *Paramecium* have a finite number of vegetative divisions and will die if they do not sexually reproduce (Chalker et al., 2013). Unlike all other studied *Paramecium*, *P. bursaria* does not only have 2 mating types and appears to have undergone gene duplication at two unlinked mating type loci. Different *P. bursaria* isolates display 2, 4 and 8 mating types (Phadke and Zufall, 2009) and form 4 or more mutually incompatible groups (Jennings, 1939). Sexually *P. bursaria* appears to have synclonal inheritance - a strictly mendelian inheritance contrary to the more complex epigenetic patterns observed in other *Paramecium* species (that led to much of the early work on epigenetics) (Siegel and Larison, 1960; Phadke and Zufall, 2009). During conjugation there is minimal cytoplasmic exchange (with no exchange of endosymbionts) (Wichterman, 1946). Contrary to other *Paramecium* species, which undergo autogamy after 75 rapid replications (Sung et al., 2012) or 30-35 while starving (Berger, 1986), *Paramecium bursaria* has not been found to naturally undergo autogamy (Siegel, 1963; Yanagi, 2004) but it can be induced by treatment of methyl cellulose (Yanagi, 2004)

In *Paramecium* the haploid size and complexity of the MIC is greater than that of the MAC as a result elimination of approximately 20-30% of DNA during reconstitution of the MAC from the MIC. Eliminated sequences are known as internal eliminated sequences (IES) and are a mixture of transposon-related repetitive sequences and nongenic single-copy sequences resulting in a gene dense low-repeat MAC (Chalker et al., 2013). Similarly, the MAC has a greater number of shorter chromosomes than the MIC due to chromosomal fragmentation during DNA elimination by imprecise deletion of internal DNA segments followed by rejoining or telomere addition (Chalker et al., 2013). This process involves 3 steps is observed in *P. tetaurelia* and features a special class of small

RNAs (scnRNAs) (Chalker et al., 2013):

- DNA amplification to high ploidy.
- DNA elimination pathway 1: accurate removal of short unique-copy elements (IES, internal eliminated sequences) that run through coding and non-coding sequences. This is achieved using bounding 5'-TA-3' dinucelotides to target double-stranded breaks and subsequent end-joining (Mayer and Forney, 1999; Bétermier, 2004)
- DNA elimination pathway 2: imprecise removal of large DNA regions (often containing transposable elements) in a manner similar to transposon silencing in other eukaryotes. This process likely involves short ncRNAs targeting heterochromatin formation via histone methylation to induce fragmentation. This fragmentation is subsequently repaired via the addition of new telomeres (Duret et al., 2008).

This process involves a special class of meiosis specific small RNAs (scnRNAs) which target aspects of DNA elimination (Chalker et al., 2013).

While the MIC appears to vary in size between subspecies of *P. bursaria* the MAC is roughly the same size and generally contains 10-30 times the amount of DNA than the diploid MIC (Cullis, 1972). Therefore, the MAC of *P. bursaria* is likely 20-60n (in contrast to the 800n MAC ploidy found in *P. tetaurelia* (Duret et al., 2008)). The MAC genome is likely to be somewhere between 20 and 100Mb and contain somewhere between 18,000 and 40,000 genes based on the size of the *Tetrahymena* (Eisen et al., 2006), *P. tetaurelia* (Aury et al., 2006), *P. caudatum* (McGrath et al., 2014) and *Oxytricha* (Swart et al., 2013) MAC genomes.

We can infer other likely features of the *P. bursaria* MAC genome from the *P. tetaurelia* sequencing project. Specifically, it is likely AT-rich (28% GC in *P. tetaurelia*), compact (78% coding density in *P. tetaurelia*), mostly repeat free with small intergenic regions and many short introns (e.g. 25bp IES elements) (Aury et al., 2006). There is also likely to be evidence of at least 1 whole genome duplications (WGD) (an ancient WGD before the divergence of *Tetrahymena* and *Paramecium* clades but not the 2 most recent WGD (see fig. 1.2.2) giving rise to the *P. aurelia* complex) with a moderate level of conservation to gene synteny and duplicated gene retention (weakly correlating with a genes GC%, expression level and functional class) (Aury et al., 2006; McGrath et al., 2014). *P. bursaria* is also likely to be have a high level of replication fidelity and relatively low rate of base-substitution mutation, traits found in *P. tetaurelia*, as *P. bursaria* shares ciliate specific modifications to the active sites of B-family polymerases α, ζ, and the proofreading exonuclease of DNA polymerase ε believed to be adaptions to improve replication fidelity and a necessary adaptation when maintaining a separate germline (Sung et al., 2012).

There is no established methodology in *Paramecium* to transform the MIC genome so the only available reverse genetic methodology is that of gene knock-down with RNA interference (RNAi) (Marker et al., 2014). However, RNAi can be induced by one of two distinct but overlapping RNAi systems in *P. tetaurelia* (Marker et al., 2014). This is by microinjection[5] of homologous transgenes (transgene-induced silencing) or by feeding *Parame-*

[5]This common RNAi pathway can be invoked by both Direct injection of dsRNA into the cytoplasm only triggers transient silencing, likely due to growth related dilution (Galvani and Sperling, 2002). Heritable silencing cannot be triggered by dsRNA (possibly due to insufficient RDR activity and absence of H3K9 histone factors in MIC) in *Paramecium tetaurelia* (Chalker et al., 2013)).

Figure 1.2.3: Figure redrawn and modified from (Duret et al., 2008). During normal vegetative growth *Paramecium bursaria* (and other *Paramecia*) divide by binary fission with the MAC elongating and "pinching" off in a process distinct from mitosis (known as amitosis) while the MIC undergoes mitosis. As the cell pinches before cytokinesis an unknown septum forms at the "neck", this stops cytoplasmic streaming which induces the endosymbionts to begin to divide. Cytokinesis then occurs largely simultaneously in host and endosymbionts (Kadono et al., 2004; Takahashi et al., 2007). The sexual cycle involves conjugation of compatible mating types (taking around an hour and lasts 24-48 hours (Jennings, 1939)) which triggers two-rounds of meosis of the MIC with one product disintegrating after each division so only a single haploid MIC remains. This undergoes mitosis to produce male and female gametes. Male gametes are then reciprocally exchanged between mating cells and fuse with the respective female gamete to create a syncaryon. Each syncaryon divides onces and one product disintegrates before undergoing two subsequent divisions. Two products differentiate into MACs by programmatic reorganisation, conjugants split and a normal binary fission occurs restoring normal 1 MAC and 1 MIC (Siegel, 1963)

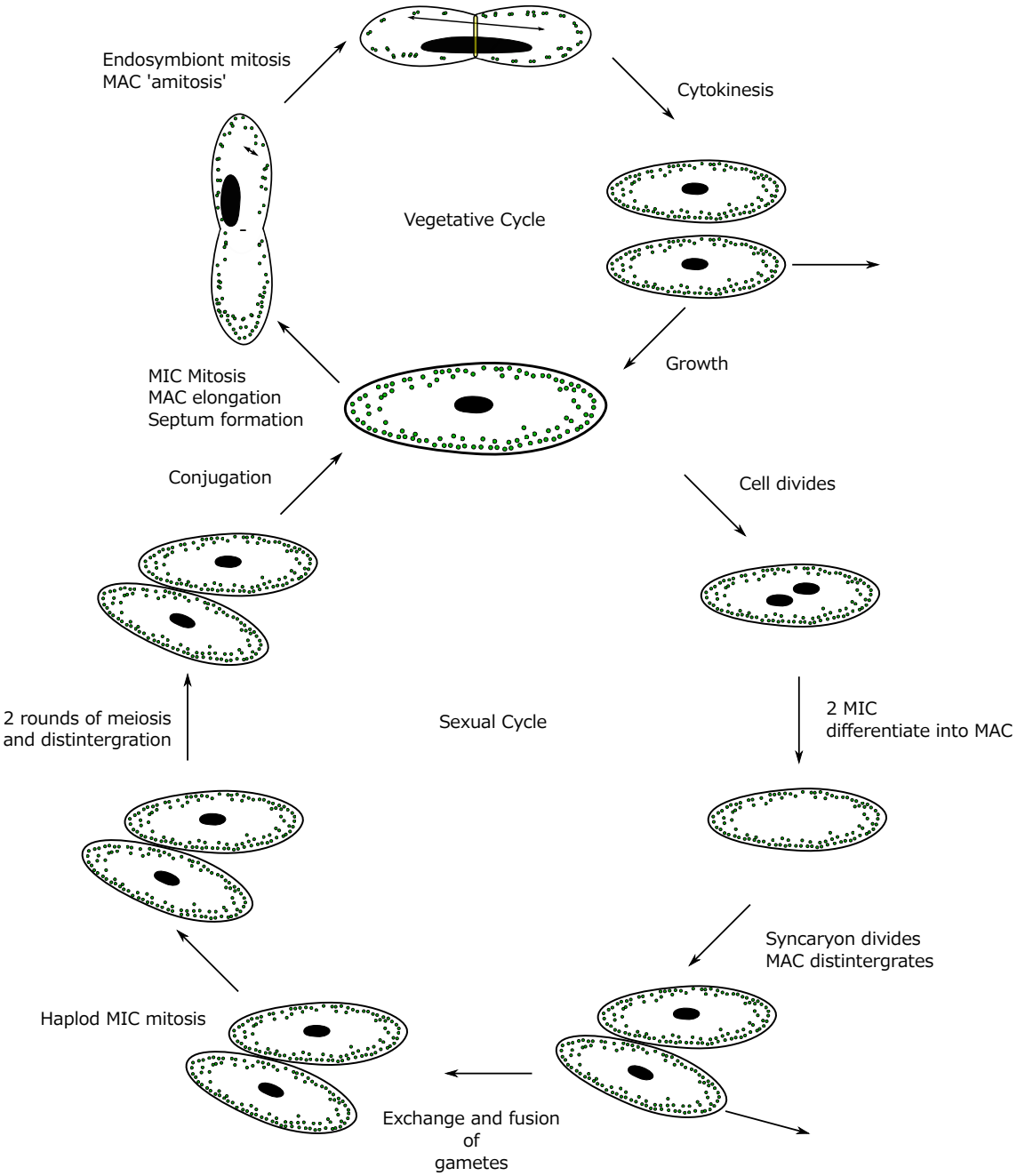

cium cells *Escherichia coli* transformed to produce sense and antisense transcripts for the target gene respectively (Galvani and Sperling, 2002) Furthermore, natural exogenous ssRNA in food bacteria of *P. tetaurelia* has been observed to produce low levels of silencing, therefore this mechanism is a likely a form of natural gene regulation used

by *Paramecium* (Carradec et al., 2015). As *P. bursaria* shares the initial ancient WGD with *P. tetaurelia* (Aury et al., 2006) based on *P. tetaurelia* genes that are the product of this WGD it currently or previously will have possessed: a pair of Dicer/Dicer-like proteins, 6 pairs of Piwi genes and a single RdRP (Marker et al., 2014). Therefore, RNAi is likely available in *P. bursaria* as a means of testing predictions generated through transcriptomic and genomic investigation.

Paramecium appears to be particularly competent for endosymbioses with an array of over 60 genetically diverse putative endosymbionts described (Görtz and Fokin, 2009). This is no surprise as ciliates have been known to have bacterial (Görtz and Fokin, 2009), archael (Wrede et al., 2012) and eukaryotic (Kodama and Fujishima, 2009) endosymbionts. These endosymbionts range in degree from mutualist to parasitic and are cytoplastmic, endomicronucleic, endomacronucleic and/or perinuclear. As a serial phagotroph, *Paramecium* species are liable to infiltration by bacterial capable of escaping or resisting the phagosomal digestive process. The *Paramecium bursaria* micronuclei frequently contains bacterial endosymbionts. The closed nature of reproduction has been suggested as a reason why endonucleobioses are common in paramecium (Görtz and Fokin, 2009) Some endosymbionts exhibit high levels of adaptation, no longer able to be found free-living and with evidence of the genome reduction distinctive of endosymbiosis (Görtz and Fokin, 2009) The most frequently identified bacterial endosymbionts in German environmental samples are that of *Holospora caryophila*, *Holospora obtusa* and *Caedibacter caryophilus* Several of these endosymbionts have been shown to require specific *Paramecium* genes for maintenance Dohra et al. (1998).

1.3 *Micractinium reisseri* and *Chlorella*

Chlorella was a key a model organism, forming the basis of the identification of the Calvin Cycle (Benson and Calvin, 1948)

Green algae have been found displaying all forms of endosymbioses: transient non-heritable associations (**?**), predation to autotrophy phases during life cycle (**?**), kleptoplasts (**?**), permanent heritable association (**?**) and metabolic co-dependence/genetic amalgamation (**?**). Above from (**?**)

Sponge and hydra endosymbiont too

Same alga in unrelated micotrophic amoebae (Gomaa et al., 2014) Mixotrophic Testate Amoebae (Amoebozoa, Rhizaria and Stramenopiles) Share the Same Symbiont (Trebouxiophyceae) Chlorella belongs to class Trebouxiophyceae, which contains most known green algal endosymbionts, living in lichens, unicellular eukaryotes (e.g. ciliates, foraminifera etc.), plants (e.g. Ginkgo), animals (e.g. cnidarians, mussels, flatworms, etc.), and even parasites such as some Coccomyxa species (Lewis and Muller-Parker, 2004, Pröschold et al., 2011, Rodríguez et al., 2008 and Trémouillaux-Guiller and Huss, 2007). (Gomaa et al., 2014)

1.3.1 Taxonomy

The initial taxonomic identity assigned to the green algal endosymbiont of *P. bursaria* was by Brandt and Beijerinck in late 19th century as *Zoochlorella conductrix* (Hoshina et al., 2010).

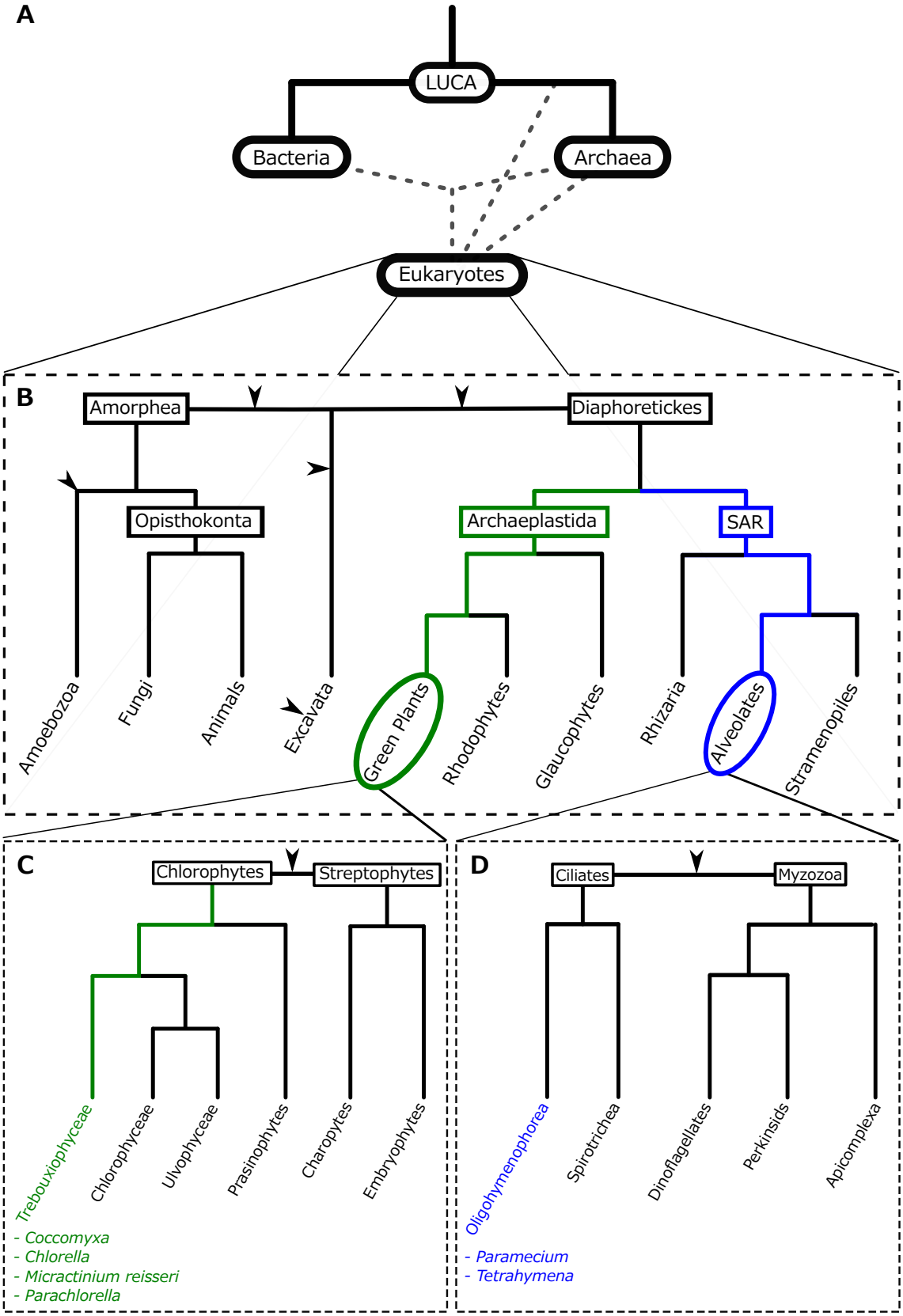

Figure 1.3.1: **A**: Schematic of the current best estimate of the tree of life demonstrating the 2D and 3D hypotheses, dashed lines indicate multiple potential branch location, arrowed lines demonstrate known endosymbiotic events (based on work reviewed in (Gribaldo et al., 2010)) **B**: Schematic of the current known eukaryotic portion of the tree of life (based on work reviewed in (Burki, 2014; Adl et al., 2013), **C**: Schematic of phylogeny of the ciliates (based on work by (Bachvaroff et al., 2011) showing Oligohymenophorea containing *Paramecium* and *Tetrahymena* and sister group Spriotrichea containing *Euplotes* and *Oxytricha*. **D**: Schematic of phylogeny of the green algae (based on work reviewed in (Leliaert et al., 2012)

1.4 *Paramecium bursaria* – *Chlorella* endosymbiosis

What is particularly interesting is that the *Paramecium bursaria*-green algal endosymbiosis is a midpoint - more phototrophic than *Noctilulca scintillans* but more heterotrophic than *Globigerinoides sacculifer*, persistent endosymbiont and on the cusp of obligate and facultative (Stoecker et al., 2009)

One aspect that distinguishes *P. bursaria - Chlorella* from similar endosymbiotic systems between green algae and corals/lichens is that it is directly heritable, specifically daughter cells receive the same symbionts retained by the mother cell (Siegel and Larison, 1960)

Chlorella produces maltose in both lit and dark conditions, in lit conditions directly from calvin cycle and in dark from starch breakdown (Ziesenisz et al., 1981)

The *Paramecium - Chlorella* endosymbiosis is established when *Chlorella* is phagocytosed by the serially phagotrophic *Paramecium* and is then able to escape the digestive vacuole. For this escape to take place, the endosymbiont must initially resist acidification caused by acidosome fusion with digestion vacuole. If the endosymbionts are able to resist this acidification they begin, through an unknown mechanism, to 'bud-off' from the initial phagosome into a new vacuole. This new perialgal vacuole (PV) is released into the cytoplasm and each PV contains an individual *Chlorella* cell (Kodama and Fujishima, 2009) The PV appears resistant to lysosome fusion and further digestive steps suggesting molecular modification of the vacuole membrane (Johnson, 2011) These perialgal vacuoles then bind the host cortex and compete for attachment with host structures known as trichocysts (Kodama and Fujishima, 2012) in a region with low to no lysosome activity (Kodama and Fujishima, 2009) This suggests the observed resistance to lysosome fusion may be a by-product of localisation. As few as a single algal cell can infect the host (Weis and Ayala, 1976) however, the majority of *Chlorella* are digested especially non-competent strains (Kodama et al., 2007). Furthermore, it has been established that *Chlorella* strains are fairly host-specific. For example, Summerer et al in 2007 (Summerer et al., 2007) showed that *Chlorella* isolated from other ciliates were able to establish endosymbioses with *P. bursaria* however, those isolated from cnidarian *Hydra* were not. This paper also showed *P. bursaria* favours its symbiotic partner over those isolated from other ciliates when given the choice, this suggests specific adaptations have taken place between host and endosymbiont (Summerer et al., 2007) Free-living *Chlorella* strains do rarely establish endosymbioses with *Paramecium* (Siegel and Karakashian, 1959), however they are generally only able to infect fewer *Paramecium* and establish much smaller endosymbiotic populations within the host than the symbiont strains (Siegel and Karakashian, 1959)

Once established, the symbiosis appears to be mutually beneficial with an observed flux of amino acids and CO_2 to the endosymbiont and oxygen and photosynthate (principally maltose) to the host as a function of light levels (Karakashian, 1963). The extent of this endosymbiosis is such that *Chlorella* is capable of supporting *Paramecium* in media without its typical bacterial food-stocks and conversely the *Paramecium* is capable of supporting the phototrophic *Chlorella* in the dark for ~2 weeks (or up to 51 endosymbiont cell divisions) suggesting considerable bi-directional nutrient flux (Siegel and Larison, 1960; Karakashian, 1963). It should be noted that for longer periods in the dark or when a bacteria-free culture is used in the dark the host will digest the endosymbionts

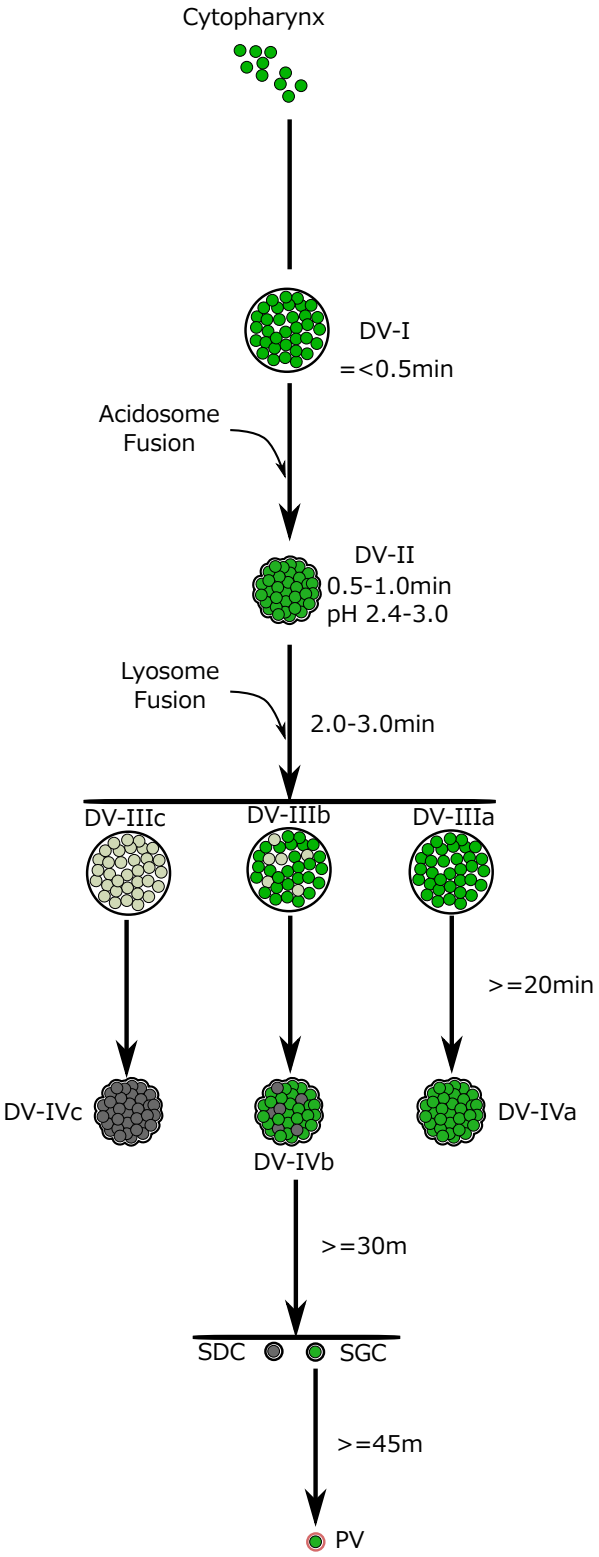

Figure 1.4.1: Process by which some endosymbiont escape digestion and generate perialgal valcuoles (PV) Figure redrawn and modified from (Kodama and Fujishima, 2009).

(Parker, 1926) From an ecological perspective, this endosymbiosis can be considered as a means of acquired phototrophy (or mixotrophy), a tactic believed to be advantageous for survival in patchy oligotrophic environments by providing fixed carbon to cover respiration requirements (Putt, 1990). This is largely supported by studies, such as Karkashian's 1963 paper, showing that with a sufficient concentration of bacterial feedstock in the media

the growth rate of asymbiotic *Paramecium* ('bleached') and *Paramecium* with *Chlorella* endosymbionts are largely equal. This threshold is estimated to lie between 10^6 and 10^7 bacteria per ml. However, as this is generally a much greater concentration than found in the natural environments of *P. bursaria* the endosymbiosis offers a considerable adaptive advantage to the host (Karakashian, 1963) As temporary acquisition of phototrophy is estimated by some research (Raven, 1997) to be less energetically costly than the permanent maintenance of plastids (via endosymbiosis or kleptoplasty) within the host this indicates that this endosymbiosis likely provides other host benefits beyond just the energetics of acquired phototrophy. These include:

- Exploitation of low oxygen environments by the host (as the photosynthesising endosymbiont is capable of providing oxygen to the host (Reisser, 1980))
- Photoprotection and protection against 257nm and 282nm UV radiation potentially via endosymbiont pigmentation and localisation to shield host nuclei (Sommaruga and Sonntag, 2009; Summerer et al., 2009; Miwa, 2009). This is especially important as the AT-rich *Paramecium* genome is likely prone to UV-damage via the formation of cyclobutane thymine dimers (Sommaruga and Sonntag, 2009)
- Protection against predation (Berger, 1980). The exact mechanism by which this occurs is unknown, however, it has been observed that mixotrophic ciliates are able to move in rapid 'jumping' movements. This is hypothesised as being an energetically costly escape reaction made possible by sugar-rich photosynthate mixotrophic ciliates gain from their algal endosymbionts (Pérez et al., 1997). Intriguingly, this protection against predation occurs despite endosymbiont displacement of trichocysts (defensive cellular structures) for attachment to the ciliate cortex (Kodama and Fujishima, 2011)
- Protection against undesired endosymbionts and/or parasites. Algae in *P. bursaria* form an antagonistic relationship with some bacterial endosymbionts but the one specific case and there is experimental evidence that *P. bursaria* can only be infected by bacteria and yeasts after *Chlorella* is eliminated (Gortz, 1982). This is consistent with bacterial symbionts having been repeatedly identified as providing resistance to parasites in organisms such as the insects (Martinez et al., 2014)
- Protection against chemical toxins, for example symbiotic *Paramecium* have a much higher survival rate (96%) to 0.5 mM nickel chloride ($NiCl_2$) than asymbiotic *Paramecium* via an undetermined mechanism (Miwa, 2009)
- Increased thermotolerance (tested at 42°C) (Miwa, 2009), again, by unknown mechanisms but potentially related to the undefined means of perialgal vacuole attachment to the cell cortex.
- Protection against excessive oxidative burden (potentially due to endosymbiont dismutases and catalases) (Hörtnagl and Sommaruga, 2007) and hydrogen peroxide (hypothesised by Miwa as being due to the improved energetics of the symbiotic host) (Miwa, 2009)

In return, the endosymbiont also appears to gain several advantages including a generally much increased level of photosynthetic activity (Sommaruga and Sonntag, 2009):

- CO_2 from the host (Parker, 1926)
- Nitrogen supply (Johnson, 2011).
- Amino acids including L-glutamine (likely an important nitrogen source) (**?**) and L-arginine, L-asparagine, L-serine, L-alanine and glycine (Kato and Imamura, 2009b).
- Host supplied divalent cations such as K^+, Mg^{2+}, and Ca^{2+}. All of which have key roles in photosynthesis (Kato and Imamura, 2009b).
- Protection against *Paramecium bursaria* – *Chlorella* Virus (PBCV) (Yashchenko et al., 2012) a large isocahedral dsDNA, 330kbp virus with 133-genes that lyses symbiotic Chlorella when isolated from the host (Van Etten et al., 1983). This potentially occurs by preventing contact between PBCV and the endosymbiont.
- Effective photo-accumulation and increased mobility (Niess et al., 1982a).

This exchange of materials between host and endosymbiont is regulated by an effective biochemical 'bartering' system with numerous feedback cycles. For example, the release of endosymbiont photosynthate is dependent on Ca^{2+}. This ion is provided by the host and also has a role in the up-regulation of photosynthesis (as proxied by oxygen evolution) (Kato and Imamura, 2009b). Once photosynthate is released into the PV lumen endosymbiont H^+-ATPases are activated which allow the generation of the H^+ gradient necessary for endosymbiont uptake of host-provided amino acids via a set of amino acid-proton symporters (in the same manner as (Camoni et al., 2006)) (Kato and Imamura, 2009b). This proton gradient will potentially lead to further photosynthate release due to observed pH-dependence of this (Kato and Imamura, 2009b). As we can see the more photosynthate supplied to the PV lumen the greater the uptake of provided nitrogen sources. Intriguingly, from experiments using cycloheximide to selectively interrupt endosymbiont but not host protein synthesis it appears that the maltose transporter that is responsible for export of photosynthate from the PV lumen into the host cytoplasm is endosymbiont derived (Muscatine, 1967). However, unless photosynthesis is also inhibited (using DCMU) the build up of photosynthate without exportation in the PV triggers the swelling of the vacuole up to 25x its original size. This removes the vacuole from the region in which it is protected from lysosome fusion and leads to the digestion of the endosymbiont (Kodama and Fujishima, 2009). So, here we can see further regulation of the relationship – in which the endosymbiont is degraded if it does not release photosynthate to the host.

On top of this system of secretion, uptake and feedback there have also been several other observed regulatory interactions between host and endosymbiont. The most apparent of these are the synchronising of cell division and circadian rhythms between host and endosymbiont with endosymbiotic *Chlorella* sufficient to recover a circadian rhythm in arrhythmic *Paramecium* mutants (Miwa, 2009) This regulation of the timing of cell division for both members of the system appears well co-ordinated and takes place in such a way that neither host or endosymbionts outgrow one another (Kadono et al., 2004; Takahashi et al., 2007). The importance of regulation of endosymbiont distribution at host division is evidence in the only natural aposymbiotic *P. bursaria* mutant which has a impairment in this mechanism and thus can't maintain endosymionts (Tonooka and Watanabe, 2002).

1.4.1 Separating host and endosymbiont

naturally aposymbiotic straings of paramecium exist but are rare

artifically reinfecting (Ohkawa et al., 2011) Reduced endsoymbiont numbers: high radiation doses excessive food supply continual darkness with plenty of good - 6 weeks - still some had chlorella so selective picking 6 rimwa

1.5 Conclusion

In conclusion, understanding the mechanisms by which primary and secondary photosynthetic endosymbioses have occurred is one of the most significant outstanding problems in understanding the evolution of the eukaryotes. *Paramecium bursaria* and its endosymbiosis with *Chlorella* offers a useful system to investigate secondary photosynthetic endosymbioses before metabolic co-dependence has become fixed. As both organisms seem highly prone to forming endosymbiotic relationships with multiple other organisms as a serial host and serial endosymbiont respectively it may be possible by identifying the key molecular components of their relationship to understand what factors contribute to such prolific utilisation of endosymbioses. Furthermore, while there is considerable supporting literature and many established methodological techniques for working on these organisms individually and in endosymbiosis there have been relatively scant efforts using the latest -omics techniques and reverse genetics such as RNAi. Considering the historical role both organisms have played independently in our understanding of endosymbiosis[6] it is perhaps apt that further insight may be gleaned by applying the latest modern techniques to interrogate their relationship.

z

[6]Margulis was strongly influenced and inspired by research conducted in organisms closely related to both *Paramecium bursaria* and *Micractinium reisseri*. Specifically, the discovery of Tracey Sonneborn of non-mendelian cytoplasmic inheritance in *Paramecium bursaria* (Sonneborn, 1950) and the multiple lines of evidence of the presence of DNA within the chloroplasts gleaned from several species of green algae related to *Micractinium reisseri* (*Spriogyra* (Stocking and Gifford Jr., 1959), *Chalymdomonas moewussii*, and *Chlorella ellipsoidea* Ris and Plaut (1962)).

Science is what we understand well enough to explain to a computer.

Art is everything else we do.

- Donald Knuth: *foreword to A = B by Petvosek, Wilf and Zeilberger*

2 Methods

2.1 Microbiology

2.1.1 Strain information

During this project 3 *Paramecium bursaria* cultures have been used. These have been obtained from the UK Culture Collection of Algae and Protozoa (CCAP) and the Japanese National BioResource Project (NBRP). Specifically:

- CCAP 1660/12: *Paramecium bursaria* SW1 with *Micractinium reisseri* SW1-ZK (Hoshina et al., 2010)
- CCAP 1660/13: *Paramecium bursaria* (unknown strain) with *Coccomyxa* CCAP 216/24 [1]
- NBRP Yad1g1N: *Paramecium bursaria* Yad1w with *Chlorella variabilis* 1N[2]

Both CCAP cultures (1660/12 and 1660/13) were isolated from the same pond in Cambridge, UK (pers. comm. Undine Achilles-Day CCAP, Oban, Scotland) CCAP 1660/12 was the principal culture and all genomic, transcriptomic and metabolomic analyses were conducted using these cultures. Theoretically, these 3 cultures provide us with *Paramecium bursaria* strains harbouring members of 3 of the 4 species of green algal *Paramecium* endosymbiont (see Chapter 1 **??** for more details).

[1] This is a mixed culture containing both CCAP 1660/12 strain with *Micractinium* and the *Coccomyxa* bearing strain, the *Coccomyxa* endosymbiont has been further isolated in CCAP under the description CCAP 216/24 (pers. comm. Undine Achilles-Day CCAP)

[2] Yad1g1N host is mating type 1 and was created by mixing of isolated and cultured endosymbiont (*Chlorella variabilis* Clone 1 (known as 1N strain))

2.1.2 Media and Culture conditions

All *P. bursaria* and green algae cultures were maintained in New Cereal Leaf-Prescott Liquid (NCL) media ($4.3g/lCaCl_2.2H_2O$, $1.6g/lKCl$, $5.1g/lK_2HPO_4$, $2.8g/lMgSO_4.7H_2O$, $1g/l$ wheat bran, gravity filtered via GF/C paper and autoclaved) (CCAP, 2012) and stored in an incubator at 15°Cwith a 12:12 light:dark cycle. The incubator was lit using 2 21*w* 865 daylight fluorescent tubes, producing 2000 lumen each. Cultures were sub-cultured approximately every 2 weeks using fresh NCL media and were inspected using light microscopy to monitor health. No bacteria was added to cultures used for "omic" analyses but otherwise the medium was bacterised with *Klebsiella pneumoniae* SMC (strain donated by the Meyer Lab, Ecole Normale Supérieure, Paris, France) the day before use.

2.2 Omics

"-omic" technologies are those aimed at globally characterising a class of biomolecules within a specific biological sample (characterising the "-ome"). The major areas of this are genomics, transcriptomics, metabolomics and proteomics. Genomics aims to characterise DNA and generally involves sequencing the genome, it is used to discover and describe genes (and non-coding DNA) and by comparison with other genomic datasets their evolution. Similarly, transcriptomics is orientated around the characterisation of the RNA present in a sample. This can include the canonical messenger RNA (mRNA) transcripts but also other RNA elements i.e. non-coding RNA (ncRNA) such as small interfering RNAs (siRNA) and micro RNAs (miRNA) and generally involves sequencing the RNA fraction of interest. Transcriptomics can be used to catalogue transcripts (and their variant splices), aid genome annotation, and/or assess transcriptional response to a given condition or cellular state (Wang et al., 2009). Metabolomics seeks, instead, to identify and quantify small biomolecules that make up the terminal and intermediate products of cellular metabolism e.g. carbohydrates, alcohols, and amino acids. Finally, proteomics characterises the proteins present in a sample. Typically, the metabolome and proteome are interrogated using various forms of mass-spectrometry. There are also a plethora of additional approaches which seek to characterise different subsets of these biomolecules e.g. epigenomics (epigenetic modification to DNA such as methylation and histone binding), gylcomics (characterisation of cellular saccharides). "Meta-…-omics" is the application of specific "omic" method to a biological sample containing multiple organisms. For example, "metagenomics" has been used to investigate the cellular community composition of marine micro-eukaryotes (Cuvelier et al., 2010) and "metatranscriptomics" has been used to analyse the transcriptomes of the microbes present in the gut of metazoa (Perez-Cobas et al., 2013).

The utility of "-omic" approaches is they allow a researcher to characterise a high proportion of a biological system's function in a way that is faster, cheaper and requires less *a priori* knowledge of the system than more targeted approaches. For example, in order to estimate the abundance of all mRNA transcripts in a sample using specific approach such as RT-PCR would require sequence knowledge to design primers as well as an infeasible amount of reactions to acquire a characterisation comparable to that obtainable by a transcriptomic approach such as RNA-Seq. Additionally, due to being "non-targeted" (or rather less targeted) "omics" also removes one aspect of researched-induced bias caused by a conscious selection of molecule specific probes. By not considering elements

of a system in isolation like the classic methodologically reductionist[3] approaches "omics" can reveal complex systemic mechanisms/features (or at the extreme "emergent properties") that would otherwise have been missed (Fang and Casadevall, 2011).

However, until relatively recently "omic" methodologies were restricted to specialised institutions and well characterised "model" organisms. While, *Paramecium bursaria* and green algae such as *Micractinium reisseri* could be considered "model" organisms throughout the early days of molecular biology, they are much less frequently studied in the genomics era (2000-today) particularly compared to organisms such as *Arabidopsis thaliana* and *Saccharomyces cerevisiae*. Fortunately, due to the development and maturation of both technologies and databases the potential for functional and adaptive analysis of non-model organisms using combined "omics" (i.e. using genomics as a reference to guide subsequent transcriptomics) approaches (e.g. (Muñoz Mérida et al., 2013; Feldmesser et al., 2014)) has recently been demonstrated. Additionally, there are two other developments which make *P. bursaria-M. reisseri* (*PbMr*) increasingly amenable to "omic" analysis: *de novo* transcriptomics which dispense with the need to generate moderately accurate genome in the relatively genomically intractable *Paramecium* (e.g. (Kodama et al., 2014) and single-cell approaches which allow fine-grained analysis of the *Paramecium bursaria* - green algal relationship on a cell-by-cell basis.

It should be noted that care must be taken with "omics" approaches as they can easily become purely descriptive, and at worse generate models that lack any biological relevance (Fang and Casadevall, 2011). This concern holds for all systems-level approaches and has been frequently raised and discussed in the context of genomics (Dougherty, 2008). Therefore, it is crucial to supplement "omic" approaches with targeted methods in a way that compensates for the weakness of each type of method. Specifically, the systems approach should be used to generate novel and interesting hypotheses which can then be tested in isolation using reductionist methods (Casadevall and Fang, 2008). For example, "omics" methods could be used to create a model of inter-organism host-endosymbiont metabolism and targeted approaches such as RNAi could then be used to test hypotheses generated by this model i.e. testing that a particular transporter protein is responsible for the transfer of metabolites by knocking out that transporter and observing the resultant phenotype: is the relationship perturbed in a predictable manner.

2.2.1 Genomics and Transcriptomics

DNA sequencing

In the majority of cases, genomics and transcriptomics are both synonymous with the sequencing nucleic acids. Earlier approaches, based upon the fluorescent marking of the hybridisation of DNA and/or RNA to arrays of short complementary probes e.g. genomic tiling arrays and the transcriptome microarrays (Mockler and Ecker, 2005), are of more limited utility. Relative to sequencing-based approaches these methods require relatively more prior knowledge of the organism and require a custom array to be designed for any novel system. Additionally,

[3]Epistemological reductionism: "explain all biology in terms of physics and chemistry" (Crick, 1966) i.e. biology is applied chemistry which is applied physics which is applied maths. Ontological reductionism: a biological system is only the sum total of its component molecules and their interactions. Methodological reductionism: examination of simple components can be used to understand complex system (Fang and Casadevall, 2011)

while microarrays can determine relative expression levels of transcripts by the comparison of the fluorescence intensity at given complementary probe(s) the continuous nature of this output, difficulty distinguishing alternative isoforms and more limited dynamic range (combined with previously mentioned limitations) has meant the sequencing of cellular transcripts (RNA-Seq) has largely supplanted microarrays (Wang et al., 2009). However, both SNP tiling arrays and microarrays do have the advantage of throughput and ease of analysis in situations where the host organism is well known and suitable arrays have already been designed and evaluated. For this reason they are still frequently encountered in specialist area of medical diagnostics.

While it is possible to directly sequence RNA transcripts (Ozsolak et al., 2009) most approaches first utilise a reverse transcription (RT) step to convert transcripts to cDNA. As ribosomal RNA makes up a sizable proportion of RNA in the cell it is often necessary to enrich or select the RNA fraction of choice in order to minimise wasted effort when sequencing (Wilhelm and Landry, 2009). For eukaryotic mRNA enrichment this can be easily achieved by using poly-T primers during RT which selectively bind to the poly-adenylated tail of these messenger transcripts. However, for bacterial/archael work and transcriptomic analyses focussing on non-poly-adenylated transcripts such as ncRNAs/siRNAs/miRNAs etc. ribosomal depletion is used (O'Neil et al., 2013). This is a process by which ribosomal probes are attached to magnetic beads. Ribosomal RNAs bind to these probes and the magnetic beads can be used to partition the majority of ribosomal sequences away from the other RNA (O'Neil et al., 2013). This means that transcripts can be sequenced using the same methods and platforms as any other DNA sample with analysis only diverging against post-sequencing. It should be noted that there are potential disadvantages to this reverse transcription step and it can potentially generate artefacts and biases in the analysis (as well as placing limitations on the quality and quantity of input RNA) (Ozsolak and Milos, 2011) however, the advantages of the more developed DNA sequencing technology outweighs these disadvantages.

These DNA sequencing technologies can largely be divided into 3 technological eras with today (2015) broadly at the transition between 2nd and 3rd generations.

1st generation (also known as Sanger) sequencing technology originated in 1970s with the work of Sanger & Coulson (Sanger and Coulson, 1975; Sanger et al., 1977a,b) which developed sequence determination via the principal of chain termination during synthesis and subsequent determination of relative fragment sizes. Briefly, by having 4 separate reactions in which DNA synthesis terminates on the incorporation of dideoxy nucleotides (ddNTP) corresponding to each of the 4 principal DNA bases (i.e. ddATP, ddGTP etc.) you can generate a series of DNA fragments of various sizes. Size fraction separation of these fragments via methods such as gel electrophoresis means the DNA sequence can be easily read from the fragment size distribution across the 4 ddNTP reactions (Sanger et al., 1977b). This technique was used to sequence the first DNA genome (bacteriophage $\varphi X174$ (Sanger et al., 1977a)). The methodology was subsequently improved by use of fluorescently labelled ddNTPs by Leroy Hood, massively simplifying automation of the process (Smith et al., 1985, 1986). Further improvements followed throughout the 1990s and early 2000s such as capillary electrophoresis and other general throughput and length enhancements (Bonetta, 2006). Transcriptomic analysis was possible using Sanger sequencing by generating clone libraries from partial or complete cDNA and randomly sequencing clones (Adams et al., 1991; Gerhard et al., 2004). However, while this did allow resolution of different isoforms and could be used to aid annotation

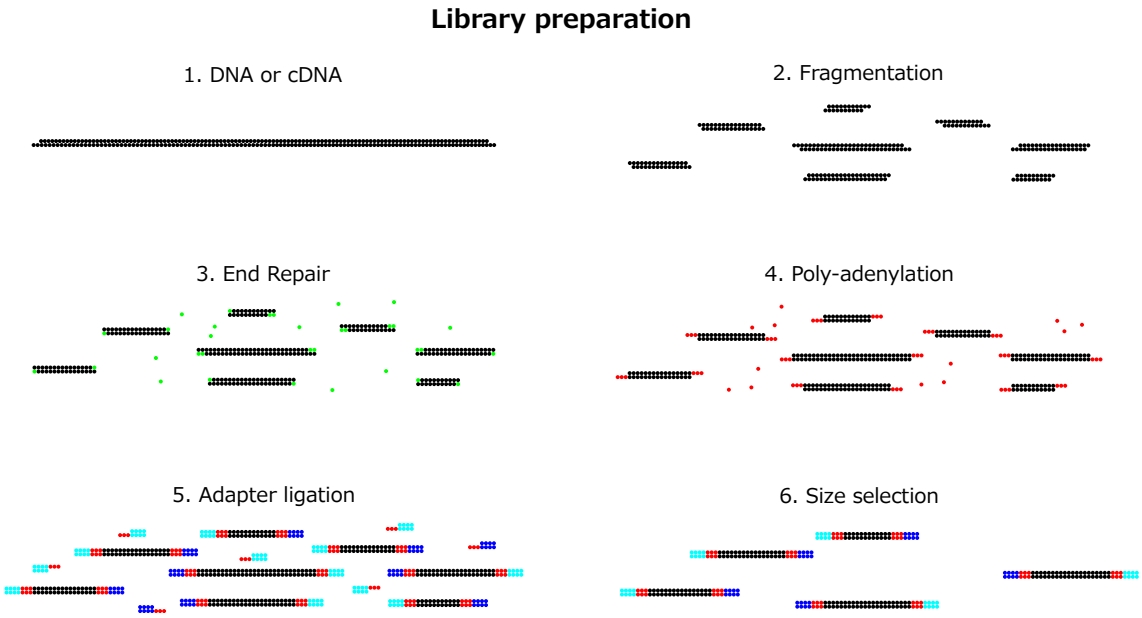

Figure 2.2.1: A brief overview of library preparation for Illumina modified from (Mardis, 2008) and Illumina TruSeq kit documentation

(Adams et al., 1991) it was not possible to investigate relative expression levels beyond a broad identification of highly expressed transcripts based on the proportion of the cDNA/EST library they made up. Sanger sequencing's main utility lies in high quality short fragment ($300 - 1000bp$) sequencing to determine or confirm the sequence of specific DNA fragments such as vectors or PCR products (Bonetta, 2006; Tsiatis et al., 2010).

2nd generation sequencing emerged commercially in 2005 with the work of both George Church and 454 Life Sciences (Margulies et al., 2005) and featured reduced individual reaction volumes, greater parallelisation (and so higher throughput), cell-free preparation without the need for time-consuming cloning of DNA fragments into bacterial vectors to generate clonal templates for sequencing, and direct sequencing detection obviating the need for size fractionation (Jaszczyszyn et al., 2014). These technologies generate huge amounts (on the order of $10^6 - 10^9$ of relatively short (on the order of $10^1 - 10^3 bp$) DNA sequences (reads) randomly sampled from the input (c)DNA.

Commercially available 2nd generation platforms include 454's GSLFLX and GSJunior (now Roche), Ion Torrent's (now Life Technologies) PGM, Applied Biosystem's (now Life Technologies) SOLiD and Illumina's (formerly Solexa) HiSeq, MiSeq and older Gene Analyzer II (**?**).

Although these platforms use a range of different implementations and tend to exhibit various different trade-offs (mainly in terms of number of reads and their respective lengths) they all largely follow the same basic process (Shendure and Ji, 2008):

1. Library generation: Randomly fragmenting input DNA into short fragments of a specific size followed by ligation of adapter sequences with some platforms allowing development of "paired-end" or "mate-pair" libraries in which each end of a fragment is sequenced separated with a known size unsequenced fragment aiding subsequent assembly (see **??**)

2. Clonal amplification: Generation of clonally identical spatially distinct clusters of DNA mainly via emulsion PCR (Dressman et al., 2003) (SOLiD, Ion Torrent, 454) or bridge PCR (Adessi et al., 2000; Fedurco et al., 2006) (Illumina) (see **??**)

3. Sequencing-by-synthesis: In which a complementary DNA strand is generated base by base via sequentially flooding and clearing a chamber with each dNTP and a polymerase (or ligase in the case of SOLiD). On incorporation of a base into a cluster a detectable signal is released such as emission of certain wavelengths of light detectable using optics (e.g. Illumina, 454, SOLiD) or release of hydrogen ion (e.g. Ion Torrent).

The explosion in sequencing throughput on 2nd-generation platforms has driven a massive decrease in per-base sequencing cost and the subsequent expansions in the amount of available data (e.g. the US National Center for Biotechnology (NCBI)'s short-read archive (SRA)) has made both genomic and RNA-Seq analysis and annotation easier and more effective.

While, 2nd generation sequencing has driven down per-base sequencing costs the cost of library preparation has fallen more slowly (Blainey, 2013). For this reason, combined with the higher throughput it has become common to multiplex difference samples during sequencing runs. Multiple distinct samples can be be sequenced in the same reaction (e.g. flowcell lane for Illumina platforms) by adding an indexed tags during library preparation. These tags can then be used to partition the reads back to their original separate samples after sequencing.

The current *de facto* standard in 2nd generation sequencing is that of the bridge amplification based (Shendure and Ji, 2008) Illumina platforms (Regalado, 2014) due to relatively low error rate ($\leq$ 0.1% (Glenn, 2011)), very high throughput (e.g. HiSeq2500 generates up to 400M 125bp reads per run (1TBase of data) (Nederbragt, 2013)) and the lowest cost per Mb ($\leq$ \$0.04 (Glenn, 2011)).

Finally, 3rd generation technologies are generally known as single-molecule sequencing. These platforms sequence individual DNA (or RNA molecules (Ozsolak et al., 2009)) without bias and error-prone amplification. The first 3rd generation platform was that of the now defunct Helicos Bioscience's Helicoscope (Harris et al., 2008) based on breakthroughs in the resolution of fluoresence visualiation using paired FRET methods (Braslavsky et al., 2003). There is only one publically available platform: Pacific Biosciences (PacBio) RS platform. PacBio operates on a similar principal of sequencing-by-synthesis as the 2nd generation platforms but uses fixed polymerases at the base of specially wave-guide structures allowing the detection of fluorescence from a single reaction instead of many parallel reactions in a clonal cluster. This produces few (compared to 2nd generation platforms) long (20kb and longer) reads but has a high cost and high error rate (14%) (Jaszczyszyn et al., 2014) Another platform, currently in testing, Oxford Nanopore's MinIon, reads individual strands of DNA through an array of pore proteins and determines the sequence at each pore based on the physical properties (impedance) of a particular set of bases.

Unfortunately, partly as an element of their relatively nascent state and partly due to the poorer signal:noise of single molecule approaches compared to analysing large batches of identical DNA sequences, 3rd generation technologies have a relatively high error rate. Thus are generally inadequate for most eukaryotic assembly tasks in and of themselves. Where they have shown great utility is in conjunction with 2nd generation datasets as a

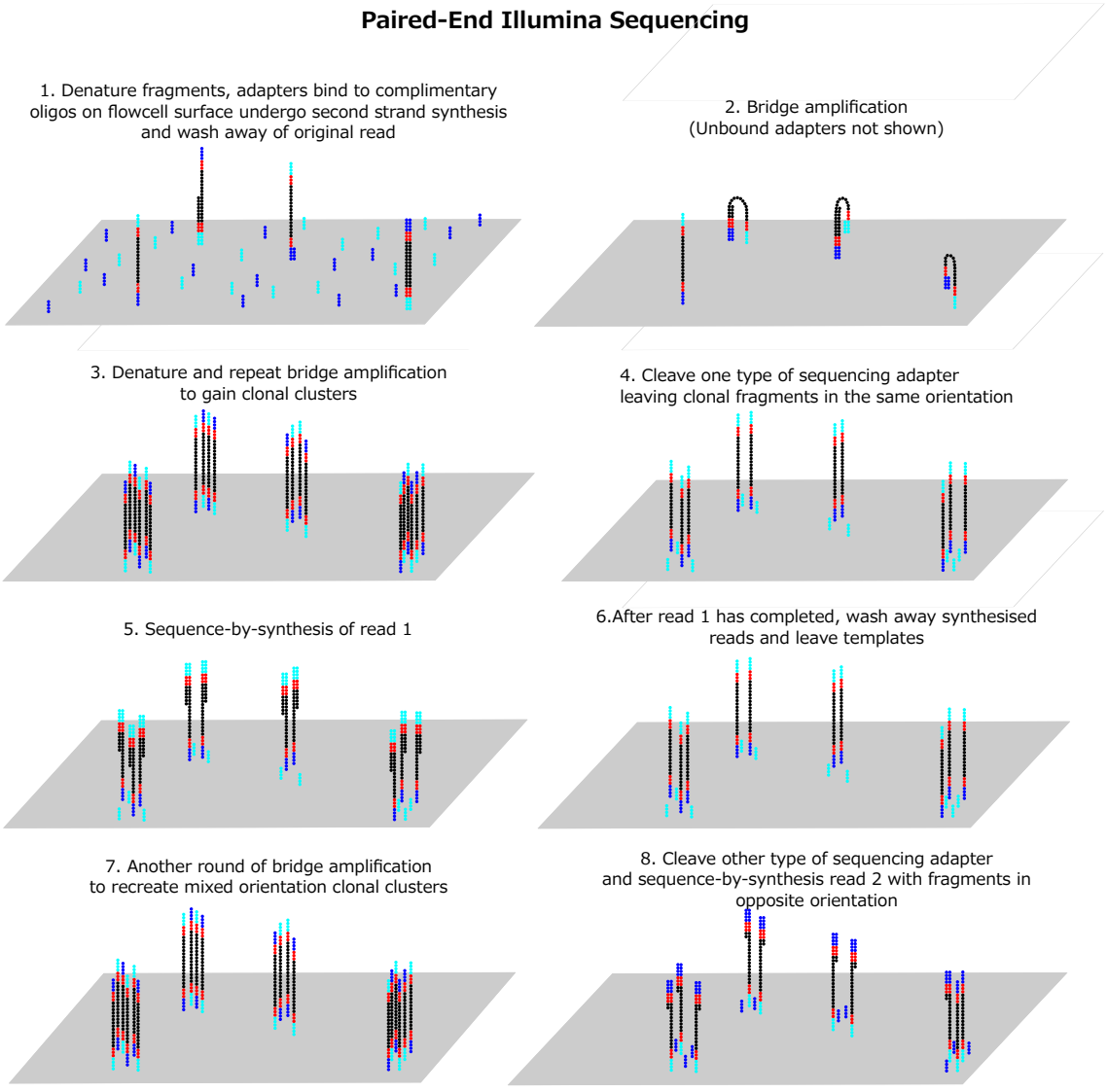

Figure 2.2.2: A brief overview of paired end sequencing in an Illumina flowcell after library preparation, derived from (Mardis, 2008) and Illumina

scaffolding tool i.e. producing long noisy reads upon which more accurate but shorter reads can be assembled.

Therefore, all genomic and transcriptomic sequencing in this PhD has been performed using the 2nd generation Illumina HiSeq platform due to its relative maturity, high-throughput, relatively accurate paired-end output making it currently the most amenable platform to effectively use *de novo* genomic and transcriptomics approaches. Additionally, Sanger sequencing has been used when accurate targeted sequencing was called for, such as investigating the taxonomic distribution of *Paramecium* green algal endosymbionts (see **??**).

Read pre-processing

Read pre-processing is a key stage in the assembly of next generation sequencing data regardless of the assembly methodology used.

Typically, this involves 4 key steps:

- Library quality control and contamination screening
- Trimming sequencing adapters and low probability reads
- Error corrections
- Digital normalisation

Arguably, trimming, error correction and normalisation are all aspects of the same process.

The specific error correction algorithms are largely based on the assumption that sequencing errors are infrequent and randomly distributed

Trimming

Error correction algorithms

normalistion

Assembly

There are two main approaches to both genome and transcriptomic assembly - referenced and *de novo*. A referenced assembly consists of the alignment of processed reads

Differential expression

Comparison of different methods of normalisation (Dillies et al., 2013)

RSEM-EVAL uses the concept of a latent true assembly for a given set of reads. Li et. al. define this as

For each read r, transcript(r) is the transcript, left(r) and right(r) are the 5' and 3' prime positoon of the transcript

a transcript is true if

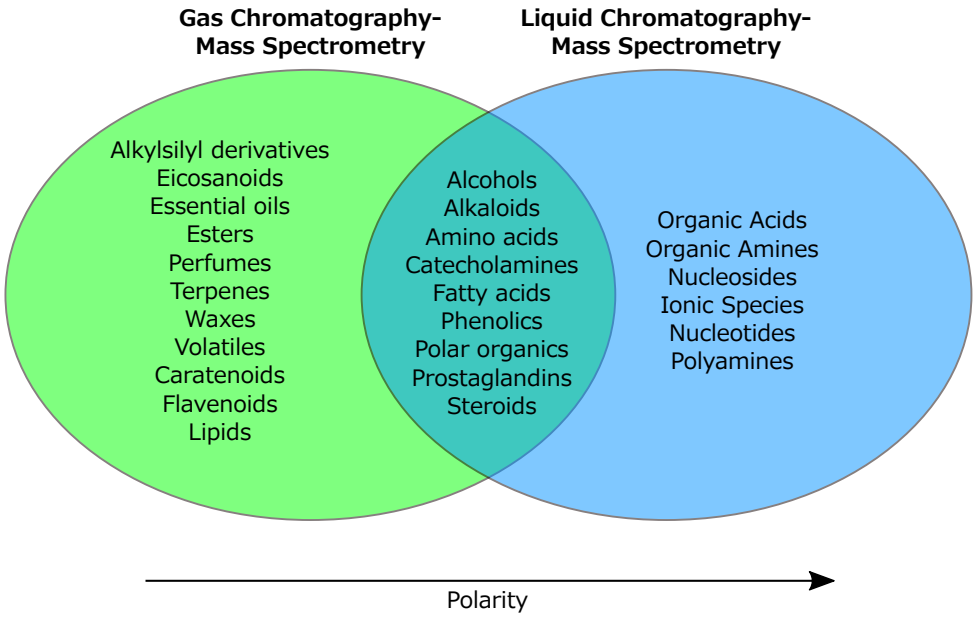

Figure 2.2.3: Groups of metabolites by which separation method is best suited for their analysis. Figure redrawn from https://www.agilent.com/cs/library/selectionguide/Public/5989-6328EN.pdf

2.2.2 Metabolomics

Metabolomics revolves around the detection and characterisation of cellular metabolites via a range of techniques. By qualitatively and/or quantitivately analysing these molecular substrates, cofactors and products of cellular metabolism a researcher can determine cellular state or response at the level.

Metabolites are direct signatures of biological activity ()

It is the final level in the path that links genotype to cellular phenotype (Fiehn, 2002)

Mteabolomics can range from target analysis (focussing on a single metabolite) to metabolic profiling (orientated on the metaboites of a specific pathway or type) to full metabolomics (uuntargeted analysis of the entire metabolome) to metabolic fingerprinting (high throughput metabolomics of a large number of organisms, also sometimes referred metabonomics) (Fiehn, 2002).

Mass spectrometry works on the principle that a charged particle moving through an electromagnetic field is subject to the following two laws: the Lorentz force law (**??**) and Newton's second law of motion (**??**)

$$F = Q(E + v \times B)$$

$$F = ma = m\frac{dv}{dt}$$

where F is the force applied to the ion, m is the mass, a the acceleration, Q the electric charge, E the electric field and $v \times B$ the cross product of the ion's velocity and magnetic flux density.

Therefore, by combining these two identities:

$$(\frac{m}{Q})a = E + v \times B$$

m/z denotes dimensionless quantityy from dividing the mass number of the ion by its charge number.

Mass spectrometry involves 4 components with numerous options and alternative methods for each optimised for different analytes:

- Sample introduction
- Ion source
- Mass analyser
- Mass detector

As mass analysers are only capable of analysing charged ions in a gaseous phase it is necessary to volatilise and charge analytes during sample introduction and ionisation respectively.

While samples can be directly introducted and vaporised using heat or similar, typically most metabolomic analyses involve the chromatographic separation of samples using either liquid (LC) or gas (GC) chromatography.

Targeted metabolomics

There are both targeted and untargeted metabolic analyses that focus on a known set of metabolites such as amino acids or a global metabolic profile respectively.

Untargeted metabolomics

These are nuclear magnetic resonance (NMR) spectroscopy, mass spectrometry (MS), light (usually infrared (IR) or ultraviolet (UV)) spectroscopy (Kafsack and Llinás, 2010).

There are 3 key techniques used

Evaluating the global metabolic profile (i.e. the presence and absence of substrates, products and cofactors)

It is possible to directly analyse samples using

By either qualtitatively characterising the presence and absence of various metabolites under varyin

First commercially available platform was the Vickers "MS-2" in 1948

One of the key issues with "-omic" platforms is the number of biological replicates tends to be far smaller than the number of parameters/metabolites/transcripts being studied.

Experimental design:

Reporting standards (Goodacre et al., 2007)

- experimental design

2.3 Machine Learning and Statistical Pattern Recognition

Machine learning is a field of computer science devoted to the challenge of developing and applying algorithms capable of automatically inferring and utilising patterns in data (Murphy, 2012). A commonly used formal definition of machine learning: "A computer is said to learn from experience E with respect to some class of tasks T and

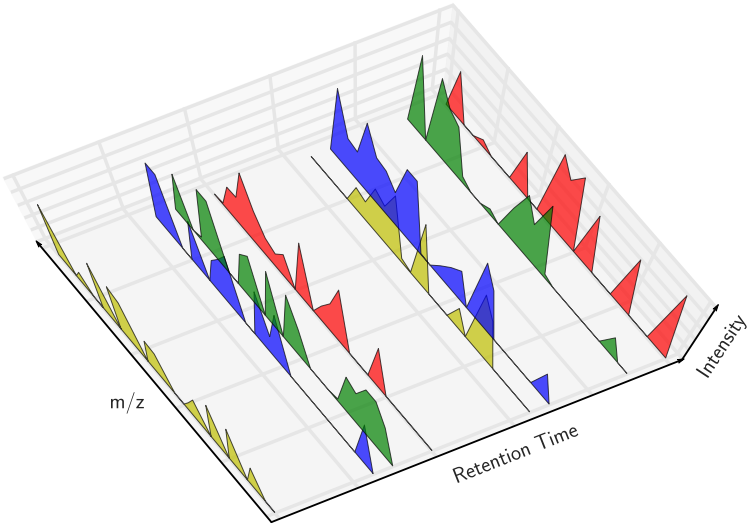

Figure 2.2.4: Visualisation of Mass Spectrometry data when coupled with chromatographic techniques. The X axis represents the m/z ratio of an ion, the Y axis the retention time within the chromatographic separation method (GC, HPLC etc.) and Z the intensity detected at a given m/z

performance measure P, if its performance at tasks T, as measured by P, improves with experience E." (Mitchell, 1997) ML encompasses techniques and methods from various areas including statistics, pattern recognition, optimisation/control engineering, neuroscience and artificial intelligence. Applications range in complexity from simple linear regression to deep convoluted neural networks with millions of free parameters running on dedicated super-computers (Wu et al., 2015) which are capable of beating human-performance on complex image classification tasks (e.g. IMAGENET (Russakovsky et al., 2014; He et al., 2015)).

Typically, we seek to set the parameters ("θ) of a function in such a way that another property is minimised. For example, in linear regression the aim is to find parameters of a straight line $h_{theta}(x) = \theta_0 + \theta_1 * x_1$ which minimise the distance between the line and the data (for example, the sum of squares distance). This distance/error is calculated using something known as the cost function e.g. $J(\theta) = \frac{1}{2}\sum_{i=1}^{m}(h_\theta(x_i) - y_i)^2$ (where m is the number of x, y pairs in the dataset for linear regression). Most algorithms will seek to minimise the value of this cost function $J(\theta)$ with respect to the parameters of the original function $h_{theta}(x)$. Typically, this is achieved using a variety of algorithmic optimisation techniques. The most prevalent of these are gradient descent based methods in which the value of "θis modified in the direction of the gradient of the cost function (determined using the partial derivative of J with respect to "θ: $\frac{\partial J_\theta}{\partial \theta}$).

In an ideal world, the best machine learning model trained using our data will generalise well for novel data generated from the same underlying process which generated the training data. This is known as generalisability and it plays into the concept of 'fit'. A model that minimises its particular cost function on the training dataset has been fit to that dataset, however, it is possible to for the model to fit the training data in such a way that it has low

error on the training data but performs incredibly poorly when applied to new data from the same process. This is typically the case when a model has overfit the data. The classic example of this is fitting a line to a set of points using a high degree polynomial. This polynomial will perfectly pass through all the points but is likely to be a worse predictor for the value of some new data than a much simpler model that while it fits the original training data, may not fit quite as well. Likewise, a model that is misspecified or cannot fit the training data well e.g. the training data follows a non-linear distribution but the model is linear, is known as underfitted. Underfitted models will perform poorly on both the training and test data. However, it isn't particularly useful to only discover how useful your model is likely to be on the test data therefore almost all machine learning analyses will use the principal of cross-validation. Cross-validation is the partitioning of the training dataset to create a validation dataset which can be used as a proxy test set.

Unfortunately, no single model will perform best for all tasks (to paraphrase and simplify Wolpert and McCreedy's "No Free Lunch Theorem" (Wolpert, 1996)), there are no shortcuts in machine learning (and many other areas) or optimisation. Therefore, testing different models (and hyperparameter values) using cross-validation is key to generating a useful model. Another important way to prevent overfitting is to introduce regularisation in the cost function, in other words a term which penalises model complexity.

Machine learning is typically divided into 2 main subsets depending on the nature of the dataset involved: supervised learning (e.g. classification and regression) and unsupervised learning (e.g. clustering, density estimation and dimensionality reduction). There are also approaches that blend features of both supervised and unsupervised learning known as semi-supervised learning as well as an alternative idea known as reinforcement learning built on the premise of the psychology of behaviour and the indirect reward of trial and error approaches (Bishop, 2006).

2.3.1 Supervised Learning

In supervised (also referred to as predictive) learning the principal aim is to learn a mapping between inputs/features x and outputs/response y from a set of inputs and their corresponding expected output. This is known as the training set i.e. $\mathcal{D} = (x_i, y_i) \forall i \in N$ where N is the cardinality (size) of the training set (Murphy, 2012). A supervised learning algorithm thus seeks to approximate $y = f(x)$ where f is an unknown function. This estimated function $\hat{y} = \hat{f}(x)$ (see 2.3.1) would then generally be applied to new data known as the test data for which the expected outputs are not known (i.e. $x_i \notin \mathcal{D}$).

$$\begin{bmatrix} x_{0,0} & \cdots & x_{0,j} \\ \vdots & \ddots & \vdots \\ x_{i,0} & \cdots & x_{i,j} \end{bmatrix} \xrightarrow{\hat{f}} \begin{bmatrix} y_0 \\ \vdots \\ y_i \end{bmatrix}$$

Supervised learning is further subdivided into two approaches depending on the nature of the expected outputs: classification and regression[4].

[4]It is worth noting that the somewhat confusingly named "logistic regression" is typically a form of classification

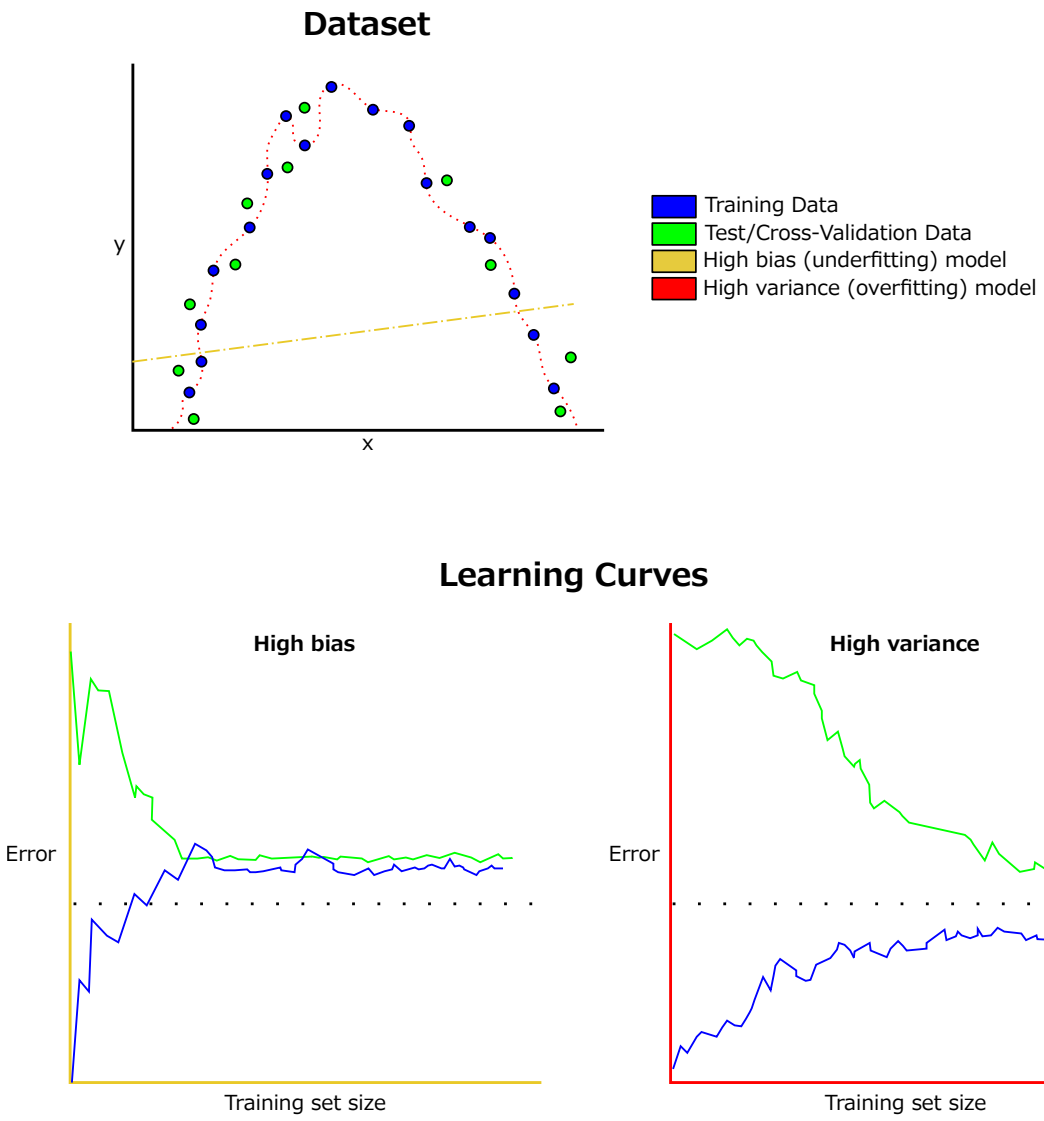

Figure 2.3.1: Plot showing a high bias (underfit) model in yellow and a high variance (overfit) model in yellow. Below are learning curves corresponding to each of these respectively. Learning curves show the effect of different training set sizes on the training and test error of misspecified models. Overfitted models show a large gap between test and training errors, they fit to the training data well but don't generalise to new data (i.e. test data). Underfit models show a very high training error and little difference between test and training data as the model is too simple to fit the training data at all.

In regression the desired outputs are real-valued (or ordinal) i.e. $y_i \in \mathbb{R}$ and we seek to estimate a particular output quantity for a specific input. The simplest example of this would be the 2-dimensional linear regression problem mentioned above in which we are determining the parameters of a line (gradient/weight and intercept/bias) which best fits the training dataset ($\mathcal{D}$) composed of pairs of x and y values. Once this line has been found we can use it to predict the value of $\hat{y}_i$ for data in the test set $x_i \notin \mathcal{D}$.

On the other hand, in classification the expected outputs are categorical or nominal variables such as class labels like "host" and "endosymbiont" ($y_i \in host, endosymbiont, ...C$). These classifications can be binary (two possible outputs i.e. $y = 0, 1$), multiclass ($|y| > 2$), or multilabel (similar to multiclass but outputs aren't mutually exclusive, i.e. an input have multiple labels) (Murphy, 2012).

Supervised learning algorithms can also be either probabilistic or non-probabilistic and generative or discriminative. Probabilistic functions will return a probability distribution associated with possible class labels or regres-

sion values whereas non-probabilistic approaches will only return the most likely class label or value. Continuing Generative algorithms, such as Naive Bayes, seek to model the process by which the output data was generated from the input i.e. learn the joint probability $p(x, y)$ and make predictions on that basis via Baye's Theorem (see 2.3.1)

$$p(x, y) = p(x|y)p(x) = p(y|x)p(y)p(y|x) = \frac{p(x, y)}{p(y)}p(y|x) = \frac{p(x|y)p(y)}{p(x)}$$

Whereas, discriminative classifiers, such as logistic regression/linear classifiers, model the posterior probability $p(y|x)$ directly or just learn mappings in the case of non-probabilistic approaches. In other words, for classification problems a generative model would determine the statistical distribution of individual classes whereas discriminative models would just determine the boundaries between them. Generative models often perform better on small training sets by preventing overfitting with discriminative classifiers performing better as the training set grows (Ng and Jordan, 2002).

Support Vector Machines

Support Vector Machines (SVMs) are a type of sparse kernel maximum-margin supervised classification algorithm. With the innovation of the kernel trick in 1992 (Boser et al., 1992) and soft-margins in 1993 (not published until (Cortes and Vapnik, 1995)) SVMs have been among the most successfully applied classification algorithms (Fernández-Delgado et al., 2014). Only relatively recently have they begun to lose ground to the deep-learning methods such as deep-convolutional neural networks (e.g. LeNet (**?**)) exemplified by the defeat of SVMs by the LeNet on the MNIST digit recognition dataset (Hinton and Salakhutdinov, 2006; Bengio et al., 2007) (Bengio et al., 2013)

The goal of SVMs is to learn a hyperplane which separates two sets of labels in the dataset. Note, for multiclass classification a series of one-vs-all classifiers are typically trained (that is for K classes, K SVMs are trained each classifying between a label k and all other labels). However, not all possible hyperplanes that could separate the labels will necessarily generalise well to novel data (and this generalisation is the ultimate goal of supervised learning). Therefore, it is necessary to determine a way to select the hyperplane which should generalise best and to do this in a manner that will be relatively efficient especially with high dimension datasets. This optimal hyperplane for separable classes can be demonstrated to be the hyperplane which maximise the margin between the two classes (Vapnik and Kotz, 1982) in other words, the optimal boundary is the one that has the largest possible distance from each class (while still separating them). Conceptually, the positioning of this boundary is only dependent on the relatively small subset of the training data $\mathcal{D}$ that is near the boundary and it would be inefficient to consider all points when placing the decision boundary. For this reason, SVMs can define the decision boundary in terms of the namesake support vectors and can reformulate their cost function in a more efficient constrained way.

A naive formulation of this problem is simple specifically we are trying to find a linear model $f(x) = \theta_0 + \theta^T x$ which can be simplified to $f(x) = \theta * x$ if we assume that the first element of x is fixed to 1. We thus want to minimise J in terms of θ to find the largest margin that correctly labels all the training data (in other words is constrained).

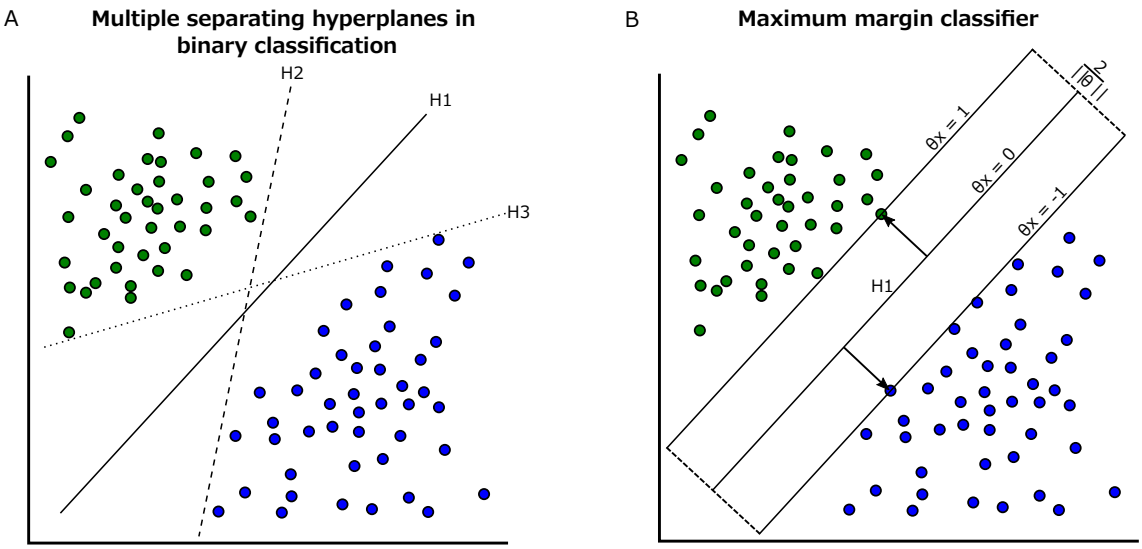

Figure 2.3.2: A: Demonstration of 3 valid decision boundaries in a 2D classification problem, B: The optimal boundary (H2) is that which maximises the separation of different classes. This optimal boundary can be defined in terms of support vectors. The bias/intercept has been folded into θ directly.

Fortunately, due to geometry the margin is property of the norm of θ i.e. $||\theta||$ but we use $\frac{1}{2}||\theta||^2$ for mathematical convenience.

$$argmin_\theta J(\theta) = \frac{1}{2}||\theta||^2 s.t. y_i(\theta x_i) \geq 1 \forall i$$

In reality, this cost function would be converted to a constrained optimisation problem using Lagrange multipliers and reformulated using the Lagrangian dual form.

The 2nd major enhancement of SVMs is that of soft-margins (Cortes and Vapnik, 1995). Soft-margins are a way of allowing a degree of misclassification if doing so would increase the size of the margin that can be generated. Specifically, a user defined penalty constant C is specified and added to the cost function penalising the degree of misclassification ξ, e.g.:

$$argmin_{theta} J(\theta) = \frac{1}{2}||\theta||^2 + C\sum_{i=1}^{n} \xi_i s.t. y_i(\theta x_i) \geq 1 - \xi_i \forall i$$

This can improve robustness to outlier data and generally improve generalisability by keeping the margin as large as possible.

Finally, the 3rd major advantage of SVMs is that despite nominally being linear classifiers they can effectively classify data which is not linearly separable in the input dimensions using the kernel trick. Conceptually, a kernel function is used to transform which transforms data from the input dimensions to a higher dimensional space in which the data is linearly separable. These transformed feature spaces can have incredibly high number of dimensions (in the case of popular kernels like radial basis function, an infinite number of dimensions). Explicitly transforming data in this way would be computationally intensive so instead the "kernel trick" is used, where instead of explicitly transforming all the data into the feature space it is done implicitly by computing the inner product of all pairs data points transformed. This is a lot more efficient and precludes the computationally intensive step

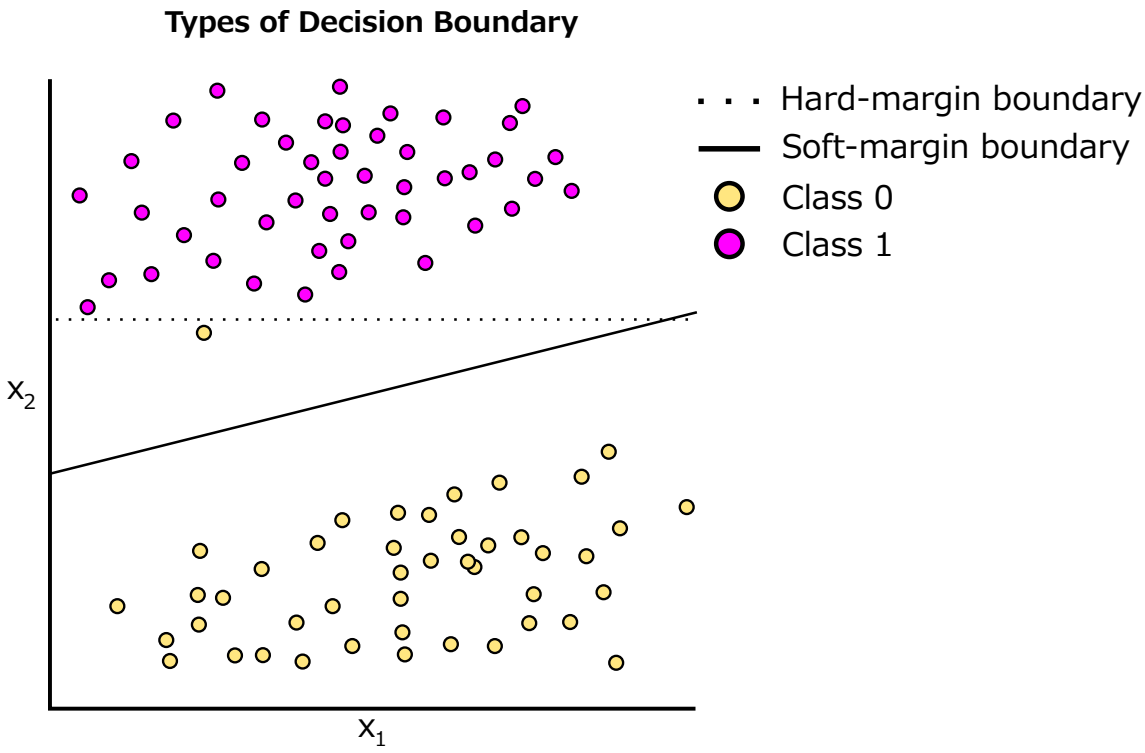

Figure 2.3.3: Demonstration of the utility of a soft-decision boundary to improve the overall fit of a decision boundary by allowing a degree of misclassification during training

of converting the data into the new, potentially infinite, co-ordinate space. Radial basis function (RBF) kernel is an example $K(x_i, x_j) = exp(-\frac{||x_i - x_j||^2}{2\sigma^2})$ kernel. Even with the kernel trick, operations on every pair of points can become infeasible for large datasets due to the combinatorial explosion in necessary operations as the dataset increases in size. However, in the same way that the decision boundary parameters are determined using only a subset of the training data (i.e. the support vectors) the kernel trick only needs evaluated on a subset of points near the decision boundary. This is the reason SVMs are sometimes referred to as sparse kernel methods.

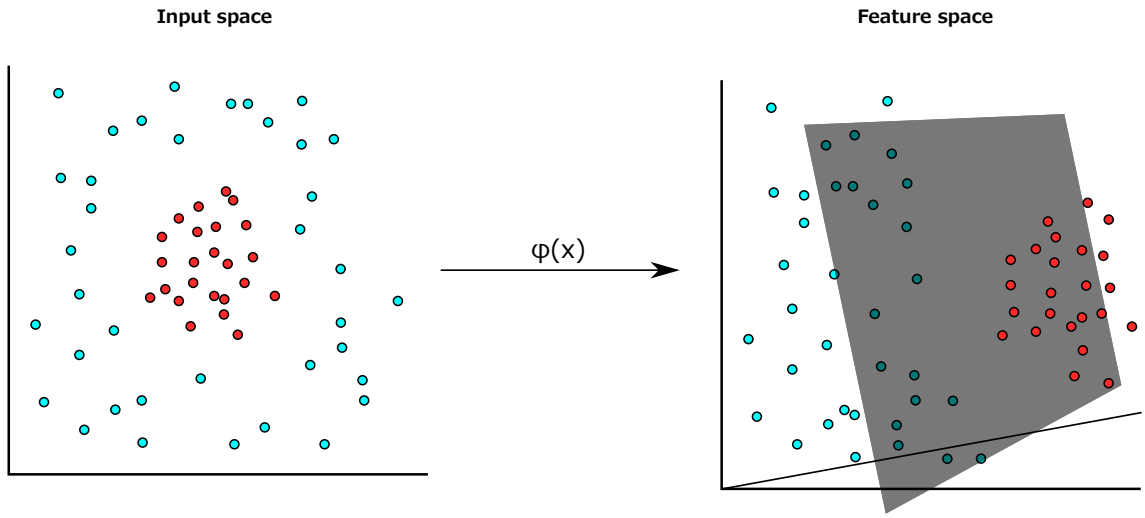

Figure 2.3.4: A kernel transform can allow SVM to produce non-linear classification boundaries by mapping the data to a higher dimensional space in which they are linearly separable. This is known as the kernel trick and the key to its efficiency in SVM is that it is only evaluated for those sets of points near the decision boundary

The advantages of SVM is that they are somewhat resistant to the curse of dimensionality i.e. they are effective with large numbers of features even if the number of features is greater than the size of the training set. By using support vectors, the kernel trick, and Lagrange bound optimisation they are relatively fast and memory efficient to train and as classification only depends on the location of the decision boundary very fast to test. Additionally, in simple form finding the hyperplane of an SVM is a true convex optimisation therefore is guaranteed to always find the global optimum (this guarantee does break with more complex kernels and soft-margins). The major disadvantage is not natively generating probabilistic output (i.e. attaching a probability to a certain classification). However, this can be achieved using methods like Platt Scaling or the related Relevance Vector Machine algorithm. The other disadvantage is that hyper-parameters such as the misclassification penalty for soft-margins (C) and kernel choice (and its parameters) need chosen, typically this is solved by training using a grid-search of permutations of these parameter settings and selecting the best model via cross-validation.

2.3.2 Unsupervised Learning

The other main form of machine learning is that of unsupervised or descriptive learning. In which the training dataset has no provided output labels (y) i.e. $\mathcal{D} = x_i \forall i \in N$ (where again N is the cardinality of this training dataset). In other words, we just have our dataset and have no additional information. This is slightly more difficult problem as it lacks an obvious error metric like supervised learning (i.e. difference between actual output and expected output) but is important and useful tool to try to discover patterns in datasets.

There are two major groups of unsupervised learning algorithms, the first of which is clustering algorithms such as K-means that seeks to partition a dataset into a set of groups (see **??** for more details). The other major group of unsupervised algorithms are those used for visualisation and/or dimensionality reduction. Dimensionality reduction is a way of projecting a multidimensional dataset into a lower number of dimensions in a way that still corresponds to "shape" of the data in the original number of dimensions.

Formally, dimensionality reduction seeks to take a set of data ($\mathcal{D}$) and convert it to a lower dimension form $\mathcal{Y}$ known as a map $\mathcal{Y} = y_i \forall i \in N$ with each individual x_i in $\mathcal{D}$ represented by a corresponding map point y_i. It also seeks to do this in a way that maintains as much of the structure found in the original data as is possible (Maaten and Hinton, 2008) therefore, if two data points are similar in the original dimensions they should still be similar in the map $\mathcal{Y}$ (and the inverse). Some dimensionality reduction approaches are well known in biology, specifically: principal component analysis (PCA) (Hotelling, 1933) and multidimensional scaling (MDS) (Torgerson, 1952) which both aim to identify hidden features within the dataset that can explain a high degree of the variation.

As ever different methodologies have a range of pros and cons, with some better at preserving global structure (e.g. isomap) and others local data structures (e.g. local linear embedding) and so on. One of the most recent innovations in this area is that of t-distributed stochastic neighbour-embedding (t-SNE) in which the similarity of data points in the input space is modelled as pairwise probabilities using Gaussian distributions. These probabilities are then translated into positions in the map $\mathcal{Y}$ and similarities re-calculated using Student's t-distributions. The position and variance of these points and distributions respectively is then optimised by minimising the difference between the similarity probabilities in the input space and on the map (Maaten and Hinton, 2008).

K-means

K-means clustering is a non-probabilistic unsupervised learning method in which we seek to partition data points in multidimensional space into K clusters. It is often used to initialise Gaussian mixture models.

Specifically, given a set of N observations $X = x_1, ..., x_N$ of $\mathcal{D}$ dimensions partition each point (x_n) into K clusters

A cluster can be intuitively considered as a group of observations/points which are "closer" to one another than to other observations and the k-th cluster can defined by a $\mathcal{D}$ dimensional vector μ_k, $where k = 1, .., K$ for all clusters. This vector represents the current "prototype" centroid of cluster.

So, with k-means clustering we actually seek the set of K cluster centroids μ_k which minimise the sum of squares distances of each data point from its closest cluster centroid. (Bishop, 2006)

If we define a 1-of-K coding scheme with $r_{nk} \in 0, 1$ as a binary variable that is 1 when x_n has been assigned to cluster k (with centroid μ_k) and 0 otherwise then we can define an objective cost function (J) that represents the sum of squares distances of each data point x_n from its assigned cluster centroid μ_k.

$$J = \sum_{n=1}^{N} \sum_{k=1}^{K} = r_{nk} \|x_n - \mu_k\|^2$$

Therefore, the goal of k-means clustering is to find values for r_{nk} and μ_k that minimise this linear function 2.3.2. (Bishop, 2006)

The standard algorithm proceeds in two alternating steps following the initialisation of μ_k with starting cluster centroid locations (Forgy, 1965; Lloyd, 1982):

1. $argmin_{r_{nk}} J$ i.e. minimise 2.3.2 w.r.t the assignment of points to clusters while keeping the cluster centroids fixed.

2. $argmin_{\mu_k} J$ i.e. minimise 2.3.2 w.r.t the position of the cluster centroids while keeping the assignment of points to centroids fixed.

Step 1 roughly corresponds to the expectation step in the expectation-maximisation (EM) algorithm and is trivially achieved by assigning each point to the cluster represented by the nearest centroid or formally:

$$r_{nk} = \begin{cases} 1, & \text{if} k = argmin_j \|x_n - \mu_j\|^2 \\ 0, & \text{otherwise} \end{cases}$$

Step 2 roughly corresponds to the maximisation step in EM is can be determined by taking the partial derivative of J w.r.t μ_k setting it to 0 and solving for μ_k:

$$\frac{\partial J}{\partial \mu_k} = 2 \sum_{n=1}^{N} r_{nk}(x_n - \mu_k)0 = 2 \sum_{n=1}^{N} r_{nk}(x_n - \mu_k)\mu_k = \frac{\sum_n r_{nk} x_n}{\sum_n r_{nk}}$$

In other words set μ_k to the mean of all data points x_n assigned to cluster k thus k-means (Bishop, 2006)

These two steps are repeated until a specified maximum number of iterations are reached or no points change cluster assignment during step 1.

J 2.3.2 will converge but is liable to get stuck in a local rather than global minimum.

K-means has many modifications and improvements such as refining the initialisation of the clusters by the Bradley-Fayyad method (clustering random samples of the dataset and then k-means clustering the resulting clusters) (Bradley and Bradley, 1998) or over-clustering (running more than k-means clustering with more than the specified number of clusters and merging clusters at the end to generate the correct number of clusters). One of the most recent and promising improvements is that of "ying-yang" k-means clustering which gains a moderate speed-up over the conventional algorithm by minimising the number of distance calculation required. This is achieved by creating upper and lower bound distance filters using the triangle inequality (i.e. $d(a,b) \leq d(a,c) + d(b,c)$ where d is a function that calculates the distance between 2 points) (Ding et al., 2015).

An efficient implementation of the k-means algorithm is available in the MLPACK C++ Machine Learning library (Curtin et al., 2013). While very efficient and effective, k-means has some limitations, it requires a user specified number of clusters and therefore diagnostics to check for obvious misspecification in the number clusters. Information criterion can be used to determine the optimal number of clusters. Additionally, it is not guaranteed to discover the global optimal clusters (can converge to local optima). This can be amortised by running multiple times with different initialisations.

2.4 Phylogenetics

Phylogenetics is an effective tool (if there is sufficient signal/resolution) to investigate the evolutionary ancestry of biological sequence data. It can be used to identify how closely related a given pair of sequences are, as well as indicate what the sequence most likely looked like in a shared common ancestor (ancestral node reconstruction). Phylogenetic methods also allow estimation of evolutionary processes such as selection pressure, migration, genome reduction, and horizontal gene transfer. In the context of endosymbiosis, phylogenetics can be used to determine evolutionary ancestry of the genes recovered in a transcriptome and to aid identification of the likely origin (host, endosymbiont, contaminant) of these transcripts. Additionally, it can pinpoint potential horizontal gene transfer events between host and endosymbiont by searching for single gene/transcript phylogenies that have an incongruent branching pattern compared to established species trees. Finally, it can be used to aid identification of the putative function of novel transcripts by comparison to other transcripts of known function from databases such as genbank.

Phylogenetics can be defined as a means of arranging a set of character sequences into an optimal hierarchial branching tree structure reflecting some measure of relatedness between the sequences. Usually, these trees will have variable branch lengths that are product of a measure of divergence between the connected nodes.

Typically, these sequences take the form of protein or DNA sequences[5] and the measure of relatedness is some

[5]Strictly phylogenetics refers to the study of molecular sequence data although the same methods are applicable to non-molecular characters such as morphological traits (and occasionally originated in this domain) as well as any other set of discrete data vectors. It has even been applied to fields such as linguistics ()

proxy for evolutionary distance ranging from simple distance measures e.g. Hamming distance ($D = \sum_{k=0}^{N} |x_k - y_k|$ for two sequences x and y of length N) to more complicated probabilistic estimations based on observed data. A character is an element of a sequence such as an individual base or amino acid, homologous characters are those in separate sequences that are descended from a common ancestor. As they were the first molecular sequences easily available much of the early work in molecular phylogenetics was conducted using protein sequences e.g. (**?**Fitch and Magoliash, 1967).

This phylogenetic estimation can be a non-trivial process (especially with more complex measures of relatedness) as the number of possible trees rapidly increases with the number of sequences $N_{trees} = \prod_{x=2}^{N_{taxa}} (2x - 3)$. However, the key stages in a phylogenetic analysis are that of sequence sampling (selection of sequences for inclusion in the analysis), alignment (in which homologous sites in the sampled sequences are aligned with one another), masking (in which sites which are evolutionarily informative – can be determined to be homologous but also non-invariant are selected), model selection (in which the best fitting evolutionary model is selected or calculated) and finally, phylogenetic reconstruction (in which the tree is generated that minimises some measure e.g. most likely tree for probabilistic models or least distance).

One implication of most current phylogenetic methods is that they implicitly assume a branching tree structure is the best representative of the evolutionary process that is being modelled. However, as the discovered prevalence of horizontal gene transfer has increased it is becoming that in some cases a network like structure may in fact be more appropriate.

Most analyses in this PhD are conducted using amino acid sequences. DNA is more likely to display a compositional bias, independence of sites is often severely violated due to the structure of codons (3rd base wobble and so on) (non-synoynmous mutations more likely to become fixed whereas synonymous mutations are prone to drift). Amino acids also have more states so are less susceptible to back mutations than DNA.

2.4.1 Sequence sampling

Sequence sampling, the selection and identification of sequences for initial inclusion in a phylogenetic analysis, is arguably the most important stage in phylogenetic analysis. Any biases introduced here will propagate throughout the rest of the analysis. While some biases can be mitigated to lesser and greater extents by careful application of various methods in the following stages, there is a degree of fundamental truth in the statement "garbage in - garbage out".

The aim of proper taxon sampling is to maximise phylogenetic accuracy and to allow testing of specific hypotheses. Phylogenetic accuracy is usually considered in terms of consistency (as data increases the analysis tends towards the correct tree), efficiency (how quickly does this convergence occur), and robustness (how sensitive is the phylogeny to violation of assumptions in reconstruction) (Nabhan and Sarkar, 2012) Typically, sequence sampling will be conducted from the basis of a single seed sequence which will be used to query existing databases using alignment tools such as BLAST and HMMs (explained in **??**) to attempt to discover potentially homologous sequences from different organisms.

The main issues caused by poor taxonomic sampling in molecular phylogenetics are that of conflicting phylo-

genetic signals, inadequate rate of evolution to resolve relationships of interest, and violations of assumptions e.g. expectation of a uniform distribution of traits (Nabhan and Sarkar, 2012).

Generally, increased taxon sampling has a strong positive effect on phylogenetic accuracy (Zwickl and Hillis, 2002) however, it can also lead to a situation where there are too many sequences to efficiently reconstruct a phylogeny. However, care care must also be taken not to unintentionally bias datasets by removing any sequences that are considered "problematic" especially when conflicting phylogenetic signal or model violations can be biologically informative. Therefore, it is usually necessary to include borderline error-generating sequences within a phylogeny initially and to iteratively remove them and repeat the phylogenetic inference. Unfortunately, the reduction of the input sequences to a representative subset by heuristics and/or naive clustering can generate biases of their own. However, tools exist that utilise taxonomic database information to automatically a subset of specified cardinality of sequences that display the maximium possible taxonomic diversity for that subset size (Zhou et al., 2014).

Another source of bias in sequence sampling is the usually heuristic choice of outgroup taxa. Most contemporary models of phylogenetic inference only infer unrooted trees. Therefore, it is common practice to "root a tree" by selecting a set of sequences from known evolutionarily distance organisms to form an outgroup. If this outgroup is correctly recovered (monophyletically) the root can be placed between it and the other sequences in the phylogeny (Yang and Rannala, 2012). However, choice of outgroup can change implications which may be drawn from a phylogeny regardless of methodology used to infer it (Milinkovitch et al., 1996). and care must be taken to ensure the selected outgroup doesn't actively distort the accuracy of inference of the rest of the phylogeny regardless of the issue of root placement (Milinkovitch and Lyons-Weiler, 1998).

The two principal ways in which putatively homologous sequences are identified in sequence databases are those based upon Basic Local Alignment Search Tool (BLAST) and its variants and Hidden-Markov Model based approaches (HMM). We seek a way of identifying and aligning homologous sequences in a target sequence database with our query sequence.

2.4.2 Multiple Sequence Alignment (MSA)

The goal of MSA is to align sets sequences such that evolutionarily homologous residues occupy the same column. In other words, any given column in the alignment theoretically should contain amino acid or nucleotide residues that derive from the same common ancestor and have evolved in each sequence lineage. It is also possible that insertion or deletion events have taken place and a particular residue is absent in the ancestral node or a sequence lineage.

This is a non-trivial computational problem which has been proven to have an NP-complete [6] computational complexity (Wang and Jiang, 1994). Specifically, the optimal alignment of N sequences has a complexity of $O(L^N)$ for N sequences of length L(Sievers et al., 2011).

Due to this complexity, the majority of MSA algorithms implement heuristic approaches in order to get, if not

[6] A decision problem for which an answer can be verified in polynomial time by a non-deterministic turing machine and to and from which any NP-hard problem can be translated (Karp, 1972).

the optimal solution, but a sufficiently good one in a reasonable amount of time.

Typically, MSA algorithms start by generating the sets of all pairwise alignments using established pairwise alignment algorithms. Pairwise alignment algorithms are almost all based upon a pair of "Ur-algorithms" with different goals: Needleman-Wunsch, a global alignment algorithms (which attempt to maximise alignment quality over entire sequence lengths) (Needleman and Wunsch, 1970) and Smith-Waterman, a local alignment algorithms (which are optimised towards producing high quality alignments in sub-strings) (Smith and Waterman, 1981). While early, MSA algorithms were typically largely derived from Needleman-Wunsch most modern algorithms seek to combine optimisation of local and global alignments. The distances used in these pairwise alignments will typically be "scored" based upon which matches or alignments are more frequent substituions (e.g. Leucine and its isomer Isoleucine or Adenine to its fellow purine base Guanine (transition)) are positively scored and gaps (extension of a gap is typically less penalised than creating a gap) or unlikely changes (e.g. the transversion of Adenine to Cytosine or Glutamine to Cysteine) penalised. This will generally be codified in a substitution matrix e.g. the PAM (Dayhoff et al., 1978), BLOSUM (Henikoff and Henikoff, 1992) amino acid matrices and their numerous subsequent derivations and improvements.

The mostly widely heuristic used to go from these series of pair-wise alignments to a useful MSA is that of progressive-alignment (Feng and Doolittle, 1987) (implemented in tools such as CLUSTAL W (Thompson et al., 1994)) in which the pairwise alignment scores are built into a distance matrix summarising the relative divergence of each pair of sequences. From this matrix a "guide-tree" is generated using simple neighbour-joining methods (in which a tree is built by recursively clustering the least dissimilar sequences (Saitou and Nei, 1987)). Sequences are then progressively aligned using their branching order within this guide-tree (Thompson et al., 1994).. This drastically reduces the $O(L^N)$ complexity to approximately $O(N^2)$ (Sievers et al., 2011). While there have been various improvements and alternative approaches created such as merging both local and global alignment (Notredame et al., 2000), rapid identification of homologous regions using Fast Fourier Transforms (Katoh et al., 2002), iterative refinement of alignments (Edgar, 2004b) and use of Hidden-Markov Models (Eddy, 1995)

There have been compelling arguments as early as 1991 that MSA in isolation from phylogenetic inference is inherently flawed as the consideration of evolutionary processes (only really done during phylogenetic inference) is key in the objective weighting and assessment of potential alignments (Thorne et al., 1991). Therefore, the phylogeny and MSA should be jointly inferred (Thorne et al., 1991; Redelings and Suchard, 2005; Bouchard-Côté and Jordan, 2013) This approach also minimises the risk of conscious or subconscious researcher bias towards alignments and subsequent phylogenies that support their pre-conceived ideas. This approach has been attempted using interesting probabilistic programming approaches i.e. BALI-phy (Suchard and Redelings, 2006), however, it is still far too slow a process to infer phylogenies in this manner on large or even moderate datasets. Therefore, for now, independent MSA estimation is here to stay, at least until computational resources and algorithmic development has continued until these more theoretically satisfying approaches become feasible.

Therefore, throughout this thesis, two progressive/iterative alignment tools will be used: Kalign2 (Lassmann and Sonnhammer, 2005; Lassmann et al., 2009) for high-throughput analyses and iteratively refined MAFFT7 (Katoh et al., 2002, 2005; Katoh and Standley, 2013) for individual accuracy critical phylogenetic analyses. Kalign

is a very high-speed and relatively accurate (Thompson et al., 2011) progessive alignment tool that uses an efficient and fast Wu-Manber approximate string-matching algorithm to calculate sequence distances (Lassmann and Sonnhammer, 2005). MAFFT, with iterative refinement, is a relatively slow but highly accurate MSA alignment method (Thompson et al., 2011) that incorporates all pairwise alignment information when refining instead of using heuristics to approximate pairwise sequence differences like most approaches.

2.4.3 Masking

Unfortunately, MSA is far from perfect, especially with the faster algorithms necessary for larger datasets and higher throughput. Therefore, it is often necessary to trim alignments to manually fix any obviously misaligned residues, and remove any ambiguously aligned or absent sites. This has been demonstrated to improve phylogenetic accuracy (Talavera and Castresana, 2007).

However, manual masking can also be a major source of researcher-bias as well as a painstaking process. For this reason, there are tools that attempt to automate this process. They typically score each column independently with criteria including number of absent character states, how similar/variable the character is and if there are multiple putative alignments - how likely is that column to be found in multiple different MSAs. These criteria can then be used to mask out certain columns based on certain thresholds and trade-offs between the length of the alignment and inclusion of low-scoring columns. TrimAL is an example of a tool that automates the masking process using this sort of methodology (Capella-Gutiérrez et al., 2009).

Similarly to MSA, for high-throughput analyses I will use TrimAL whereas for individual accuracy critical analyses masking will be done manually using the graphical tool Seaview (Gouy et al., 2010).

2.4.4 Substitution model selection

While the simplest means of phylogenetic inference - parsimony i.e. finding the tree that requires the fewest sequence changes does not require any explicit model of sequence evolution, all other means of phylogenetic inference do (Le and Gascuel, 2008).

A substitution model is in its simplest sense the same as the PAM and BLOSUM matrices used in pairwise and MSA. They are a means of scoring and weighting the significance of different character changes, is an A to a G a more evolutionarily rare state change than an A to a T for example.

Substitution models typically assume neutrality, independence and finite sites. With the probability of substitution rates having an independently identical distribution (i.i.d) (Hasegawa et al., 1985) This measure of distance can be naive models where rates of change between character states and the frequency of each state is equal (e.g. $p(x \rightarrow y) \forall x \forall y \in G, C, T, A \text{where} x \neq y$ (Jukes and Cantor, 1969)) to models fully parameterised in terms of character frequency and rates of change by the masked alignment (e.g. the generalised time-reversible (GTR) model (Tavare, 1986)) While models like GTR can feasibly be fully parameterised with DNA sequence data due to DNA's relatively few character states it is usually necessary to use empirically-defined models for amino acid datasets. These are substitution matrices that have been determined using the empirically observed substitution rates for various amino acids changes in many large MSAs (Le and Gascuel, 2008).

Unfortunately, a single substitution model will rarely hold true over an entire alignment with the rate of evolution varying both across and within sites (heterogeneity and heterotachy). The frequency of character states also frequently changes across a phylogeny. It is important to control for these phenomena, because, as mentioned earlier, violation of model assumptions can decrease phylogenetic accuracy.

The most frequent violation that is controlled for is allowing the rate of substitution to vary across sites by using a Γ distribution $Var = \frac{\alpha}{\beta^2}, \mu = \frac{\alpha}{\beta}$ with a given shape α and trivial scale factor β depending on the dataset to scale rates at each site. For datasets that have a high degree of rate heterogeneity a low valued α produces a broad distribution of rates, whereas a high value will generate a narrow distribution for datasets with low rate heterogeneity (Yang, 1993). For reasons of computational efficiency Γ is typically approximated as a discrete distribution of 4 to 8 categories of equal probability (Yang, 1994). A more limited version of this is the invariant sites model in which sites are divided into 2 classes, one considered invariable while the other has normal substitution rates applied[7](Hasegawa et al., 1985).

Unfortunately, these models still assume other model parameters namely the equilibrium frequencies and relative rates are the same across sites (but just scaled). However, some models have been proposed with multiple rate matrices (Lartillot and Philippe, 2004) and state frequency can be defined at each site (**?**) but needs lots of taxa (Lartillot and Philippe, 2004) An alternative to this is the CAT model which a mixture model mixture model with K classes each containing a different state frequency. If $K = N$ then this is the same as Bruno's model however, generally $K < N$. A probabilistic process known as a Dirichlet Process Prior is used to assign columns to various state frequency classes and simultaneously determines the optimal value of K during this process (Lartillot and Philippe, 2004). An alternative to this approach is explicitly partitioning a masked alignment and generating a model and state frequencies for each partition, some consider this equivalent to a CAT model depending akin to preferences for fixed-effects vs random-effects models (Yang and Rannala, 2012). However, personally, automated partitioning using a Dirichlet process has the advantage of not requiring arbitrary user-defined partitions, which could be a source of bias.

Finally, the rate of evolution can vary even with a site itself (a process known as heterotachy) especially when large numbers of divergent taxa are included in a masked alignment. One model modification which attempts to control for this is that of the covarion model. It allows sites to switch between on and off using an infinite mixture model. The proportion of on and off sites is determined at each site (Zhou et al., 2010)

Generally, simpler models such as the "null" parsimony model or basic models that don't account for complex evolutionary phenomena are more susceptible to artefacts such as long-branch attraction (LBA)[8] (Yang, 1996).

However, in the grand tradition of "no-free lunch", there is no universally best model for all datasets. Therefore, it is necessary to test multiple competing models using a provided MSA. Typically, these models are then compared for their fit to the observed data using information criterion (Sullivan and Joyce, 2005) such as Akaike's (AIC) which assess fit while penalising model complexity in a standard regularisation trade-off ($AIC = 2k - 2ln(L)$

[7]This can also be used with Γ and is approximately equivalent to the addition of another discrete Γ category

[8]LBA is a distorting effect in which long branches (rapidly diverging) are incorrectly placed close to one another regardless of actual shared homology. This is due to the increased chance of rapidly diverging sequences to share independently acquired residues (Bergsten, 2005)

where k is the number of parameters and L the model likelihood (Akaike, 1974)). Other criteria include corrected AIC (Sugiura, 1978), Bayesian Information Criteria (Schwarz, 1978) and Decision Theoretic criteria (Minin et al., 2003) based approaches (Sullivan and Joyce, 2005).

Throughout this thesis, I will use 2 tools which incorporate these various criteria to infer the best fitting model depending on the input data. ProtTest3 (Abascal et al., 2005; Darriba et al., 2011) will used for analyses involving protein sequences and jModelTest2 (Posada, 2008; Darriba et al., 2012) for phylogenetic inference of DNA datasets.

2.4.5 Phylogenetic inference

The simplest phylogenetic inferences are that of distance matrix methods. Distance matrix methods (Fitch and Magoliash, 1967) work on the basis of generating a matrix representing the pairwise distances of each sequence using the selected substitution model and inferring a phylogeny from this. The simplest case would be searching tree space for the optimal tree using a standard least-squares criteria between actual and expected branch lengths (i.e. distances) (Fitch and Magoliash, 1967; Cavalli-Sforza and Edwards, 1967).

However, the most common is that of neighbour-joining which begins with the distance matrix and a star topology tree in which all leaf node branches are connected to a single shared central node. Then:

1. Find the closest two branches in the distance matrix
2. Join the closest pair into a single branch with a new internal node connected to central node
3. Generate a new distance matrix reducing the selected pair to the new node (the distance of the selected pair of leafs to the new internal node and the distance between every other leaf and the new internal node)
4. Repeat the process with the new matrix (Nei, 1987)

It works on the assumption that the true tree has the smallest expected length (minimum evolution) and a short tree that has similar topology can be achieved using the fast simple agglomerative algorithm. NJ is one of the best distance methods and is more reliable than maximum-parsimony which can be asymptotically inconsistent While already efficient (possibly efficient as possible) NJ can be made more efficient using effective heuristics to search tree space (Kumar, 1996) As well as improvements where variance is minimised instead of pure distance improving performance in datasets with high substitution rates e.g. BIONJ (Gascuel, 1997)

Distance methods are very fast but can perform very poorly for divergent sequences with large sampling errors as they don't generally account for variance in distance estimates (Yang and Rannala, 2012) (BIONJ partially adds this). They are also particularly sensitive to gaps in the alignment.

Parsimony approaches (Camin and Sokal, 1965) on molecular sequences (Eck and Dayhoff, 1966) seek to infer the maximum parsimony (MP) tree. That is the tree which requires the smallest number of character changes (has the best tree score). Where the tree score is the sum of all character lengths (the minimum number of changes for each site in the alignment). Any site that is invariable is not informative for generation of a parsimony tree. It

has no explicit assumptions relative to other methods however, this means it is difficult to build in prior knowledge of sequence evolution when generating a tree. It also fails when multiple substitutions have occurred at the same site or with parallel changes in two long branches and therefore is especially prone to long-branch attraction (Felsenstein, 1978). Prestige of parsimony methods declined with discoveries that they can produce statistically inconsistent phylogenies (Felsenstein, 2001)

A majority consensus tree will typically be presented with each node annotated with the number of bootstrapped trees that supported its existence.

Maximum likelihood

Maximum likelihood (ML) methods seek to discover the maximum-likelihood estimates (MLEs) of the tree parameters (topology τ, branch length θ_l and usually substitution model parameters θ_μ) for the data i.e. MLE of $L(\tau, \theta_l, \theta_\mu)$.

These MLEs are estimated numerically using standard iterative optimisation algorithms. They were developed relatively early in molecular phylogenetics using relatively simple models (Neyman, 1971) but more efficient implementations e.g. (Felsenstein, 1981) and increased computational power has made them one of the more popular means for phylogenetic inference.

Generally, an ML approach will sequentially perturb a starting tree topology (often BIONJ or simple ML tree itself) using branch swapping operations such as Nearest-Neighbour Interchanges (NNI) or Subtree-Prune-and-Regraph (SPR) where whole subtrees are removed and reattached to a different part of tree. SPR is slower but less prone to get caught in local optima than NNI and thus will lead to higher likelihood phylogenies overall (Criscuolo, 2011) Expectation-maximisation can then be used to find the MLE for branch length and model parameter. For example, PhyML uses an initial BIONJ and standard hill-climbing which perturbs topology and branch lengths simultaneously

The advantage of ML approaches is that they have explicit model assumptions (which can therefore be tested), are relatively robust to model misspecification, are relatively efficient in a phylogenetic sense, and can make use of sophisticated evolutionary models and thus compensate for many pathological data features (heterotachy, state and rate heterogeneity within and across sites). (Yang and Rannala, 2012). Almost all published phylogenies are Bayesian or ML (or ideally both) for this reason. Unfortunately, ML inference is also relatively slow to calculate especially in comparison to distance methods.

In order to get an estimate for the robustness of a particular phylogenetic ML inference, the masked alignment can be repeatedly resampled (boostrap samples) with replacement and phylogenies regenerated. Each node can then be scored based on the proportion of these boostrap samples in which it is recapitulated (Felsenstein, 1985). A similar approach, known as jackknifing, uses random subsets of the alignment instead of samples (Miller, 1974; Lapointe et al., 1994). Finally, approximate likelihood-ratio tests (aLRT) can be used on branches to give support values by comparing the likelihood of existence of a given branch compared to its non-existences (Anisimova and Gascuel, 2006). There is considerable literature evaluating the pros and cons of different support schemes. However, bootstrap supports are the *de facto* method of inferring a variance of phylogenetic error (Stamatakis et al.,

2008) as they are both simple and conservative (but are computationally expensive) (Anisimova and Gascuel, 2006). It should be noted that all of the above methods of determining phylogenetic robustness can be applied to distance and parsimony methods as well.

In this work, for high-throughput analyses FastTree2 was due to its considerable greater speed relative to ML inference tools (?Price et al., 2010). For individual phylogenetic analyses ML trees were inferred using RAxML8 (Stamatakis, 2014) and non-rapid bootstrap supports.

Bayesian

Bayesian inference is, as the name suggests, based on the Baye's theorem. $p(\tau, \theta_l, \theta_\mu)|D) = \frac{p(\tau,\theta_l,\theta_\mu)p(D|\tau,\theta_l,\theta_\mu)}{p(D)}$ with $p(\tau, \theta_l, \theta_\mu)$ being the prior probability for model parameters (topology τ, branch length θ_l, substitution model θ_μ) $p(D|\tau, \theta_l, \theta_\mu)$ being the likelihood of the data given a certain set of parameters with $p(D)$ as the marginal probability.

Due to the computational difficulty directly calculating the marginal likelihood (integrated over all possible parameter values in all dimensions) phylogenetic inference uses a process known as Monte-Carlo Markov-Chains (MCMC) to sequentially randomly sample the posterior probability distribution. Conceptually, these can be considered as random walkers on the probability distribution that are more likely to accept new movements that increase likelihood than decrease.

An advantage of Bayesian inference is that the posterior probability (PP) of a given node means "support" values are built-in to the inference and additional bootstrapping is unnecessary. Unfortunately, posterior probabilities are sensitive to model violations and have been found to not be very conservative estimators (Simmons, 2003) (although again there has been considerable work comparing Bootstraps to PP (Anisimova and Gascuel, 2006)). Additionally, the prior distribution in Bayesian Inference allows information that is already known about the dataset to effectively built-in to the inference potentially improving phylogenetic accuracy.

All in-depth individual phylogenetic analyses presented in this thesis were inferred using both Bayesian (via MrBayes3 (Huelsenbeck and Ronquist, 2001; Ronquist and Huelsenbeck, 2003; Ronquist et al., 2012)) and ML methods. Phylogenies are then presented with both PP and bootstrap support values on each node inferred using both methodologies.

2.5 Informatics languages and hardware

2.5.1 Languages and Libraries

Several programming languages and a range of libraries were used throughout this PhD depending on the suitability of a particular tool for a task. The full details of the specific tools used for the main analyses are outlined during the description of these analyses, however, the tools used for prototyping as well as those used for smaller tasks not covered in detail are omitted elsewhere.

Languages and libraries were chosen depending on their best fit for a particular task. Performance sensitive code such as those dealing with large datasets (e.g. high-throughput sequencing libraries or image data) were prin-

cipally conducted using the C++ language in line with the C++11 standard (ISO International Standard, 2011)

The main C++ libraries used in addition to the C++11 standard library were:

- Seqtk - fastq/a sequence parsing library (Li, 2015)
- MLPACK - a high-performance machine learning library http://www.mlpack.org/ (Curtin et al., 2013)
- OpenCV3 - widely used computer vision library (Bradski, 2000)
- Armadillo - numerical computation library (Sanderson, 2010)

The majority of tasks were accomplished using the high-level python language (python2.7 or python3.4 depending on the application) (). In addition to the standard library, the numerical computation libraries numpy () and theano (), machine learning library scikit-learn (), statistical and scientific libraries scipy () and pandas (), the bioinformatics libraries scikit-bio () and biopython (), and plotting libraries holoviews (), matplotlib () and bokeh () were all used extensively. Frequent use was made of literate programming offered by environments such as the ipython notebook (recently renamed jupyter).

The statistical programming language R (R Core Team, 2015) was used for some data analysis and visualisation primarily using ggplot2 (Wickham, 2009) and dplyr (Wickham and Francois, 2014). This was primarily done using the R-Studio http://www.rstudio.com/ integrated development environment) and R-markdown (Allaire et al., 2014).

All code was version controlled using git http://git-scm.com/ and remotely hosted using github https://github.com/ and bitbucket https://bitbucket.org/ services. Unit tests were automatically run on synchronisation ('push') with these remote servers using the Travis https://travis-ci.org/ Continuous Integration service.

Incidental scripting was done using zsh and bash languages and all code was written using a simple vim terminal.

2.5.2 Hardware

All analyses were conducted on either the lab cluster (running Ubuntu Server LTS 12.04 and 14.04 http://www.ubuntu.com:

- PowerEdgeM910 with 2 x Intel Xeon CPU $E6510@1.73GHz$, $512GB$ RAM
- PowerEdgeM910 with 2 x Intel Xeon CPU $E7-4807@1.87GHz$, $512GB$ RAM
- PowerEdgeM620 with 2 x Intel Xeon CPU $E5-2650v2@2.60GHz$, $512GB$ RAM

Or on two workstations both running continuously updated versions of Arch Linux https://www.archlinux.org/.

- Apple MacPro with 2 x Intel Xeon CPU $E5520@2.27GHz$, $16GB$ RAM
- Dell Precision T7500 with 2 x Intel Xeon $E5620@2.4GHz$, $48GB$ RAM

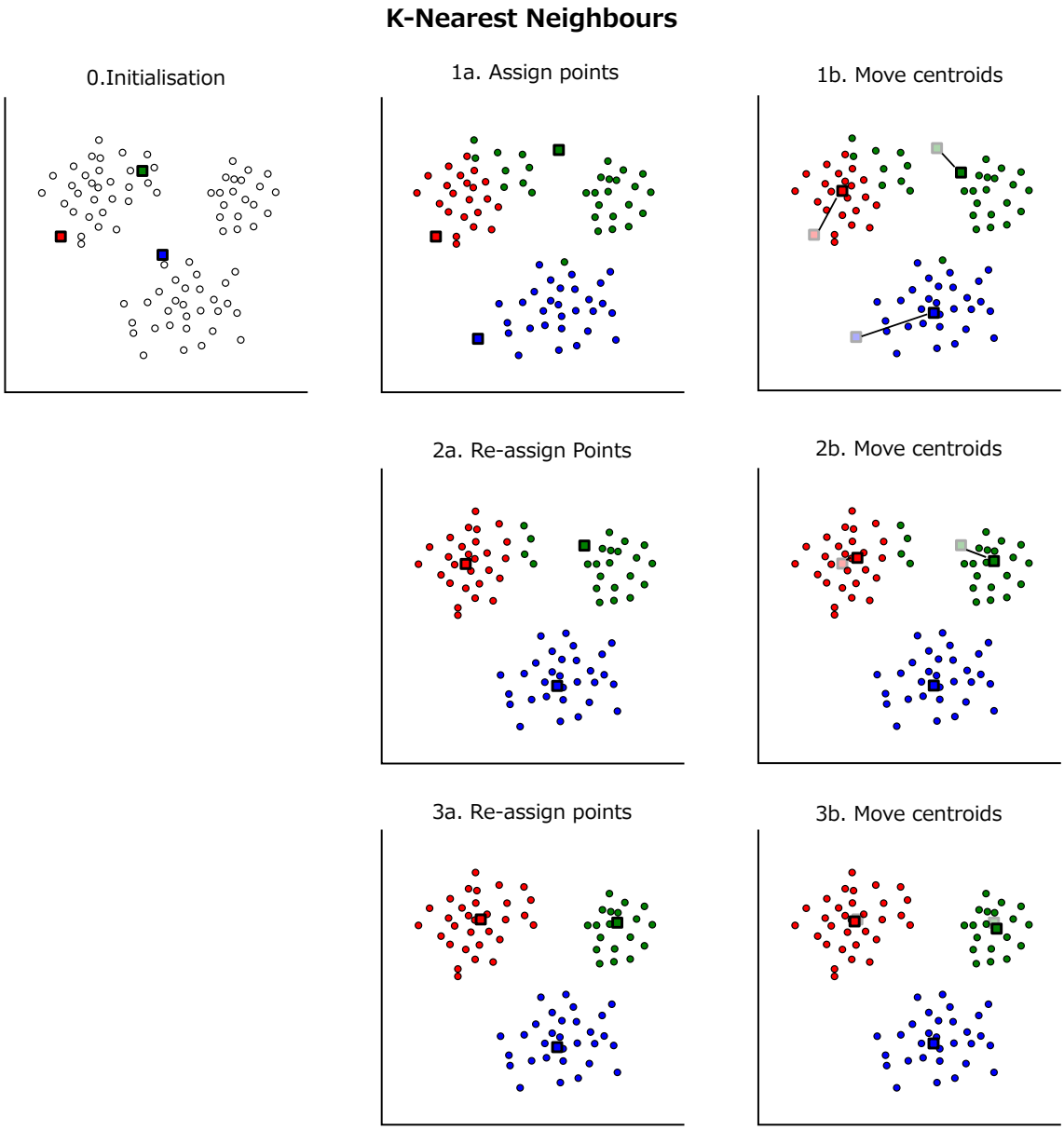

Figure 2.3.5: Demonstration of the K-means algorithm applying 3 rounds of Expectation-Maximisation to cluster a group of 2 dimensional samples. The 3 cluster centroids (represented by coloured rectangles) are randomly initialised in 0 before undergoing 3 rounds of EM. This involves the successive assignment of samples to their nearest centroids (1a, 2a, 3a) and then the movement of the centroids to the center of the points currently assigned to that centroid (1b, 2b, 3b). Assignment of a given sample to a centroid is indicated by a shared colouring and centroid relocation by an arrow with a faded version showing the initial location.

Taxonomy is described sometimes as a science and sometimes as an art,
but really it's a battleground

- Bill Bryson: *A Short History of Nearly Everything*

3

Endosymbiont Diversity

3.1 Introduction

3.1.1 Endosymbiont taxonomy and clonality

Over 50 strains of green algal photobionts have been identified in *Paramecium bursaria* species (Hoshina et al., 2010, 2004; Hoshina and Imamura, 2009; Summerer et al., 2008; Vorobyev et al., 2009). These form at least 4 distinct species groups, supposedly represented in the following cultures:

- *Micractinium reisseri* (e.g. former "European" group endosymbionts such as those attributed to CCAP 1660/12)
- *Chlorella variabilis* (e.g. former "American" group endosymbionts such as *Chlorella variabilis* NC64A)
- *Chlorella vulgaris* (e.g. the endosymbiont attributed to CCAP 1660/10)
- *Coccomyxa* sp. (e.g. the endosymbiont attributed to CCAP 1660/13)

These species display a polyphyletic distribution within the green algae providing evidence for multiple separate origin events for the *P. bursaria* endosymbiosis (Hoshina and Imamura, 2008, 2009) Furthermore, there is emerging evidence, in the form of intron HGTs and ITS2 sequencing data that strains of *P. bursaria* are capabale of hosting double and triple co-habitations of different photobiont species (Hoshina, 2012). Therefore, before an

effective analysis can take place of an endosymbiotic system it is important to carefully define the species (singular or plural) involved.

Unfortunately, the systematics of the Chlorophyta has experienced a relatively high degree of flux, with multiple redefinitions even since the initial use of molecular phylogenetics of ribosomal sequences (Hori et al., 1985; Gunderson et al., 1987) in the 1980s (Leliaert et al., 2012; Hoshina et al., 2010). The algal endosymbionts of *Paramecium bursaria* in particular have gone through a range of names and classifications starting with *Zoochlorella* in 1882 and through various species of the genus *Chlorella* (Hoshina et al., 2010).

Initially, all symbiotic algae were named as single *Chlorella paramecii* species but this name was rejected and *Chlorella variabilis* was defined (Shihira and Krauss, 1965) but this was in turn rejected and fell out of use. Later, the first discovery of the existence of multiple distinct strains of photobiont was published (Douglas, 1986). With this came the understanding that the endosymbionts of *P. bursaria* are likely to be divergent but not distinct species to other described free-living *Chlorella* (Hoshina et al., 2010).

To add further confusion to the system, the most recently accepted terms defined species of endosymbiont merely as "American" and "European". This lead to several misidentifications (e.g. (Kodama et al., 2007)) (Hoshina et al., 2010). Recently, these two organisms have been redescribed as distinct species *Chlorella variabilis* and *Micractinium reisseri* respectively (Hoshina et al., 2010). Therefore, care must be taken when reading older literature to distinguish the earlier less well-defined *C. variabilis* from the modern usage.

One source of complication in the systematics of the photobionts have been plagued with cases of mislabelling and loss of cultures by various culture collections and in papers. For example, the initial culture which the original *Chlorella variabilis* was described from was lost and a supposedly identical culture from a different collection was found to have wildly different biochemical properties (Hoshina et al., 2010). These complications and confusions add to the importance of accurate endosymbiont species identification.

The most widely accepted means of rapidly taxonomically profiling archaeplastida (and indeed a range of eukaryote species) is that of nuclear ribosomal internal transcribed spacer 2 (ITS2) (see fig. 3.1.1) barcoding. ITS2 has shown particular utility in the identification and separation of closely related green algal species (Buchheim et al., 2011; Heeg and Wolf, 2015) due to being universal, reliably amplifiable and highly variable (Hershkovitz and Lewis, 1996).

ITS2 barcoding has been recommended as a superior marker to other universal archaeplastida DNA barcodes such as the *rbcL* (Chen et al., 2010). The conserved nature of the flanking 5.8S and 18S sequences allows near universal primers to be designed which efficiently amplify ITS2 sequences unlike the broadly distributed but highly variable *rbcL* (Buchheim et al., 2011).

Not only will ITS2 sequencing identify the endosymbiont species in both CCAP 1660/12 and CCAP 1660/13 cultures, it will offer an tool in which to investigate the presence of clonality within the photobiont populations. By amplifying and sequencing a large number of ITS2 fragments from the same culture there is a reasonably good probability that all the ITS2 level diversity will be sampled. If on analysis these sequences form multiple clades or display divergent groupings this could be strong evidence for a multiple photobiont co-habitation within the *P.*

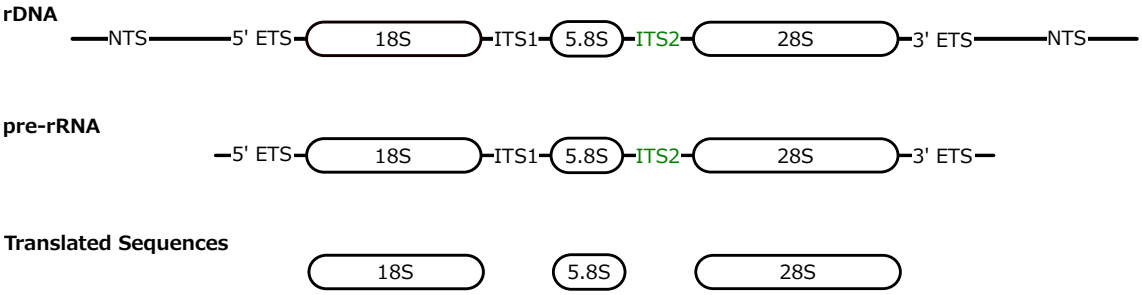

Figure 3.1.1: Structure of Eukaryotic nuclear ribosomal DNA. rRNA genes exist in tandem repeats separated by nontranscribed spacers (NTS). ITS2, which forms an effective taxonomic barcode at sequence level for eukaryotic species analyses. Similarly, the secondary structure shows a greater level of conservation and can be used to investigate lower distance systematic relationships. The location of ITS2 is highlighted in green. Figure was redrawn from (Shi, 2005)

bursaria host.

Finally, one last means in which we saught gain additional insight into the host-endosymbiont system was through the use of multiple-displacement amplification (MDA) based sequencing (Lasken, 2007). Due to difficulties in obtaining sufficient culture densities and the prevalence of putative sources of contamination within the culture bulk genome sequencing was considered to be prone to major difficulties. Therefore, MDA offered a way in which we could further investigate this question of photobiont clonality while also generating a resources with potential use for further analysis. The utility of this genomic resources hinges on our ability to partition recovered genomes/contigs into the originating host and endosymbiont genomes. It is particularly important to do this and effectively discard contaminant contigs derived from bacteria (food and symbionts) and viruses associated with the host.

3.1.2 Isolation of hosts

One avenue that is important for an effective analysis of a host-endosymbiont system is the ability to analyse the partners in isolation. This can be used to test individual hypotheses regarding each partner and allowing controlled reintroduction experiments. Unfortunately, the majority of extant well-characterised endosymbioses display metabolic co-depdendence and therefore, host and endosymbiont cannot be isolated without one or other dying (i.e. they form an obligate relationship as supposed to a facultative one).

Fortunately, there have been numerous studies that have investigated the separation of host and symbiont in *P. bursaria* - green algal systems e.g. (Hosoya et al., 1995; Achilles-Day and Day, 2013b; Karakashian, 1963). Most recently, the only transcriptomic analysis of this system by (Kodama and Fujishima, 2014). investigated the differential global metatranscriptome profile of *P. bursaria* Yad1g strain with and without its *Chlorella variabilis* 1N endosymbiont (Kodama and Fujishima, 2014). While, this is a different strain of both host and endosymbiont to the CCAP1660/12 strains (*P. bursaria* and *Micractinium reisseri*) reproduction of this endosymbiont clearing offers a potential avenue by which to further investigate and, combined with RNAi to test the functional underpinning of this relationship.

There have been several published methods for clearing endosymbionts from host cells namely, the herbicide paraquat (Hosoya et al., 1995), culturing under constant dark (Karakashian, 1963), herbicide DCMU (**?**), X-ray

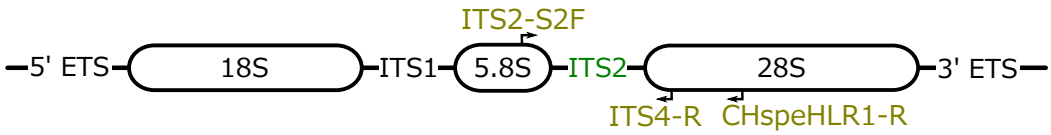

Figure 3.3.1: Schematic diagram showing the location of the forward (ITS2-S2F) and reverse primers (CHspeHLR1R, ITS4-R) used for the amplification of ITS2 sequences in this study. CHspeHLR1R binds within the 28S whereas ITS4-R binds closer to the 5' end of the 28S. Both primer sets recover the full ITS2 sequence.

(Wichterman, 1948), and cyclohexamide (Weis, 1984; Kodama et al., 2007). Therefore, we attempted 3 of these methods: specifically Paraquat, Cyclohexamide, and constant darkness treatments with bacterial feeding in order to clear endosymbionts from the host *Paramecium*.

3.2 Aim

In this chapter I will determine the exact algal endosymbiont strains present in the principal *Paramecium bursaria* cultures used throughout this thesis and their relationships relative to one another and to other green algae.

I will also use this data and single cell genomics to investigate whether the algal endosymbiont present in the *Paramecium bursaria-Micractinium reisseri* CCAP 1660/12 strains form a clonal population.

Finally, I will discuss the attempts to remove the endosymbiont in the *Paramecium bursaria* CCAP 1660/12 strain from the host.

3.3 Methods

3.3.1 Taxonomic Investigation

ITS2 Sequencing

Paramecium bursaria CCAP 1660/12 and *Paramecium bursaria* CCAP 1660/13 cultures were maintained in New Cereal Life (NCL) media at 18°C with 12:12 hour light/dark cycle. In order to mitigate the risk of sequencing free-living algae in the CCAP 1660/13 culture, ITS2 sequences were acquired from both pure culture samples and carefully purified samples. Purification involved successive filtering and washing steps of isolated cells in sterile NCL media. Specifically, filtration using a 10μm filter, washing off, resuspension and 3 serial subcultures in sterile NCL media.

ITS2 sequences were amplified using 2 pairs of primers: ITS2-S2F primer (*ATGCGATACTTGGTGTGAAT*) binding to conserved 5.8S sequences from (Chen et al., 2010) with the CHspeHLR1R (*CACTAGACTACAATTCGCCAGCC*) reverse primer specific to chlorophyte 28S (**?**) and the ITS4 primer (*TCCTCCGCTTATTGATATGC*) (White et al., 1990) (see fig. 3.3.1). The reason for the dual primer approach was that it was observed in the smaller biological samples created during the cleaning process that the ITS2-S2F - CHspeHLR1R primer pair wasn't amplifying ITS2 very efficiently therefore the alternate primer pair was used.

PCR conditions used were 94°C for 5 minutes followed by 40 cycles of 30 seconds at 94°C, 30 seconds at

56°C, and 45 seconds at 72°C. This was followed by a final elongation step of 10 minutes at 72°C.

PCR products were then cleaned up, cloned, sequenced and processed using the same protocol as (Maguire et al., 2014). Briefly, the successfully amplified PCR products were gel-purified (Wizard SV Gel and PCR Clean-Up kit, Promega). These products were then TA-cloned using Agilent's PCR StrataClone Cl e-white screened and 5 clones selected for each PCR product. Clones were then externally Sanger sequenced using the M13Rev primer at MWG Eurofins. Flanking vector and primer sequences were removed: sequenced trimmed to areas of high chromatograph quality and ambiguously defined bases corrected using Sequencher (Corporation, 2015).

From the 3 *Paramecium bursaria* CCAP 1660/12 biological replicates 14, 9, and 11 ITS2 sequences were obtained respectively. Similarly, from the 2 *Paramecium bursaria* CCAP 1660/13 biological replicates 8 were obtained from sequences obtained from the culture directly, and 10 from the purified, washed samples (7 using ITS2-S2F-ITS4 primers and 3 using ITS2-CHspe).

In order to mitigate the risk of sequencing error masquerading as true sequence divergene any sequences found in later phylogenetic analysis to demonstrate single nucleotide changes from the consensus of its clade placement was resequenced at MWG Eurofins in reverse using M13Uni. Specifically, these were ITS-B18, ITS-2, ITS-19, ITS-B6, ITS-B3, ITS-A7, ITS-6, ITS-B15, ITS-10, ITS-9, ITS-15, and ITS-1.

Phylogenetics

ITS2 sequences used in (Hoshina et al., 2010), (Hoshina and Fujiwara, 2013) were retrieved from genbank. The trimmed sequences and the established database sequences were then aligned using MUSCLE (Edgar, 2004a). This alignment was manually masked in the graphical SeaView (Gouy et al., 2010) package. jModelTest2 (Guindon and Gascuel, 2003; Darriba et al., 2012) was then used to pick an appropriate substitution model. Finally, phylogenies were inferred using the maximum likelihood method via RAxML version 8 (Stamatakis, 2014) with 1,000 bootstrap replicates. Similarly, MrBayes (Huelsenbeck and Ronquist, 2001) was used to infer the phylogeny using the bayesian formulation. MrBayes used 2 indepdendent runs of 4 Monte-Carlo Markov-Chains (MCMC) for 3,750,000 million generations (at which point the 2 runs were considered to have converged, as determined in Tracer v1.4 (Rambaut and Drummond, 2007). Trees were estimated from the MCMC results with a burn-in of 250,000 generations. Trees were then visualised and support values combined using TreeGraph2 (Stöver and Müller, 2010).

3.3.2 Single Cell Genomics

DNA Extraction

Individual *P. bursaria* CCAP 1660/12 cells were removed from culture and washed three times in a successive series of 10μl drops of sterile modified New Cereal Leaf-Prescott (NCL) medium to minimise prokaryotic contamination from bacterial foodstocks in the culture media. Cells were added to a final 10μl drop of sterile water before being added to a microcentrifuge tube.

DNA was then extracted using a Cetrimonium bromide based method adapted from (Winnepenninckx et al.,

1993). In brief, 748.5μl of CTAB extraction buffer (at 37°C and 100μl beads (Sigma, 425600μm; acid washed) were added and the tube was vortexed for 5 minutes. The tube was incubated for 50 minutes at 37°C, vortexed again for 5 minutes and incubated for 50 minutes at 60°C. DNA was extracted three times with phenol/chloroform/isoamylacohol (25:24:1, pH 8), washed with 70% ethanol and re-suspended in 2.5μl TE (pH 8). Whole-genome amplification of purified genomic DNA was performed using the multiple-displacement amplification based (MDA) Qiagen REPLI-g Single Cell Kit. The REPLI-g amplified gDNA was purified using a QIAamp DNA mini kit and eluted in 100μl elution buffer.

Illumina Sequencing

5 prepared libraries were put forward for sequencing (Pb-3, Pb-4, Pb-6, Pb-7 and Pb-8). Samples were multiplexed and were rapid sequenced in an Illumina HiSeq 2500 in 150bp paired-end mode.

Read pre-processing

Trimmomatic (Bolger et al., 2014) was used to trim sequencing adapters (using sequences provided by Exeter Sequencing Service) via the ILLUMINACLIP setting. Reads were then quality trimmed at a minimum average SLIDINGWINDOW quality thresholds of Q5 and Q30.

Q5 and Q30 trimmed reads were then error corrected using BayesHammer (Nikolenko et al., 2013) as built into the SPAdes assembler (Bankevich et al., 2012).

Trimmed and error corrected libraries were also then digitally normalised (Brown et al., 2012) to a coverage of 20 and with a K-mer size of 25. K-mers were then abundancy filtered (Zhang et al., 2014, 2015) using the Khmer package (Crusoe et al., 2015).

Assembly

Assemblies were then generated using the following sets of data:

- Q5 trimmed reads with error correction
- Q30 trimmed reads with error correction

The following assemblers were used:

- SPAdes assembler (Bankevich et al., 2012; Nurk et al., 2013)
- SPades assembler with "careful" thresholding (runs MismatchCorrector and minimises the risk of indels)
- MEGAHIT (Li et al., 2015)
- Platanus (Kajitani et al., 2014)

Assembly assessment

Assemblies were assessed and compared using the QUality ASsessment Tool for genome assembly (QUAST) (Gurevich et al., 2013) and key assembly metrics were compared (N50, N90, contig number and length and total assembly size).

Assembly binning

Contigs were subsequently cut into 10kb fragments for consistency in binning and taxonomic assignment. Reads were mapped back onto the final assembly using Bowtie2 (Langmead and Salzberg, 2012)

Using the metagenomic binning tool, CONCOCT (Alneberg et al., 2014) contigs were binned into clusters based on sequence composition and coverage features (derived from mapping data). Coverage features were derived from a coverage and linkage table generated via CONCOCT scripts built around BEDTools (Quinlan and Hall, 2010; Quinlan, 2014), Picard `http://broadinstitute.github.io/picard/` and Samtools (Li et al., 2009) based parsing of the bowtie2 alignment files. Clustering was conducted using a Gaussian Mixture Model (GMM) (Bishop, 2006) and the number of clusters determined through variational Bayesian inference (Corduneanu and Bishop, 2001).

All CONCOCT analyses were completed using a provided pre-configured Docker Image (Merkel, 2014), a form of lightweight distributable process isolation container. This was downloaded from DockerHub `https://hub.docker.com/r/binpro/concoct/` on 2015-10-25.

Additionally, the cut contigs were taxonomically assigned using TAXAssign `https://github.com/umerijaz/TAXAassign` against the NCBI nt database. The BLAST database was downloaded using update_blastdb.pl script `http://www.ncbi.nlm.nih.gov/blast/docs/update_blastdb.pl` and TAXAssign was run in parallel (using GNU parallel (Tange, 2011)) with a maximum of 10 reference matches per contig a minimum percentage identity for assignment to a given taxonomic level of 60, 70, 80, 95, 95, and 97 for Phylum, Class, Order, Family, Genus and Species respectively.

CONCOCT clusters were then evaluated using the taxonomic assignments from TAXAssign using the provided "validate.pl" script.

Finally, another attempt at taxonomic assignment was attempted:

- ORFs with a minimum size of 300 were called using Tetrahymena and Universal encodings from contigs over 500bp
- ORFs were then clustered at 90% identity using CD-HIT
- Diamond BLASTP searches were then done against the NR protein database
- Taxonomy was assigned to each contig based on the lowest common ancestor of all its ORFs with hits (via the "lca_mapper.sh" accesory script in MEGAN)
- Contigs were then binned based on the identity of this taxonomic assignment:

- Endosymbiont contigs were all those assigned to Archaeplastida or descendent node.
- Host contigs were all those assigned to Aveolata or a descendent node.
- Eukaryote was a super group containing all Eukaryote assigned contigs
- Contaminant contigs were all those assigned as Bacterial
- Viral contigs were all those assigned as Viral sequences.

3.3.3 Endosymbiont elimination

CCAP 1660/12 and YADGN1 cultures in NCL media with were treated under the following conditions to attempt to remove the endosymbiont. *P. tetaurelia* were used as a control culture and was given the same treatment.

Paraquat was added at both $1mg\mu l^{-1}$ and $0.5mg\mu l^{-1}$ concentrations. Cultures were maintained under normal 12:12 lit:dark conditions at 15°C. Cultures were inspected daily using light microscopy and assessed for "bleaching".

Cyclohexamide was added to cultures at both $1mg\mu l^{-1}$ and $10mg\mu l^{-1}$, again cultures were maintained under standard 12:12 lit:dark condition and 15°C. Cultures when looking clear were subcultured and resuspended in NCL without cyclohexamide.

Cultures were maintained in the dark without a lit phase at 15°C and inspected every 2 weeks for clearing. This was to prevent providing too much light and further encouraging endosymbiont growth.

3.4 Results

3.4.1 ITS2 Phylogeny

The ITS2 phylogeny demonstrates a clear and well supported relationship in all samples between the CCAP 1660/12 and CCAP 1660/13 endosymbionts and the species described as *M. reisseri* (see fig. 3.4.1).

There are a variety of SNPs but never more than a single SNP difference from the basal *M. reisseri* polytomy. These SNPs were grouped into 3 categories: 4 different SNPs that were not found in the reverse complement and therefore represent likely sequencing error (1660-13-purified-K4, K8, K6 and K7), 3 different SNPs that were found in both forward and reverse sequencing (1660-12-B6, 1660-12-19 and 1660-12-18) and therefore represent either true diversity or PCR error and finally 1 SNP that was found in forward and reverse sequencing and in two separate PCR reactions from different biological replicates (1660-12-A7 and 1660-12-6). This featured a single base change from A to G (see fig. 3.4.2) at position 126 in the full masked alignment.

With the exception of these SNPs these sequences were identical to 3 from previously sequenced *M. reisseri* endosymbionts, specifically CCAP 211/83 culture with *P. bursaria* Pbi host (AB206547.1), the SW1-ZK symbiont from a *P. bursaria* PB-SW1 host (AB506070.1), and TP-2008b from the SAG241.80 culture (FM205851.1) (see fig. 3.4.1).

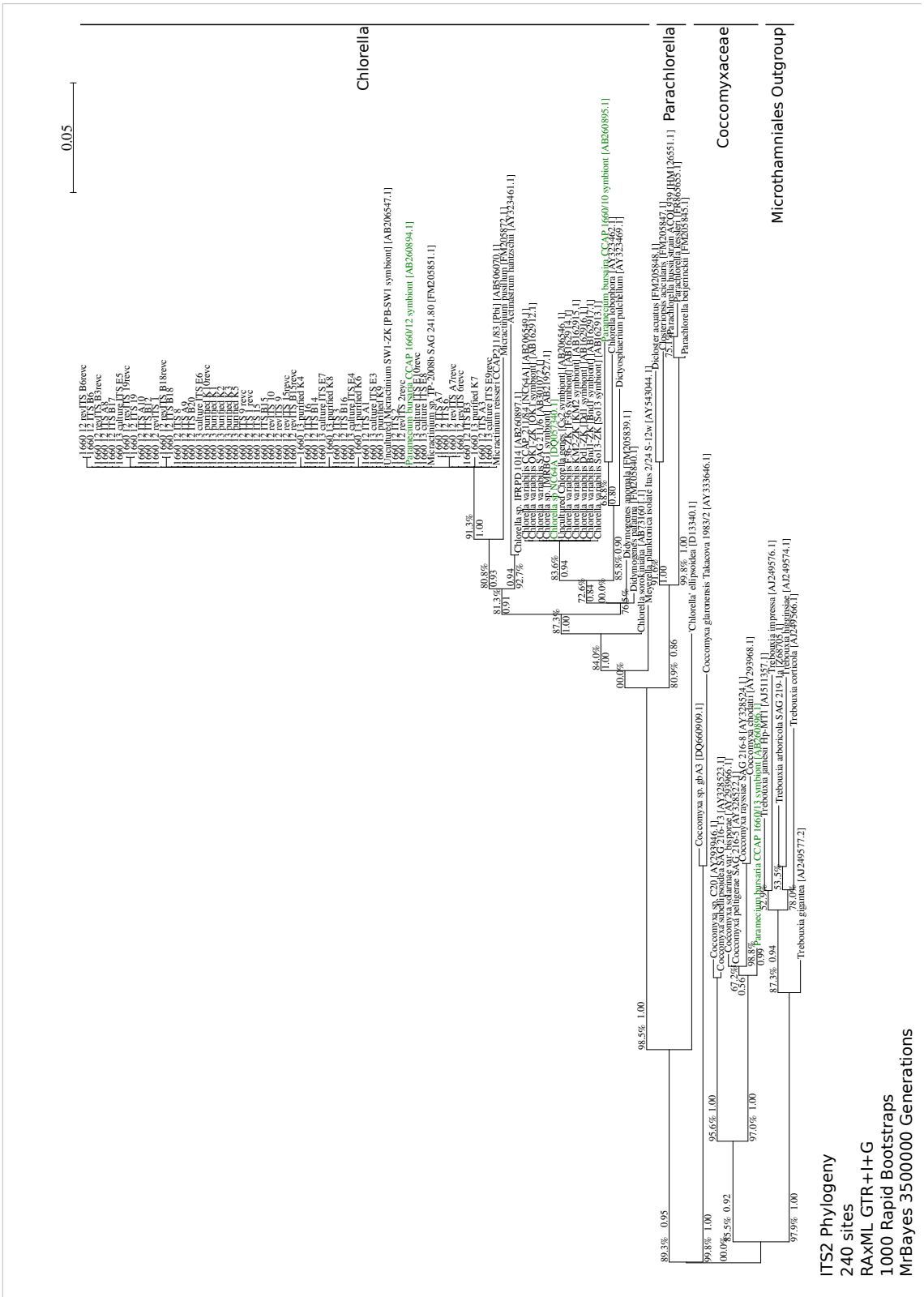

Figure 3.4.1: Combined MrBayes and RAxML phylogeny of all ITS2 sequences along with numerous reference ITS2 sequences from (Hoshina et al., 2010; Hoshina and Fujiwara, 2013). This phylogeny highlights a single example of each of the 4 major groups of *P. bursaria* green algal endosymbionts i.e. *Coccomyxa*, *Micractinium reisseri*, *Chlorella vulgaris* and *Chlorella variabilis*. As can be observed all ITS2 sequences derived from CCAP 1660/12 replicates, and purified and non-purified CCAP 1660/13 replicates form a single polytomy with established *M. reisseri* sequences. This indicates that CCAP 1660/12 and CCAP 1660/13 endosymbionts are *M. reisseri* and despite a few SNPs form clonal populations.

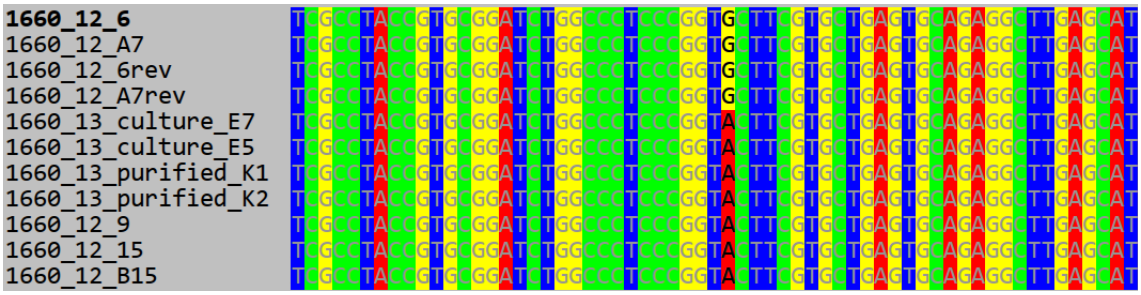

Figure 3.4.2: Alignment showing the sole SNP (at pos 126 in masked ITS2 alignment) that is likely to represent true diversity. This indicates that the endosymbiont population is largely clonal with a small marginally divergent sub-population that has possibly arisen during the endosymbiosis itself.

Sample	Raw PE Reads	Q30 Trimmed PE Reads	Q5 Trimmed PE Reads
Pb-3	$3.523 \cdot 10^7$	$1.951 \cdot 10^7$	$2.737 \cdot 10^7$
Pb-4	$3.228 \cdot 10^7$	$2.606 \cdot 10^7$	$3.035 \cdot 10^7$
Pb-6	$3.291 \cdot 10^7$	$2.437 \cdot 10^7$	$2.962 \cdot 10^7$
Pb-7	$4.023 \cdot 10^7$	$2.642 \cdot 10^7$	$3.404 \cdot 10^7$
Pb-8	$3.869 \cdot 10^7$	$2.613 \cdot 10^7$	$3.246 \cdot 10^7$

This polytomy as the sister clade to other *Micractinium pusillum* taxa was highly supported in both ML and Bayesian phylogenies (91.3% of bootstraps and with a posterior probability of 1.00). There was similarly high support for the separate branching of these sequences from the clade containing the *C. variabilis* and *C. vulgaris* endosymbionts (87.3%/1.00) and the existence of a clade comprising these 3 endosymbionts to the exclusion of any *Coccomyxa* sequences was well supported (89.3%/0.95.

3.4.2 Single Cell Genomes

Sequencing and Pre-processing

The number of remaining reads in each library after trimming at a minimum average sliding window quality threshold of 30 and 5 can be found in section 3.4.2.

After error correction the combined Q30 trimmed libraries comprised $1.218 \cdot 10^8$ paired end reads. Similarly, the Q5 trimmed libraries comprised $1.538 \cdot 10^8$ reads.

Assembly

Assemblies were compared using generated contigs and QUAST. Assembly statistics were tabulated to allow comparison (table 3.4.1). As we are interested in recapitulating as much genomic sequence as possible from this complex metagenome but not necessarily to generate "clean" polished closed genome assemblies, the fact that the Q30-SPAdes assembly generated both the longest total assembly (over twice the size of the nearest assembly even when considering only contigs over 1kbp) as well as the highest N50 and within 2kbp of the longest contig of all assemblies (generated by Q5-SPAdes) was compelling.

Generally, the SPAdes assemblers out-performed Platanus and MegaHit, likely due to being specifically designed for MDA based data. Note, that all assemblies were completed with BayesHammer corrected reads so the

Assembly	Q30-MegaHit	Q30-Platanus	Q30-SPAdes-Careful	Q30-SPAdes	Q5-SPAdes
# contigs ($\geq$ 0 bp)	131057	**25789**	73698	127976	94384
# contigs ($\geq$ 1000 bp)	14960	**486**	13301	21808	12614
Total length ($\geq$ 0 bp)	73350696	6289036	73691706	**142281712**	81478234
Total length ($\geq$ 1000 bp)	28064499	2191750	52704642	**105269748**	58162565
# contigs	41221	**776**	24923	42180	24109
Largest contig	13847	78624	207156	207157	**209873**
Total length	46095605	2398106	60731204	**119241116**	66064486
GC (%)	38.81	33.68	37.78	37.85	39.27
N50	1246	6386	4949	**7163**	6334
N75	769	**2875**	1845	2277	2188
L50	10444	**112**	2937	3530	2241
L75	22405	**249**	7974	11103	6716

Table 3.4.1: Assembly statistics generated by an analysis of contigs using QUAST. Best values are highlighted in bold. All statistics are based on contigs of size $\geq$ 500 bp, unless otherwise noted (e.g., "# contigs ($\geq$ 0 bp)" and "Total length ($\geq$ 0 bp)" include all contigs). N50 and N75 are the minimum contig length at which all contigs of that length are larger comprise 50% and 75% of the total assembly size. Similarly, L50 and L75 are the number of contigs that are summed for a given N50 and N75 (i.e. lower is better). This table shows that Q30 Platanus assembly generated the fewest and longest contigs overall, however the Q30-SPAdes assembly generated the longest assembly by a considerable margin with the highest N50. The Q5 SPAdes assembly generated the longest single contig.

difference in perfomance cannot be attributed to this aspect of the assembly pipeline.

Plots of assembly GC (fig. 3.4.3), cumulative length (fig. 3.4.4) further support Q30-SPAdes as both the longest assembly but an assembly with similar GC profile to the other assemblies and contig length distribution. Finally, the plot of Xs indicates that Q30-SPAdes isn't merely a highly gapped assembly (fig. 3.4.5).

Therefore, Q30-SPAdes assembly was selected for further analysis and size filtered to exclude all contigs shorter than 500bp to give 21,090 contigs.

Binning

From the selected Q30-SPAdes assembly, the 21,090 contigs were cut to 10kb fragments for decomposition to generate 64,852 contigs. 18,277 of these 64,852 contigs were successfully given a phylum level assignment, table 3.4.2.

Contigs were clustered into 34 unique clusters by Concoct. These taxonomic assignments were then used to validate the 34 contig cluters generated in Concoct (visualised in fig. 3.4.6) by considering them as the "ground-truth".

Recall that Precision and Recall can be defined as follows: $Precision = \frac{TP}{TP+FP} Recall = \frac{TP}{TP+FN}$ where TP are True Positives and FP and FN are False Positives and Negatives respectively (see table 3.4.3 for an explanation of what these terms mean in the context of clustering).

CONCOCT assigned clusters were relatively precise 0.912608 therefore there were relatively few FP i.e. the majority of clusters contained contigs with the same taxonomic assignments.

However, recall was relatively poor 0.542250 suggesting a fair number of FN i.e. contigs with the same taxo-

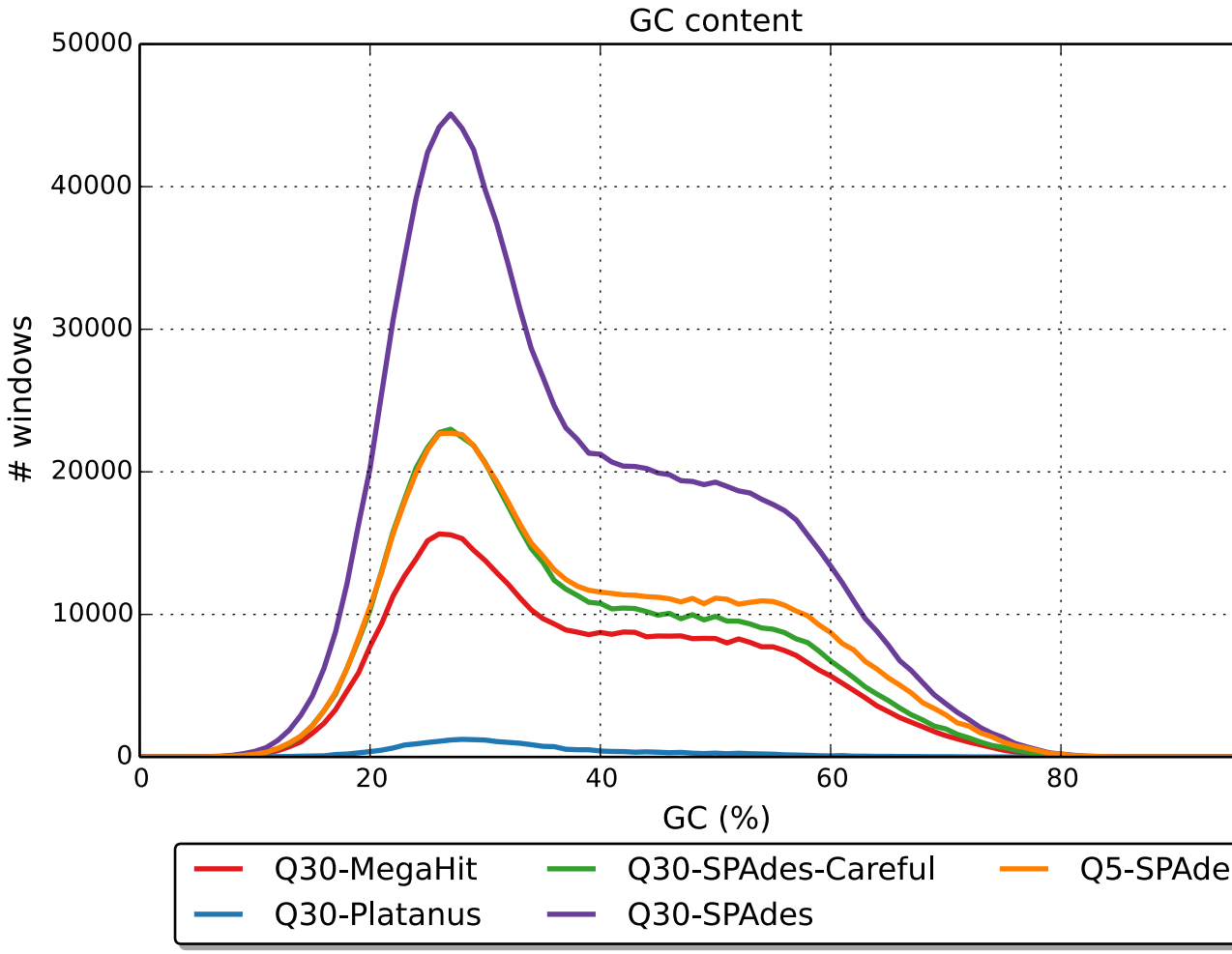

Figure 3.4.3: GC densities of the compared genome assemblies. As expected all display a clear peak around 30% representing that the majority of the assemblies by length contigs are likely to be derived from the GC rich. The height of the Q30-SPAdes peak reflects the relative size of this assembly. Peaks around 50% GC may reflect endosymbiont contigs and possibly bacterial contamination.

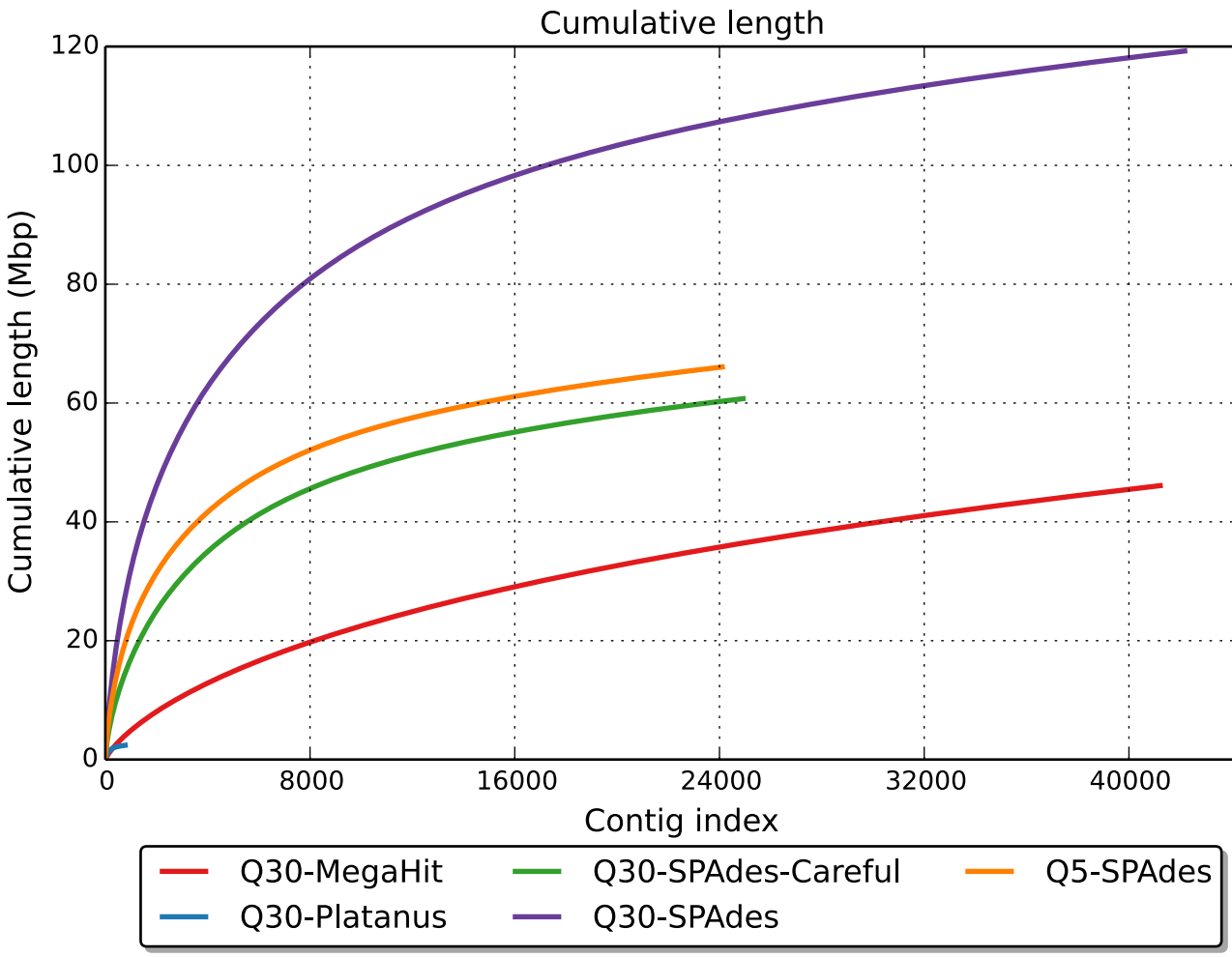

Figure 3.4.4: The cumulative length of contigs as a function of contig number. Again, this plot reflects that Q30-SPades generated the largest assembly by a considerable margin and while generating clean consistent contigs Platanus failed to recover many contigs found in other assemblies.

Source Group	Number of Contigs	Total Length	Phylum-Level Breakdown
Host	13	38,209	Intramacronucleata
-	2	140	Apicomplexa
-	1	163	Colponemidia
Endosymbiont	12	2,758	Chlorophyta
-	12	3,987	Streptophyta
-	1	1,674	Cyanobacteria
Bacterial Contamination	16,230	13,435,718	Proteobacteria
-	468	669,751	Firmicutes
-	329	135,928	Actinobacteria
-	128	68,337	Bacteroidetes/Chlorobi group
-	1	241	Deinococcus-Thermus
Eukaryotic Contamination	605	640,915	Ascomycota
-	380	206,354	Chordata
-	74	38,529	Arthropoda
-	12	3,623	Basidiomycota
-	7	2,150	Nematoda
-	1	61	Platyhelminthes
-	1	102	Cnidaria
Unknown	540	345,834	Unclassified

Table 3.4.2: Summary of taxonomic assignments via TAXAassign grouped into putative "source groups" reflecting the most probable source of 10kb chunked contigs of that specific taxonomic provenance. Of note, is the disproportionate number of contigs from contaminating sources. Specifically, bacteria such as Firmicutes and potential user contaminant in the form of Chordate assigned contigs.

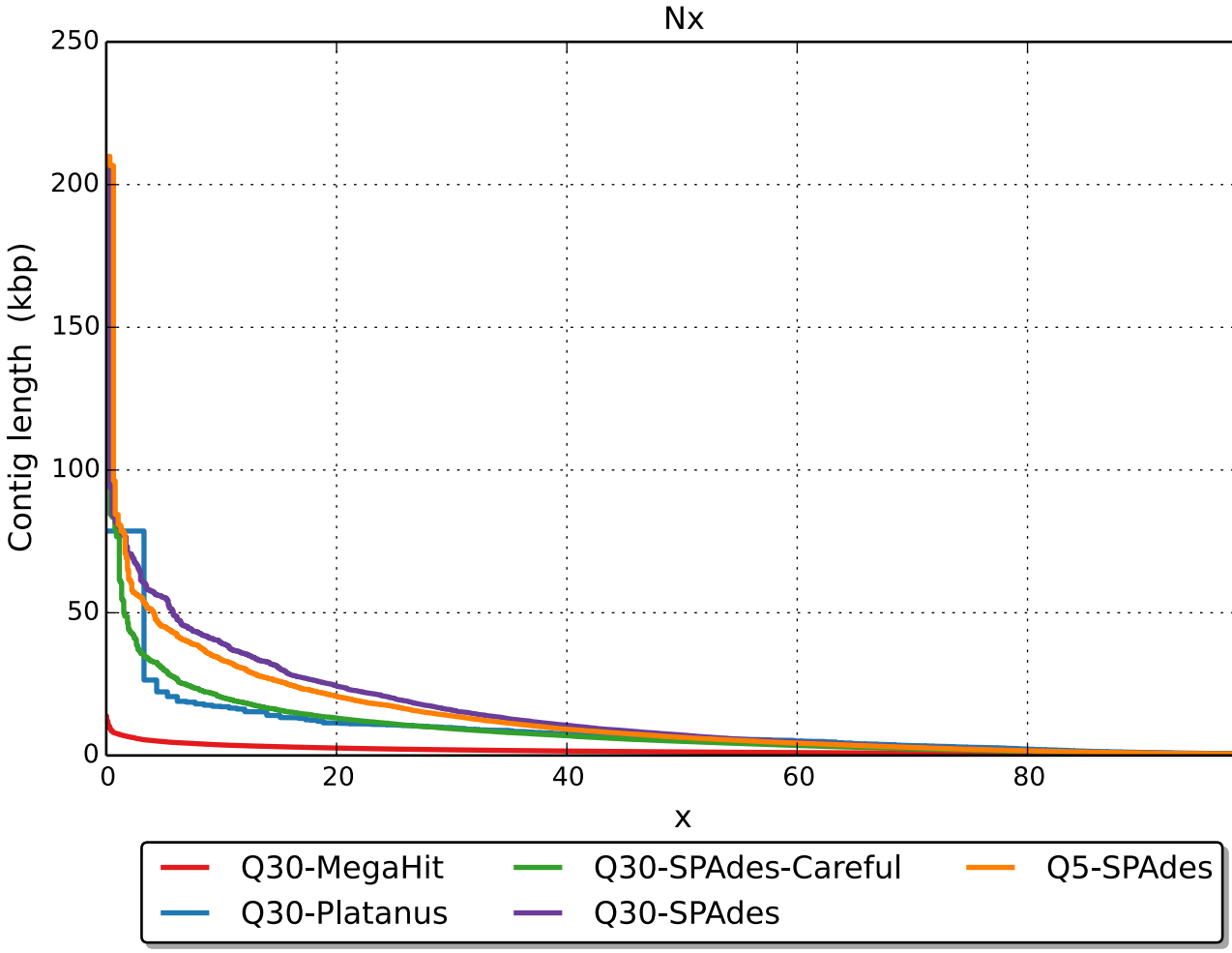

Figure 3.4.5: The number of X (i.e. gap) in the assembled contigs as a function of their length. This demonstrated that generally few Xs were assembled - however, it should be noted that these are contigs and not assembly scaffolds and thus fewer Xs would be expected.

-	Positive	Negative
True	Contigs with **same** taxonomic assignment are assigned to the **same** cluster	Contigs with **different** taxonomic assignments are assigned to **different** clusters
False	Contigs with **different** taxonomic assignments are assigned to the **same** cluster	Contigs with the **same** taxonomic assignment are assigned to **different** clusters

Table 3.4.3: A contextual explanation of True and False Positive and Negatives in the context of contig binning/clustering. Top left indicates what a True Positive (TP) means in this context, bottom left a False Positive (FP). Similarly Top Right explains a True Negative (TN) and Bottom Right a False Negative (FN)

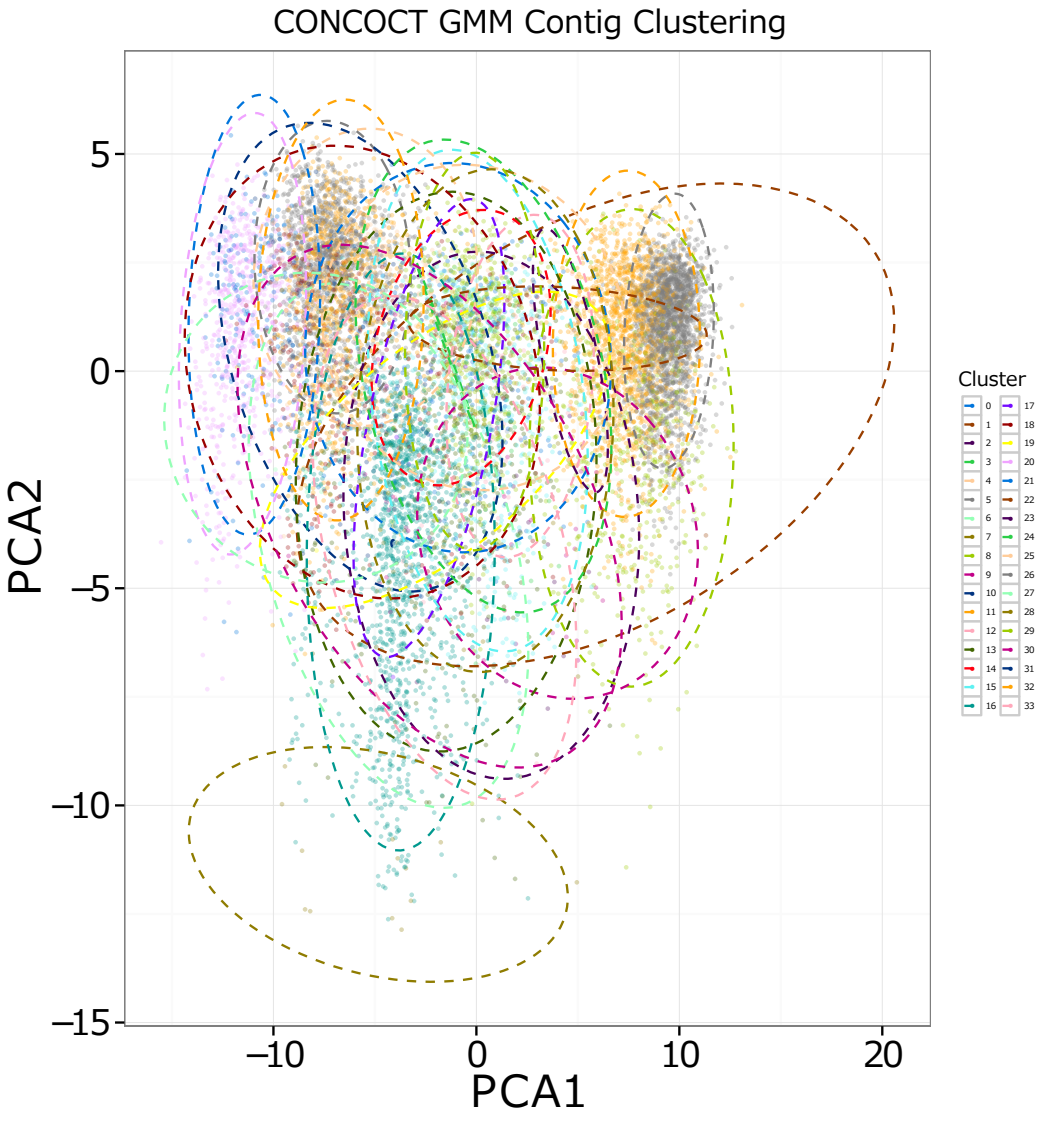

Figure 3.4.6: A low dimensional Principal Component representation of genomic contig cluster assignments. Clusters are assigned via a Gaussian Mixture Model (GMM) based on sequence compositional and coverage features as implemented in CONCOCT. Unfortunately, as can be observed clusters are both poorly distinguished even in the dimensions of the 2 principal components (PCA1 and PCA2) and are numerous (34). This figure highlights how poorly resolved and noisy the decompositon of this single cell metagenome.

Bin	Number of Contigs	Total Size (in bp)
Endosymbiont	782	1,767,324
Host	3,451	24,294,611
Other Eukaryotic	1,646	7,237,238
Bacterial and Unknown	15,211	26,342,475

Table 3.4.4: Results of the customised taxonomic binning, note the far less conservative binning compared with TAXAssign. Note this only consisted of contigs over 500bp in length

.

nomic assignments were not confined to a single cluster and were spread over main clusters.

The F_1[1] score for CONCOCT clustering was therefore 0.680389 under the, slightly flawed, assumption that TAXAssign represents the ground-truth.

It is also worth noting that the 34 clusters had a relatively high level of mutual information (Normalised Mutual Information of 0.332022 and a Rand Index of 0.499741) suggesting many small but highly similar clusters were created. This level of similarity combined with the poor recall suggests a greater number of clusters were inferred than was present in the taxonomic assignment ground-truth.

3.4.3 Elimination

After 1 week $10\mu gml^{-1}$ Paraquat cultures were partially bleached. Unfortunately, after 2 weeks and despite regular feeding all *Paramecium* were also dead. The same pattern was observed with $1\mu gml^{-1}$ treated cultures just a slower process. After 6 weeks, cultures began to clear and then promptly died.

A similar pattern was observed with both concentrations of cycloheximide where $10\mu gml^{-1}$ treatment led to a reduction in endosymbiont abundance by 90% after 1 week followed promptly by host death. The lower concentration $1\mu gml^{-1}$ displayed the same pattern but over a 6 week period.

Finally, with subculturing and feeding cultures maintained in constant darkness did lead to gradual bleaching over 4-8 weeks. However, after 10 weeks the cultures ended up dead.

3.5 Discussion

3.5.1 CCAP 1660/12 and CCAP 1660/13 contain largely clonal *M. reisseri* symbionts

Phylogenetic analysis demonstrates that the endosymbiont present in the CCAP 1660/12 and CCAP 1660/13 is *M. reisseri*. The ITS2 sequences derived from these 2 cultures across 5 different biological replicates (using both primer sets and with or without extra purification steps to minimise contamination from any algae present in the media) were all identical (with the exception of individual SNPs) to 3 separate previously published *M. reisseri* ITS2 sequences. That this formed a well supported clade with other *Micractinium* sequences and was clearly a distinct grouping from the other *P. bursaria* endosymbiotic green algal species further supports the identity of the 1660/12 and 1660/13 endosymbionts as *M. reisseri*.

While 8 different SNPs were identified in the ITS2 sequences, these never occurred in the same sequence and

[1] $F_1 = 2 * \frac{precision * recall)}{(precision + recall)}$

half are easily attributable to sequencing error as they couldn't be recapitulated in reverse sequencing of the same clone. Of the remaining 4 SNPs that were validated as not being sequencing error, only 1 was discovered in separate PCR reactions and biological replicates and thus can putatively be attributed to genuine biological diversity and not merely PCR error (ITS2-6 and ITS2-A7, A to G transition). Therefore, on the basis of ITS2 sequences we cannot say the endosymbionts in CCAP 1660/12 and 1660/13 form a clonal population. However, a single SNP in the hypervariable ITS2 region represent very recent and minor divergence. The most likely explanation is that this represents the emergence of a slightly modified line of endosymbionts within the clonal endosymbiont population of the CCAP 1660/12 culture. Due to the uniformity of the ITS2 sequences there is no evidence of multi-strain photobiont co-habitation as described by (Hoshina, 2012).

It should be noted that the majority of ITS2 based studies make use of the secondary structure (predicted using tools such as RNAstructure (Mathews et al., 2004)) in inference (Schultz and Wolf, 2009). This increases reliability of phylogenetic inference (Keller et al., 2008) allows ITS2 to be used to distinguish higher taxonomic levels (Coleman, 2003), and plays a role in resolving the thorny problem of species determination (Müller et al., 2007). However, as the endosymbiont species ITS2 secondary structures have already been extensively investigated (e.g. (Hoshina and Imamura, 2008; Hoshina et al., 2010)) it was proved as unneccessary in this analysis as at the taxonomic level of the inquiry.

3.5.2 Reliability of Culture Collection

One clear result and point worth raising is that contrary to previous studies (accession *AB*260896.1 (Hoshina and Imamura, 2008)) and CCAPs culture description CCAP 1660/13 does not contain a *Coccomyxa* endosymbiont and contains an identical *M. reisseri* endosymbiont to the CCAP 1660/12 culture. Unfortunately, on communication with CCAP it emerged that the 1660/12 strains in their collection are no longer available and that CCAP 1660/13 had apparently become overgrown by free-living *Coccomyxa*. Therefore it is likely that the previous finding of *Coccomyxa* "endosymbionts" in CCAP 1660/13 (Hoshina and Imamura, 2008) represents accidental contamination and sequencing of the free-living *Coccomyxa* also present in the culture.

The identical nature of the CCAP 1660/12 and CCAP 1660/13 endosymbioses is perhaps not surprising when it is emphasised that these cultures were isolated from the same pond (Cambridge, UK) by CCAP.

This demonstrates the necessity of not taking culture collection labels and taxonomic assignments on faith. It is critical to thoroughly determine that all received cultures actually contain the organism

3.5.3 MDA metagenomes are non-trivial

The biases induced by MDA in single cell genomes are known to be formation of chimeric sequences and the amplification of undesired contaminant sequences (Binga et al., 2008). Additionally, despite a theoretical basis that the amplification coverage bias should be random (Hosono et al., 2003) there is evidence disputing this in practice (Ellegaard et al., 2013b). The magnitude of this bias is related to the starting quantity of DNA (Ellegaard et al., 2013a). Fortunately, there does not appear to be any bias related to GC (Ellegaard et al., 2013a). An increase in the number of starting cells to the range of a few hundred to a few thousand bacterial cells improves amplifciation

considerably (Ellegaard et al., 2013a). Unfortunately, increasing the number of cells in the case of CCAP 1660/12 *P. bursaria - M. reisseri* system would likely compound issue with bacterial contamination due to both a greater sample volume leading to greater inclusion of food bacteria living in the media and an increase in the number of partially digested bacterial (and viral) symbionts associated with the host.

SPAdes, by far, generates the best assemblies of complex MDA-based metagenomes of the assembly tools trialled. This cannot be attributed to the effective read error correction implemented as part of SPAdes via BayesHammer as all assemblies were completed on BayesHammer error corrected reads. The performance of SPAdes is likely attributable to 2 factors: it is specifically designed to handle MDA-based single cell assemblies and thus is highly tolerant of the coverage variability observed and secondly it is the lone genome assembly that effectively utilised paired-end data during assembly. The vast majority of assemblers will only utilise this data in ad-hoc post-assembly heuristic operations to improve contigs and scaffold the dataset. On the other hand, SPAdes generates the assembly de-Bruijn using siamese retangular graphs that incorporate both forward and reverse reads and their respective insert. In future, it may be worth re-analysing this data using other MDA-specific tools such as HyDA to assess their performance.

The relative performance of Q30-SPAdes with and without the "careful" setting is interesting. This setting minimises the risk of mismatch and indels found in the assembly. This led to assembly with statistics relatively similar to that of the Q5-SPAdes assembly. However, on correspondance with the developers of SPAdes it emerged that there was a bug in this setting in the version of the assembler used within this study leading it to be highly conservative and discard many assembled contigs that were unlikely to be mismatches.

Finally, the poor performance of CONCOCT suggests that coverage and composition are not effective metrics by which to decompose an MDA-based metagenome into constituent "bins". The poor recall and high similarity indices between the clusters suggests that a greater number of clusters were inferred than was present in the ground truth of the taxonomic assignments. This likely represents the effect of biased amplification in MDA (therefore heterogeneous variable coverage) on the variational inference of the number of clusters and the utility of the coverage feature in general. This means, therefore, in MDA-based metagenomes standard metagenomic binning pipelines that are reliant on coverage metrics (even partially as in the case of CONCOCT) are not effective.

This problem is somewhat symptomatic of the current state of the tool ecosystem for MDA-based eukaryotic metagenomes. The few MDA-orientated analysis tools focus on the assembly of bacterial systems whereas the majority of the metagenomic tools are based on features and metrics such as coverage that are only consistent in convential non-MDA bulk genomic studies. Ideally, future research will improve the ease of analysis and assembly of datasets such as this.

3.5.4 Metabolic co-dependence in the CCAP 1660/12 system

Due to the repeated failure to create endosymbiont free *Paramecium* hosts from the CCAP 1660/12 cultures using 3 of the major accepted methodologies (cultivation in darkness (Karakashian, 1963), paraquat (Hosoya et al., 1995; Tanaka et al., 2002) or cycloheximide (Weis, 1984)) we are forced to address the possibility that the *Micractinium reisseri* endosymbiont and *P. bursaria* system in CCAP 1660/12 and CCAP 1660/13 cultures forms

an obligate system. By some unidentified mechanism, metabolic co-dependence may have become fixed in this culture.

Cycloheximide does partially inhibit host protein synthesis (Weis, 1984; Kodama et al., 2007; Kodama and Fujishima, 2008, 2009) therefore it is possible that in the host strain found in the CCAP 1660/12 culture that this partial inhibition is lethal to both host and endosymbiont. However, the failure of this method in conjunction to Paraquat, a herbicide which theoretically should only affect the endosymbiont, and constant dark culturing suggests it is the loss of endosymbiont photosynthetic activity that is lethal to the host cells (as adequate bacterial foodstocks were included in these cultures).

The one major method that wasn't attempted was the use of 3-(3,4-dichlorophenyl)-1,1-dimethlyura (DCMU) an established blocker of photosystem II (van Gorkom, 1974). However, DCMU has previously been found to be mildly toxic in *P. bursaria*, affecting the sexual reproduction system (Miwa, 2009) therefore, this would have proven unlikely to show different results in either the case of a particularly "sickly" host strain or obligate endosymbiosis.

This result indicates the presence of key differences between the current state of this endosymbiosis and the previously studied *C. variabilis* endosymbiosis studied by (Kodama and Fujishima, 2014). Therefore, a comparative analysis of these systems could theoretically shed light on the mechanism by which metabolic co-depedence has become fixed in one system. Alternatively, this difference may just reflect the nature of two different, independently acquired endosymbioses with different species and strains of both host and endosymbiont.

Another avenue of study that we did not investigate was that of isolation of endosymbiont into free-living cultures (Achilles-Day and Day, 2013a). This would allow us to establish whether green algae such as *Micractinium* that have obligate hosts are themselves obligate endosymbionts. There is some evidence pointing towards this in nature, with the widespread predation of *M. reisseri* and *C. variabilis* by their specific PBCV virotypes as well as the relative paucity of natural free-living strains of these species. To my knowledge, there has only been a single isolated and characterised free-living *M. reisseri* (Abou-Shanab et al., 2014) example and no *C. variabilis* examples. However, this said, algae have previously been isolated from the CCAP 1660/13 culture (Achilles-Day and Day, 2013a). We have demonstrated via ITS2 sequencing that the endosymbionts in CCAP 1660/13 are the same as those in CCAP 1660/12. Therefore, if these isolated algae are actually endosymbionts (as supposed to the free-living *Coccomyxa* sp. that overgrew the culture shortly after this study was published) then the *M. reisseri* endosymbiont is capable of living without the host and is not an obligate endosymbiont despite *P. bursaria* being an obligate host.

3.6 Conclusions

Therefore, on the basis of ITS2 sequencing the CCAP 1660/12 culture endosymbiont is a strain of *Micractinium reisseri*. Additionally, the CCAP 1660/13 endosymbiont has been misclassified as a strain *Coccomyxa* and is the same *Micractinium reisseri* species found in the CCAP 1660/12 culture. Despite poor performance in genome assembly, the evidence of the genomes and ITS2 data seem to indicate that this endosymbiont forms a clonal or

near clonal population within the CCAP 1660/12 endosymbiont. At a minimum, a single strain of *M. reisseri* comprises the sole green algal endosymbiont in the CCAP 1660/12 and 1660/13 cultures although it may be actively evolving as evidenced by a small divergent sub-population.

Finally, the *Micractinium reissieri* endosymbiont in cultures CCAP 1660/12 CCAP 1660/13 has potentially become metabolically co-dependent with the host. The host appears incapable of survival without the endosymbiont, therefore, it is important to attempt to identify the differences between the demonstrably facultative relationship between the Japanese Yad1g1N strains (used in (Kodama and Fujishima, 2014)) and the obligate CCAP 1660/12. Identifying these differences may pinpoint the mechanism by which metabolic co-dependence becomes fixed in *P. bursaria* - green algal endosymbioses.

"even after the observation of the frequent or constant conjunction of objects, we have no reason to draw any inference concerning any object beyond those of which we have had experience;"

- David Hume: *A Treastie of Human Nature, 1738*

4

Transcriptomic analysis of the *Paramecium bursaria* and *Micractinium reisseri* endosymbiosis

4.1 Introduction

The *Paramecium bursaria-Micractinium reisseri* (PbMr) endosymbiosis conveys phototrophy (Karakashian, 1963), numerous photobiological traits (e.g. (Berk et al., 1991; Saji and Oosawa, 1974; Nakajima and Nakaoka, 1989; Niess et al., 1982b; Iwatsuki and Naitoh, 1988; Summerer et al., 2009), partially reviewed in (Sommaruga and Sonntag, 2009)) and its establishment and maintenance is dependent on photosynthetic activity and enigmatic light-induced factors (Karakashian, 1963; Hosoya et al., 1995; Kodama et al., 2007; Kodama and Fujishima, 2014). Therefore, a relatively unbiased global metatranscriptomic profile of host and endosymbiont in both lit and dark conditions would potentially identify key transcripts which play a role in the establishment, maintenance, and characteristics of this endosymbiosis.

"Dual-RNAseq" is a form transcriptomics which characterises transcripts in a small number of defined organisms simultanously (Westermann et al., 2012). It has proven an effective method in several studies investigating host-chloroplast interactions (Nowack et al., 2011; Jiggins et al., 2013; Xiang et al., 2015), and host-pathogen systems (Tierney et al., 2012; Kawahara et al., 2012; Jones et al., 2014; Hayden et al., 2014). It differentiates itself from both standard metatranscriptomics, such as those common in microbial ecology (Poretsky et al., 2005;

Aliaga Goltsman et al., 2014), by being conducted on samples of known, or mostly known composition, and from classical transcriptomics by not depending on axenic samples.

Paramecium bursaria and its green algal endosymbionts form a system well-posed for "dual-RNAseq" analysis. Firstly, there is a plethora of literature on the physiology and behaviour of host and endosymbiont, both together and individually (e.g. (Iwatsuki and Naitoh, 1988), see (Kato and Imamura, 2009b) and the Introductory Chapter for more details), presenting a key resource by which results can be contextualised. Additionally, transcriptomic analysis has proven feasible in reasonably close relatives of both host (Arnaiz et al., 2010; Kolisko et al., 2014) and endosymbiont (Guarnieri et al., 2011; Rowe et al., 2014; Bashan et al., 2015). Even more promisingly, there has been an analysis of the host-endosymbiont system (although in a different strain: Yad1g1N) (Kodama et al., 2014). Unfortunately, this study focussed only on the expression pattern of the host alone with and without its endosymbiont and discarded endosymbiont derived data during analysis.

This said, the PbMr system does also present some severe difficulties in terms of its transcriptomic tractability. Specifically, the system is highly genomically and transcriptomically complex with *P. bursaria*'s ciliate nuclear dimorphism and high order polyploidy (Raikov, 1995), the presence of sexual reproduction in both host (Jennings, 1939) and endosymbiont species (Blanc et al., 2010), and a large range of GC biases (Kodama et al., 2014). Therefore, care must be taken to optimise sequencing, and assembly methods to mitigate these complications.

These difficulties are compounded by the lack of available reference genomes for either *Paramecium bursaria* or *Micractinium reisseri* and thus necessitating *de novo* transcriptome assembly. However, the utility of sequenced genomes from divergent ciliate species (i.e. *Tetrahymena thermophila* (Eisen et al., 2006), *Paramecium tetraurelia* (Aury et al., 2006) and *Paramecium caudatum* (McGrath et al., 2014)) and endosymbiotic green algae *Chlorella variabilis* NC64A (Blanc et al., 2010) and *Coccomyxa subellipsoidea* C-169 (Blanc et al., 2012) (see fig. 1.2.2 in the Introductory Chapter and **??** in Chapter 1 for respective phylogenetic context of these genomes) as references for assembly was investigated. It should also be noted that the existing *Paramecium bursaria* (Kodama et al., 2014), *Paramecium duboscqui* (Kolisko et al., 2014) and *Chlorella vulgaris* (Guarnieri et al., 2011) transcriptomes mentioned above were successfully recapitulated *de novo* (without a reference genome).

The mixotrophic nature of the host *Paramecium* (Dolan, 1992) means there are partially digested bacterial prey species, as well as numerous associated bacteria (Görtz and Fokin, 2009; Fokin and Görtz, 2009; Schrallhammer and Schweikert, 2009) and viruses (Van Etten et al., 1983) which all present potentially obfuscating sources of contamination in the analysis of host-endosymbiont interaction. Therefore, it is key to effective analysis of this system to develop methods to minimise the effects of contamination at all stages of analysis. To address this, we investigated methods to reduce contamination during library preparation such as washing steps, cell picking and single cell sequencing techniques; methods to screen and/or filter sequenced libraries for contaminants before inclusion in assembly and methods to effectively sort assembled transcripts into bins relating to their likely originating organisms (i.e. "host", "food" or "endosymbiont" derived).

To this end, bulk RNAseq libraries from cultured PbMr was sequenced using 76bp paired-end reads and the Illumina Gene Analyzer II platform taking care to mininmise contamination by filtering and washing cultures and carefully assessing culture health to maximise the number of healthy PbMr sequenced. Unfortunately, due to

limitations in the maintainable culture density of the *Paramecium bursaria* CCAP 1660/12 and thus the quantity of extractable mRNA it was necessary to pool all day and night replicates into a single pair of day and night libraries.

While this provided sufficient material for sequencing it precluded accurate inference of differential expression between day or night by masking the biological replicates (Auer and Doerge, 2010). We, therefore, also sequenced a set of 3 (followed later by an additional 5) dark and 3 light biological replicates using single-cell RNAseq (sc-RNAseq) methods. This also allowed a finer-grain control over cell selection and potentially a method to reduce culture based contamination.

While reasonably nascent, sc-RNAseq has shown a lot of promise in well characterised systems such as human cell cultures (Bengtsson et al., 2005; Shalek et al., 2013) and *Saccharomyces cerevisiae* (Lipson et al., 2009) and there are high expectations of their utility for "dual-RNASeq" (Westermann et al., 2012). sc-RNAseq addreses the key difficulties of analysing unculturable or poorly culturable organisms (Murray et al., 2012) and investigating cell-cell heterogeneity in expression patterns (Raj and van Oudenaarden, 2008; Shalek et al., 2013)). Uninvestigated, this heterogeneity (either from biological and/or genomic variance or just the stochasticity of gene expression), can lead to a Yule-Simpson effect (Yule, 1903; Simpson, 1951), where the false amalgamatation of distinct expression patterns in previously cryptic but distinct cellular subpopulations could generate a spurious expression pattern contrary to either subpopulation.

There are a range of possible sc-RNAseq methods (whose advantages and disadvantages are covered in the Methods Chapter). We used Qiagen's Repli-G Whole Transcriptome Amplification (WTA) MDA-based kit as MDA is well established and characterised in single cell genomics (e.g. (Spits et al., 2006)), has a simple methodology not requiring additional equipment, and is potentially more successful at recovering transcripts from a wide range of abundance levels than other methods i.e. recovers many lowly expressed transcripts[1]. Unfortunately, despite the publication of empirical comparisons of single cell transcriptomic methods (Wu et al., 2014), Qiagen's Repli-G WTA MDA-based kit has yet to be directly assessed relative to other approaches and thus its performance has not been independently verified. Briefly, this method involves the ligation of reverse transcribed cDNAs using oligo-dT primers (after lysis and removal of gDNA) before MDA by a φ29 DNA polymerase with a 5'-3' exonuclease proofreading activity (reducing error-rate of amplification to $9.5 \cdot 10^{-6}$ errors per nucleotide (Paez et al., 2004) compared with 10^{-4} to 10^{-5} for Taq (Tindall and Kunkel, 1988; Eckert and Kunkel, 1990)) (Korfhage et al., 2015).

Unfortunately, despite its utility sc-RNAseq generates a new set of difficulties. First and foremost, there has only been a single published use of sc-RNAseq, to my knowledge, in non-model unicellular eukaryotes. This study by (Kolisko et al., 2014), briefly addressed the issues of bias, contamination and gene discovery effectiveness in a set of model and non-model eukaryotes and constitutes an important proof-of-concept. However, it also used a different sc-RNAseq approach (SMART), focussed on single organisms, and didn't address, in-depth, the optimal way to process, assemble and utilise single cell datasets from protists. While some work has been done invesigating the optimal pre-processing of bulk RNAseq datasets (e.g. (Macmanes and Eisen, 2013; Macmanes,

[1] https://www.qiagen.com/gb/shop/sample-technologies/rna-sample-technologies/total-rna/repli-g-wta-single-cell-kit/ as of 2015/08/25

2015)) the effect of different trims and error correction on sc-RNAseq has yet to be characterised. There are also some early indications of problems of cryptic bacterial contamination from samples and/or reagents in sc-RNAseq is particularly problematic (Kolisko et al., 2014). This further increases the importance of library screening and post-assembly transcript binning.

4.2 Aims

Therefore, this chapter will investigate the optimal use of 2nd generation bulk and sc-RNAseq libraries in a characterising a complex reference-free system. Specifically, it will look at the screening of RNAseq libraries for contamination before assembly, the optimal preprocessing (partitioning, trimming, digital normalisation and error correction), assembler and assembly parameters (including the utility of divergent reference genomes from related species) in recapitulation of host and endosymbiont transcripts. Finally, I will address the problem of the attribution of recovered transcripts into their appropriate likely originating organism.

4.3 Methods

4.3.1 Sample Preparation and Sequencing

Bulk transcriptome RNA preparation

For bulk transcriptomic analyses CCAP 1660/12 cells were harvested in a way to minimise contamination from bacterial prey species in the culture. $\sim 10^6$ cell aliquots were strained through 40μm sieves, filtered on 10μm nylon filters, before finally being filtered on 8μm TETP polycarbonate filters using a low-pressure filtration pump. Collected samples were either immediately quick-frozen in liquid nitrogen for storage (-20°Cfor short-term storage and -80°Cfor longer storage) or harvested by centrifugation. In order to investigate the two main metabolic states of the symbiosis (i.e. under light conditions during active photosynthesis and in the dark when no photosynthesis is taking place) samples were extracted 5 hours into the light and dark phase of the 12:12 hour day-night cycle.

To ensure extracted RNA was representative of healthy and interacting host and endosymbionts care was taken to the number of dead/dying cells from which RNA was extracted. In order to do this, a subsample was taken from each culture during the process of harvesting and scored for dead/dying cells. Cell assays were formed by taking 1-2ml of each harvest cell pellet and fixed using 40μl Lugol's solution (0.5g I_2 and 1g KCl in 8.5ml of MilliQ water). Dead/dying cells were identified as broken or puckered cells and counted using light microscopy. Samples containing >10% dead/dying cells were discarded and no RNA extracted from them.

In order to lyse collected samples, cells were washed from the filter or the pellet was resuspended in 1ml TriReagent (Sigma) heated to 60°C. Cells were vortexed with sterile 300μm glass-beads for 15s, incubated at room temperature for 10 minute, vortexed for 15s, quick-frozen in liquid nitrogen and stored at -20°C before further processing. Samples were defrosted, vortexed for 15s, placed in a heat-block set to 60°C for 10 minutes while continuing to be vortexed, removed from heating and vortexed again for 15s. RNA was extracted by adding 0.2ml

of Chloroform to the glass-bead-trizol-sample solution, shaking for 15s, incubating for 5 minutes at room temperature and centrifuging at 12,000g for 15 minutes at 4°C. The upper-phase was then transferred to an RNAse-free 1.5ml tube and an equal volume ($\sim$ 0.5*ml*) of isopropanol was added before shaking for 15s. The isolated RNA was then incubated at −20°Cfor 10 minutes (up to several hours) before being collected as a pellet using a centrifuge at 10,000g for 10 minutes at 4°C (supernatant was discarded). The RNA pellet was then washed with 1ml of 75% ethanol and centrifuged twice at 10,000g for 10 minutes at 4°Cwith the supernatant being discarded after each centrifugation. The pellet was then dried before being resuspended in 100μl of RNAse-free water. The RNA was cleaned further using the Qiagen RNeasy clean-up kit before being assessed for quality using ND-1000 (NanoDrop) and BioAnalyzer (Agilent).

Single cell RNA preparation

For single cell transcriptomics, a "cell-picking" approach was used in which *P. bursaria* cells (from the CCAP1660/12 culture) were inspected on an inverted light microscope before being picked using an orally aspirated drawn-glass Pasteur pipette (Garcia-Cuetos et al., 2012). In order to mininmise contamination from food bacteria present in the media these picked cells were washed 3 times by serial transfer to 10μl droplets of sterile NCL media. The washed cell was then transferred to a 10μl droplet of sterile water. Cells were picked 5 hours into both the lit and dark phase of the 12:12 hour day-night cycle identically to the bulk analyses. As cells were picked individually, health status could be exhaustively assessed during picking and therefore the subsampling and scoring method used to check the status of cells in bulk preparations was unnecessary.

cDNA was generated and amplified using the MDA-based Qiagen REPLI-g WTA Single Cell Kit (Korfhage et al., 2015) with additional cell disruption steps. Specifically, cells were transferred from their respective 10μl droplets of sterile water to a PCR tube containing 6μl water and 4μl lysis buffer. Due to the robust chitin cell walls of *M. reisseri* (Kapaun and Reisser, 1995) it was important to ensure thorough cell lysis. Therefore, samples underwent mechanical disruption by bead beating (Sigma, 425 − 600μm, acid-washed) followed by freeze-thaw via submersion in liquid nitrogen for 5 seconds. In order to compare disruption methods, extractions and amplifications were also conducted using just lysis buffer, bead beating and vortexing (i.e. without freeze-thaw), and just the lysis buffer. Samples were then quantified using a ND-1000 (NanoDrop) and as extraction methods produced near identical DNA concentrations the maximal disruptive method of freeze-thaw, beat beating, vortexting and lysis buffer described above was used for further purification and library preparation. The samples were then vortexed for 1 minute before a gDNA removal step.

mRNA was selectively amplified and reverse transcribed to cDNA using poly-A selection (i.e. oligo-dT) primers to prevent amplifying ribosomal sequences. Prior to MDA by a φ29 DNA polymerase cDNA were ligated into long fragments due to lower MDA efficiency for short fragments (Korfhage et al., 2015). This reduces size-dependent amplification bias but could potentially lead to the creation of chimeric transcripts in which paired-reads cross boundaries of adjacently ligated cDNA transcripts. Analysis of this is discussed below.

The amplified cDNA was then purified using a QIAamp DNA mini kit and eluted in 100μl elution buffer. This kit operates by binding the DNA to a QIAmp membrane in a spin column followed by successive washing steps

to remove impurities such as remaining proteins and cations. To create 3 dark cDNA samples (Dark1-2, Dark1-3, Dark1-5) and 3 light samples (Light1-9, Light1-10, Light1-11).

Due to low quantities of eukaryote identifiable reads in the initial 3 sequenced single cell dark libraries a set of additional single cell extractions were conducted. These followed the same protocol as above but also featured an additional final PCR-based screening of synthesised cDNA using primers specific for *Paramecium* Bug22 sequence. Bug22 is a highly conserved ciliary protein found in a large number of organisms including the ciliates (Smith et al., 2005b; Laligne et al., 2010), green algae (Keller et al., 2005; Laligne et al., 2010; Meng et al., 2014), higher plants (Hodges et al., 2011), and animals (Mendes Maia et al., 2014) we used as a marker for *Paramecium* derived cDNA. Primers used were Bug22BFWD "GCATTCTAGACCAATCTGGCTTTCTGTCAA" and Bug22BREV "GCATTTCGAATTTGAGGCTCTAAATCTTCTTCTCA", under standard PCR conditions. 5 (Dark2-2, Dark2-3, Dark2-6, Dark2-7, Dark2-8) samples with bands of appropriate size were then taken forward for library preparation and sequencing.

Illumina library preparation

For both bulk and single cell preparations each cDNA sample was fragmented in $130\mu l$ 1xTE buffer on the Covaris E220 with a target size of $225bp$ (duty factor of 10%, 200 cycles per burst, peak incident power of 175, $200s$ at 7^oC). Fragment sizes were checked on a BioAnalyzer (Agilent) 7500 DNA chip. cDNA was then concentrated using a GeneRead kit column with a elution in $35\mu l$. Fragmentation step was then repeated 3 times ($110s$) until majority of cDNA in each library was between $200 - 250bp$

cDNA ends were then end-repaired, adenylated and adapters ligated using the NEXTFlex (Biooscientfic) sequencing kit according to the manufacturer's instructions and using NEBNext (New England Biolabs) indices. Also following the NEXTFlex kit instructions, MgNa bead purification was done before and after PCR amplification using NEBNext reagents. Finally, prepared libraries were size selected using a Blue Pippin machine at a size selection of $350bp$ (range $315 - 385bp$).

A final bioanalyzer step was conducted with individual library concentrations ranging from $0.66 - 4.09nM$.

Sequencing

The bulk day and night library were paired-end (PE) $76bp$ sequenced using an Illumina Genome Analyzer II by the Exeter University Sequencing Service. The two libraries were sequenced on separate flowcells (Bulk-Light, Bulk-Dark).

Single cell libraries were paired-end $150bp$ using an Illumina HiSeq 2500 by Exeter Sequencing Service. 3 dark (Dark1-2, Dark1-3, Dark1-5) and 3 light (Light1-9, Light1-10, Light1-11) samples were multiplexed sequenced on a single flowcell lane. The 5 additional dark samples (Dark2-2, Dark2-3, Dark2-6, Dark2-7, Dark2-8) were multiplexed and sequenced on a single flowcell lane in a separate sequencing run.

4.3.2 Library contamination screening

Taxonomic analysis

Sequenced libraries were initially screened using the standard metrics implemented in the FastQC to check for standard seqencing issues such as flowcell defects, library degaradation, and adapter read-through (Andrews, 2015).

To further investigate potential contamination, a taxonomic profile and GC% probability density was determined for each library.

The former was conducted using a custom tool dubbed "DueyDrop" which functions as follows. Briefly, for each library 5 batches of 10,000 PE reads were sampled using the reservoir sampler (Vitter, 1985) implemented in Heng Li's seqtk library (Li, 2015). Despite 5 batches of 10,000 reads theoretically being equivalent to 50,000 random samples by splitting sampling and using a different random seed any problems from poor randomisation implementation was minimised and consistency of taxonomic profiles could be easily assessed. These randomly sampled reads were subsequently aligned to NCBI's Protein NR RefSeq database (Pruitt et al., 2007) using the efficient short-read optimised BLASTX implementation of DIAMOND (Buchfink et al., 2015) (at a expectation of e^{-5} and top hits for each read retained. Gene identifiers (GI) were extracted from these tops hits and queried against a local copy of the NCBI taxonomy database (Federhen, 2012) to recover a hit taxonomic lineage for each read that aligned to a sequence within NR database. These lineages were then interactively tallied at several different taxonomic levels (e.g. domain level - eukaryote vs bacteria, or lower level - viridiplantae vs ciliate) and variances calculated. Results were then tabulated and libraries compared to assess whether any libraries appeared abberrant. This whole analysis was repeated for both untrimmed reads and reads quality trimmed to a high quality threshold of an average Q30 over a sliding window of size 4 using Trimmomatic (Bolger et al., 2014) to assess the impact trimming has on this profiling. Taxonomic profiles were additionally visualised in Krona (Ondov et al., 2011) using the tabular BLAST hit import functionality.

Scripts used to conduct this analysis are available in the following github repository:
`https://github.com/fmaguire/dueydrop`

To determine how representative profiles created using small subsamples consisting of <1% of reads are to profiles of entire libraries a similar analysis was done using full libraries. All libraries were pre-trimmed at the harsh threshold of the Q30 sliding window discussed above. The forward read from each trimmed library was used used in a similar DIAMOND based BLASTX search however all hits were retained. Multiple hits for a given read were collapsed into a single lowest common ancestor (LCA) using the LCA algorithm (Gabow and Tarjan, 1985) implemented in MEGAN (via the "mtools" package) (Huson et al., 2007; El Hadidi et al., 2013). LCA were then summarised and tabulated using a script in the CGAT collections ("lca2table.py") (Sims et al., 2014) and visualised using Krona (Ondov et al., 2011).

On the basis of the resultant taxonomic profiles libraries were excluded or included from downstream preprocessing and assembly. The libraries selected for inclusion during these analyses are referred to as the "taxonomically filtered" single cell libraries.

GC density estimates

Each library's GC% probability density was estimated from per-read GC proportions (calculated using awk (Aho et al., 1987)) via Kernel Density Estimation (KDE) (Rosenblatt, 1956; Parzen, 1962) (implemented in the seaborn package (Waskom et al., 2015)). This involved a standard gaussian kernel and a bandwith determined by "Scott's normal reference rule" (Scott, 1979). Again this analysis was repeated with both untrimmed and Q30 trimmed reads.

4.3.3 Optimising read pre-processing

Trimming

To investigate the optimal trimming parameters for single cell libraries, random subsamples were trimmed using a range minimum quality thresholds and then the effects investigated by mapping against 3 draft *de novo* transcriptomes.

Specifically, 5000 PE reads were randomly sampled without replacement from each of the raw FASTQ libraries using the streaming reservoir sampling (Vitter, 1985) algorithm implemented in Heng Li's seqtk C library ((Li, 2015)). To guarantee that pairing was maintained the same random seed was used for the left and right read of each library and incremented between libraries.

Trimmomatic (Bolger et al., 2014) was run on these samples with adapter clipping (ILLUMINACLIP) using sequencing service provided fasta file of adapters, a maximum mismatch count of 2, a palindromic clip threshold of Q35 and a simple clip threshold of Q15, a sliding window quality trim of size 4 and average window quality thresholds of Q0, Q2, Q5, Q10, Q15, Q20, Q25, Q30, Q35, and Q40. Finally, a minimum length trimmed read length critera of 40bp was used.

The trimmed samples were then mapped to 3 different *de novo* draft transcriptome assemblies using bowtie2 (Langmead and Salzberg, 2012) with maximum and minimum insert sizes of 37bp and 1161bp (derived from library preparation fragment size distribution and histrograms of mapped insert sizes for untrimmed reads against bulk reference).

These 3 draft assemblies were a "baseline" bulk RNASeq transcriptome reference consisting of a Trinity (Haas et al., 2013) assembly of the light and dark bulk libraries preprocessed to remove low quality bases (<Q20) and adapters using Fastq-MCF (Aronesty, 2013); and two Trinity assemblies of the taxonomically filtered sc-RNASeq libraries previously trimmed at an average window quality threshold of Q5 and Q30 respectively.

For each library and set of quality thresholds the total number of concordantly mapping (i.e. forward and reverse PE reads mapped to transcripts within the range of the insert sizes used) reads was recorded. This heuristic measure was chosen because the number of concordantly mapping reads generally correlates with the assembly quality (MacManes, 2014). The proportion of surviving reads which mapped was not used as a metric because this could be spuriously inflated in cases where a particular set of trimming parameters has caused the majority of reads to be discarded.

The number of concordantly mapping reads were tallied and plotted in seaborn for each library, reference

transcriptome and set of trimming parameters. The shape of this line was then used to determine the optimal quality threshold to use for further assembly.

Scripts used to conduct this are available in my thesis scripts github repository: https://github.com/fmaguire/thesis_scripts/tree/master/chapter_2_assembly_and_binning/trimming_optimisation

GC Partitioning of Reads

To assess the utility of pre-assembly read partitioning an unsupervised clustering tool was created: Paired Arrangement of Reads via K-means On Unlabelled Reads (parKour). This C++ tool implements a fast and efficient K-means clustering of reads based on the dual features of GC% in forward and reverse paired reads and designed to exploit the wildly differing GC biases of *P. bursaria* and *M. reisseri*.

ParKour operates as follows:

1. Parse user input of paired FASTQ files corresponding to Forward and Reverse Paired-End reads, and desired number of clusters
2. Simultaneously iterate over the pair of FASTQ files calculating the GC% for each loading results into an Armadillo $2xN$ matrix (Sanderson, 2010) where N is the total number of PE reads
3. Bradley-Fayyad K-means (Bradley and Bradley, 1998) clustering as implemented in the MLPACK library (Curtin et al., 2013)
4. Re-read the two input FASTQs assigning them to output files based on the assigned cluster of the pair

GNUplot (Williams et al., 2010) was used to visualise classification and cluster assignment. This approach was attempted using a range of expected clusters from 2 to 5.

Scripts used to conduct this are available in a github repository: https://github.com/fmaguire/parKour

Error correction

The effect of error correction on assemblies involving single cell libraries was assessed by applying two different error correction algorithms to the screened, trimmed reads before assembly. These were a Bayeshammer (Nikolenko et al., 2013) implemented as part of the Spades genome assembler (Bankevich et al., 2012) and optimised for MDA-based single cell genomic data, and "SEECER" (Le et al., 2013) which is optimised for RNAseq (but not necessarily sc-RNAseq data). The impact of each of these error correction algorithms at the read level was assessed as well as their subsequent impact on downstream assembly metrics, particularly RSEM-EVAL likelihood score as will be expanded upon below in the description of assembly assessment.

Kmer normalisation and trimming

Taxonomically screened sc-RNAseq libraries trimmed at a minimum sliding window quality threshold of Q30 and bulk libraries were Kmer normalised and trimmed using the Khmer package (Crusoe et al., 2015)

Specifically, reads were interleaved (Döring et al., 2008) and then digitally normalised using diginorm (Brown et al., 2012) with a K-mer size and coverage cut-off of 20. Low abundance and likely erroneous K-mers were then filtered relative to the read coverage i.e. low abundance k-mers were removed from high coverage reads but would be more likely to be retained for low coverage reads (Zhang et al., 2015, 2014).

Filtered data was then assembled using Trinity (with minimum K-mer coverage of 2) and the subsequent assembly partitioned into transcript families in Khmer (Pell et al., 2012).

The final assemblies were then compared to un-normalised and k-mer trimmed assemblies (see section 4.3.4 for details.

4.3.4 Assembly

Referenced and *de novo assemblies* were attempted using a range of assemblers and assembly parameters.

Firstly, trimmed bulk and taxonomically filtered single cell libraries were mapped to *Chlorella* NC64A, *Coccomyxa C169*, *Tetrahymena thermophila* and *Paramecium caudatum* macronuclear (MAC) genomes. The former pair being the closest available genomes to the endosymbiont and the latter to the host. Mapping was done using the TopHat2 spliced aligner (Kim et al., 2013) against the genomes and was supplemented with and without annotated ORF information (in the form of gtf). GTF files were generated from best avaiable gene annotations in the form of GFF files using gffread (part of cufflinks). Cufflinks (Trapnell et al., 2011) was then used to extract isoforms from the spliced alignments.

For *de novo* assembly, assemblies were conducted using following assemblers with default settings unless specified otherwise:

- Trinity v2.0.6 (Grabherr et al., 2011) with and without a minimum K-mer coverage of 2
- SOAPdenovo-Trans v1.03 (Xie et al., 2014) with K-mer sizes of 20, 32, 64, and 80
- TransAbyss v1.5.3 (Robertson et al., 2010) with K-mer sizes 20, 32, and 64
- Velvet v1.2.10 (Zerbino and Birney, 2008) and Oases v0.2.08 (Schulz et al., 2012) with K-mer size of 21, a minimum K-mer coverage of 2 and a minimum transcript length of 100.
- Iterative de Bruijn Graph Assembler (IDBA)-tran (Peng et al., 2010, 2012, 2013)
- IDBA-MTP (Leung et al., 2014), IDBA-UD (Peng et al., 2012), IDBA-MT (Leung et al., 2013) workflow.
- Bridger (Chang et al., 2015).

Trinity was used for all further downstream assembly optimisation due to its performance and consistency. Specifically, a minimum K-mer coverage of 1-3 were attempted as well as various combinations of libraries (i.e. bulk and screened sc-RNAseq libraries) and also sequencing data from Kodama's previously published *P. bursaria* bulk RNAseq analysis (Kodama and Fujishima, 2014).

To assess the utility of combining assemblies as discused in (Nakasugi et al., 2014), the best assemblies from Bridger and Trinity (as assessed below) were combined using the EvidentialGene tr2aacds pipeline (Gilbert,

2013). Additionally, the best assemblies from all assemblers that ran to completion i.e. Bridger, Trinity, SOAPdenovo-Trans, Transabyss and IDBA-tran were also combined and assessed.

Assembly assessment

Resultant assemblies were compared using standard assembly statistics (e.g. contigs number and size, bases assembled) as implemented in a perl script supplied with Trinity (Haas et al., 2013) and TransRate (Smith-unna et al., 2015). Additionally, reference free probabilistic assembly assessment RSEM-EVAL package (part of DETONATE) (Li et al., 2014) to produce likelihood scores for various completed assemblies.

ORF calling

ORFs were called from assembled transcripts using TransDecoder (Haas et al., 2013) with a minimum protein size of 100aa.

TransDecoder operates as follows

1. All ORFs are found in transcripts by identification of sequences between a start codon and an in-frame stop codon. Partial ORFs are also identified as sequences between the 5' transcript terminus and a stop codon or a start codon and the 3' transcript terminus.
2. The top 500 longest of these ORFs was selected and used to train a reading-frame specific 5th-order Markov model.
3. All of the ORFs were then scored for each reading frame as a sum of the per-base log odd scores (log probability of a given base and reading frame given its preceding 5 bases normalised by the relative frequency of that nucleotide across all transcripts).
4. The highest scoring reading frame is retained as a candidate
5. Any of the initial ORFs with homology to proteins in PFAM and Swissprot (as determined by HMMR and BLASTP (minimum e-value of $1e^{-5}$)) are also retained.

Paramecium uses an alternative genetic code in which two universal stop codons (UAA, UAG) are reassigned to glutamine. For the purposes of initial BLAST based binning ORFs were called and translated using both universal encoding and this alternative code. However, for the later BLAST-based bin accuracy verification purposes and subsequent automated phylogeny based binning all ORFs were initially only called using the alternative ciliate encoding. The ciliate encoding was used instead of universal because it was spuriously extended transcripts were considered favourable to falsely truncated ones. This greatly reduced redundancy in the later binning analyses.

4.3.5 Transcript Binning

Initial BLAST based bins

Initially, 10,000 randomly chosen, translated transcripts from an earlier iteration of the assembly process were binned into their predicted source - Host (H), Endosymbiont (E), Food (F) and Unknown (U).

Each of the assembled transcripts were BLASTP-ed against a database consisting of the following predicted proteomes: *Chlorella* NC64A, *Chlamydomonas reinhardtii*, *Coccomyxa* C169, *Paramecium tetraurelia*, *Tetrahymena thermophila*, *Arabidopsis thaliana*, *Homo sapiens* (help- ing to identify contamination), *Saccharomyces cerevisiae*, *Schizosaccharomyces pombe*, *Bacillus cereus* ATCC 14579, *Escherichia coli* 536, *Escherichia coli* O157 H-7, *Salmonella typhimurium* LT2 and *Escherichia coli* K-12 (the last 5 genome datasets helping to identify food bacterial genes). Then initial bins were determined as follows:

- Endosymbiont (E): Transcript's highest scoring BLAST hit at an expectation of $\leq e^{-50}$ was to *Coccomyxa*, *Chlamydomonas* or *Chlorella*. Or transcript's highest scoring hit at e^{-20} was one of those species and the longest likely coding region in the transcript was using the universal codon table.
- Host (H): Transcript's highest hits at $\leq e^{-50}$ were to *Paramecium tetraurelia* or *Tetrahymena thermophila*. Or highest hit at e^{-20} was one of those species and longest likely coding region was using the *Tetrahymena* codon table.
- Food (F): Transcript's highest scoring BLAST hit at an expectation of $\leq e^{-50}$ was to one of the *E. coli* species or *Salmonella*. Or transcript's highest scoring hit at e^{-20} was one of those species and the longest likely coding region in the transcript was using the universal codon table.
- Unknown (U): highest scoring hits to *Arabidopsis*, *Homo sapiens*, *Saccharomyces* or *Schizosacharomyces* or any sequence not fitting into the above categories.

The accuracy of the BLAST based binning was then determined by generating phylogenies using the method described below. Resultant phylogenies were then manually parsed and assessed for phylogenetic congruence with their bin. For example, do host binned sequences predominantly branch with other ciliate sequences? Do endosymbiont binned sequences mainly branch with archaeplastida sequences?

Automated Phylogeny Generation Pipeline - Dendrogenous

To rapidly generate phylogenies an established lab tree generation pipeline, known as "Darren's Orchard" (Richards et al., 2009) was modified and ported to python3 from perl5. This new pipeline "Dendrogenous" takes in a multi-fasta set of inputs and a set of genomes to search against. For each input sequence:

1. The user specified genome database is queried using BLASTP
2. The results are parsed and a fasta file of putative homologues is created, with inputs that have fewer than a specified number of hits (default of 5) ejected.
3. A multiple sequence alignment (MSA) is created from this fasta using Kalign (chosen for its speed) (Lassmann et al., 2009)
4. This MSA is then masked automatically to remove ambiguous sites using TrimAL (Capella-Gutiérrez et al., 2009) and masked alignments with fewer than a specified number of sites (default of 30) are ejected from the pipeline.

5. A rapid maximum-likelihood phylogenetic tree is generated using FastTree2 (Price et al., 2010)

6. Finally, encoded taxonomic information is recovered from the "cider" database of the original "Darren's Orchard" pipeline and the trees are named with full species names.

The two key improvements are that of full and efficient parallelisation of the tree generation process (see fig. 4.3.1) and increased use of filestreams to pass data between pipeline stages. This latter modification reduces costly and slowly file reading and writing operations.

In the process of creating this modified phylogenetic pipeline I upgraded the general purpose python phylogenetic toolkit ETE (Huerta-Cepas et al., 2010) to support python3. As ETE is an open source project I submitted these changes to the maintainer and they have subsequently been merged into the master. These changes compose a significant proportion of the latest major release version of this toolkit `https://github.com/jhcepas/ete/pull/105`.

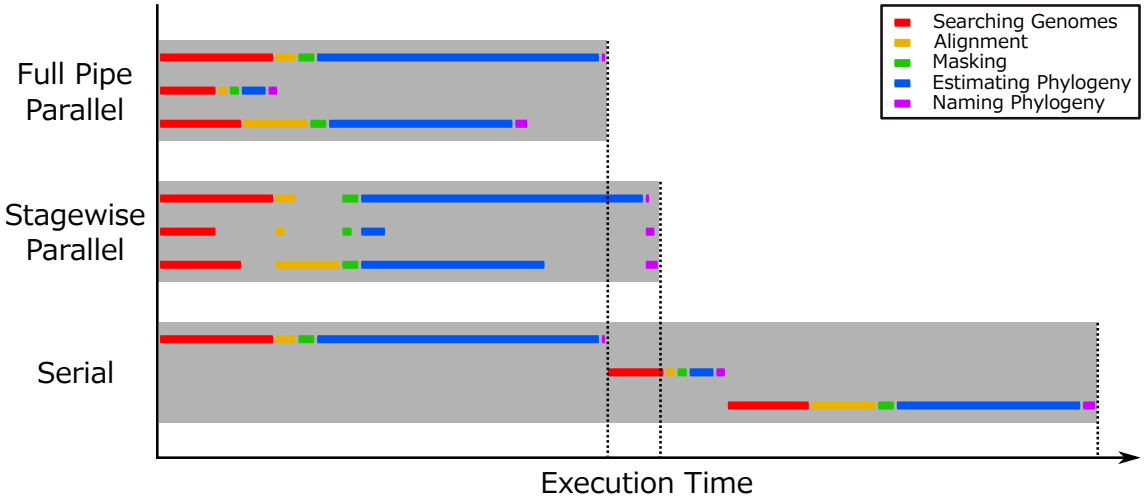

Figure 4.3.1: A explanatory plot showing 3 different possible architectures for a tree generation pipeline. Serial, in which each phylogeny is run one after another. This form makes no use of multiprocessing facilities, however, a moderate but significant performance improvement can be achieved by allowing each stage in the pipeline to utilise multiple cores i.e. the trees are generated serially but during their generation alignment and blasting making use of multiple processors. Stagewise parallel, where for example, all alignments for each input sequence are run side-by-side and masking begins once the last sequence has finished alignment. The disadvantage of this is a single slow stage for one input sequence can hold up the whole pipeline and leave resources idle. Additionally, by running many of the same type of process at the same time, each with similar resource requirements, the risk of hardware bottlenecking is increased compared to a more heterogenous load. Finally, fully parallel runs each input sequence through the pipeline stage-by-stage separately from all other inputs to the pipeline. This prevents blocking and allows efficient using of resources.

40 genomes covering the diversity of the tree of life, with a particular focus on green algal and ciliate representatives were selected for this phylogenetic generation: *Arabidopsis thaliana, Chlamydomonas reinhardtii, Ostreococcus tauri, Micromonas pusilla CCMP1545, Chlorella variabilis NC64A Chlorella vulgaris C-169, Physcomitrella patens, Saccharomyces cerevisiae S288C, Neurospora crassa OR74A, Homo sapiens, Mus musculus, Dictyostelium discoideum, Paramecium caudatum, Paramecium tetraurelia, Tetrahymena thermophila macronucleus, Oxytricha trifallax, Toxoplasma gondii, Guillardia theta, Bigelowiella natans, Emiliania huxleyi CCMP1516, Aureococcus anophagefferens, Ectocarpus siliculosus, Schizosaccharomyces pombe, Bacillus cereus ATCC 14579, Escherichia coli str. K-12 substr. MG1655, Escherichia coli O157 H7 str. Sakai, Salmonella enterica subsp. enterica serovar Typhi str. CT18, Amy-*

colatopsis mediterranei U32, Aquifex aeolicus VF5, Borrelia burgdorferi B31, Chlamydophila pneumoniae CWL029, Chlorobium tepidum TLS, Deinococcus radiodurans R2, Caulobacter crescentus CB15, Sulfolobus islandicus M.14.25, Nanoarchaeum equitans Kin4-M, Haloferax mediterranei ATCC 33500, Methanococcus maripaludis S2, Cenarchaeum symbiosum A.

Automated Phylogenetic Transcript Binning - Arboretum

In order to automate phylogeny based transcript binning the 10,000 manually verified phylogenetic bins from the initial BLAST based binning and analysis were used as a training dataset for supervised classification.

The supervised classification was implemented in a script called "Arboretum" The cardinalities of each label in training set was relatively balanced (i.e. all within the same order of magnitude) 1975 endosymbiont phylogenies, 2600 host, 3456 food, and 1969 unknown.

"Arboretum" parses phylogenies and identifies the k (default of 10) nearest branches to the seed transcript the phylogeny was generated from. The species of these closest leaves is queried taxonomically using the NCBI taxonomy local database implemented in the ETE toolkit. With a set of look-up filters e.g. sequences from ciliates can be defined as "host-like", a set of vectors is created for each phylogeny. These are N-dimensional vectors where N is the number of class labels being used. For example, in this specific case: "endosymbiont", "host", "food/bacterial", and "unknown". The magnitude of each dimension is the summed reciprocal phylogenetic distance between the root node and all of the nearest branches that have been identified as being indicative of a certain class. Specifically, if $\gamma(x, y)$ is the phylogenetic distance between the terminal nodes x and y, $\psi(x)$ represents the look-up filters and returns the label of the terminal node x e.g. "host". and δ_{ij} is the Kronecker delta[2], then for a phylogeny A:

$$X_{A,class} = \sum_{k=1}^{K} \left(\frac{1}{\gamma(A_k, A_{root})} * \delta_{\psi(A_k),class} \right)$$

Where in this specific example "class" is one of the set $\{endosymbiont, host, food, unknown\}$ although naturally the classes will be encoded using integer labels. Therefore, the dimensions of X are $|A|, |class|$ i.e. the number of training phylogenies by the number of pre-defined class labels.

Training data was visualised using Radial Visualisation (RadViz) (Hoffman et al., 1997; Fayyad et al., 2001). RadViz is a form of radial co-ordinate visualisation that non-linearly maps a set of N-dimensional points onto a plane for easy 2D visualisation. This mapping operates on the physical principle of "springs" anchored evenly around a unit circle with "spring" stiffness determined by the normalised $0 - 1$ value of that dimension for that point. Each point therefore rests at the point of mechanical equilibrium between the "springs" (Novakova, Lenka and Stepankova, 2006).

1,000 vectors from this training set were held out to form the test set and all models were then trained using 5-fold cross-validation (CV) on the remaining 9,000 training vectors. We evaluated Support Vector Machines

[2] $\delta_{ij} = \begin{cases} 1, & i = j \\ 0, & i \neq j \end{cases}$

(SVMs) with both linear and radial basis function (RBF) kernels (Vapnik and Lerner, 1963), naive Bayes, K-neighbours, Decision Trees (DT) (Quinlan, 1986), DTs ensembles in a Random Forests (Breiman, 2001) and Extremely Randomised Trees (ExtraTrees) (Geurts et al., 2006), adaptively boost (AdaBoost) DTs (Freund and Schapire, 1997), Linear Discriminant Analysis (LDA) and Quadratic Discriminant Analysis (QDA). Models were trained and hyperparameters were optimised using a randomised search instead of the less efficient grid search (Bergstra and Bengio, 2012) using Bayesian optimisation in the HPOlib library (Eggensperger et al., 2013; Komer et al., 2014) over the CV-folds. Finally, each model was assessed using the held out test set and performance was evaluated by inspection of label-wise classification reports containing various metrics e.g. label F1-scores and confusion matrices.

The best performing model and hyperparameters were then used to classify the remaining unlabelled phylogenies.

TAXAassign comparison

To assess the performance of supervised learning and phylogeny based system (Arboretum) described above a stand-alone sequence identity binning tool TAXAssign (`https://github.com/umerijaz/TAXAassign`) was run against the 70,605 CDS sequences.

TAXAssign queried each CDS against the entire NCBI nt database. The nt BLAST database was downloaded using update_blastdb.pl script `http://www.ncbi.nlm.nih.gov/blast/docs/update_blastdb.pl` and TAXAssign ran BLASTN in parallel (using GNU parallel (Tange, 2011)) with a maximum of 10 reference matches per CDS a minimum necessary percentage identity for assignment to a given taxonomic level of 60, 70, 80, 95, 95, and 97 for Phylum, Class, Order, Family, Genus and Species respectively.

Results were then tabulated and compared with the Dendrogenous-Arboretum assignments.

4.4 Results

4.4.1 Library contamination screening

Libraries were screened for inclusion in assemblies by inspection of their taxonomic profiles (see table 4.4.1 and table 4.4.2) as determined by DueyDrop and their GC% probability densities (via KDE).

The GC density estimates of the single cell libraries show a clear bimodal GC density with a high 70GC% peak (fig. 4.4.1) in all dark single cell libraries. With the exception of Dark1-2 and Dark2-3 this high GC peak is a greater density than the expected peak 30-50GC% (from known GC% found in genomes of sequenced relatives of both host and endosymbiont).

When these KDE are compared to the densities estimated from the Q20 trimmed bulk reads (bottom right pane in fig. 4.4.1) and raw bulk RNAseq reads from (Kodama et al., 2014) (see fig. 4.4.2) it is apparent that this high GC% peak is likely originating from a high GC% bacterial contaminant in the Dark single cell libraries.

One other observation when comparing the bulk RNAseq analyses to the single cell libraries is that the main

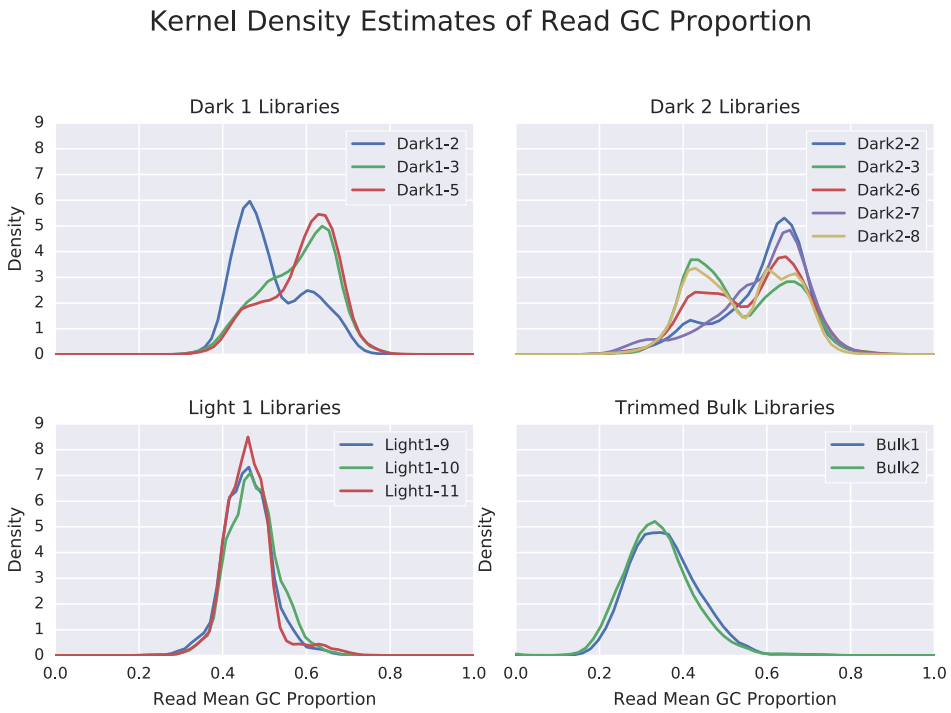

Figure 4.4.1: Probability densities of per-read GC proportions for the raw data (apart from pre-trimmed bulk explained previously) from each sequenced library. Densities were derived using Kernel Density Estimation implemented in Seaborn. Dark 1 (Dark1-2, Dark1-3, and Dark1-5) and Light 1 (Light1-9, Light1-10, Light1-11) were sc-RNAseq from the first round of SCTs sampled during the mid-dark and light culture phases. Similarly, Dark 2 (Dark2-2, Dark2-3, Dark2-6, Dark2-7, Dark2-8) were the libraries sampled in the dark from the second round of SCT. Bulk1 and Bulk2 are the bulk RNAseq libraries sequenced under lit and dark conditions. The bulk and single cell light libraries demonstrate similar shaped distributions although the bulk has a greater proportion of low GC% reads potentially representing more *Paramecium* derived data. All single cell dark libraries demonstrate a bimodal density with up to the majority of reads deriving from an unknown high 70% GC population. The dark single cell libraries exhibiting a relatively larger peak at 70% GC than at 40-50%GC (i.e. Dark1-3, Dark1-5, Dark2-2, Dark2-7) were the same libraries which were identified as potentially contaminated in taxonomic screening (see table 4.4.1).

GC peak is slightly lower in the bulk (and Kodama dataset), around 30GC% versus 45-50GC%. This possibly indicates a greater proportion of reads deriving from the low GC% *Paramecium bursaria* host and fewer from the 50GC% endosymbiont in bulk libraries relative to single cell libraries.

By comparing the results of the KDE GC analysis with and without read trimming it is apparent that trimming of reads makes nearly no difference in the density estimates. The KDE of Q30 sliding window trimmed single cell reads in fig. 4.4.3 is nearly identical to that of the raw reads fig. 4.4.1.

The taxonomic profiles of single cell (table 4.4.1) and bulk libraries (table 4.4.2) generated by DueyDrop are summarised in the tables below. It is readily apparent that Dark1-3, Dark1-5, Dark2-2, and Dark2-7 display an aberrantly low number of reads aligning to known alveolate (or even eukaryote) sequences. Forward and reverse reads within a library display similar profiles with a slightly lower proportion of hits in the reverse reads. This can likely be attributed to the lower read quality found in reverse reads relative to forward reads in paired-end Illumina sequencing.

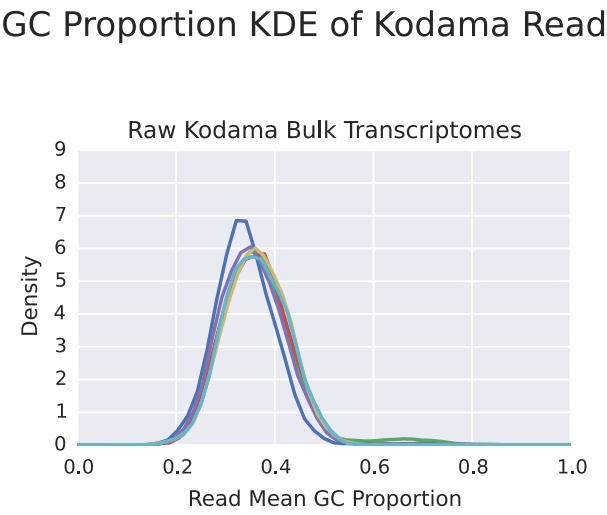

Figure 4.4.2: Probability density of the per-read GC proportion for 6 raw libraries derived from (Kodama et al., 2014) transcriptome analysis of a different *P. bursaria* species (Yad1g) with and without its *Chlorella variabilis* 1N endosymbiont. Individual libraries are indicated in the key using their DDBJ accession. This dataset displays densities relatively similar to the bulk RNAseq conducted in this project - "Trimmed Bulk Libraries" in fig. 4.4.1.

The bulk libraries demonstrate a very low level of hits compared to single cell libraries (see table 4.4.2), to the point where if they were single cell libraries they would be taxonomically excluded. However, it should be noted that the bulk libraries were sequenced on a Gene Analyzer II and are on average half the length of single cell reads (76bp vs 150bp). Due to the difficulty aligning short reads to references the difference between libraries may be attributable to this alone. Additionally, the vast majority of the lower number of hits do align to eukaryote (and alveolate) taxa consistent with an non-contaminated library.

To identify the likely source of the high GC% contamination and to assess how representative the taxonomic profiling of small random subsamples of reads $\leq 1\%$ to full scale analyses Krona was used to create interactive hierarchial plots of the taxonomic profiles[3] From this, Rhizobia species are the most prevalent high GC% species found in the libraries with this high 70GC% peak in the KDE plots and therefore are the most likely source of this particular aspect of contamination.

Therefore, small random subsamples are representative of the full library and read-level taxonomic assignment can be used to screen single cell libraries for contamination.

4.4.2 Read pre-processing

Trimming Optimisation

The optimal trimming threshold was determined by a combination of read mapping statistics against 3 preliminary reference assemblies as well as the impact on resultant *de novo* assemblies at that threshold.

A rapid decrease in the number of concordantly mapping PE reads (i.e. within insert distance of one another) was observed above a Q30 quality threshold. This proves true regardless of the reference assembly being mapped

[3]Accessible at http://finlaymagui.re/dueydrop_analysis

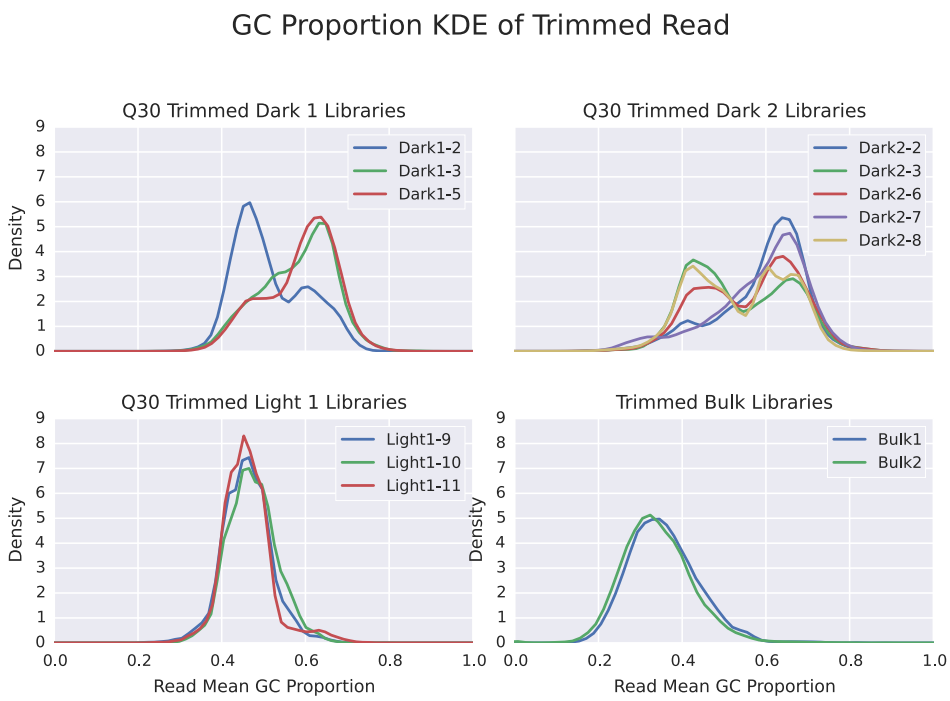

Figure 4.4.3: Probability densities of per-read GC proportions for trimmed reads. To ensure probability densities estimated in fig. 4.4.1 weren't biased by low quality ambiguous reads the same analysis was repeated using reads trimmed using a sliding window approach with a stringent average quality threshold of Q30. In all cases the densities produced appear near identical to the analysis of the raw data.

to (see fig. 4.4.7). Q30 relative to Q20 appears to induce a very slight decrease in total number of mapping reads but not drastically so.

Additionally, naive assemblies in Trinity of taxonomically screened single cell libraries at different sliding window quality threshold trims of Q5, Q20, and Q30 (table 4.4.3) were created. These show that more permissive trims (Q5 and Q20) lead to a greater number of assembled bases and transcripts however the likelihood of these assemblies are also lower than that generated using the more conservative Q30 trim. However, it should be noted that the difference in the number and size of assembled transcripts at different thresholds was less than was found using different assemblers and assembly parameters.

Therefore, due to increasing the assembly likelihood while only very marginally decreasing the number of contigs and mapping reads relative to more permissive trims Q30 was determined to be the optimal trimming threshold. It can be considered from this data that Q30 forms a maximum feasible stringency for trimming.

GC Partitioning

GC partitioning was conducted on Q30 trimmed reads using K-means clustering as implemented in the parKour tool described above to attempt to remove GC% rich contamination from single cell libraries.

The 2 different clustering schemes attempted using 2 and 3 target clusters. Additionally, both clustering schemes were also run with an initial overclustering factor of 3 i.e. parKour originally found 6 and 12 clusters

SCT Library	*PE*	Eukaryote	Bacteria	Alveolate	Viridiplantae		Total Hits
Light1-9	*R1*	51.89 +/- 0.45	9.37 +/- 0.26	25.15 +/- 0.71	7.45 +/- 0.33		69.49 +/- 0.37
	R2	51.75 +/- 0.25	8.82 +/- 0.24	24.85 +/- 0.56	7.49 +/- 0.21		68.75 +/- 0.29
Light1-10	*R1*	46.35 +/- 0.56	15.72 +/- 0.46	22.96 +/- 0.24	6.94 +/- 0.26		68.73 +/- 0.30
	R2	46.12 +/- 0.83	15.14 +/- 0.48	23.13 +/- 0.38	6.99 +/- 0.37		68.73 +/- 0.30
Light1-11	*R1*	58.28 +/- 0.47	3.62 +/- 0.12	28.68 +/- 0.43	8.20 +/- 0.40		71.38 +/- 0.49
	R2	57.74 +/- 0.27	3.50 +/- 0.10	28.23 +/- 0.36	8.41 +/- 0.31		70.42 +/- 0.20
Dark1-2	*R1*	28.64 +/- 0.51	22.88 +/- 0.61	12.23 +/- 0.28	4.93 +/- 0.19		60.31 +/- 0.49
	R2	28.29 +/- 0.24	21.06 +/- 0.21	12.13 +/- 0.28	4.87 +/- 0.34		57.65 +/- 0.35
Dark1-3	*R1*	9.48 +/- 0.43	25.07 +/- 0.42	2.15 +/- 0.13	2.60 +/- 0.27		41.43 +/- 0.68
	R2	8.89 +/- 0.19	23.11 +/- 0.52	2.13 +/- 0.16	2.45 +/- 0.18		38.50 +/- 0.46
Dark1-5	*R1*	5.56 +/- 0.19	23.99 +/- 0.44	1.07 +/- 0.07	2.89 +/- 0.11		36.72 +/- 0.33
	R2	4.94 +/- 0.21	21.75 +/- 0.53	1.02 +/- 0.11	2.33 +/- 0.17		33.06 +/- 0.52
Dark2-2	*R1*	12.32 +/- 0.25	9.81 +/- 0.19	3.73 +/- 0.16	4.33 +/- 0.17		27.65 +/- 0.47
	R2	11.53 +/- 0.15	9.00 +/- 0.17	3.67 +/- 0.22	3.74 +/- 0.12		25.71 +/- 0.39
Dark2-3	*R1*	32.07 +/- 0.31	7.43 +/- 0.15	12.81 +/- 0.21	4.71 +/- 0.21		48.42 +/- 0.53
	R2	32.47 +/- 0.24	6.68 +/- 0.21	13.11 +/- 0.43	4.58 +/- 0.12		47.92 +/- 0.28
Dark2-6	*R1*	24.11 +/- 0.28	8.55 +/- 0.11	9.04 +/- 0.35	5.27 +/- 0.15		41.69 +/- 0.45
	R2	22.89 +/- 0.55	7.44 +/- 0.17	8.74 +/- 0.49	4.36 +/- 0.24		38.85 +/- 0.58
Dark2-7	*R1*	9.96 +/- 0.24	16.89 +/- 0.27	4.22 +/- 0.24	2.83 +/- 0.17		37.06 +/- 0.40
	R2	8.77 +/- 0.18	15.00 +/- 0.43	3.94 +/- 0.14	2.16 +/- 0.11		32.86 +/- 0.29
Dark2-8	*R1*	28.24 +/- 0.48	4.45 +/- 0.13	12.00 +/- 0.32	4.69 +/- 0.06		40.50 +/- 0.37
	R2	28.22 +/- 0.47	4.30 +/- 0.22	11.98 +/- 0.37	4.32 +/- 0.24		40.05 +/- 0.22

Table 4.4.1: Taxonomic profiles of raw single cell libraries generated using "DueyDrop". All values are percentage of reads mapping to that category +/- the standard deviation between sample replicates. The analysis was conducted for both forward and reverse reads from each library (indicated as R1 and R2 in the paired-end (PE) column). Libraries highlighted in bold were those excluded from subsequent analysis on the basis of their very low numbers of reads identifiable as eukaryotic (or specifically alveolate or archaeplastida). All forward and reverse read pairs display similar profiles to one another suggesting the problem of "MDA chimeras" may be minor.

Bulk Library	*PE*	Eukaryote	Bacteria	Alveolate	Viridiplantae	Total Hits
Light	*R1*	9.66 +/- 1.55	0.18 +/- 0.13	6.28 +/- 1.41	0.86 +/- 0.3	10.10 +/- 1.48
	R2	9.62 +/- 0.81	0.26 +/- 0.09	6.58 +/- 0.36	1.04 +/- 0.41	10.16 +/- 0.95
Dark	*R1*	4.90 +/- 0.78	0.36 +/- 0.11	3.14 +/- 0.58	0.50 +/- 0.16	5.40 +/- 0.93
	R2	5.50 +/- 1.25	0.22 +/- 0.19	3.82 +/- 0.81	0.50 +/- 0.12	6.02 +/- 1.22

Table 4.4.2: Taxonomic profile of the two trimmed (Q20) bulk transcriptome libraries generated using "DueyDrop". All values are the percentage of reads mapping to that taxonomic category +/- the standard deviation between sampling replicates. The analysis was conducted for both forward and reverse reads from each library (indicated as R1 and R2 in the paired-end (PE) column). Overall only a very small number of bulk reads could be assigned to any taxonomic class by "DueyDrop".

Trim Threshold	Number of Transcripts	Bases Assembled	Assembly Likelihood $(-\log)$	
Q5	112,182	52,511,552	$-3.168 * 10^{10}$	
Q20	107,955	50,809,686	$-3.015 * 10^{10}$	
Q30	99,784	47,313,963	$-2.832 * 10^{10}$	

Table 4.4.3: Comparison of Trinity assemblies of taxonomically screened single cells reads (no bulk reads) at 3 different sliding window minimum average quality trimming thresholds. Trimming largely does not cause a major difference between assemblies in terms of number of contigs recovered or overall assembly likelihoods. Harsher (Q30) trims result in slightly smaller but slightly more likely assemblies than permissive trims (Q5).

and then merged them to produce the target 2 and 3 clusters respectively.

2 and 3 target clusters with and without an initial overclustering factor of 3 (i.e. initially finding 6 and 12 clusters originally before merging to produce final 2 and 3 cluster targets).

Therefore, over-clustering made a minimal effect on cluster centroids and read assignment.

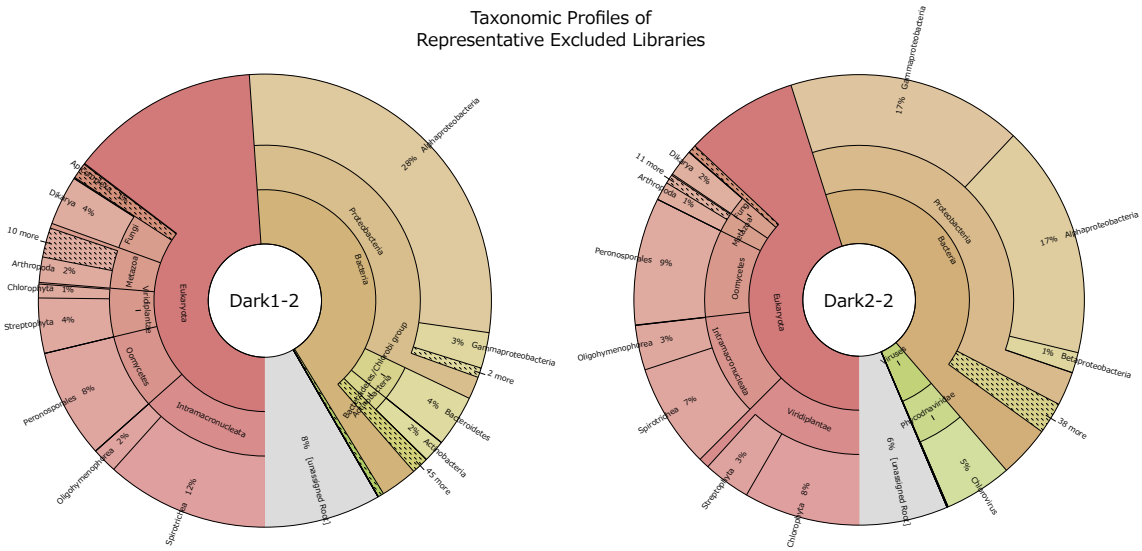

Figure 4.4.4: Krona visualisation of taxonomic profiles of two representative single cell libraries (Dark1-2, Dark2-2) that were excluded from further analysis due to aberrant profiles (typically large proportion of reads being assigned to Bacteria than Eukaryota). Note that nearly 50% of each library is identified as bacterial.

Library	Number of raw PE Reads	Number of Q30 trimmed PE Reads
Dark1-2	$6.460 * 10^7$	$3.355 * 10^6$
Dark2-3	$2.243 * 10^7$	$1.478 * 10^7$
Dark2-6	$2.431 * 10^7$	$1.443 * 10^7$
Dark2-8	$2.761 * 10^7$	$1.866 * 10^7$
Light1-9	$1.524 * 10^7$	$1.382 * 10^7$
Light1-10	$1.614 * 10^7$	$1.478 * 10^7$
Light1-11	$1.474 * 10^7$	$1.334 * 10^7$

Table 4.4.4: Summary of the library size of the taxonomically selected single cell libraries before and after trimming at a minimum average SLIDINGWINDOW quality threshold of Q30. Of interest, Dark1-2 was generally of poor quality and thus was disproportionately minimised by trimming. Additionally, the two bulk RNAseq libraries were trimmed at Q20 in FastQ-MCF resulting in total library sizes of $2.458*10^7$ and $2.779*10^7$ respectively

Unfortunately, as might have been foreseen, the resultant assemblies from individual read clusters displayed high levels of fragmentation regardless of the clustering regime used. For example, in the case of the 2 cluster (without over-clustering) and subsequent individual Trinity-based assemblies resulted in 268,806 transcripts of marginally shorter average length than the equivalent un-pre-partitioned assembly (99,784 transcripts).

The same pattern, consistent with assembly fragmentation, was observed when only dark single cell libraries were clustered using 2 or 3 clusters. Therefore, GC-based pre-assembly read partitioning proved incapable of improving the assembly of this highly heterogeneous RNAseq dataset.

Error Correction

Error correction was attempted on both lightly trimmed (Q5) and harshly trimmed (Q30) taxonomically selected SCT reads.

Bayeshammer, as implemented in the Spades genome assembler, even on permissively trimmed ($Q > 5$) reads corrected only a maximum 0.0007% of reads in the 7 taxonomically selected SCT libraries. As this affected on the order of 10s of reads it was not considered worth pursuing this tool further.

"SEECER", an RNA-Seq specific error correction tool was used to correct lightly trimmed (Q5) and harshly

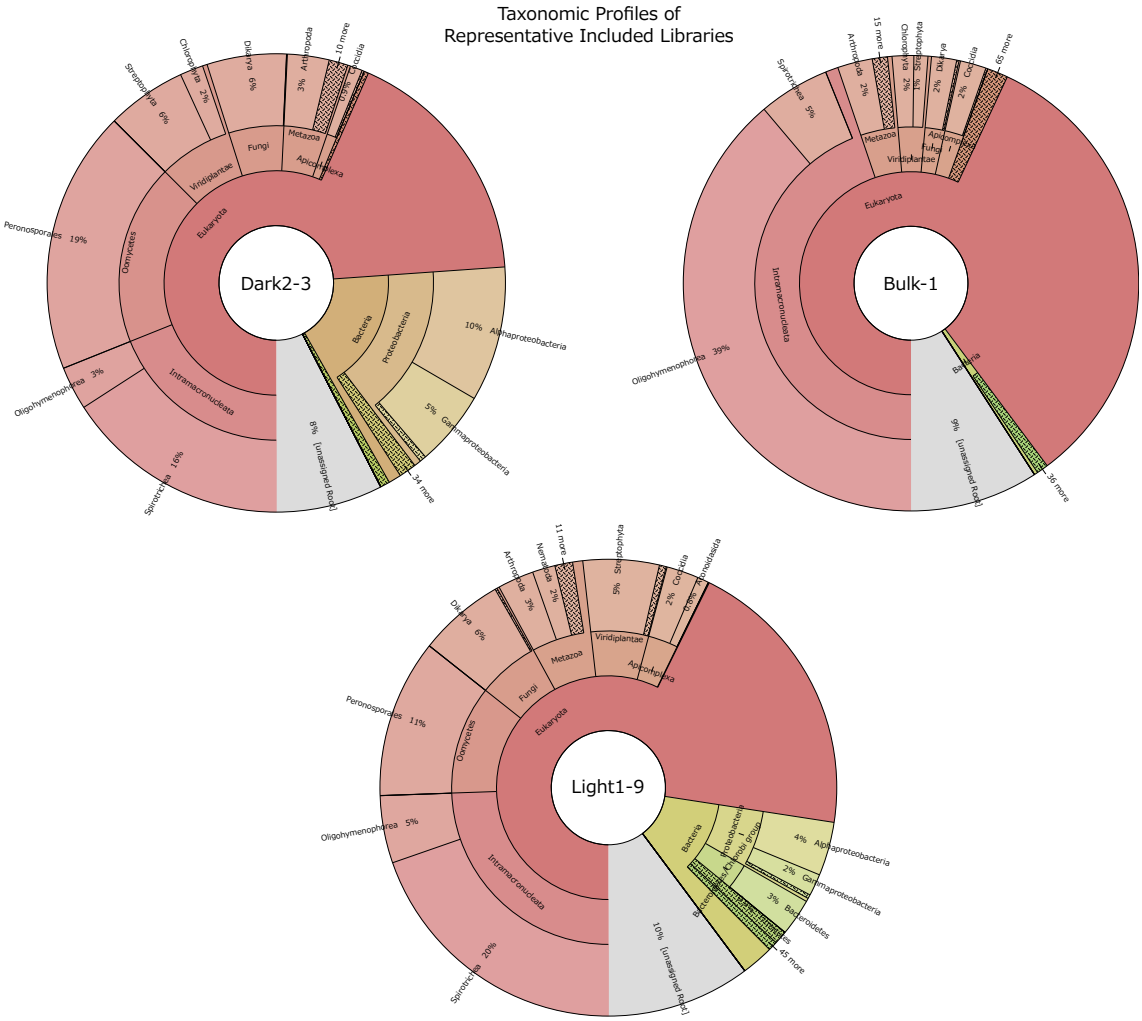

Figure 4.4.5: Krona visualisation of the taxonomic profiles of representative RNAseq libraries (Bulk1, Dark2-3, and Light1-9) that were retained in the analysis after taxonomic screening. The key thing this figure shows is that in retained libraries the vast majority of reads were identified as eukaryotic in origin.

trimmed (Q30) SCT reads. Approximately, 5.37% of Q5 trimmed SCT reads were corrected in "SEECER". 0.51% of Q30 trimmed SCT reads were corrected.

Trinity assemblies of taxonomically selected single cell libraries (without bulk libraries) were then compared with and without "SEECER" error correction (see table 4.4.6).

As can be observed, error correction of SCT reads made minimal effect in the overall likelihood of assemblies for this dataset even with lightly trimmed reads. Error corrected Q5 trimmed reads performed worse than Q30 trimmed reads without error correction. Additionally, Q30 trimmed reads generated marginally less likely assemblies with error correction than without.

Therefore, error correction was considered ineffective for this dataset and thus was not used used for further analysis. Instead, we elected to use uncorrected, taxonomically selected, Q30 trimmed reads from this point on.

Digital Normalisation

Digital normalisation and removal of likely erroneous k-mers (i.e. low abundance) via Khmer reduced the total input reads from the Q30 trimmed taxonomically filtered SCT and bulk libraries from $2.912 \cdot 10^8$ to $8.473 \cdot 10^6$

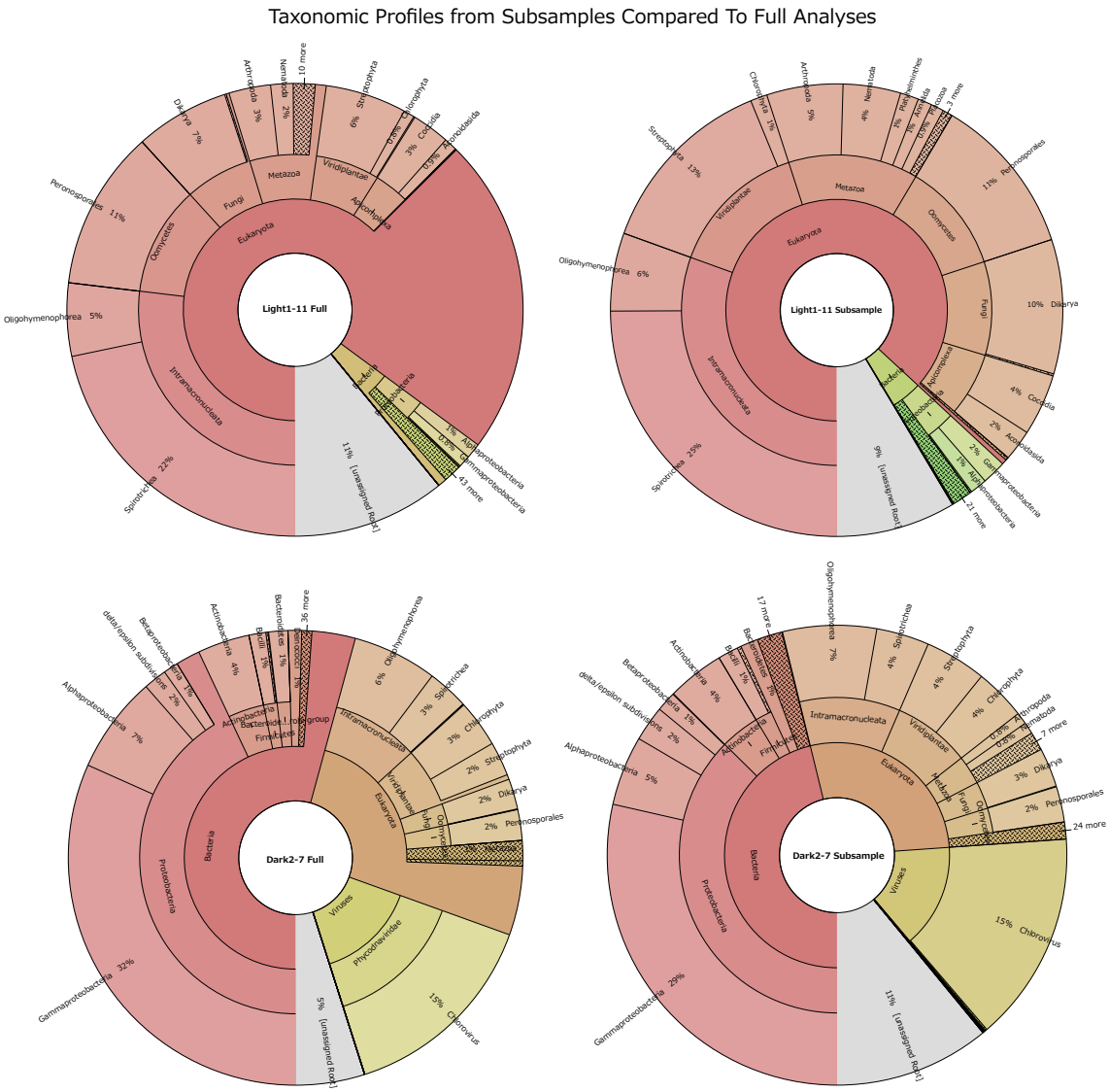

Figure 4.4.6: Comparison of taxonomic profiles derived from small $\leq 1\%$ random subsamples of libraries compared to profiles generated using the full library. Light1-11 and Dark2-5 are used as representative examples as they display the trends common for all single cell libraries. All subsamples demonstrated taxonomic profiles with relatively similar proportions to full analyses. For example, in the Light1-11 subsample of reads with hits the proportion of eukaryote to Bacteria was 87:4 % vs 85:4% of the root for the full analysis. Similarly the ratios for Dark2-7 shown eukaryote to bacteria are 26:54 for full analysis and 28:46 for subsample. The key difference is the assignment of a greater proportion of reads to intermediate taxonomic levels in the full analyses due to the difference in resolution of multiple hits per read. Principally, the full library analyses retain all hits and assign level based on a lowest common ancestor algorithm whereas the subsample analysis just uses the top hit.

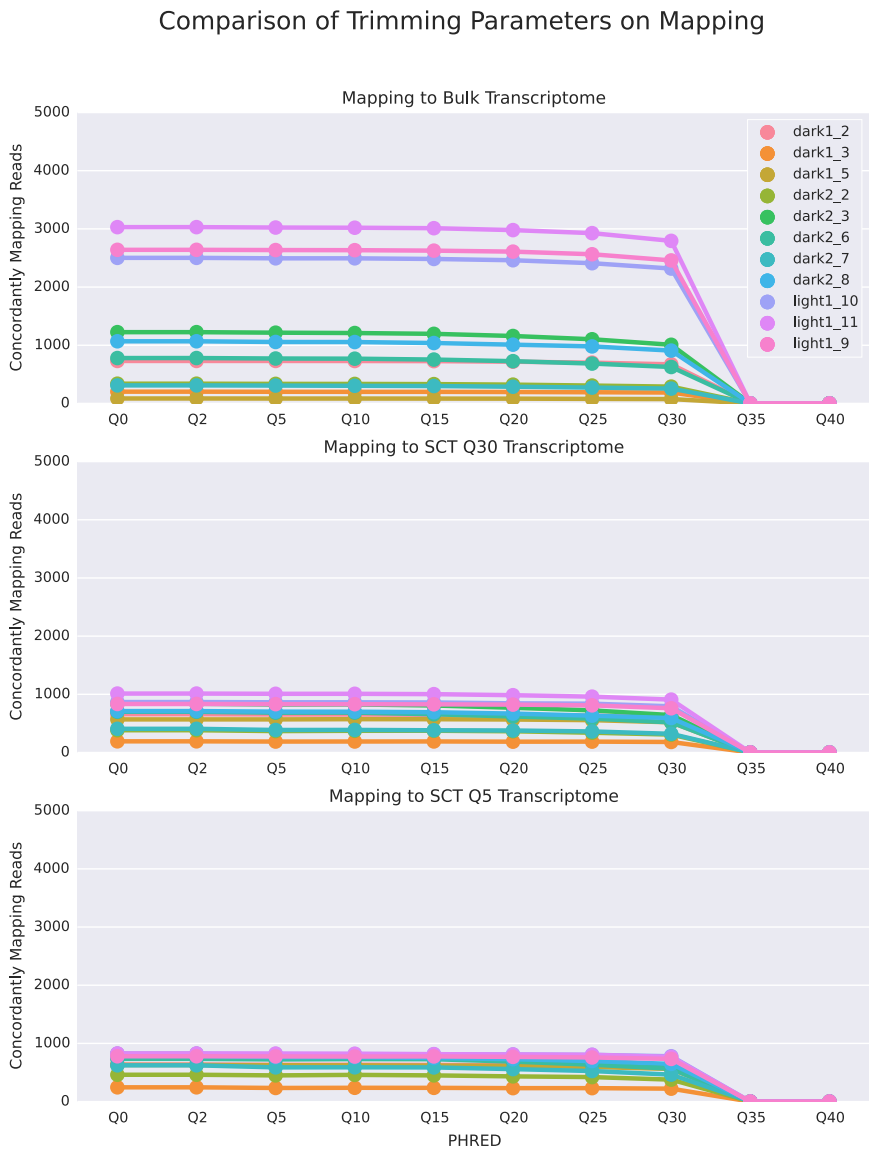

Figure 4.4.7: Assessment of the optimal minimum average quality threshold in Trimmomatic's sliding window (size 4) trim. Plots display the number of concordantly mapping reads (i.e. the forward and reverse read map to assembly at a distance of approximately their insert) at a range of different trimming thresholds. 5000 randomly sampled PE reads from each single cell library are mapped against 3 different reference assemblies. The key finding is above a threshold of Q30 there is a huge decrease in the number of mapping reads.

Clustering Scheme	Centroids	Number of Reads Assigned
2	(0.6674, 0.6177)	57.3M
	(0.4557, 0.4393)	81.6M
2 (over-clustering)	(0.6672, 0.6168)	57.7M
	(0.4555, 0.4392)	81.2M
3	(0.5363, 0.5092)	44.0M
	(0.6924, 0.6394)	43.3M
	(0.4231, 0.4096)	51.6M
3 (over-clustering)	(0.5365, 0.5090)	43.9M
	(0.6921, 0.6396)	43.6M
	(0.4235, 0.4098)	51.7M

Table 4.4.5: Final cluster centroids and number of reads assigned to each cluster in parKour using various run settings. Centroids are the mid-point of each cluster, therefore in the 2 cluster scheme "parKour" identified one cluster of reads centered around 66.74% GC for the forward read and 61.77% for the reverse read. Note that overclustering made a minimal impact on cluster location.

Trim Threshold	**Number of Transcripts**	**Bases Assembled**	**Assembly Likelihood** $(-\log)$
Q5	112,182	52,511,552	$-3.168 \cdot 10^{10}$
Q5 SEECER Corrected	111,853	51,847,128	$-3.147 \cdot 10^{10}$
Q30	99,784	47,313,963	$-2.912 \cdot 10^{10}$
Q30 SEECER Corrected	96,494	46,312,469	$-2.995 \cdot 10^{10}$

Table 4.4.6: Naive Trinity assembly of Q5 and Q30 trimmed taxonomically selected single cell libraries with and without SEECER error correction. While assembly likelihood increases after error correction for Q5 trimmed reads it is still lower than Q30 uncorrected. For Q30 trimmed reads error correction marginally decreases assembly likelihood.

paired reads.

Of those, $6,231 \cdot 10^6$ derive from the bulk and $2.253 \cdot 10^6$ from single cell libraries. Therefore, as Q30 trimmed single cell libraries comprised $9.318 \cdot 10^6$ paired end reads and bulk libraries consisted of $52.377 \cdot 10^6$ reads digital normalisation and abundance filtering resulted in a retention of 2.418% of single cell PE reads and 11.891% of bulk PE reads.

Of these surviving single cell PE reads $9.762 * 10^5$ were from the 3 selected light libraries (Light1-9, Light1-10, and Light1-11) and $1.277 * 10^6$ were derived from the dark libraries (Dark1-2, Dark2-3, Dark2-6, and Dark2-8). Therefore, abundancy filtering and digital normalisation did not disproportionately remove light or dark single cell reads.

This Khmer based pre-processing had a very positive effect on assembly likelihoods. The standard Trinity assembly improved in likelihood by an order of magnitude while assembling more transcripts of near equal length (based on median contig length). The Khmer processed assembly marginally increased median contig length at the expense of a lower N50.

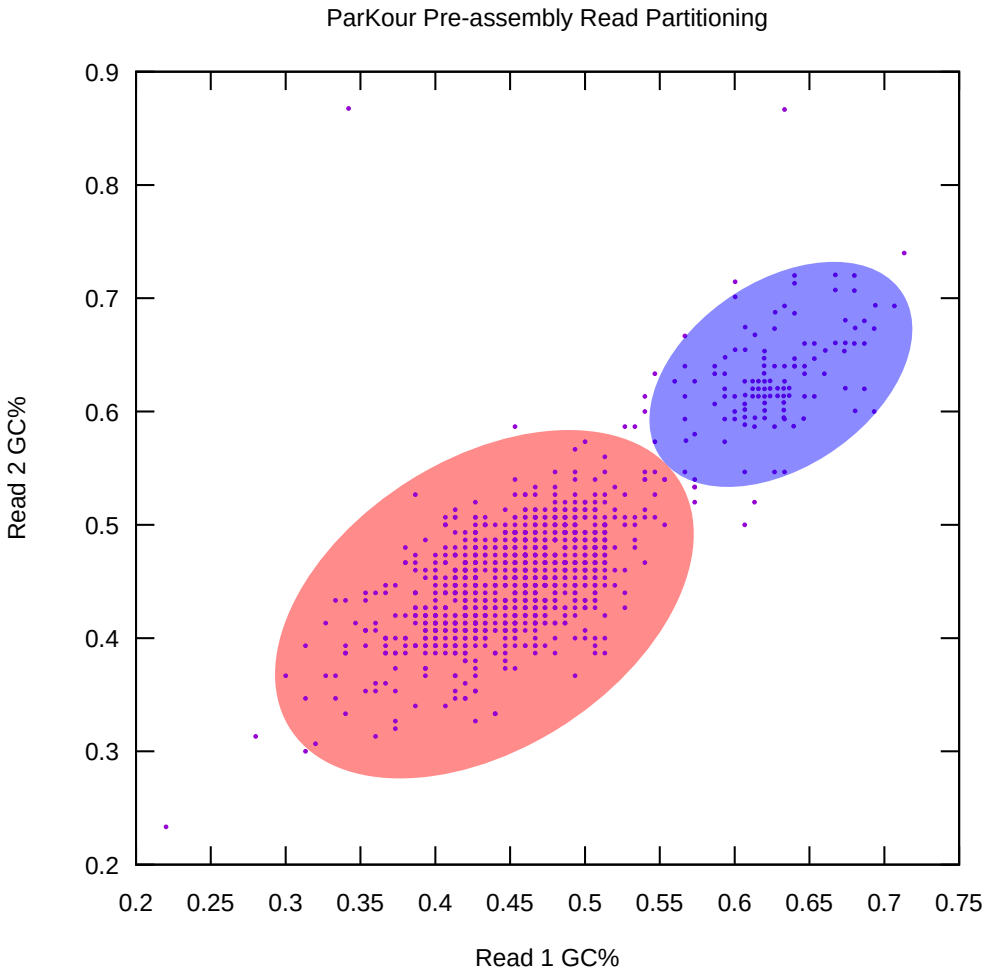

Figure 4.4.8: Visualisation of GC-based paired read K-means clustering on a small random subset of all single cell transcriptome reads. 2 initial centroids were specified without an overclustering factor and approximate final centroids (0.6674, 06177) and (0.4557, 0.4393) are indicated by highlighted areas. 57.3M and 81.7M were assigned to each respective cluster. Comparison to other clustering regimes can be found in table 4.4.5. This supports the finding of the fig. 4.4.1that there is a clear and identifiable cluster of high GC% reads present in the sample and it is possible to identify and group these reads using unsupervised learning.

Preprocessing	**Number of Transcripts**	**Bases Assembled**	**Contig N50**	**Median Contig**	**Assembly Likelihood** $(-\log)$
Q30 and Bulk	127,508	83,264,944	851	411	$-2.832 \cdot 10^{10}$
Q30 and Bulk with Khmer processing	147,902	92,395,841	789	423	$-1.224 \cdot 10^{9}$

Table 4.4.7: Trinity assemblies (with –min-kmer-cov 2) of Q30 trimmed, taxonomically selected single cell and bulk libraries with and without Khmer digital normalisation and K-mer abundance filtering. Khmer preprocessing improved the assembly likelihood by an order of magnitude, and significantly increased the total size of the assembly while only having a marginally negative effect on contig N50s.

As Khmer pre-processing both significantly improved assembly run time as well as the overall assembly quality (as assessed in the Trinity assembly comparison metrics above table 4.4.7) digitally normalised and K-mer abundance filtered bulk and taxonomically selected Q30 trimmed SCT were determined to be the optimal preprocessing for this dataset.

4.4.3 Assembly

Referenced

Referenced assembly using the divergent *Chlorella NC64A*, *Coccomyxa subellipsoidea* C-169, *Tetrahymena thermophila*, *Paramecium caudatum* genomes as references was largely ineffectual. Of all bulk and SCT reads only 0.3 and 0.4% mapped to the algal references respectively. Similarly, only 0.6 and 0.9% of reads mapped to the related ciliate genomes. This level of mapping is on the order of random chance. Of the read which mapped, a high proportion ($73 - 82\%$) mapped non-uniquely. This suggests mapping was occurring in low complexity regions and is a statistical artefact for the most part instead of biological significance.

The addition of gene junction annotation files for the reference genomes to improve spliced mapping only improved the percentage of reads mapping by $0.05 - 0.3$ percentage points. With so few reads mapping, any attempt to class transcripts from this using cufflinks resulted in $10 - 23$ total transcripts.

Therefore, referenced assembly using divergent related genomes proved impossible for this dataset.

de novo assembly

The results of the initial assembler comparison using the Q30 trimmed taxonomically selected SCT libraries (Light1-9, Light1-10, Light1-11, Dark1-2, Dark2-3, Dark2-6, Dark2-8) and bulk libraries are shown in table 4.4.8.

Assembler	**Parameters**	**Number of Contigs**	**Bases Assembled**	**Assembly Likelihood** $-\log$
SOAPdenovo-Trans	K23	374,325	$7.64 \cdot 10^7$	$3.778 \cdot 10^{10}$
	*K64	-	-	-
	*K80	-	-	-
TransAbyss	K20	3,272,137	$1.722 \cdot 10^8$	-
	K32	853,079	$1.321 \cdot 10^8$	-
	K64	376,280	$9.755 \cdot 10^7$	-
	Merged	3,055,851	$2.71 \cdot 10^8$	$-3.113 \cdot 10^{10}$
Oases*	-	-	-	-
IDBA-tran	-	54,113	$2.7 \cdot 10^7$	$-4.589 \cdot 10^{10}$
IDBA-MTP/UD/MT**	-	-	-	
Trinity	min_kmer_cov 2	127,508	$8.326 \cdot 10^7$	$-2.832 \cdot 10^{10}$
Bridger	K25	114,582	$9.707 \cdot 10^7$	$-2.587 \cdot 10^{10}$

Table 4.4.8: *De novo* assemblies of Q30 trimmed taxonomically selected single cell libraries and bulk libraries (but not digitally normalised or K-mer abundance filtered) with a range of assemblers and parameters. K-mer size used for assemblers with that option are indicated in the Parameters column e.g. K23 indicates a 23-mers. Bridger and Trinity outperformed other assemblers in terms of assembly likelihood and rational contig numbers and sizes. * indicates assemblies programs that failed to run to completion due to insufficient computational resources (despite using a server with 500GB of memory) ** indicates assemblies which failed due to coding errors in the application.

Critically, Oases, the IDA-MTP/UD/MT pipeline and SOAPdenovo-Trans at higher K-mer values all failed to run to completion correctly with the dataset. In the case of Oases and SOAPdenovo-Trans at higher K-mer values this was due to exhaustion of system memory and in the case of IDBA-MTP/UD/MT workflow an unresolved coding error resulting in repeated segmentation faults.

However, Trinity and Bridger both consistently generated assemblies of approximately equal size (100-130,000

contigs of rational sizes: N50s of 700-850 and mean and median contig sizes of 600-660 and 410-470) across a variety of assembly parameters (not shown). Furthermore, they both consistently generated the assemblies with the greatest likelihoods (from RSEM-Eval), and ran most computationally efficiently.

Trinity and Bridger assemblies using digitally normalised and K-mer abundance filtered, taxonomically selected, Q30 trimmed, single cell and bulk libraries performed even better in terms of assembly likelihood and read incorporation.

Assembler	**Parameters**	**Contigs**	**Bases Assembled**	**Assembly Likelihood** $(-\log)$
Bridger	K19	102,686	$8,209 * 10^7$	$-1.729 * 10^9$
	K25	113,106	$9.866 * 10^7$	$-1.183 * 10^9$
	K31	112,391	$8.941 * 10^7$	$-1.143 * 10^9$
Trinity	Minimum K-mer Coverage of 1	176,097	$1.113 * 10^8$	$-1.214 * 10^9$
	Minimum K-mer Coverage of 2	147,902	$9.239 * 10^7$	$-1.238 * 10^9$

Table 4.4.9: Asssembly summaries of Q30 trimmmed taxonomically selected SCT and bulk reads after digital normalisation and K-mer abundance filtering. Parameters used in the assembly indicates any special parameter settings used in the assembly i.e. K19 indicates a K-mer size of 19 was used.

Smaller K-mer values (19-mer) performed worse in the case of the Bridger assembly with the optimal assembly in terms of contig number and size was the K-mer size of 25. This was slightly lower in terms of likelihood than the 31-mer Bridger assembly. The digitally normalised and filtered Trinity assemblies generated much larger assemblies overall but still produced good likelihoods.

Assembly combination

Two assemblies were combined using the tr2aacds.pl script in EvidentialGene and a minimum CDS size of 100. The first consisted of all successfully completed assemblies of non-normalised/filtered reads i.e. SOAPdenovo-Trans, TransAbyss (multiple K-mer assembly merged using built-in tool), IDBA-tran, Trinity and Bridger in table 4.4.8. The second, of the 3 Bridger digitally normalised assemblies and two Trinity assemblies described in table 4.4.9.

Assembly	**Input Contigs**	**Collapsed Contigs**	**Assembly Likelihood** $(-\log)$
Non-normalised Assemblies	3,726,379	46,063	$-4.347 * 10^{10}$
Normalised Assemblies	652,182	53,628	$-1.823 * 10^9$
CD-HIT 90% meta-clustering	99,691	94,628	$-5.133 * 10^{10}$

Table 4.4.10: Summary of merged multi-assemblies. Collapsed contigs is the number of contigs found in the merged set by the EvidentialGene pipeline. The level of assembly reduction and redundancy removal is high and, at first appearance, is impressively consistent between meta-assemblies despite differences in preprocessing. However, CD-HIT metaclustering at 90% identity shown at the bottom demonstrated that there was very little overlap between these two minimised assemblies. Even the merged normalised assemblies generated a meta-assembly of lower overall likelihood than the best individual constituent assemblies.

The combination of all non-normalised assemblies produced a surprisingly small set of contigs, however, also both assemblies also had lower likelihoods than any of their constituent assemblies. It is of interest that despite both generating similar numbers of contigs there was next to no overlap between the two combinations as assessed by clustering using CD-HIT at a similarity of 90%.

Therefore, the assembly selected for downstream binning and analysis was Bridger assembly of bulk and library screened single cell normalised and K-mer abundancy filtered reads with a K-mer size of 31 as it displayed the best likelihood while maintaining assembly statistics within expected ranges.

4.4.4 Binning

ORF Calling

From the 112,391 contigs in the final selected assembly (31-mer Bridger Normalised and Taxonomically Selected SCT and Bulk) - 1,005,370 ORFs longer than 30 amino acids were identified using a "Tetrahymena" encoding. Using the 500 longest of these ORFs to train a Markov Model and removing shorter ORFs that lay entirely within a longer ORF resulted in a final set of 70,605 ORFs.

Performance of BLAST-based binning

10, 000 of these ORFs were randomly selected and used to search the NCBI nr database with BLASTP with an expectation of $1e-5$. Based on the taxonomic provenance of the top-hit these ORFs were assigned to a particular originating bin. The initial identification and binning of recovered transcripts into host and endosymbiont categories was tested using this phylogenetic approach. The results of this analysis is plotted below. This demonstrates that the initial bin identifications were accurate for endosymbiont ($\sim 92\%$) and food ($\sim 94\%$) derived transcripts.

Phylogeny-based bin classification

The 70,095 transdecoder called peptide sequences were then run through the automatic phylogeny generation pipeline ("Dendrogenous") against the 40 representative genomes described above. Of these, 38,193 had no BLAST hit against any genome database sequence and thus were not used to generate phylogenies. A further 9,335 had less than 4 hits and thus were not used to generate phylogenies but were taxonomically sorted based on the BLAST hit binning criteria to give 8,574 "host" sequences, 258 "endosymbiont", 395 "food' and 108 "unknown". An additional 9 sequences had insufficient numbers of sites when masking to generate a phylogeny (≤ 30). Finally, 10 phylogenies were malformed due to a latent bug in FastTree2. Therefore, 22,672 phylogenies were successfully generated and named from the input sequences. [4]

The training dataset and test datasets were visualised to ensure that the training dataset (generated during a previous iteration of these analyses) was representative of the test dataset. These plots demonstrate a possible under representation of "Unknown" and/or "Food" samples (fig. 4.4.10) but do reflect a training dataset that largely encompasses a good quantity of the same feature space as the test dataset (fig. 4.4.11).

[4] However, in speed testing "Dendrogenous" did prove very efficient at rapidly generating phylogenies with its fully parallelised mode capable of generating 100 phylogenies randomly selected transcripts against 41 genomes in an average 2:22.50 minutes. The same pipeline run serially took an average of 23:41.39 minutes and the stage-wise parallel was very marginally faster at an average of 21:45.02 minutes.

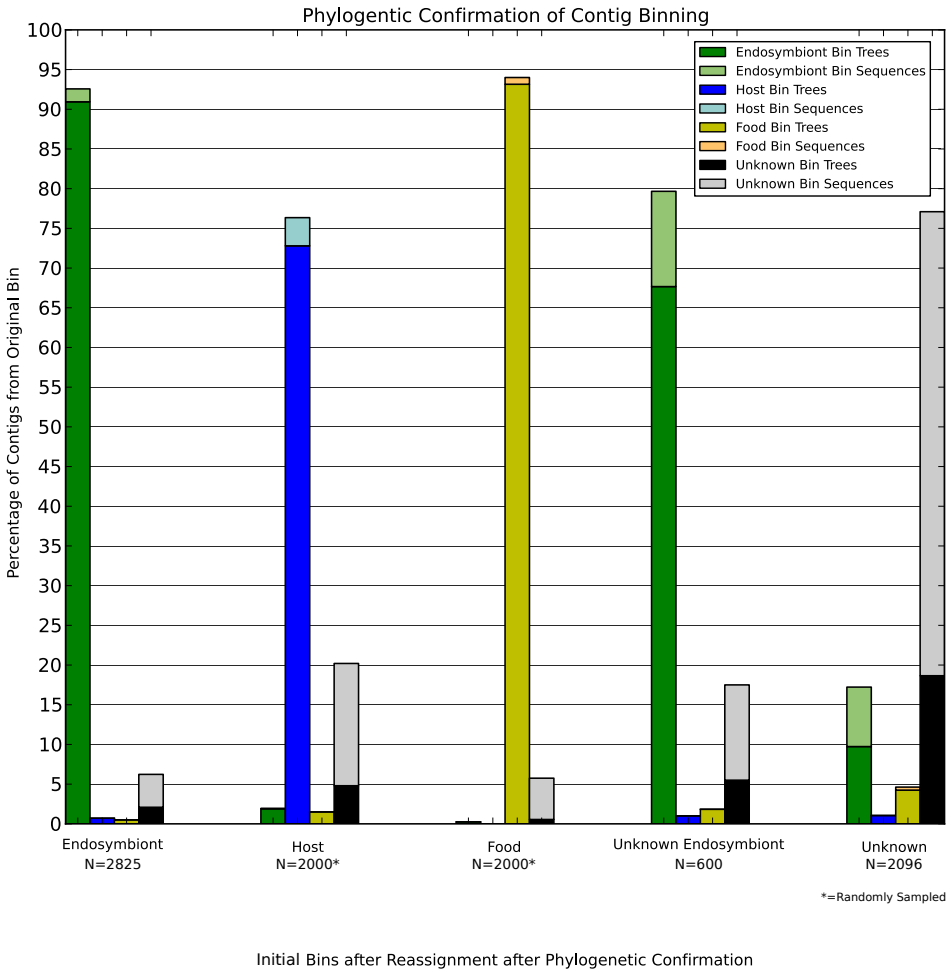

Figure 4.4.9: Preliminary analysis of change in binning after manual phylogenetic confirmation. This analysis was based on an earlier iteration of the assembly and ORF calling.

The large range of classification algorithms were fitted to this training dataset and hyperparameters were efficiently optimised using random search and Bayesian optimisation on the cross-validation folds. The average F-1 scores across classes were tallied and compared revealing K-Neighbours the most effective classification algorithm for this dataset (fig. 4.4.12).

As can be seen in the confusion matrix (and manual parsing of the classification reports from each classifier (see appendix <++>)) K-neighbours (like the majority of classifiers) poorly classified "Unknown" samples but largely performed well ($0.89 - 0.9$ for each class (table 4.4.11).

When the trained K-Neighbours model was used to classify the unlabelled 22,672 phylogenies: 415 were "endosymbiont", 2253 "unknown", 19476 "host" and 531 "food".

Therefore, of the 70,095 called ORFs in total there were: 28,050 were "host" derived, 673 "endosymbiont", 40446 "unknown" and 926 "food".

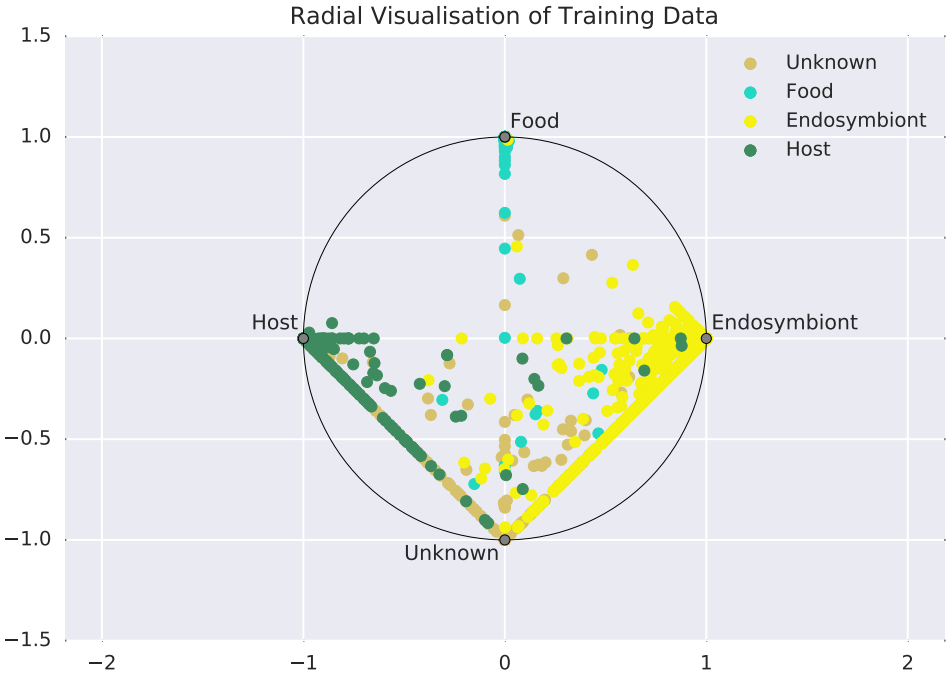

Figure 4.4.10: Radial Visualisation of Manually Parsed Training Data. All input features are normalised to unit magnitudes. Each point represents a single training sample (i.e. phylogeny) and its relative proximity to the cardinal points of the unit circle represents a the number of closely related taxa considered part of that "class". Unknown and Food classes can be seen to be particularly problematic and poorly partitioned. represents the

Label	Precision	Recall	F1-Score	Support
"Unknown"	0.96	0.84	0.90	156
"Food"	0.98	0.99	0.99	426
"Host"	0.90	0.99	0.98	787
"Endosymbiont"	0.97	0.99	0.89	359
average / total	0.95	0.96	0.95	1728

Table 4.4.11: Classification report of a trained and optimised K-Neighbours Classifier using a leaf size of 30, minkowski distance metric and 50 neighbours. Note the poor performance on "Unknown" samples but generally good ($\geq$ 90%) on other labels. This can likely be explained by the "miscellaenous" nature of this label and the diverse phylogenies that comprise it.

Performance relative to TAXAssign

TAXAssign performed relative poorly at taxonomic classification/binning of transcripts. Of 70,605 CDS sequences only 2,043 (2.893%) were assigned a phylum level taxonomic identity (table 4.4.12).

Of these top level assignments:

This can be contrasted with the 29649/70605 or 41.99% classified using the phylogeny and supervised classification system..

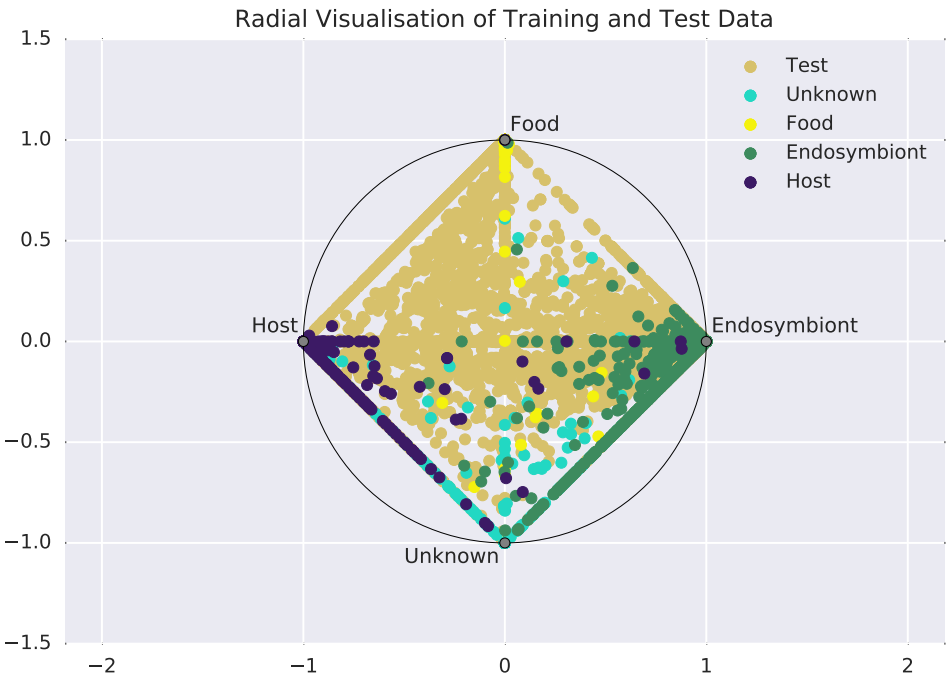

Figure 4.4.11: Radial Visualisation of Test Data and Training Data. All input features are normalised to unit magnitudes. Each point represents a single training sample (i.e. phylogeny) and its relative proximity to the cardinal points of the unit circle represents a the number of closely related taxa considered part of that "class". Test shows the position of all unlabelled phylogenies. This plot shows where the training data is poorly sampled - specifically phylogenies that only contain "host" and "food" taxa or "host" and "endosymbiont" taxa. These phylogenies may prove problematic to easily classify.

4.5 Discussion

4.5.1 Library screening is a key stage in sc-RNAseq

Despite evidence and hope that nanoscale methods can greatly reduce levels of contamination (Blainey and Quake, 2011), the taxonomic profiling conducted here indicates a high level of bacterial (and viral) contamination in the scRNA-Seq. Therefore, much as library contamination is one of the key issues with single cell genomics (Blainey, 2013; Lusk, 2014), it is also highly important in SCT. This is in concordance with the findings of (Kolisko et al., 2014), in which enigmatic, bacterial contamination was a problem in single cell eukaryotic transcriptomes.

Single cell methods are particularly prone to contamination issues from reagents, laboratory environment and enigmatic nucleic acids within the biological samples themselves. This is due to the low-input concentration and high amplification necessary in these approaches (Blainey, 2013) leading to enrichment of non-target sequences, especially bacterial contaminants present around or within the *P. bursaria* host. It is critical to identify and discard highly contaminated libraries in *de novo* assemblies as contaminant reads severely complicate the assembly graph thus increasing the computational difficulty and reducing the accuracy of the de-Bruijn graph path resolution. This was highlighted by observations in the preliminary stages of this project that the inclusion of certain (SCT) libraries would increase assembly run-time and lead to the generation of fragmented transcripts relative to assemblies without those libraries.

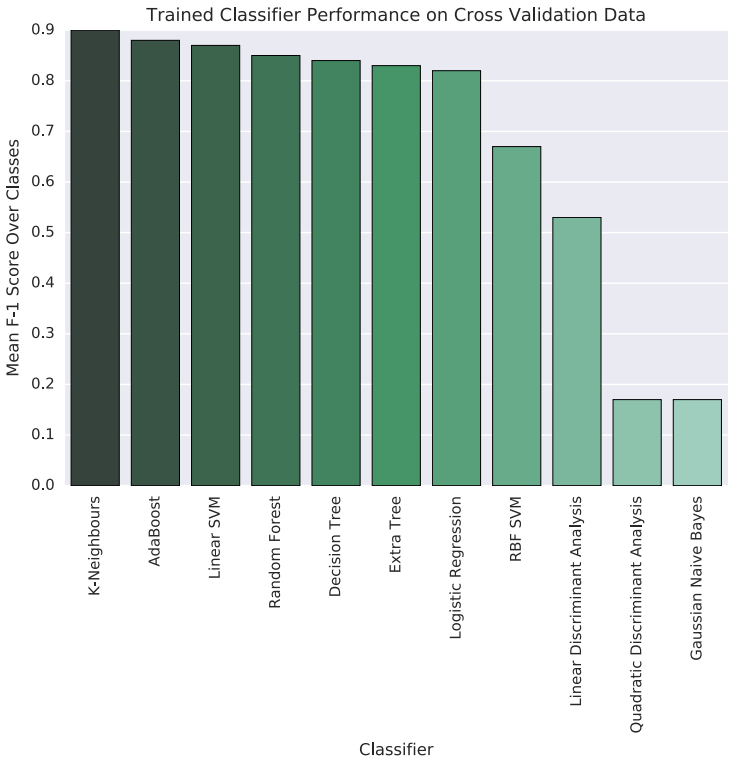

Figure 4.4.12: Classification report must be straightforward - a report of P/R/F-Measure for each element in your test data. In Multiclass problems, it is not a good idea to read Precision/Recall and F-Measure over the whole data any imbalance would make you feel you've reached better results. That's where such reports help.

Taxonomic profiling also reveals other features of the dataset that wouldn't necessarily be obvious otherwise. For instance, our profiles revealed systematically low low levels of Viridiplantae related reads across both bulk and sc-RNAseq libraries and in both lit and dark conditions. Despite care being taken to ensure thorough lysis of the chitinous *Micractinium* cells during RNA extraction and a ratio of $\sim$ 300 : 1 endosymbiont to host cell ratio this may be related to lytic inefficiences (Korfhage et al., 2015) or potentially just relatively fewer endosymbiont transcriptomic activity relative to host and associated bacteria species. Finally, it is possible that due to the endosymbiont being largely provisioned by the host it may be relatively transcriptionally inactive and thus relatively fewer transcripts can be recovered.

Intriguingly, taxonomic profiling of the bulk libraries showed a very low percentage of reads mapping to any sequence in the nr protein database. This was significantly lower than the sc-RNAseq libraries. While this finding is concerning it is likely to be an artefact of the older sequencing platform the bulk data was generated on. These paired reads were sequenced via the GAII and were half the length of the HiSeq2500 reads used for the SCTs. Shorter reads and a relatively higher technical error rate on this platform may have played a role in this marked decline in recognisable reads. Despite this the relative proportion of bacterial reads to eukaryote reads among the recognisable reads is much lower for bulk libraries than SCT. This does however suggest, that read length is highly important to accurate contamination screening/taxonomic profiling.

Taxonomic profiling of reads/libraries proved surprisingly robust to trimming. The profiles generated in "DueyDrop" were largely identical regardless of whether the input library had been trimmed or not (even at high

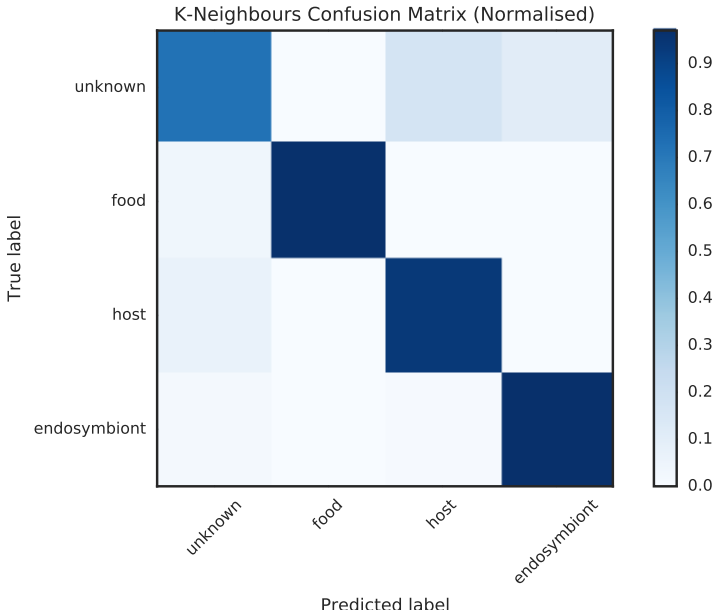

Figure 4.4.13: Normalised Confusion Matrix for K-Neighbours. These plots highlight the problematic classes in the cross-validation dataset. The heatmap corresponds to the proporiton of samples classified with a given predicted label compared with their true labels. "Host" samples are accurately classified however a small number are erroneously classified as "Unknown". Similarly, "Unknown" samples are relatively poorly classified in general.

stringency thresholds). This indicates that screening can occur before the computationally expensive trimming process without loss of accuracy. While the results presented here demonstrate that the profile generated from a relatively small random subsample of a library is largely consistent with that of the profile generated from the library as a whole.

"DueyDrop" could potentially be improved in such a way that an entire library can be screened quickly instead of just subsamples. Briefly, this would involve quantifying exact K-mer matches between library reads and a pre-generated database of known taxa using efficient probabilstic hashing datastructures such as a bloom filter, or more likely count-min sketch and an efficient k-mer counting library such as Jellyfish (Marçais and Kingsford, 2011). This would have a major speed advantage compared to the BLASTX-based method of "dueydrop" and would

Class	Phylum	Sequences Assigned
"Host"	Intramacronucleata	97
"Endosymbiont"	Streptophyta	101
	Chlorophyta	58
	Cyanobacteria	1
"Food"	Proteobacteria	1270
	Firmicutes	80
	Actinobacteria	35
	Bacteriodetes/Chlorobi	29
"Unknown"	Chordata	365
	Chlorovirus	94
	Arthropoda	7

Table 4.4.12: Phylum level TAXAssign assignments for $(2,043/70,605)$ CDS called from the Bridger 31-mer assembly. Only 2.893% were assigned using this method relative to 39.72% for the phylogenetic supervised learning (Dendrogenous-Arboretum) method. Therefore, this demonstrates the the how well this method works relative to conventional binning approaches like TAXAssign.

thus allow entire libraries to be checked in reasonable time. A similar approach to this has been implemented as a service by https://www.onecodex.com/, although this focuses specifically on screening for medically relevant taxa. However, it would require laborious workarounds to handle K-mers shared between multiple taxa in the database, translation of reads and/or database sequences into a matching sense and form (e.g. protein), and use of a locality-sensitive hash function to handle scenarios where there is no exact k-mer match. This latter issue is particularly problematic for libraries consisting of transcripts from poorly sampled sections of the tree of life where exact matches would become commensurately rarer as sampling sparsity increases. While still affected by this problem, the BLASTX/Diamond approach implemented in the "DueyDrop" scripts are relatively more robust to these problems due the explicit probabilistic modelling of sequence divergence built into the BLAST alignment algorithm (e.g. E-values). Other potential improvements to "DueyDrop" would be to incorporate some degree of automatic clustering of phylogenetic profiles using unsupervised learning and possibly manifold embedding, potentially including a form of anomaly detection to discover contaminated libraries. Robustness of taxonomic inference for each profile can also be improved by taking all hits instead of just the top one and resolving conflicting phylogenetic signal using a lowest common ancestor algorithm over all the hits.

4.5.2 Combining single cell and bulk transcriptome data creates new challenges

Contrary to previous studies in optimising conventional RNA-seq assemblies where: permissive trims (MacManes, 2014), error correction (Macmanes and Eisen, 2013; Macmanes, 2015) and the combination of multiple assemblies (Nakasugi et al., 2014) have been demonstrated as effective tactics in recapitulating a comprehensive set of transcripts *de novo*, MDA-based SCT and bulk datasets such as the one investigated above exhibit different properties. It is important to pick a trimming threshold which minimises sequence error (mostly substitutions (Yang et al., 2013)) as these result in assembly of spurious sequences but doesn't discard reads necessary to complete transcripts (Macmanes and Eisen, 2013; MacManes, 2014). For the *P. bursaria - M. reisseri* bulk and SCT dataset the optimal trimming threshold - based on both mapping statistics to preliminary assemblies and final assembly likelihoods proved to be a harsh threshold of Q30.

Following a similar theme, despite numerous indications that error correction is important for improving the accuracy of genomic and transcriptomic assemblies using Illumina reads (e.g. (Molnar and Ilie, 2014; Macmanes, 2015)) in the case of this dataset error correction appeared to be have a minimal effect with few reads being corrected and downstream assemblies being largely equivalent to those without error correction. In fact, permissively trimmed (Q5), error corrected assemblies were shown to have lower likelihoods and smaller assembly sizes than more conservatively trimmed assemblies (Q30). It should be noted that SEECER, while an RNAseq specific error correction tool is not optimised for single cell MDA-based datasets, and Bayeshammer is not optimised for transcriptomic data. Therefore, the poor performance of error correction in this dataset might be a consequence of the lack of error correction tools designed for MDA-based sc-RNAseq datasets. It will likely prove beneficial, as datasets of this type become more prevalent, to develop tools for this specific use case combining the most effective features of the MDA aware BayesHammer and the RNA-seq optimised SEECER. This said, there are several other available Illumina RNA-Seq error correction tools which were not trialled, "SEECER" was chosen in

accordance to the recommendations based on dataset and hardware heuristics ($> 50M$ reads and the availability of a high memory system) (Macmanes, 2015) but as we've demonstrated the limitations of such heuristics on new types of data it might be worth investigating these alternative tools further.

Finally, merging multiple assemblies proved a sub-optimal strategy with all merged assemblies generating lower likelihood assemblies than the best individual assembly. While not merging assemblies might mean specific transcripts might not have been recovered, especially assemblies at a range of K-mer sizes (short K-mers generally recover lower expression transcripts and vice versa for long K-mers), the much higher likelihoods meant the best performing individual assembly (Bridger using 31-mers, Q30 trimmed taxonomically selected SCT and bulk libraries) was preferred.

These results suggest that MDA-based single cell transcriptomic datasets do not behave in a qualitively similar way to bulk RNA-seq in terms of pre-processing and assembly parameters. This means care must be taken incorporating advice and heuristics derived from studies based on analysis bulk RNA-seq datasets (e.g. (Macmanes and Eisen, 2013; MacManes, 2014; Macmanes, 2015; Nakasugi et al., 2014)). As further studies using MDA SCTs are completed (e.g. (Kolisko et al., 2014)) a greater understanding of the optimal analysis of this type of dataset will emerge.

4.5.3 Pre-assembly read partitioning is non-trivial

As we expect the PbMr metatranscriptome to contain predominantly a highly AT-rich organism, *Paramecium*, (ranging from 24.1 to 28.2%GC in *P. aurelia* species complex and *P. caudatum* (Aury et al., 2006; McGrath et al., 2014)) and a very GC-rich organism, *Micractinium*, (*Chlorella variabilis* NC64A genome is approximately 67.1%GC, the highest found in a sequenced eukaryote genome (in 2010) (Blanc et al., 2010)), the utility of pre-assembly read partitioning was assessed. This GC pattern was supported by the clear bimodal GC distribution that can be observed in fig. 4.4.1. However, under careful observation it was apparent that the bimodal GC distribution was more attributable to the presence of a GC-rich contaminant such as Rhizobiales (Peralta et al., 2011). Therefore, in practice pre-read partitioning was mainly attempted to try to remove these contaminant reads from screened libraries. Theoretically, accurate pre-assembly read partitioning could transform a complex assembly graph into two relatively simpler assembly tasks. As well as simplifying path resolution accuracy, if this method could speed up assembly considerably and thus allow more iterations to optimise other assembly parameters.

This pre-assembly partitioning has been tried with mixed success in other meta-omic analyses (e.g. (Dröge and Mchardy, 2012)). However, a lack of fast efficient tools to accomplish this led to the creation of "parKour". The developed GC partitioning package proved very effective at rapidly and relatively computationally efficient clustering of PE RNAseq data. ParKour generated clusters with centroids reasonably where they may be expected from inspection of per read GC probability densities (see fig. 4.4.3) i.e. partitioning out the GC rich potentially contaminant reads likely from *Rhizobia* bacterial species. Unfortunately, in the case of this dataset clustering proved ineffective at improving assembly accuracy and fully removing groups of contaminant reads with large GC skews. The likely explanation for this is that even 150bp paired end reads are too short to consistently statistically demonstrate the GC-AT bias of the originating organism. This means any partitioning is likely to remove a significant

number of reads necessary to complete transcripts due to local variation in AT bias. The high number of shorter contigs is indicative of the kind of assembly fragmentation that would be expected in this situation.

However, the relative efficiency and theoretical benefits of this type of clustering indicates there may be some potential to utilising a similar but less naive approach in future work. It may be possible to combine "DueyDrop" and "ParKour" to all read-level screening and partitioning of reads on the basis of taxonomic profile and compositional characteristics such as GC% and tetramer frequencies. This could improve resolution of clusters and decrease the observed contig fragmentation effect while performing accurate taxonomic screening.

Other improvements could include the consideration of alternative clustering algorithms such as k-medoids (Kaufman and Rousseeuw, 1987) with more robust outlier stability or large scale database clustering algorithms such as DBSCAN (Ester et al., 1996) or BIRCH (Zhang et al., 1996) (allowing non-convex clusters). Silhouette coefficients and analysis[5] (Rousseeuw, 1987) can be incorporated to aid determination of the expected number of clusters when it cannot be determined *a priori* from inspecting the data as well as validation of generated clusters. Unfortunately, other validation and analysis systems are somewhat limited due to the lack of ground truth labelling available. Alternatively, a variational Bayes approach could be implemented to determine the optimal number of clusters (e.g. CONCOCT (Alneberg et al., 2014)). Finally, memory efficiency can be improved by use of streaming clustering algorithms (e.g. those discussed in (O'Callaghan et al., 2002)) in which all data does not require to be loaded into a matrix at a given time and be clustered as they are parsed.

4.5.4 Digital normalisation greatly improves assemblies

Digital normalisation, a method to remove redundant read data from libraries and thus reduce the computational burden of assembly (Brown et al., 2012), was also investigated for this dataset and found to be a highly effective strategy in improving assemblies of mixed bulk and MDA SCT data.

Interestingly, some have argued that error correction is special case of general digital normalization (Krasileva et al., 2013). This is supported by the fact that many error correction algorithms operate on similar principal of attempting to remove low abundance K-mers from input datasets. K-mers with a low abundance are more likely to be due to sequencing errors than representing novel biological diversity. This said digital normalisation has the potential to spuriously discard true variation that is merely undersampled in our libraries due to the high level of contamination.

This hypothesis is somewhat supported by the disproportionate retention of bulk reads relative to noisy single cell reads. However, within the context of the single cell reads the more highly contaminated Dark reads were retained in roughly equal proportion to the light reads. Suggesting, MDA derived data may also just display a greater quantity of low-level sequencing error.

It should be noted that the digitally normalised and K-mer abundance filtered assemblies also incorporated more bases overall than the equivalent assembly using the full libraries therefore resultant assemblies were just high confidence (and li elihood) subsets of the initial input data.

[5] $s = \frac{b-a}{max(a,b)}$ where s is Silhouette coefficient, a is the mean distance between a sample and all other points in the same class and b is the mean distance between a sample and all other points in the next nearest cluster (Pedregosa et al., 2011). Therefore, s is a measure of cluster definition.

One factor that has not been adequately analysed in the context of this work is that of sequencing depth. Future studies will need to carefully consider sufficient sequencing depth given the noise and prevalence of contamination in MDA based data.

4.5.5 Assembly and assembly assessment

While we have demonstrated that some progress can be made identifying optimal pre-processing parameters using measures such as mapping metrics it is very difficult to identify the parameters (preprocessing or otherwise) which will leads to the "best" *de novo* assembly without actually generating the assembly. Assembly can be considered an example of Wolpert and Macready's "No Free Lunch Theorems" (Wolpert and Macready, 1995, 1997) as (in the case of *de novo* assembly) it is fundamentally a hamiltonian/eulerian cycle search problem (equivalent in the de-Bruijn formulation) and therefore any two assembly implementations (in different assemblers and/or with different parameters) should ultimately be equivalent across all possible input datasets.[6]. For this reason, it is necessary to try assembly using a random of assembly parameters and indeed a range of both *de novo* and referenced assemblers.

Unfortunately, the task of identifying the "best" *de novo* transcriptome assembly is also a non-trivial task (Neil and Emrich, 2013). Many widely used assembly assessment metrics have been shown to be inconsistent measures in simulated sequencing data, especially those metrics related to invidual contigs (theoretically different transcript splices). Metrics such as average length and N50 prove consistent across both simulated sequencing depth and read lengths i.e. they improve towards (Neil and Emrich, 2013). Furthermore, the number of possible metrics is greatly reduced if assessment is mainly conducted in a reference-free manner (Li et al., 2014). As the majority of assemblies were *de novo* and the suitability of the related but divergent genomes proved lacking it was necessary to restrict to reference-free assembly assessments. Therefore, a model-based reference-free assembly scoring algorithm (RSEM-EVAL (Li et al., 2014) was, along with standard (if imperfect) metrics, used to evaluate different assemblies in this study. The assumption of the accuracy of the RSEM-EVAL likelihood is a strong one, and deserves careful re-consideration in further work.

In terms of referenced assembly using divergent relatives, it is safe to conclude that despite other findings that even divergent (up to 15%) genomes can generate transcriptomes of higher-quality than *de novo* (Vijay et al., 2013), the potential references are too divergent in the case of the PbMr to be of any utility.

Overall, a comparison of *de novo* assemblies using a range of assemblers and parameters on "optimally" pre-processed read data demonstrated the clear superiority of both "Bridger" and "Trininty" Trinity comes with the advantages of being a generally better developed tool that interlocks effectively via several plugins and utility scripts with other tools and analysis pipelines.

However, despite being relatively newer and consisting of a less mature and tested codebase, Bridger proved to be a slightly more effective assembly tool overall. Unfortunately, coding problems and a lack of public active development means it is non-trivial to successful use this tool. In the process of implementing the above analyses

[6]This should be taken with a pinch of salt, a proof of this theorem applied to the case of assembly is beyond both the scope of this thesis and my abilities

it was necessary to fix several bugs present in the assembler. These upgrades were merged into the code and are available on GitHub https://github.com/fmaguire/Bridger_Assembler. Hopefully, by rehosting this code on a public development and collaboration platform (as well as adding continuous integration) will spur further development of this promising tool.

Interestingly, despite strong evidence supporting the need to combine assemblies due to the size of the disjoint sets of transcripts recoverable from different algorithms and parameter choices (Lowe et al., 2014) assembly merging systematically led to worse overall assemblies with this dataset (as assessed by RSEM-EVAL likelihood scores). The likelihood of the merged assemblies were worse than the best individual constituent assemblies.

4.5.6 Binning

However, even once a good assembly has been generated it is still necessary to identify the likely originating species of a given transcript i.e. host, endosymbiont, food bacterial contaminant or other contaminant. While a successful partitioned pre-assembly strategy may simplify this process it would still be sensible to confirm bins using downstream analyses that use full length assembled transcripts and thus more potential data than are present in shorter individual PE reads. Rough, approximate bins were generated using a simple "top BLAST hit" approach following ORF calling (using Tetrahymena and Universal encodings) against a set of representative predicted proteomes. In order to assess how accurate these bins were likely to be, 10,000 were randomly selected and rapid maximimum-likelihood phylogenies were generated using the transcript sequence as a seed to sample the entire RefSeq protein nr database. This was accomplished using "Dendrogenous", a rewritten and modified version of a pipeline originally known as "Darren's Orchard" which first appeared in (Richards et al., 2009). Phylogenies were manually assessed to check whether the resultant topology was congruent with the BLAST based binning i.e. are supposedly "endosymbiont" transcripts branching principally with archaeplastida taxa. However, due to the slow largely manual nature of this phylogeny assessment process it would be infeasible to repeat this for all transcripts generated from a single assembly, let alone investigating several.

Therefore, this became a fundamental classification problem with the 10,000 manually verified phylogenies forming a handy training dataset for supervised learning. To determine the best performing classification algorithm and hyperparameters for this dataset an automated search was conducted using bayesian optimisation. This was then converted to a binning script named "Arboretum". High throughput phylogeny generation, parsing and supervised classification is a more sensitive and powerful way in which to bin transcripts into their likely originating organisms provided a reasonable level of *a priori* knowledge of the system at hand. This demonstrably operates better than established although simpler approaches such as TAXAssign or top BLAST hit. While, classification accuracy (and F-1) is sub-optimal for "Food" and "Unknown" bins it (table 4.4.11) a decent level of precision and recall for the target bins of "Host" and "Endosymbiont".

However, this classification is still a work in progress and could potentially be improved by the addition of anomaly detection in place of the catch-all (and subsequently poorly classified) "Unknown" classes. Furthermore, there are several potential possible improvements in the classification itself that could be made. Specifically, unsupervised clustering pre-training could potentially forgo the need for laborious manual generation of the training

Transcript Bin	Number of Transcripts	Called ORFs
Endosymbiont	8,975	4,275
Host	18,793	17,920
Food	18,516	-
Unknown	66,107	-

Table 4.6.1: Summary of transcriptome assembly and binned sequences

dataset and minimise the difficulties in handling these aberrant phylogenies. An AutoML bagging estimator such as one of those implemented in the AutoML project (Eggensperger et al., 2013), a variational autoencoder pre-processing following by a deep neural network classifier or using a phylogeny specific kernel function (Vert, 2002) in a Gaussian process or SVM system all offer potential algorithmic improvements. Finally, incorporation of additional sequence related features such as K-mer coverage and composition into each samples may help greatly improve the fidelity of classification.

4.6 Conclusion

In conclusion, for this dataset the optimal pre-processing was determined to be careful taxonomic screening of input libraries, followed by trimming at a high (Q30) threshold and subsequent digital normalisation and low-abundance K-mer filtering. The optimal assemblies were generated using larger (25-31 K-mer) sizes and utilised the Bridger (and to lesser extent Trinity) assembly algorithms. While pre-assembly read partitioning proved ineffective in this implementation, in future a less naive method that incorporated both read-level taxonomic data and compositional information could potentially improve assemblies of complex eukaryotic metatranscriptomes, especially those that combined bulk and single cell RNAseq data. Generally, MDA-based single cell datasets are noisy and difficult to work with. Potentially, they require the existence of robust references to aid assembly or a much greater depth of sequencing.

Finally, I have demonstrated that BLAST based transcript binning alone is ineffective at accurately binning transcripts. Fast, automated phylogeny generation and the subsequent use of supervised learning (particularly large ensemble models such as Random Forests and those AutoML algorithms) can potentially improve the quality of such binning. Further work in the implementation of unsupervised clustering of generated phylogenies could conceivably forgo the laborious process of manually generating a training dataset.

Points arising in this analysis:

- It is possible to generate a functional working transcriptome combining bulk and MDA based RNAseq (see table 4.6.1)
- sc-RNAseq libraries generated from dark samples are problematic.
- Binning methodologies may prevent easy finding of novel genes due to a lack of homology.

"All models are wrong, but some are useful"

- George E.P. Box & Draper: *Empirical model-building and response surfaces, 1987*

5

Metabolic integration

5.1 Introduction

The linking of metabolism between host and endosymbiont is a fundamental stage in endosymbiotic integration (Bhattacharya et al., 2007; Karkar et al., 2015). Complementation of respective metabolic deficiencies/limitations in host and endosymbiont allow exploitation of novel niches and provide the key selective benefits of endosymbiosis (Hoffmeister and Martin, 2003).

In order to identify points of metabolic integration it is necessary to identify the primary "points of contact" between the metabolic networks of host and endosymbiont. These "points of contact" comprise two major classes of proteins, transporters and secreted proteins. Specifically, host and endosymbiont transporters which localise to the perialgal vacuole (PV) membrane and the outer-membrane of the endosymbiont, and proteins which are secreted by host and endosymbiont into PV. These points of contact can then be used to aid interpretation and supplement inferred host and endosymbiont metabolic networks.

Another way to investigate metabolic integration is the annotation and analysis of known metabolic pathways in host and endosymbiont from binned transcripome sequences. This allows identification of pathways being expressed while in the endosymbiotic relationship and potentially indicates further likely sites of integration.

Finally, a direct analysis of metabolites present in the system shows final evidence of metabolic integration. This has the benefits of not relying on abstracted measures such as transcript abundance or gene copy to attempt

to infer biological activity. By not treating the metabolic state of the system as a latent variable novel information about the cellular dynamics can be revealed. For example, the existence of cryptic regulatory systems that breakdown direct mapping from genes to transcripts to protein to metabolites. By using both targeted and untargeted chromatography and mass spectrometry metabolomics approaches it is possible to survey the combined pool of host and endosymbiont both qualitatively and quantitatively. These inferences can then be correlated.

By utilising 3 separate streams of metabolic analysis: comparative transcript annotation and mapping, directed identification and analysis of transporters and secreted proteins and metabolomics, we maximise the strength of any inferences and reduce the chance of false negatives preventing the identification of biologically important metabolic integration.

First, I will summarise what is currently known about the metabolic integration of *P. bursaria* and its green algal endosymbionts, before briefly discussing the nature and identification of evidence of further metabolic integration.

5.1.1 Metabolism of Host and Endosymbiont

The most obvious point of metabolic integration in any endosymbiosis featuring a photosynthetic partner is that of the flow of photosynthates from endosymbiont to host.

This is believed to primarily be in the form of carbohydrates such as maltose (Muscatine, 1967) In return, the host facilitates increased rates of photosynthesis in the endosymbiont (Sommaruga and Sonntag, 2009), via supply of CO_2 (Parker, 1926), one or several forms of nitrogen (Johnson, 2011), and mono- and divalent cations such as K^+, Mg^{2+}, and Ca^{2+}. All of which have key roles in photosynthesis (Kato and Imamura, 2009b).

Therefore, I will briefly review the current state of knowledge of nitrogen and carbon/carbohydrate metabolic uptake and utilisation in green algal endosymbionts.

Carbohydrate Metabolism

The transfer of matlose, glucose, fructose and malate from endosymbiont to host has been observed using radiolabelling (Brown and Nielsen, 1974). Furthermore, green algae strains competent to form endosymbioses were found to inducibly release significantly more photosynthate (in the form of $\sim$ 95% maltose) than strictly free-living strains in the presence of $NaHCO_3$ on the order of $5.4 - 86.7\%$ vs. $0.4 - 7.6\%$ of total photosynthate (Muscatine et al., 1967).

In terms of the uptake of saccharides by the endosymbiont, at least one free-living *C. vulgaris* strain has an inducible system for active hexose uptake (Tanner et al., 1974). In order of highest to lowest uptake rate the free-living *C. vulgaris* took up sucrose, glucose and maltose but not fructose (Kato and Imamura, 2009b). Additionally, studies in *C. variabilis* F36-ZK endosymbiont strains indicates an inability to directly utilise sucrose or maltose in free-living culture (Kamako et al., 2005) as well an inability to import glucose or fructose (Kato and Imamura, 2008b). Interestingly, export of photosynthate from the PV to the host cytoplasm may be dependent on a transporter derived from the *C. variabilis* 1N in its respective *P. bursaria* endosymbioses (Kodama and Fujishima, 2008).

Additionally, there are a few transporters mainly associated with intracellular transport such as vacuolar glucose transporter I (VGT1), ERD-like transporters and tonoplast monosaccharide transporters. Therefore, this analysis of sugar transporters will feature both general screening for transporters as well as targeted homology searches for elements of these transporter families.

Nitrogen Metabolism

Nitrogen is the most transferred material between host and endosymbiont after carbon (Kato and Imamura, 2009b). There has been considerable research and interest in exactly what form this nitrogen exchange takes (Kato et al., 2006; Kamako et al., 2005; McAuley, 1986).

C. variabilis (both NC64A and the Japanese F36-ZK) have been found to be able to use amino acids effectively as a nitrogen source but only minimally effectively utilise ammonium (NH_4^+) and being unable to use nitrate (NO_3^-) or nitrite (NO_2^-) (Kamako et al., 2005; **?**). Similar patterns have been observed in *M. reisseri*, although all strains tested could utilise nitrate and 3/4 could use nitrite to greater or lesser degrees (Kessler and Huss, 1990). On the other hand, free-living species such as *Parachlorella kessleri* can effectively utilise all of the nitrogen sources mentioned (Kato and Imamura, 2009b) (although amino acid utilisation has to be induced with glucose (**?**)).

In terms of amino acids as a nitrogen source, there unfortunately, isn't a high degree of correlation between the ability to uptake an amino acid and its usage. Even rate of uptake does not indicate utilisation (Kato and Imamura, 2009b). For example, while *C. variabilis* F36-ZK can uptake all 20 amino acids, only 6 (L-arginine, L-asparagine, L-glutamine, L-serine, L-alanine) were found to promote growth (Kato et al., 2006). This was despite some these 6 being taken up at lower rates than non-utilised amino acids such as L-proline, L-cysteine or L-leucine (Kato et al., 2006).

Similarly, *C. variabilis* NC64A was found to have stimulated growth in the presence of L-arginine and L-glutamine, whereas another *C. variabilis* strain, 3N813A, used every amino acid apart from L-lysine and L-glutamic acid (McAuley, 1986; Kato and Imamura, 2009b).

Glutamine synthetase likely plays a role in the endosymbiotic utilisation of amino acids that can be broken down to generate intracellular ammonium after uptake (Rees et al., 1995; Kato and Imamura, 2009b).

There is also evidence that the expression of this protein is light-dependent in *C. variabilis* (Kato et al., 2006).

Unfortunately, this ability to utilise amino acids isn't totally correlated with the ability of a green algae to uptake the amino acid (Kato and Imamura, 2009b).

The free-living *C. vulgaris* NIES-227 on the other hand was found to not utilise any amino acid apart from low levels of uptake of L-arginine (Kato et al., 2006).

Therefore, even within the *C. variabilis* strains there was a range of traits in terms of amino acid uptake and utilisation.

Kinetic analyses and competitive assays indicate 3 amino acid transport systems in *C. variabilis* F36-ZK, a general amino acid tranporter for all amino acids except L-alanine, a basic transporter for L-arginine and L-lysine and a specialised L-alanine transporter (Kato and Imamura, 2009a,b). All of these are constitutively expressed, active, amino-acid symporters (Kato and Imamura, 2009a,b).

Although glucose did increase the rate of amino acid uptake by some partially defined sensing system and resorted uptake in the casoe of calcium ihibtion (Kato and Imamura, 2008a, 2009b).

(although glucose and maltose did stimulate growth (Kamako et al., 2005) it was via a mechanism which promoted increased uptake of a nitrogen source (Kato and Imamura, 2009b)).

As *P. bursaria* cannot import nitrate (Albers et al., 1982) the heterogeneous loss of nitrate and nitrite utilisation in endosymbiotic strains is perhaps not surprising (**?**). As there is no pressure to maintain enzymes necessary for this pathway when an endosymbiont this may explain the appearance This reduced selection pressure for nitrate and nitrite utilisation when in the endosymbiot milieu may explain the presence of low-activity mutatant Nitrate Reductase (NR) and Nitrite Redutase (NiR) (**?**). On the other hand in free-living organisms utilisation of the usually rare inorganic sources of nitrogen such as ammonium, nitrate and nitrite often a major limit on growth and productivity (Giordano and Raven, 2014).

Putatively, this reflects an early stage in the genomic streamlining that frequently takes place in endosymbionts.

Constitutive expression is another adapation to endosymbiosis and metabolic integration as the free-living *C. vulgaris* strains tested must have induced expression of these transporters (**?**).

Ca_2^+ and Mg_2^+ inhibit affects amino acid uptake (Kato and Imamura, 2008a) in the general amino acid transporters of *C. vulgaris* and F36-ZK

Respiration of the host plays a role in the gas exchange of CO_2 and O_2 to the endosymbiont, with the algae displaying higher levels of photosynthetic activity while in association with the host due to the increase host related CO_2 respiration (Reisser, 1980). Addition of glucose, which likely increases host respiration rate and thus CO_2 evolution increases the rate of photosynthetic oxygen production commensurately (Reisser, 1980)

Proton gradient dependent transport of maltose/photosynthate out of the (Schussler and Schnepf, 1992) pH induces release of maltose in many algae ()

5.1.2 Identifying Direct Points of Contact

Transporter Proteins

The most important group of proteins in the control and evolution of metabolic integration is that of host and endosymbiont transporter proteins. This is due to their role in facilitating diffusion and active transport across the lipid membranes that exist between host and endosymbiont.

Without transporters many metabolically important large uncharged polar molecules (e.g. carbohydrates, amino acids) and charged molecules (e.g. the various biologically relevant cations and anions such as H^+) are incapable of significant rates of diffusion across membranes even in the presence of high concentration gradients. Therefore, the presence of transporters is vital to facilitating any interaction involving these groups of metabolites. However, there are also several metabolites that are capable of unfacilitated diffusion across lipid membranes at significant rates. These include important respiratory gases such as O_2 and CO_2, hydrophobic compounds like benzene and small uncharged polar molecules (e.g. H_2O and ethanol) (Cooper, 2013; Alberts, 2015). Despite this, transporter proteins have evolved to facilitate even more rapid diffusion of some of these metabolites e.g.

aquaporins (Agre et al., 1993). Finally, certain transporters can provide the ability to actively transport metabolites against concentration gradients. This involves the expenditure of energy (typically in the form of ATP) to directly pump compounds or generate an opposing gradient which can be exploited (primary vs secondary active transport).

There are 5 functional groups of transporters (Saier et al., 2014):

- Channel/Pore types which catalyse diffusion of metabolites along concentration gradients e.g. porins and the Mitochondirla and Plastid Porin (MPP) family.

- Electrochemical Potential-driven transporters which use a carrier-mediated process to catalyse uniportation (single metabolite) or cotransportation (two species in the same direction, symportation, or two species in opposite direction, antiportation). These make use of chemiosmotic gradients but generally do not directly make use of cellular energy molecules such as ATP. However, many make use of a gradient/potential generated by the active transport of solutes by another complex, in this case they can referred to as secondary active transporters. Electrochemical Potenital-driven transporters are a very large family and include the ubiquitous major facilitator superfamily (MFS) and Cation Diffusion Facilitator (CDF) families.

- Primary active transporters which use a direct source of chemical, electrical or light energy such as ATP, voltage or photon to drive transport against concentration gradients. Transporters of this type form many of the components fundamental to life as they allow an organism to decouple itself directly from environmental and intracellular gradients. They include rhodopsins, ATP-binding Cassette (ABC) Superfamily, and the general Secretory Pathway (Sec) family.

- Group translocators, which modify a substrate during transportation e.g. polysaccharide synthesis during secretion in the Polysaccharide Synthase/Exporter family and the Fatty Acid Group Translocation (FAT) family which can acylate fatty acids during transport.

- Transmembrane Electron Carriers which transport single electrons from a donor to an acceptor across a membrane. The major groups of these include the cytochrome and Photosystem I complexes.

This analysis will primarily focus on transporters of the first 4 classes. In the case of *P. bursaria* and its endosymbiont we are particularly interested in the host the host perialgal vacuole membrane and the outer membrane of the green algal endosymbiont in the case of *P. bursaria*.

Therefore, the first step to the successful analysis of the metabolic integration of host and endosymbiont is accurate identification of transporter proteins present in their respective binned transcriptome sequences. By identifying both the identity of these proteins and qualitatively investigating the relative day:night expression targets can be generated for further analysis, validation, and proof of localisation to the PV and algal outer membrane.

Transporter proteins can be identified primarily via annotation and homology searches to previously identified transporters (Saier et al., 2006, 2009, 2014) and direct identification of transmembrane (TM) domains motifs. All transporters feature at least 1 TM helix, usually considerably more (von Heijne, 2006). However, as not necessarily

every sub-unit of a transporter will contain a TM domain and the presence of partial transcripts in our assemblies it is necessary to not rely totally on TM prediction to discover transporter proteins.

One obvious target of such an analysis is based on the most obvious point of metabolic integration between a host and its photosynthetic endosymbiont. The exchange of photosynthate and the provision of a nitrogen source. Specifically, we wish to discover sugar transporters which facilitate the secretion and uptake of photosynthate and ammonium and/or amino acid transporters which facilitate transfer of a nitrogen source between host and endosymbiont.

Secreted Proteins

The next major class of proteins involved in endosymbiosis from the perspective of the endosymbiont as those which are secreted. These proteins are secreted into the perialgal vacuole and thus are likely to be play some form of role in the maintenance of the endosymbiosis. For example, the endosymbiont derived sugar transporter responsible for the export of photosynthate from the PV hypothesies by (Kodama and Fujishima, 2008).

Secreted proteins can be effectively identified by searching for the presence of N-terminal signal peptides.

These are short 15-30 amino acid N-terminal sequences cleaved during translocation. They aren't conserved sequences but are present across the tree of life.

Feature a biochemical compositional fingerprint of positively charged residues, hydrophobic residues and polar uncharged residues with distinctive points before site.l (Emanuelsson et al., 2007)

Not all have signal peptides either

SignalP (Nielsen et al., 1997) has proven the most effective method of predicting the presence of signal peptides (Lee et al., 2009; Petersen et al., 2011).

This method uses a standard feed-forward artificial neural network with 8-41 hidden units (depending on whether the organism is eukaryotic, gram positive or gram negative) trained with back-propagation.

By analysing the identified signal peptides it is possible to

Subcellular localisation of a given protein can be inferred using tools such as the WoLF PSORT (Horton et al., 2007). This tool implements a standard K-neighbours classifier trained on localisation labelled proteins from SwissProt and uses PSORTII (Nakai and Kanehisa, 1992; Nakai and Horton, 1999; Horton and Nakai, 1997) and iPSORT (Bannai et al., 2002) derived sequence features and automatic inference of weightings (Horton et al., 2006).

from Swiss-Prot using their localisation annotations.

The key amino acid features used are found using PSORTII () and then weighted for revlance with WoLF

5.1.3 Metabolic mapping

Metabolic pathways form the functional backbone of all biological processes. The Kyoto Encyclopedia of Genes and Genomes (KEGG) (Ogata et al., 1999; Okuda et al., 2008; Kanehisa et al., 2014) and MetaCyc (Caspi et al., 2007) databases form an important resource for contextualising genomic and transcriptomic scale results into these networks. The utility of this approach is emphasised by the presence of numerous tools and analytical

pipelines to explore these databases e.g. (Okuda et al., 2008; Nakao et al., 1999; Karp et al., 2002, 2010; Antonov et al., 2008; Klukas and Schreiber, 2007)

By comparison of the relatively complete predicted peptides from the endosymbiotic algae *C. variabilis* NC64A and *Coccomyxa subellipsoidea* C-169 genome projects to the predicted endosymbiont binned peptides from the transcriptomes of *M. reisseri* and *C. variabilis* 1N it is possible to infer what the endosymbiotic metabolic pathways

what metabolic pathways are likely

5.1.4 Metabolomics

A pilot untargeted global metabolomic profile was generated for *P. bursaria-M. reissieri* CCAP 1660/12 culture to test the feasability of this approach and help optimise chromatography and

Finally, a proof of concept for the targeted metabolomic analysis of this system was conducted used HPLC-QQQ to determine the relative abundances of amino acids in the culture between day and night conditions.

In the case of *P. bursaria* and its green algal endosymbionts there are

Untargeted Global Profiling

GCMS, LCMS,

Targeted Analysis of Key Classes of Compounds

Mass spectrometry also offers methods by which a targeted analysis of key classes of compounds can be conducted.

While few Amino acids

5.2 Aims

The principal aim of this chapter is to identify likely points of metabolic integration between host and endosymbiont to generate targets for subsequent targeted mass spectrometry, RNAi and qPCR based validation experiments.

This will be achieved by:

- identifying transporter proteins present in the endosymbiont binned transcripts from the CCAP1660/12 RNA-Seq analysis and analysing them for qualitative differential expression between day and night.
- identifying secreted proteins present in the endosymbiont binned transcripts from the CCAP1660/12 RNA-Seq analysis and analysing them for qualitative differential expression between day and night.
- Comparative analysis of metabolic pathways between host and endosymbiont relative to sequenced green algal genomes.
- A pilot untargeted global metabolomic profile of the system and comparison of day to night.
- Targeted quanitative analysis of amino acid concentrations between day and night.

5.3 Methods

5.3.1 Transporter Analysis

Transporter identification pipeline

Transporters were identified in the 4 sets of sequences (*C. variabilis*, *M. reisseri*, *C. vulgaris* and *C. subellipsoidea*) using the following set of pipelined filters:

1. Transmembrane (TM) domains were predicted for each sequence using an HMM approach implemented as part of TMHMM2 (Sonnhammer et al., 1998; Krogh et al., 2001) and sequence predicted to contain at least 1 TM domain was extracted.

2. These sequences were then used to search a PFAM database of profile HMMs (**?**) via HMMER3's hmmscan utility (Eddy, 1995; Johnson et al., 2010; Eddy and R, 2011; Mistry et al., 2013) and sequences with a hit to a PFAM domain at an independent E-value of $1e^{-5}$ were retained.

3. These hits were then finally filtered for PFAM domains which mapped to transporter families classified by the Transporter Classification Database (TCDB) (Saier et al., 2006; **?**, 2009, 2014) mapping files.

Additionally, to ensure thorough discovery of all *M. reisseri* transporters *M. reisseri* binned sequences were BLASTP-ed against the NR protein database with an e-value of $1e^{-3}$ and 20 hits. InterproScan (Zdobnov and Apweiler, 2001) was then used to further annotate these proteins incorporating results from BlasProDom (Servant et al., 2002), FPrintScan (Attwood et al., 1994), HMMER (**?**) scans against the PIR (Barker et al., 1998), PFAM (Bateman, 2002), SMART (Schultz et al., 1998), PANTHER (Thomas, 2003) and TIGRFAM databases (Haft, 2003), ProfileScan (Gribskov et al., 1988), HAMAP (Lima et al., 2009), PatterScan, SuperFamily (Gough and Chothia, 2002), SignalP (Petersen et al., 2011), TMHMM (Sonnhammer et al., 1998), Gene3D (Buchan et al., 2002), Phobius (Käll et al., 2007) and Coils. Results were then mapped to GO terms (Ashburner et al., 2000; Harris et al., 2004) and annotated via BLAST2GO (Conesa et al., 2005).

Finally, all proteins annotated to have a GO term associated with "transport" and "transport activity" specifically, GO:0005215, GO:0005478 and GO:0006810 and their child terms were extracted.

Qualitative expression analysis

Kallisto (Bray et al., 2015) was used to pseudoalign and estimate abundances for all taxonomically screen single cell libraries (4 dark and 3 light) to the called "endosymbiont" binned CDS sequences from the *P. bursaria* CCAP 1660/12 transcriptome (see Chapter 2).

Kallisto doesn't align reads to references in the same manner as conventional short read alignment algorithms such as Bowtie2 (Langmead and Salzberg, 2012). Instead of specifically mapping a read to a set of co-ordinates it instead determines which transcripts are compatible with the alignment of a given read. This is achieved via decomposition of transcripts in de-Bruijn graphs and fast k-mer hashing to compare reads to transcript graph

nodes in constant time. These k-compatability classes are then used with boostrapped expectation-maximisation to estimate transcript quantification and determine uncertainty (Bray et al., 2015).

Results were visualised and analysed using "sleuth" and the seaborn plotting library (Waskom et al., 2015).

5.3.2 Secretome prediction

A conservative set of secreted proteins were predicted using the following pipeline:

1. Signal peptides are detected using SignalP4.1 and mature sequences created for each sequence with a signal peptide
2. Sequences detected to have a TM domain (by TMHMM) within either the mature sequence or full length for proteins without signal peptides were discarded.
3. Signal peptides were re-added to mature sequences and the remaining sequences were then filtered using for those predicted as secreted by TargetP1.1
4. These sequences were then filtered down to those which had extracellular localisation in WoLFPSORT 0.2
5. Finally, for the endosymbiont, secreted protein found to have a Chloroplast targeting signal (via ChloroP1.1) were removed.

5.3.3 Metabolic mapping analysis

First, predicted proteomes were obtained or generated for *Coccomyxa subellipsoidea* C-169, *Chlorella variabilis* NC64A, *Chlorella variabilis* 1N, and *M. reisseri*.

For *M. reisseri* the endosymbiont binned sequences from the transcriptomic sequencing project discussed in the previous chapter were used. *Coccomyxa subellipsoidea* C-169 genome project (Blanc et al., 2012) version 2.0 JGI annotated proteins (created 12-01-2014) were downloaded from JGI's Phyotozome v10.3.1 (Goodstein et al., 2012). Similarly, the "best" annotated proteins from version 1 of the *Chlorella variabilis* NC64A genome project (Blanc et al., 2010) were downloaded from JGI's genome portal (Grigoriev et al., 2011; Nordberg et al., 2014)

However, to obtain *C. variabilis* 1N endosymbiont peptides a reassembly and binning of raw sequencing data from (Kodama et al., 2014) was conducted (discussed below).

Once all sequences were acquired they were annotated using KEGG orthology. This was achieved using the KEGG Automatic Annotation Server (KAAS) (Moriya et al., 2007) single-directional best hit with both BLAST and GHOSTZ (Suzuki et al., 2014, 2015) method against the following 40 gene sets: *Homo sapiens*, *Drosophila melanogaster*, *Caenorhabditis elegans*, *Arabidopsis thaliana*, *Gylcine max*, *Vitis vinifera*, *Oryza sativa*, *Ostreococcous lucimarinus*, *Ostreococcus tauri*, *Micromonas* sp. RCC299, *Cyanidioschyzon merolae*, *Galdieria sulphuraria*, *Saccharomyces cerevisiae*, *Candida albicans*, *Neurospora crassa*, *Aspergillus nidulans*, *Coccidioides immitis*, *Schizosaccharomyces pombe*, *Ustilago maydis*, *Encephalitozoon cuniculi*, *Monosiga brevicollis*, *Dictyostelium discoideum*, *Acanthamoeba castellanii*, *Plasmodium falciparum* 3D7, *Cryptosporidium hominis*, *Tetrahymena thermophila*, *Paramecium tetraurelia*, *Phaeodactylum tricornutum*, *Emiliania huxleyi*, and *Guillardia theta*.

KEGG annotations were then plotted onto KEGG metabolic networks and compared to identify key aspects of differences between the algal species and host and endosymbiont metabolic.

Chlorella variabilis 1 N assembly

232.3*M* 100bp paired-end reads from (Kodama et al., 2014)'s bulk RNAseq transcriptome of *Paramecium bursaria* Yad1g (syngen 3, mating type 1) bearing *Chlorella variabilis* 1N endosymbionts were downloaded from the DNA Data Bank of Japan (DDBJ) (Tateno et al., 2002; Kaminuma et al., 2011) in Sequence Read Archive (SRA) format (Leinonen et al., 2011; Kodama et al., 2012) (accession DRA000907 (Kodama et al., 2014)).

These reads were then converted to fastq using "fastq-dump" using the SRA Toolkit (National Center for Biotechnology Information, 2011). Reads were then trimmed for sequencing adapters using ILLUMINACLIP and SLIDINGWINDOW with a window size of 4 and a minimum average quality of 5 in Trimmomatic (Bolger et al., 2014).

Reads were then error-corrected using "SEECER" with a k-mer size of 25 and default settings otherwise (entropy of 0.6 and a cluster log-likelihood of -1) (Le et al., 2013). Error-corrected reads were digitally normalised using a K-mer size of 25 and a coverage of 20 (Brown et al., 2012) and low abundance K-mers in high coverage reads were filtered (Zhang et al., 2014, 2015) using the Khmer software package (Döring et al., 2008; Crusoe et al., 2015).

Assemblies were completed in a modified/fixed version of Bridger 2014-12-01 (Chang et al., 2015) (available at `https://github.com/fmaguire/Bridger_Assembler`) and Trinity v2.0.6 (Grabherr et al., 2011; Haas et al., 2013) both with K-mer sizes of 25.

An alternative Trinity assembly was also completed using SLIDINGWINDOW Q30 trimmed reads without normalisation or error correction.

Assemblies were then compared using RSEM-EVAL (Li et al., 2014) and the best overall assembly selected on the basis of likelihood.

ORFs were called from the best assembly using universal and tetrahymena encodings via TransDecoder (Haas et al., 2013) retaining the best scoring sequences and those with HMMR hits to PFAM and BLASTP hits to the swissprot database.

Phylogenies were generated for each sequence using the same approach and pipeline described in Chapter 2. These phylogenies were subsequently classified using the same trained K-Neighbours supervised learning algorithm. Any sequence that didn't have enough BLAST hits in the genomes used to generate a phylogeny (5) were parsed based on what hits were retrieved. Those with no hits were classified as "unknown" and those with hits were classified based on the origin of those hits e.g. hits to green algae and plant genomes were considered "endosymbiont" and so on.

Finally, the ORF bins for host and endosymbiont from both encodings were manually combined and reconciled to generate transcript bins. With the transcripts binned into "host" and "endosymbiont" ORFs were recalled from them using the appropriate encodings.

3 mass spectrometry analyses were conducted to investigate the presence/absence and relative abundances of polar and non-polar metabolites.

Finally, a targeted mass spectrometry analysis was conducted using LC-QQQ to quantitatively assess

Untargeted LC-QTOF Profiling

Sample preparation for mass spectrometry followed standard protocols. Briefly, 5 biological replicates were sampled from *P. bursaria* CCAP 1660/12 cultures at the midpoint of both the day and night cycles. Samples were then dried, flash-frozen in liquid nitrogen, and homogenised using a cell disruptor.

For each sample, $10mg$ was dissolved in $400\mu l$ of a solution of 80% MeOH containing $7.2mgml^{-1}$ of an umbellifrone internal standard. This solution was kept on ice and vortexed for 30s every 10 minutes for 30 minutes. Samples were sonictated in ice cold water for 15 minutes and then centrifuged at 13k rpm for 10 minutes. Retaining the supernatant in a separate tube, the pellet was resuspended in $400\mu l$80% MeOH and vortexing, sonication and centrifugation steps repeated. The two supernatants were combined and filtered through a $0.2\mu m$ syringe filter (Chromacol). Samples were sub-divided into two a $5\mu l$ of each was loaded into an Agilent 1200 Series HPLC with a $3.5\mu m$, $2.1 \times 150mm$ Eclipse Plus C18 Agilent column. One sample was then analyses using a positive electron spray ionisation and the other a negative ionisation on an Agilent 6520 accurate mass quadrupole time of flight (Q-TOF) mass spectrometer. Data was captured using the standard Agilent data acquisition software and converted from ".d" format to the open mzXML format (Pedrioli et al., 2004). The same process was repeated for 7 blank samples under both ionisation conditions as well as an apigenin QC standard.

Samples were analysed primarily using the XCMS R package (Smith et al., 2006; Tautenhahn et al., 2012b). Peak features were detected in each samples using the centWave algorithm with a 30ppm tolerated m/z deviation, minimum peak width of 10 and maximum peak width of 60 (Tautenhahn et al., 2008). Peaks were aligned with a 0.025 m/z width overlap, and a maximum bandwidth 5 retention time deviation. Using the aligned peaks, the retention time deviation between samples were calculated. The samples were then realigned correcting for retention time deviation and integrated using fillPeaks.

In order to determine differential presence of globally detected metabolites unpaired Welch's *t*-tests were conducted comparing the 5 day samples to the 5 night samples. Welch's tests were used as they don't assume equal sample sizes or variances between the two groups(Welch, 1947)[1]

P-values from this were corrected for multiple comparisons using false discovery rates (FDR). FDR is a less conservative correction than, the classic family-wise error rate correction, Bonferroni adjustment[2] but allow maintenance of a greater proportion of statistical power with a slightly evelated risk of Type-I errors.

Features were then annotated using the METLIN metabolite database (Smith et al., 2005a; Sana et al., 2008; Tautenhahn et al., 2012a). Extracted ion base peak chromatograms were manually inspected for each significantly

[1] $t' = \frac{\mu_1 - \mu_2}{\sqrt{\frac{s_1^2}{n_1} + s_2^2 n_2}}$ with degrees of freedom determined via the Welch-Satterwaite-equation: $df = \frac{(\frac{s_1^2}{n_1} + \frac{s_2^2}{n_2})^2}{\frac{(\frac{s_1^2}{n_1})^2}{n_1 - 1} + \frac{(\frac{s_2^2}{n_2})^2}{n_2 - 1}}$ (Ruxton, 2006)

[2] P-value threshold α is adjusted relative to the number of comparisons (n). Specfically, significance is determined as a P-value $\leq \frac{\alpha}{n}$.

Preprocessing	PE Reads
Raw Reads	$2.323 \cdot 10^8$
Q30 Trimmed	$1.75 \cdot 10^8$
Q5 Trimmed	$2.127 \cdot 10^8$
Q5 Error Corrected	$2.021 \cdot 10^8$
Q5 Digital Normalistion	$1.09 \cdot 10^7$
Q5 K-mer abundance filtering	$1.055 \cdot 10^7$

Table 5.4.1: Summary of read pre-processing stages for tthe Kodama library demonstrating the massive amount of redundancy that digital normalisation removes from the assembly. The low amount number of reads removed during K-mer abundance filtering indicates that there were relatively few low abundance

Assembly	Contigs	Likelihood $(-log)$
Trinity Q5 Normalised	101,957	$1.216 \cdot 10^9$
Bridger Q5 Normalised	62,504	$1.285 \cdot 10^9$
Trinity Q30	53,938	$5.619 \cdot 10^9$

Table 5.4.2: Summary of Kodama assembliesj

expressed feature and any that weren't clear distinct peaks were discarded. Any sample without an annotation against METLIN was similarly discarded. Finally, annotations were manually parsed and samples with impossible annotations (e.g. chemotherapeutic drugs) discarded.

Untargeted GC-QTOF Profiling

Targeted Amino Acids Quantitative Analysis

5 Day and 5 Night samples were prepared for liquid chromatography using the same approach as the untargeted LC-QTOF analysis. In addition to this, the Day1 and Night1 samples were analysed at both $2x$ and $0.5x$ titrations. 3 blank samples were run as well as standards consisting of a complete amino acid mix from Sigma at $0.5\mu M$ and 4 samples consisting of Asparagine-Glycine-Tryptamine and Leucine-Glutamine-Lysine respectively.

After chromatography samples were ionised using electronspray ionisation and analysed using multiple reaction monitoring optimised for amino acids with an Agilent Technology 6410B enhanced sensitivity triple quadrupole mass spectrometer (QQQ).

Results were analysed using the Agilent Quantiative Analysis software package with peaks normalised in respect to the umbelliferone standard. Results for any

Agilent 6410 enhanced sensitivity triple quadrupole (QQQ) with Agilent 1200 series HPLC stack

5.4 Results

5.4.1 Kodama Assembly

Therefore, the optimal assembly chosen for further analysis was the Trinity Q5 normalised assembly on the basis of RSEM-EVAL score.

From the 101,957 transcripts 193,906 ORFS were called using tetrahymena encoding and 20,875 universal.

Bin	Number of Transcripts
Food	3,873
Endosymbiont	8,627
Host	53,295
Unknown	36,162

	C. variabilis 1N	*M. reisseri CCAP 1660/12*	*C. vulgaris NC64A*	*C. subellipsoidea C-169*
Peptides	5,565	4,275	9,791	9,629
1+ TM domains	695	419	1,722	1,709
1+ TM and TCDB	251	185	690	697

These were subsequently binned using the same approach as used in Chapter 3.

Finally, "Host" and "Endosymbiont" binned transcripts were re-ORF called using the appropriate encodings to result in a host ORF bin of 61,239 sequences and an endosymbiont bin of 5,565 peptides.

5.4.2 Transporter Identification

To identify transporters present in the translated protein dataset of the endosymbiont bins of the CCAP1660/12 and YADGN1 *Paramecium bursaria* transcriptome assemblies, as well as the Chlorella NC64A and Coccoymxa C-169 predicted proteomes the following process was used:

A set of 233 transporter proteins were also identified in the *M. reisseri* binned peptides by parsing the results of a BLAST/InterProScan and GO term based annotation pipeline. Of, these 77 were redundant to proteins already identified using the TM/TCDB pipeline, therefore 156 were novel.

This means a total of 341 transporters were identified belonging to the CCAP 1660/12 endosymbiont from the SCT transcriptomes.

5.4.3 Kallisto quantification analysis

Using the nucleotide CDS sequence of the called peptides identified as transporters from the primary SCT transcriptome.

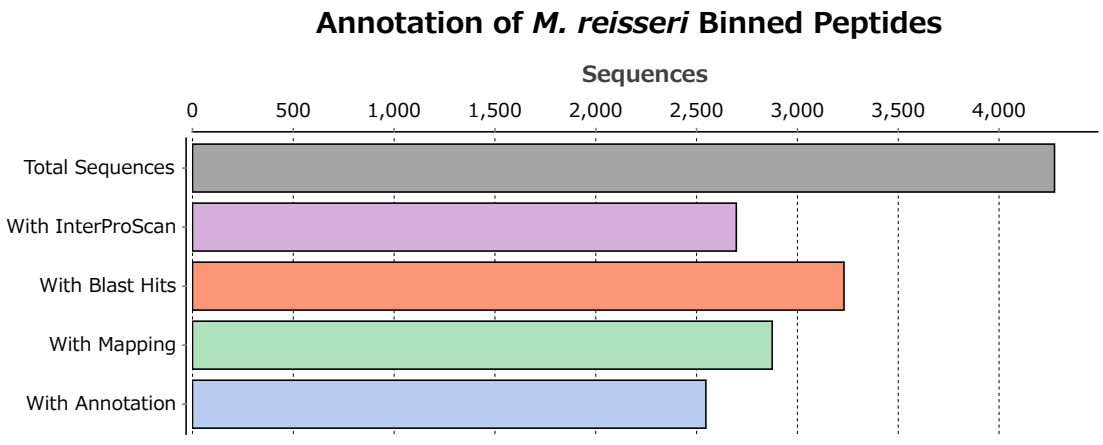

Figure 5.4.1: More stringent

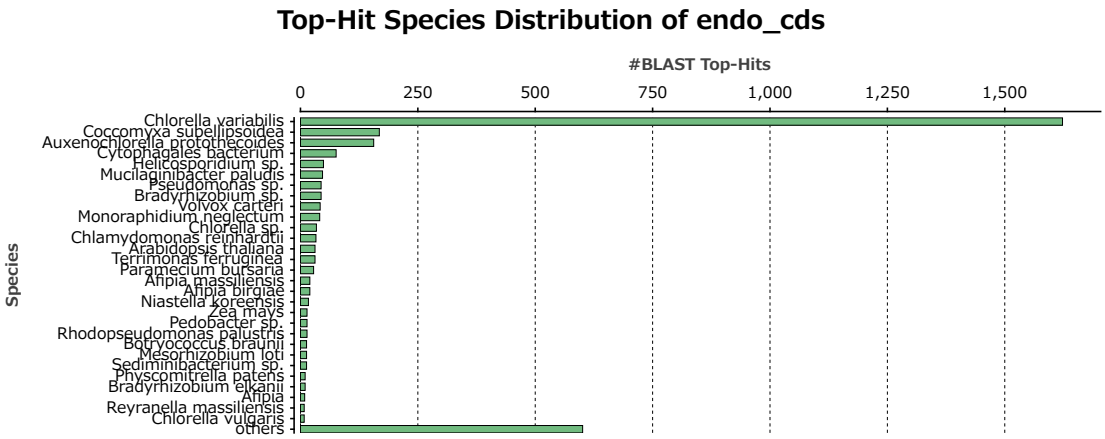

Figure 5.4.2: asdasd

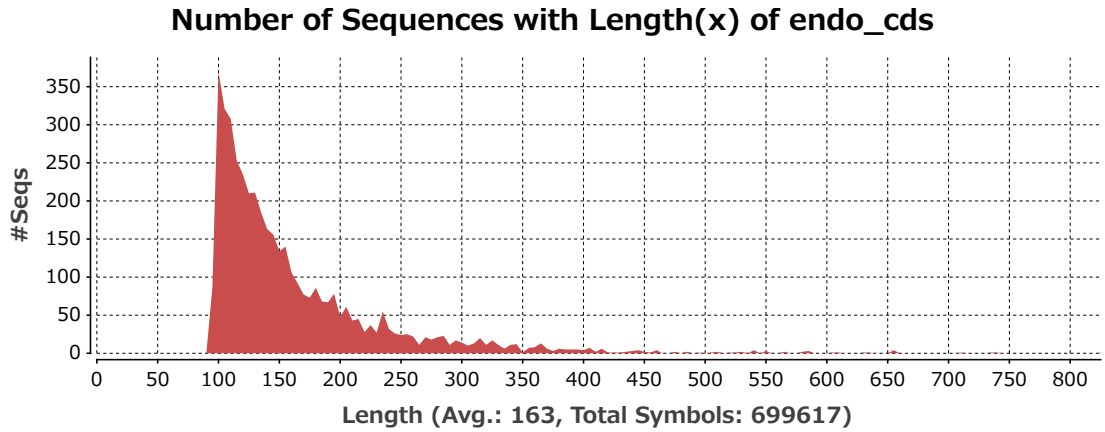

Figure 5.4.3: asdasd

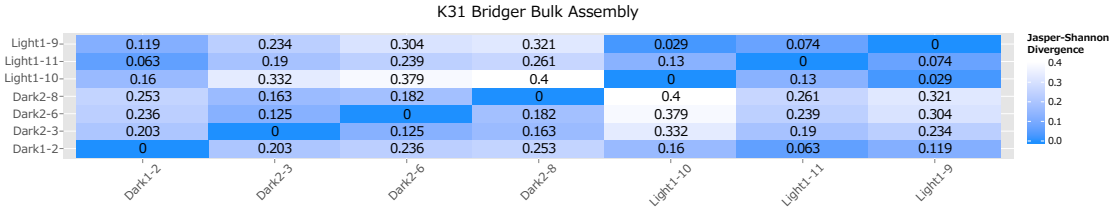

Figure 5.4.4: Comparison of single cell libraries

Due to the compositional/coverage biases of MDA-based single cell transcriptomics Kallisto statistical inference was likely to be spurious and relate to the well-documented coverage biases of MDA. Therefore, a simple presence/absence filter was implemented for the single cell libraries where an estimated Transcripts per million (TPM) was above 0 for at least 1 biological replicate in each condition. TPM is an estimate of the

Of these only 2 were expressed in all 4 bulk libraries 34 in all 3 light libraries, 14 in all taxonomicall screened SCT libraries.

After filtering photosystems and cytochrome related transporters = number left

2 homologs of HUP1,2,3 - m.12814 m.17059 (latter in b2go has no TM domain - partial ?)

Nitrate Reductase - m.43047 NADH-glutatamte reductase dehyodrgenase ? gluatmine synthetase ? No high e-value hit for Nitrite reducatase

Ammonium transporter m.62060 in b2go not in TM pipe

5.4.4 Secreted proteins

This resulted in a set of 44 proteins for endosymbiont

One of the most intriguing of this set is that of a putative raffinose synthase

comp65133_seq0|m.57547 Alpha amylase catalytic domain family 1.38e-10 homologous to Raffinose synthase or seed imbibition protein Sip1

low number of reads mapping in 1 day and 1 night library

Constitutive expression in both bulk samples

5.4.5 Metabolic Maps

All prok transporters? One interesting aspect of comparison between the *M. reisseri* endosymbiont and the other endosymbiotic green algae was the unique presence of 3 additional sub-units of the branched-chain amino acid ABC transporter. *M. reisseri* binned sequences contained the LivK, LivG, LivF sub-units as well as the LivH and LivM units shared by all the remaining algae. This suggests either.

There are also putatively RbsB and RbsA subunits of a Ribose/D-Xylose ABC transporter not present in and a LptB element of the ABC-2 lipopolysaccharide transporter and OppD oligopeptide transporter.

Uracil-xanthine transporters

State	Name	TCDB Identity	
All Dark Libraries	comp11781_seq0|m.10145	PF00448.18	
	comp20734_seq0|m.20988	PF00122.16	
All Light Libraries	comp34406_seq1|m.34111	PF02705.12	
	comp55761_seq0|m.51120	PF07690.12	
	comp26454_seq0|m.27109	PF03239.10	
	comp12997_seq0|m.11462	PF02653.12	
	comp2196_seq0|m.2436	PF00361.16	Proton-conducting membrane t
	comp30376_seq0|m.30648	PF01490.14	
	comp8796_seq0|m.7077	PF01241.14	
	comp16529_seq0|m.15912	PF00032.13, PF00033.15	
	comp39264_seq0|m.37815	PF01970.12	
	comp12686_seq0|m.11025	PF01970.12	
	comp18033_seq0|m.17793	PF03401.10	
	comp16603_seq1|m.16010	PF00860.16	
	comp1093_seq1|m.1645	PF00860.16	
	comp8621_seq0|m.6954	PF00033.15	
	comp23923_seq0|m.24587	PF00032.13	
	comp23290_seq0|m.23888	PF00115.16	
	comp19868_seq0|m.19974	PF00115.16	
	comp47698_seq0|m.44756	PF01061.20	
	comp27137_seq0|m.27822	PF06472.11	
	comp33855_seq0|m.33598	PF00528.18	
	comp38129_seq0|m.36919	PF00528.18	
	comp29161_seq0|m.29630	PF00528.18	
	comp30550_seq0|m.30821	PF02417.11	
	comp36383_seq0|m.35530	PF02487.13	
	comp2716_seq1|m.2811	PF01490.14	
	comp31515_seq0|m.31652	PF00146.17	
	comp15817_seq0|m.15012	PF02990.12	
	comp23811_seq0|m.24460	PF03030.12	
	comp12244_seq0|m.10668	PF03030.12	
	comp17395_seq0|m.16982		
	comp38285_seq0|m.37041		
	comp61444_seq0|m.55210		
	comp12398_seq0|m.10763		
All SCT libraries	comp23196_seq0|m.23818	PF00223.15	
	comp16798_seq0|m.16234	PF00223.15	
	comp13220_seq1|m.11682	PF00223.15	
	comp13220_seq0|m.11681	PF00223.15	
	comp1772_seq0|m.2188	PF00421.15	
	comp1772_seq1|m.2192	PF00421.15	
	comp2799_seq0|m.2876	PF00361.16, PF06455.7, PF00662.16	
	comp2799_seq0|m.2878	PF00361.16, PF06455.7, PF00662.16	
	comp2682_seq0|m.2777	PF03911.12	
	comp2682_seq2|m.2790	PF03911.12	
	comp6740_seq0|m.5524	PF00119.16	
	comp16837_seq0|m.16280	PF00510.14	
	comp428_seq0|m.891	PF01333.15	
	comp15996_seq1|m.15230		

Table 5.4.3: A list of CDS identities that were predicted to be expressed in all the single cell libraries of a given type.

Figure 5.4.5: KEGG Maps contrasting endo bin with other algae

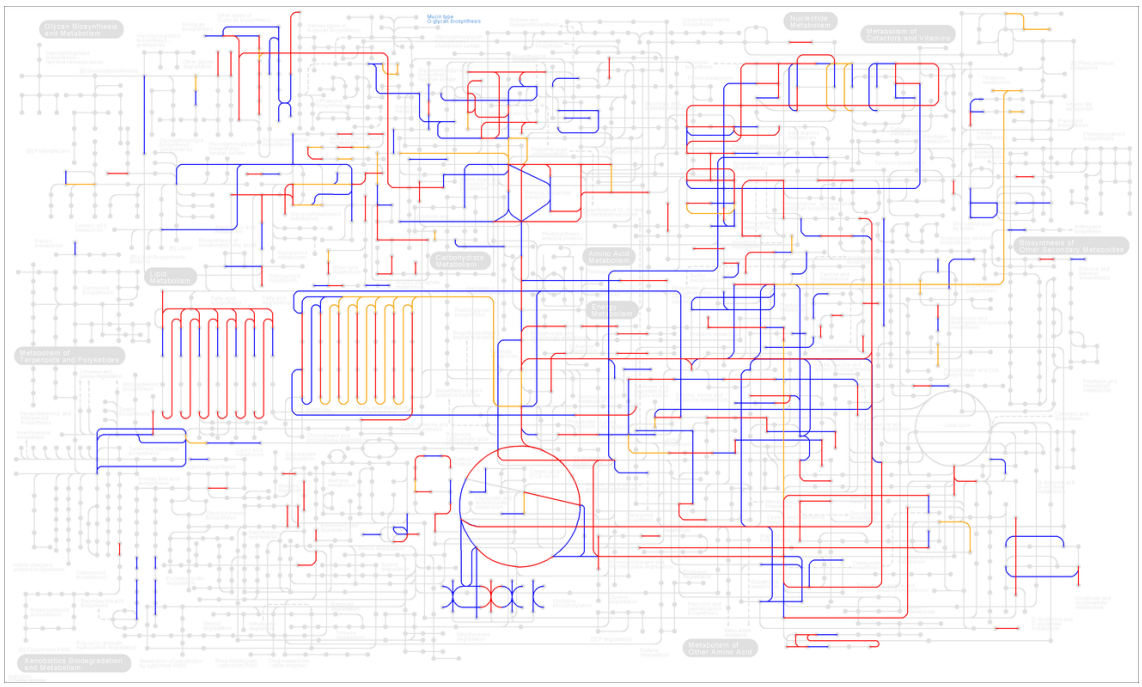

Figure 5.4.6: KEGG Maps contrasting host bin with other host

Malate-Fumarate fumarate hydratase not present in other algae

5.4.6 Metabolomics

Global profiling

Only one metabolite putatively with a m/z matching glucose was identified with no significantly different expression.

GCMS- down reg of putative 6-Acetly-D-glucose -1.24

Again one interesting peak is that of in negative 9.7 0.04846 DOWN with a fold vlaue of 9.7 putatively raffinose>? 503.1698 vs actual 503.169

Xylitol or arabinose likely play a role Arabinose is likely to play a role with the signficant (2.7) fold up-regulation of arabinosyl glucoside in LC-QTOF pos, Arabitol/Xylitol of 1.52 and 2.24 In GCMS Arabionic acid/xylonate 3.1 up

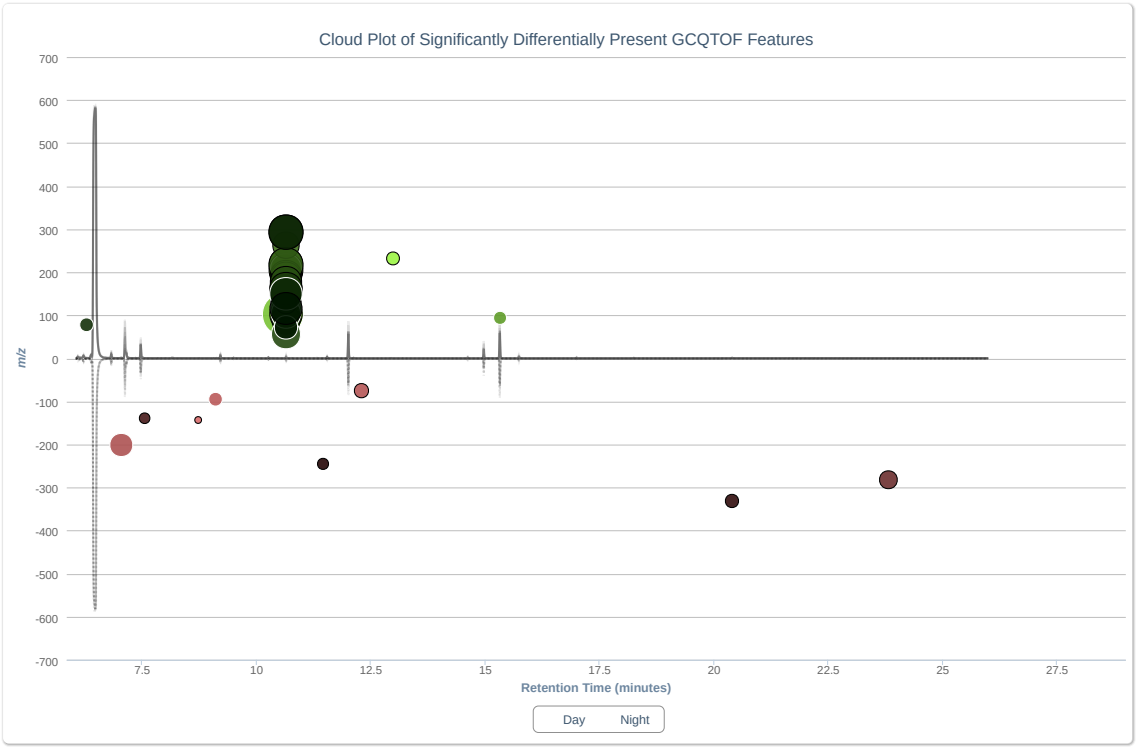

Figure 5.4.7: Cloud point showing for the GCQTOF analysis. The radius of a given point reflected its fold change. Data is filtered to those 50 points with significantly different expression (FDR corrected P-value of 0.01 shown by depth of colour)

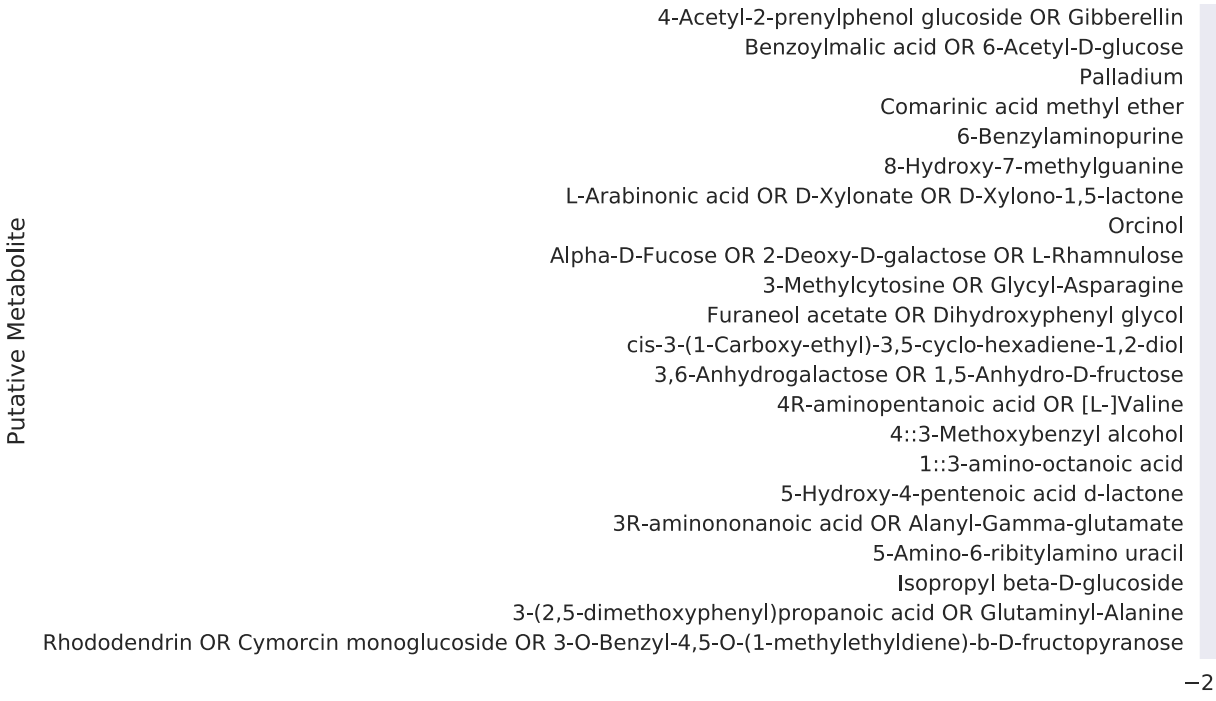

Figure 5.4.8: Plot showing the fold change of the 23 putatively identifiable significantly differently present metabolites from GC-QTOF. 5 peaks were discarded after inspection of the EIC. 8 were discarded as there was no sensible annotation, 14 had no annotations.

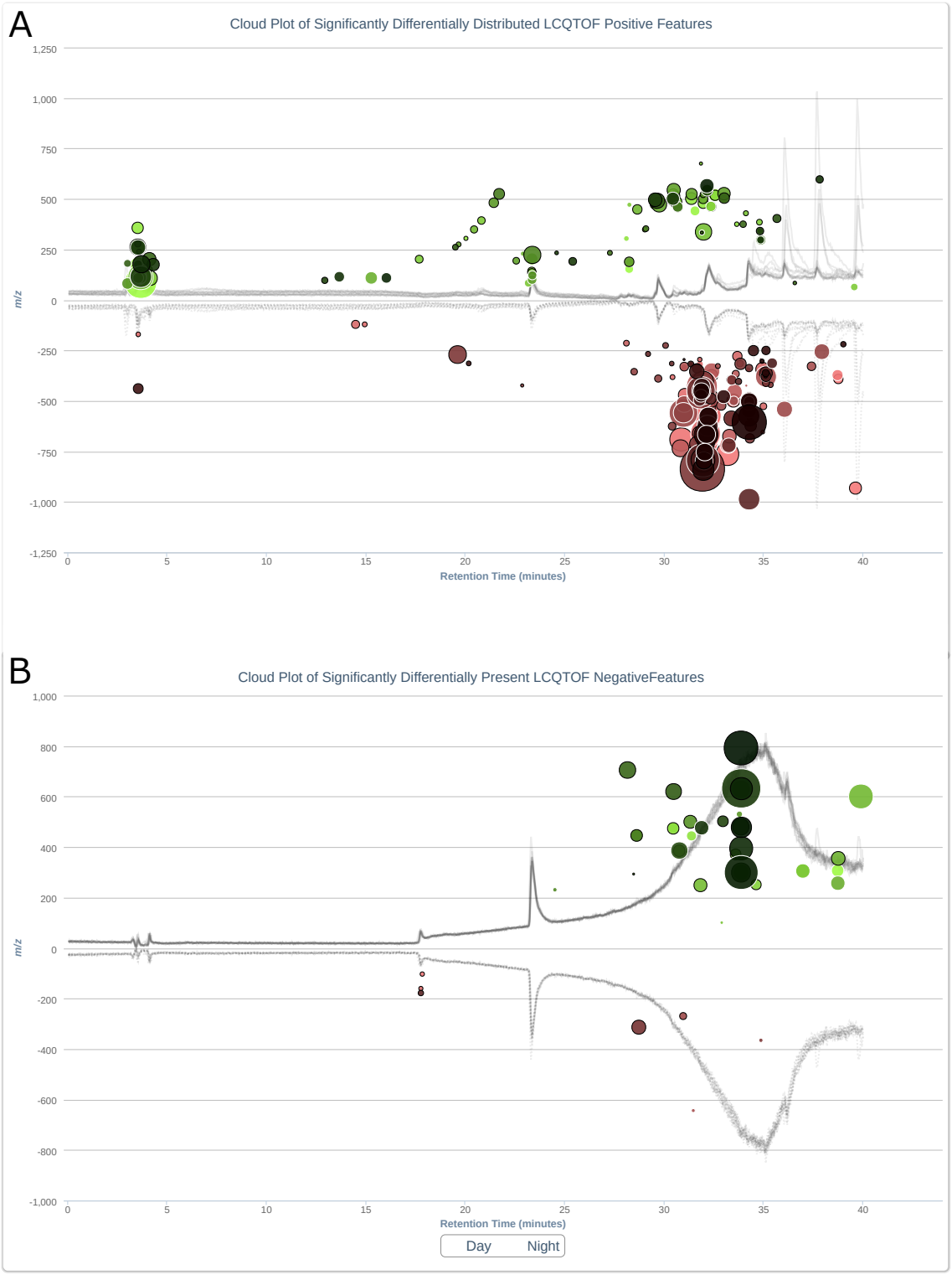

Figure 5.4.9: A: Positive 254, B: 43

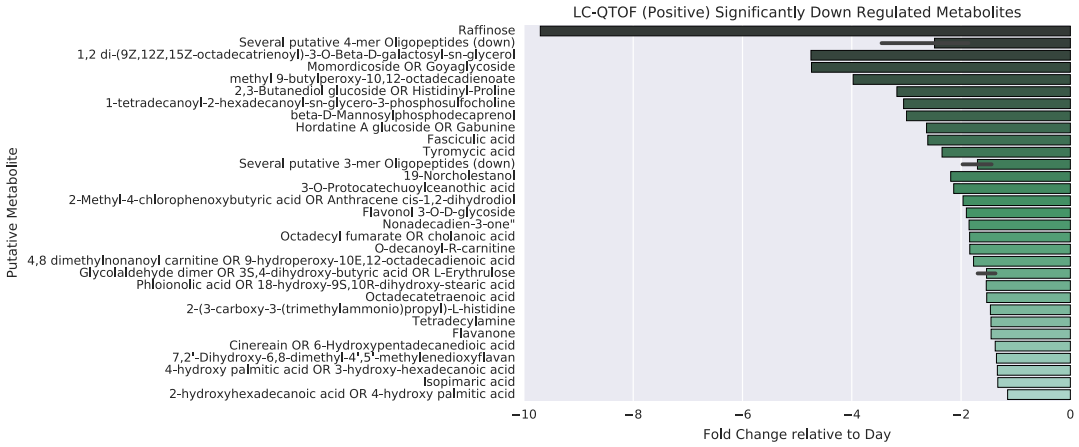

Figure 5.4.10: Of the 254 positive significantly different present metabolites, 19 were removed after manual inspection of peaks, 95 were removed due to having no METLIN hits

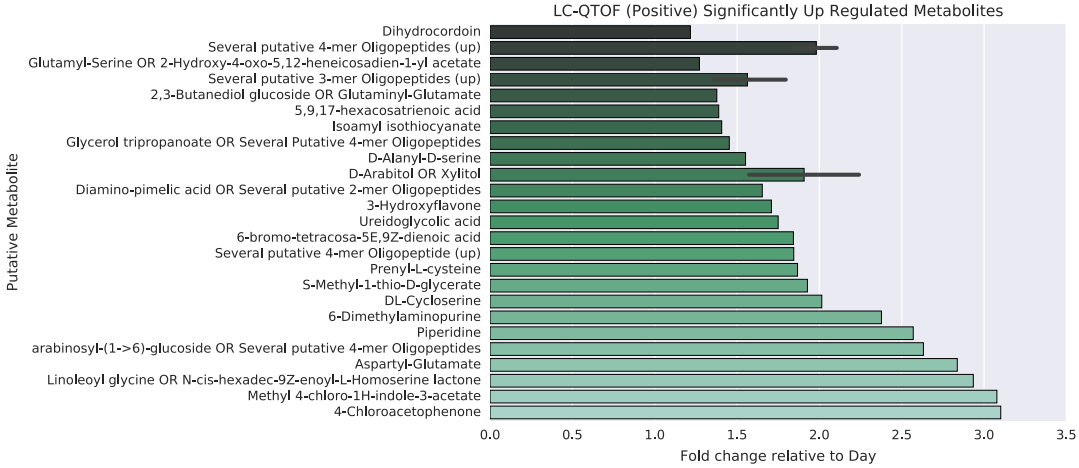

Figure 5.4.11: Of the 254 positive significantly different present metabolites, 19 were removed after manual inspection of peaks, 95 were removed due to having no METLIN hits

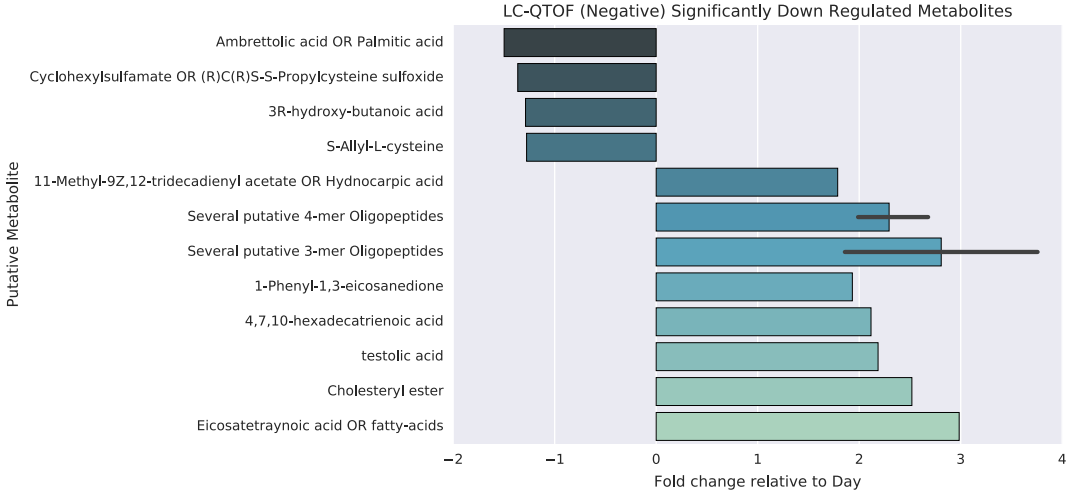

Figure 5.4.12: Of the 43 positive significantly different present metabolites, 3 were removed after manual inspection of peaks, 17 were removed due to having no METLIN hits

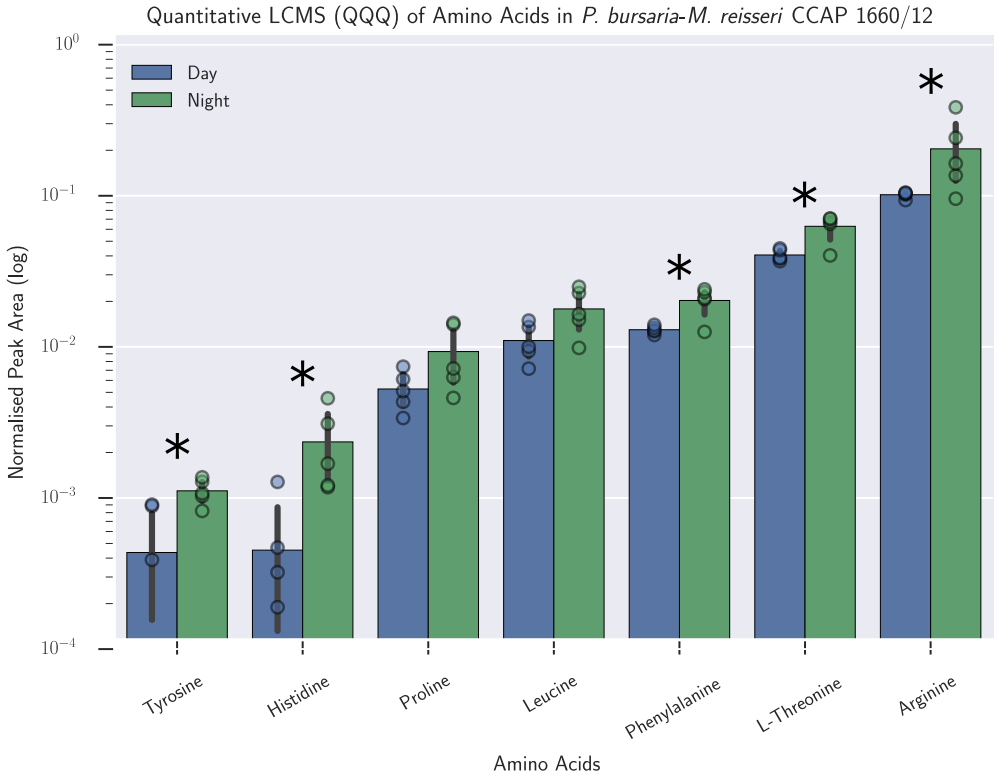

Figure 5.4.13: LC-QQQ analysis of amino acid abundances. Normalised Peak Areas Calibration was conducted using Day1 and Night1 samples at two titrations, as well as Asn-Gln-Tryptamine and Sigma AA mixes Calibration and quantitative analysis failed for the following amino acids: Glutamic Acid, Tryptamine, Asparagine, Trpytophan, Isoleucine, Methionine, Valine, Serine, Glutamate, Glutamine, Aspartic acid, Cystein or Lysine. Significant concentration differences between day and night (as determined via Welch's '*t*' are indicated by an astrerisk.

5.5 Discussion

SEECER and K-mer abundance filtering may be mutually exclusive

5.5.1 Quantification in MDA

MDA has amplification bias with GC content - problem for PbMr (Macaulay and Voet, 2014)

5.5.2 All methods have limitations

Can't identify traits related to acquistion of endosymbionts.

Another possible benefit is to apply similar methods to cultures gaining their endosymbiont

All the methods included here have major limitations.

Firstly, the identification and analysis of secreted and transporter proteins, as well as the metabolic mapping is fundamentally reliant on the quality and completion of the host and endosymbiont transcriptomes. Any transcript missing from these bins either due to failure to assemble, cryptic MDA biases, or erroneous binning into bins other than host or endosymbiont.

This incorporates the issues with false negatives.

However, there is also the issue of false positives. This is especially important for the transporters where a minimal (as few as a single amino acid) divergence is sufficient to convert them to non-transporting sensor proteins (Lalonde et al., 1999; Bianchi and Díez-Sampedro, 2010).

Therefore, it is key that the functionally important

blah has to be tested

5.5.3 Limits of metabolomics analysis

A more intelligent hypothesis testing than corrected unequal variance 't'-test could be used such as Kurschke's Bayesian BEST algorithm (Kruschke, 2013). This also has the advantage of a Bayesian inference which can be made robust to multiple comparisons without need for extensive correction procedures by using standard multi-level approaches (Gelman et al., 2009).

5.5.4 Potentially missing transporters

One potential issue with the binning methodology used is that any recently horizontally acquired host or endosymbiont transporters or other metabolic pathway proteins will have been misclassified and potentially discarded into the "food" or "unknown" bin.

This is problematic as there is evidence for bacterially acquired hexose-phosphate transporters playing a key role in the establishment of primary plastid endosymbiosis (Price et al., 2012; Karkar et al., 2015).

Ideally, future work could expand this transporter analysis over the "unknown" and "food" binned sequences in combination with synteny analyses using genomic sequences to investigate and identify potential horizontally acquired transporters that may play a role.

Another issue with the binning approach used is the possibility of totally novel transporter (and other proteins) not being classified due to the dependence of the binning on homology to known sequences. Therefore, totally novel proteins would not have been identified as "host" or "endosymbiont". Unfortunately, this problem could only properly be resolved with a thorough and robust draft quality genome for both host and endosymbiont which was outside the scope of this analysis.

The final source of obfuscation in an accurate analysis of this data is that of host-endosymbiont gene transfer. This is well observed phenomenom that has resulted in the eventual loss of the endosymbiotic in the majority of algal secondary endosymbiotic organelles as genes are transferred to the host nucleus (Keeling and Palmer, 2008; Archibald, 2005; **?**).

It is unknown and difficult to determine to what extent the unusual nuclear dimorphism and germline sequestration of the host effect's the rate of this form of transfer.

Fortunately, this binning method means that while some peptides may have been falsely assigned to wrong bin all "host" and "endosymbiont" ORFs that were not either so novel they lacked any homology to known proteins or were recently acquired from bacteria were still included in this analysis.

However, as some *M. reisseri* and *Chlorella* endosymbionts have been demonstrated as capable of free-living it is unlikely that HGT has occurred between host and endosymbbiont as extensively as that observed in established photosynthetic organelles.

5.5.5 Secretome

Without knowledge of *P. bursaria*'s intracellular trafficking system it is not possible to easily infer which host peptides are secreted into the PV. For this reason, analysis of secreted proteins focussed on the endosymbiont bin as the secretion signal are generally better conserved and established.

Unfortunately, much as incorrect

5.5.6 Metabolomics shows promise

The pilot application of metabolomics demonstrated mixed results. There was poor performance of mass

GC/MS failed for comprehensive profiling of carbohydrates. Possibly due to miscalibration of the GC parameters or the capture paramters on the initial quadrupole.

All globally profiled metabolites required comprehensive validation with a secondary mass spectrometry.

The failure of accurate quantification in the second round of MRM LC-QQQ spectrometry for the majority of amino acids is problematic. However, this targeted approach still revealed useful information regarding the relative abundance of amino.

Particularly, both the high concentration of arginine as well as its significantly differential abundance between day and night indicates that this amino acid may well form a major component of host provided nitrogen for

M. reisseri. This is in concordance with previous findings suggesting the importance of this amino acid in the *C. variabilis* endosymbiosis (Kato et al., 2006).

Despite not have been implicated in previous analyses as one of the key amino acid nitrogen sources, the identification of both high quantities and differential abundant threonine and phenylalanine suggests that these amino acids may play a role in the host-endosymbiont barter system of *P. busaria-M. reisseri*.

This alternative behaviour suggests that the feeding experiment results by (Kato et al., 2006) and (**?**) need to be re-evaluated for *M. reisseri*. This also adds further support to the diversity of endosymbiotic relationships between *P. bursaria* and its various algal endosymbionts.

Unfortunately, a failure to accurately quantify and calibrate for several amino acids means this targeted metabolomic analysis is incomplete. Of particular interest, is the remaining 5 amino acids implicated in *C. variabilis* F36-ZK's endosymbiosis.

In future, metabolomics needs further optimise for the discovery of carbohydrates.

Additionally, advanced novel techniques such as nanoscale secondary ion mass spectrometry combined with microscopy and isotope labelling could theoretically allow direct analysis of metabolites present in the PV (Kopp et al., 2015; Legin et al., 2014).

5.5.7 Novel Sugars Implicated in the Endosymbiosis

Several sugars not previously associated with this endosymbiosis have been identified in this analysis as putatively playing important roles.

Specifically, the significantly upregulated Arabinose/Xylitol Arabinose not implicated

Contrary to dinoflagellate coral endosymbioses that don't detecet arabinose (Markell and Trench, 1993).

and significantly down-regulated Raffinose.

Putatively novel role for Raffinose in endosymbiosis?? galactinol + sucrose → myo-inositol + raffinos/

Unfortunately, the GCQTOF analysis failed to successfully identify sugars in the

Raffinose has been associated with cold shock in *Parachlorella kessleri* (formerly *C. vulgaris*), accumulating duing cold exposure and disappearing after return to normal culture temperatures

It is unclear if raffinose is a (Salerno and Pontis, 1989)

Raffinose and another Raffinose Family Oligosaccharide (RFO) stachyose are generated from sucosrse in gymnopserls during the cold season (Kandler and Hopf, 1982).

Raffinose has been found to inhibit growth under isosomotic conditions in a *C. vulgaris* (Setter and Greenway, 1979).

Specifically, it has also been directly associated with cryoprotection of thykaloid membranes (Lineberger, 1980). And no chlorop targeting sequence though

But that doens't explain secretion.

Bacterial raffinose transport system?

In archaeplastida RFOs are related to stroage and transport of carbon.

What about trehalose? sucrose? phylogeny?

It does appear that the raffinose synthase is constitutively expressed unless both light and dark conditions are exposed to cold stress.

Culture temperature was 18°C, so this is unlikely.

Needs confirmed with qPCR.

Putative galactose related compounds were signficantly up-regulated (deoxy-D-galactose and)

5.5.8 Endosymbiont Nitrogen Metabolism

The presence of amino acid transporters.

The identification of a partial oligopeptide transporter combined with the high concentrations of various 3- and 4-mer oligopeptides suggests that previous studies focussing exclusively on endosymbiont utilisation and uptake of individual amino acids (e.g. those reviewed in (Kato and Imamura, 2009b)) may have missed on the role of these in host-endosymbiont nitrogen flux.

The difference in amino acids abudances for several of those fitted as well as differential numbers of reads mapping to putative amino acids transporters indicates light-dependent amino acid uptake in the endosymbiont.

One the balance of the evidence of significantly higher concentrations of specific amino acids.

There is reason to believe that *M. reisseri* CCAP 1660/12 endosymbiont displays a similar system to that of the Japanese *C. variabilis* F36-ZK strain in terms of amino acid usage.

Intriguingly, the transcriptome reveals the presence of all sub-units of the ABC-type branched amino-acid transporter not present in the other endosymbiotic green algae. However, the non-differential abundance of Leucine makes it hard to determine.

Due to the huge range of possible

While, NR and NiR are present in the *M. reisseri* transcriptome it is possible that these are non-functional like the mutants in NC64A and F36-ZK.

5.6 Conclusion

This preliminary analysis of host-endosymbiont metabolic integration has lead to some promising results. Namely, discovering quantitative data supporting the mechanism by which the host likely provides a nitrogen source to the endosymbiont. Specifically,

Ultimately, the key finding from this analysis is that *M. reisseri* much like various strains of *C. variabilis* exhibit a range of adaptations to endosymbiosis and a given host displays different behaviours.

However, further work is needed to confirm both the role and loc

In biology, nothing is clear, everything is too complicated, everything is a mess, and just when you think you understand something, you peel off a layer and find deeper complications beneath. Nature is anything but simple.

- Richard Preston: The Hot Zone

6 RNAi Analyses

6.1 Introduction

RNAi is a highly useful experimental methodology through which many biological hypotheses can be tested.

23nt siRNA from Dcr1 in *P. tetaurelia* (Lepere et al., 2009)

6.1.1 RNAi pathway in *Paramecium* sp.

Is there significant cross-talk between endosymbiont and host? - is this why RNAi doesn't seem to work

What of the required RNAi components from Marker are present in genome and transcriptome host bins

What is the phylogeny of these components compared to other Paramecium/ciliate species?

eDicer experiment results - what is the overlap with host orthologs of known yeast lethal genes

rnai as cross-kingdom communication (Weiberg et al., 2015)

FIGURE 5. Dating of genome duplication events

6.2 Aims

Induce RNAi based knock-down using transformed bacterial vectors.

RNAi via microinjection

Gene	Function	RNAi phenotype in *P. tetaurelia*	Vector Design
epi2	Epiplasmin	"Monstrous" cells	500bp via *Pst*I and *Hi*
NSF	Membrane fusion factor	Lethal	500bp via *Pst*I and *Hi*
pTMB.422c	Binding protein	Lethal	500bp via *Pst*I and *Hi*
bug22	Basal body/ciliary protein	Slow swimming and death	313bp via *Xba*I and *H*
BBS7	Ciliary ion transport	Fewer, shorter ciliar	486bp via *Xho*I and *H*
PGM	PGM endonuclease	Post-autogamous cells unable to resume normal growth	500bp via *Pst*I and *Hi*

Table 6.3.1: Details of RNAi vectors used. All constructs were cloned into a L4440 vector and used an Ampicillin resistance market

Gene	*P. tetaurelia* Accession	Length	Role
Rdr1	PTETG8500012001	4319	Exo
Rdr2	GSPATG00036857001	4162	Exo and Endo
Rdr3	GSPATG00006401001	3292	Endo
Cid1	PTETG9100013001	1051	Exo
Cid2	PTETG13400003001	1083	Exo and Endo
PSD1	PTETG600032001	2084	Exo
Dcr1	GSPATG00021751001	5394	Exo and Endo
Ptiwi12	GSPATG00001709001	2315	Exo
Ptiwi13	PTETG4800007001	2483	Exo and Endo
Ptiwi14	PTETG16300003001	2428	Endo
Ptiwi15	GSPATG00005370001	2315	Exo

Table 6.3.2: (?)

Identify required components for endogenous or exogenous RNAi in *P. bursaria* CCAP 1660/12 from transcriptome and genome

Investigate the possiblity of "host" - "endosymbiont" collision as a reason for disabling.

6.3 Methods

6.3.1 RNAi feeding experiments

Methods modified from ParameciumDB

PGM was identified in the genomic contigs (see chapter 1).

6.3.2 RNAi microinjection

6.3.3 Analysis of RNAi pathway

Genomic survey for components

BLASTP using sequences from Marker against transcriptome and genome

6.4 Results

6.4.1 RNAi feeding experiments

Fail

6.4.2 RNAi microinjection experiment

Fail

6.4.3 RNAi required components

BLASTX

Cid

6.5 Discussion

6.5.1 Exogenous RNAi is non-functional in *P. bursaria* CCAP 1660/12

PSD1 is totally absent.

Degenerate PCR was attempted using sequences from *P. tetaurelia* and the other *aurelia*

6.5.2 Endogenous RNAi is methodologically difficult

While RNAi by microinjection repeatedly failed there is a still a high possibility that this is more related to the methodological difficulty of this technique rather than necessarily any fig. 6.5.1

6.5.3 Deactivation requires confirmation

6.5.4 Endosymbiont "collision" hypothesis

Hypothetically, one explanation for the deactivation/loss of RNAi in *P. bursaria* CCAP 1660/12.

- need to confirm

6.6 Conclusions

RNAi induced phenotypes could not be created in *P. bursaria* CCAP1660/12 by either feeding experiments or direct transgene microinjection.

Therefore, assembled transcriptomic and genomic data from *P. bursaria* CCAP 1660/12 and YADG1N were analysed for factors identified as essential in the function of these pathways in *P. tetaurelia* (**?**).

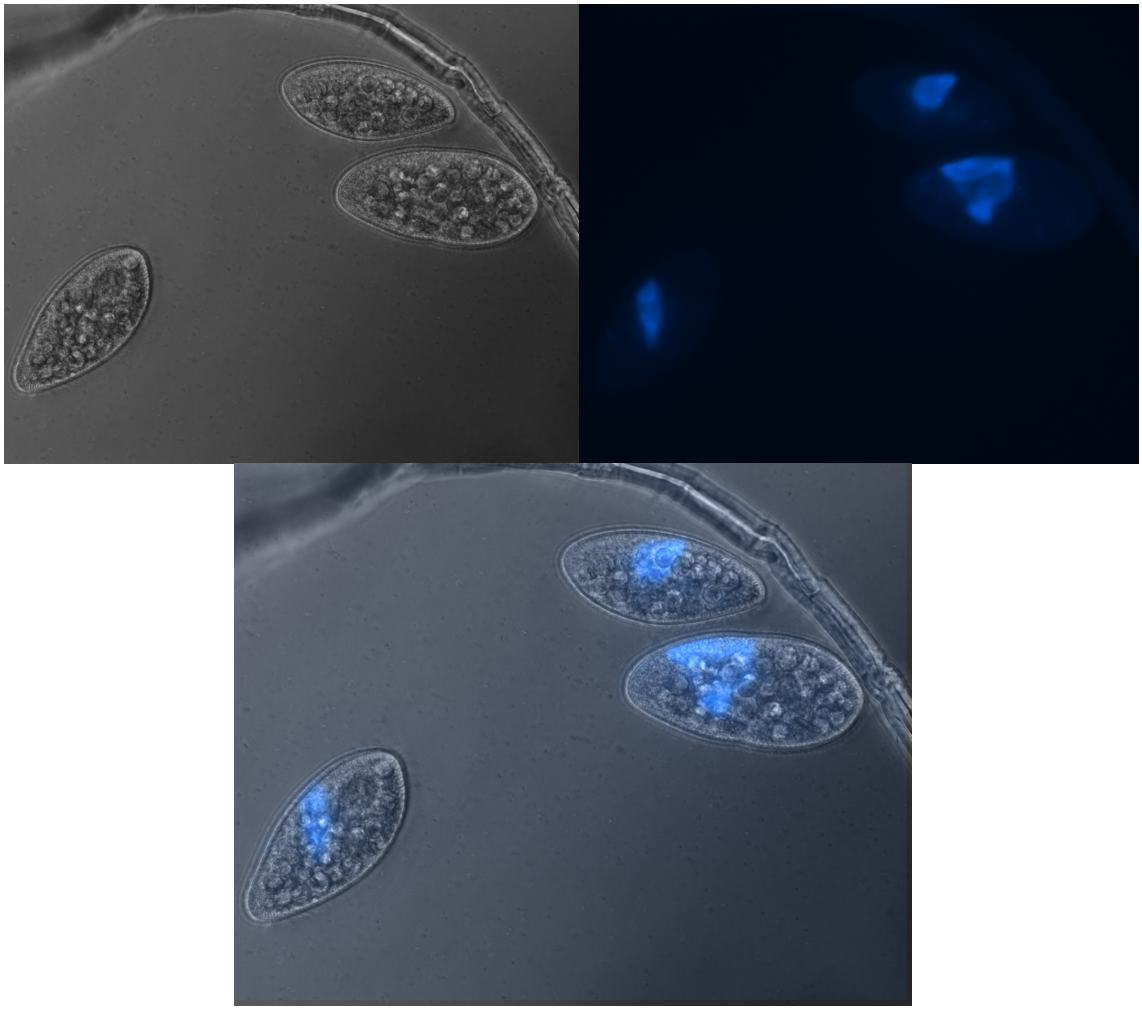

Figure 6.5.1

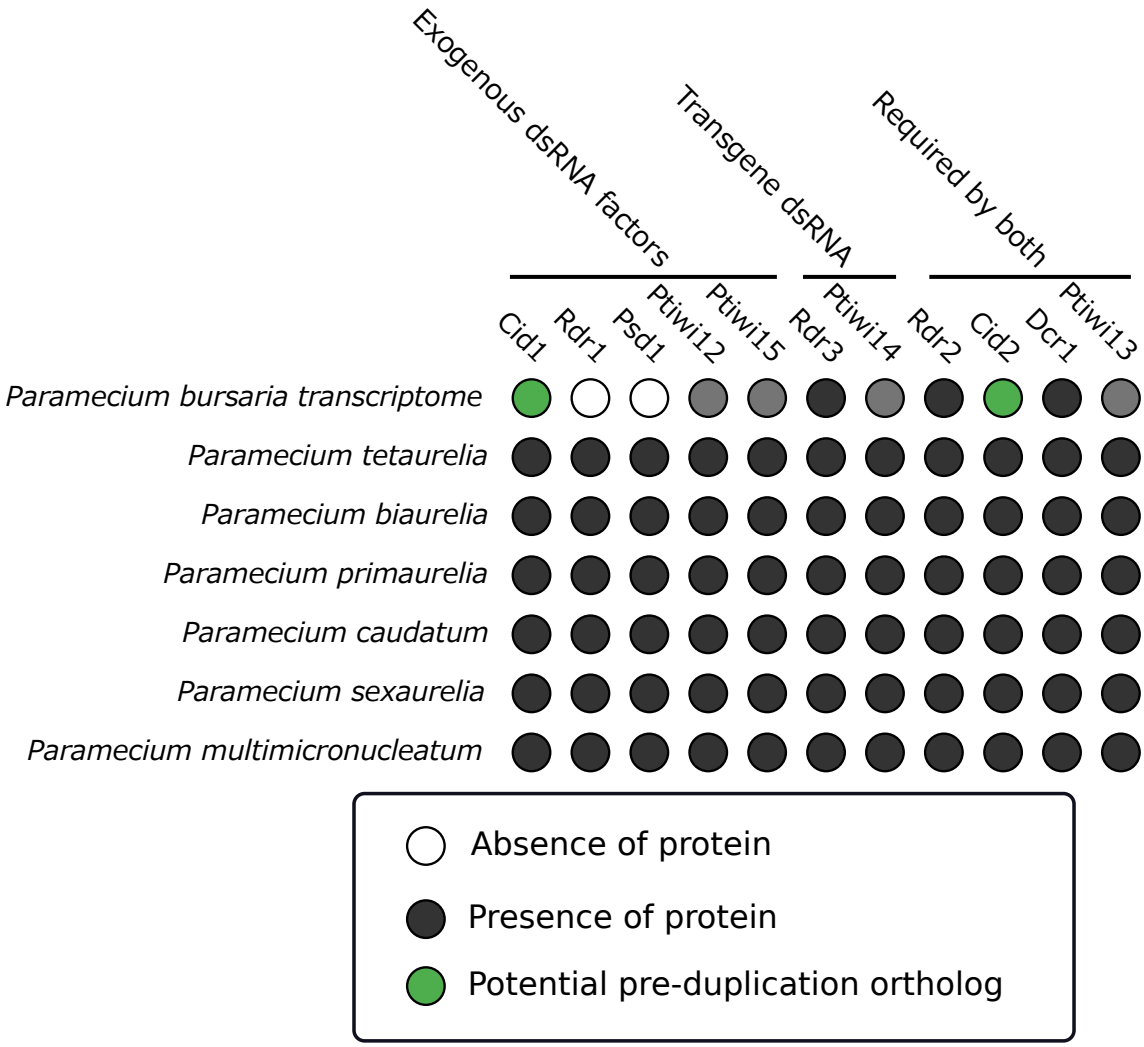

Figure 6.6.1: Summary of the discovery of RNAi figures in *P. bursaria*

Two proteins essential for the function of the exogenous dsRNA induced RNAi pathway in *P. tetaurelia*, Psd1 and Rdr1, were not found in the partial genome and transcriptome of *P. bursaria* CCAP 1660/12 or the transcriptome of *P. bursaria* YADG1N. This suggests that this pathway may not be active/present in *P. bursaria*. Either,

However, assuming the likely pre-duplication orthologue of Cid2 and the necessary unresolved Ptiwi's are functional in the transgene dsRNA pathway of *P. bursaria* then this pathway is theoretically active. Unfortunately, methodological difficulties in microinjection have thus far failed to generate RNAi-induced phenotypes.

"a typical symbiotic Chlorella strain common to all P. bursaria strains does not exist"

- Reisser et al. (1988)

7

Discussion and Conclusions

PROFOUND THOUGHTS

Endosymbiosis is widespread across the tree of life and ecologically

Forms a key part of the evolution of the euks

Understanding endosymbiosis in all its form is fundamental to answering both high-concept key questions pertaining to the evolution of the eukaryotic cell as well as specific mechanistic and utilitarian questions about using endosymbiosis, bioengineering, shit.

Green algal phylogenetics and taxonomy is a messy field still undergoing a high degree of flux.

MDA-based genomes are difficult and prone to contamination

MDA-based transcriptomics

Digital normalisation and error correction in general is a hugely important technique by which

The analysis of complex messay

7.0.1 Why not further integration?

Why is there not evidence of tighter integration in this system.

Firstly, the protein import systems considered necessary for extensive EGT to start taking place are complicated in the cases of secondary and tertiary endosymbioses than basic plsatids due to the increased number of membranes that may need to be traversed especially for import directly to the secondary plastid from the host

(Hirakawa et al., 2012).

Secondly, the unusual nuclear dimorphism of the host *P. bursaria* may prove a barrier to the vast majority of EGT activity.

For successful transfer to take place between host and endosymbiont it would be necessary for the gene to transfer not just from the endosymbiont to the transcriptionally active host MAC but to the germline MIC. Even then integration into the MIC would have to occur in such a way that it would be correctly spliced and duplicated during the conversion of the MIC back to the MAC. Compounding this with sexual reproduction further decreases the probability of effective integration.

It should be noted that the prototypical hosts of the endosymbiotically "promiscuous" green algae - *Chlorella*, *Coccomyxa* and *Micractinium* all display germline sequestration either through the aforementioned dimorphism in *P. bursaria* or via standard metazoan germlines in the case of *Hydra* and the kleptoplastic sacoglossan sea slugs.

Bibliography

Abascal, F., Zardoya, R., and Posada, D. (2005). ProtTest: Selection of best-fit models of protein evolution. *Bioinformatics*, 21(9):2104–2105.

Abou-Shanab, R. a. I., El-Dalatony, M. M., EL-Sheekh, M. M., Ji, M.-K., Salama, E.-S., Kabra, A. N., and Jeon, B.-H. (2014). Cultivation of a new microalga, Micractinium reisseri, in municipal wastewater for nutrient removal, biomass, lipid, and fatty acid production. *Biotechnol. Bioprocess Eng.*, 19:510–518.

Abrams, P. (1987). On classifying intractions between populations. *Oecologia*, 73:272–281.

Achilles-Day, U. E. and Day, J. G. (2013a). Isolation of clonal cultures of endosymbiotic green algae from their ciliate hosts. *J. Microbiol. Methods*, 92(3):355–357.

Achilles-Day, U. E. M. and Day, J. G. (2013b). Isolation of clonal cultures of endosymbiotic green algae from their ciliate hosts. *J. Microbiol. Methods*, 92(3):355–7.

Adams, M. D., Kelley, J. M., Gocayne, J. D., Dubnick, M., Polymeropoulos, M. H., Xiao, H., Merril, C. R., Wu, a., Olde, B., and Moreno, R. F. (1991). Complementary DNA sequencing: expressed sequence tags and human genome project. *Science*, 252(1990):1651–1656.

Adessi, C., Matton, G., Ayala, G., Turcatti, G., Mermod, J. J., Mayer, P., and Kawashima, E. (2000). Solid phase DNA amplification: characterisation of primer attachment and amplification mechanisms. *Nucleic Acids Res.*, 28(20):E87.

Adl, S., Simpson, A., Lane, C., Lukeš, J., Bass, D., Bowser, S., Brown, M., Burki, F., Dunthorn, M., Hampl, V., Heiss, A., Hoppenrath, M., Lara, E., LeGall, L., Lynn, D., McManus, H., Mitchell, E., Mozley-Stanridge, S., Parfrey, L., Pawlowski, J., Rueckert, S., Shadwick, L., Schoch, C., Smirnov, A., and Spiegel, F. (2013). The Revised Classification of Eukaryotes. *J. Eukaryot. Microbiol.*, 59(5):1–45.

Agre, P., Preston, G. M., Smith, B. L., Jung, J. S., Raina, S., Moon, C., Guggino, W. B., and Nielsen, S. (1993). Aquaporin CHIP: the archetypal molecular water channel. *Am. J. Physiol.*, 265:F463–F476.

Aho, A. V., Kernighan, B. W., and Weinberger, P. J. (1987). *The AWK Programming Language*. Addison-Wesley Longman Publishing Co., Inc., Boston, MA, USA.

Akaike, H. (1974). A new look at the statistical model identification. *IEEE Trans. Autom. Control*, 19:716–723.

Albers, D., Reisser, W., and Wiessner, W. (1982). Studies on the nitrogen supply of endosymbiotic chlorellae in greem paramecium bursaria. *Plant Sci. Lett.*, 25:85–90.

Alberts, B. (2015). *Molecular biology of the cell*. Garland Science, Taylor and Francis Group, New York, NY.

Aliaga Goltsman, D. S., Comolli, L. R., Thomas, B. C., and Banfield, J. F. (2014). Community transcriptomics reveals unexpected high microbial diversity in acidophilic biofilm communities. *ISME J.*, 9(4):1014–1023.

Allaire, J. J., Horner, J., Marti, V., and Porte, N. (2014). *markdown: Markdown rendering for R*.

Alneberg, J., Bjarnason, B. S., de Bruijn, I., Schirmer, M., Quick, J., Ijaz, U. Z., Lahti, L., Loman, N. J., Andersson, A. F., and Quince, C. (2014). Binning metagenomic contigs by coverage and composition. *Nat. Methods*, 11(11):1144–1146.

Álvarez Loayza, P., White, J. F., Torres, M. S., Balslev, H., Kristiansen, T., Svenning, J. C., and Gil, N. (2011). Light converts endosymbiotic fungus to pathogen, influencing seedling survival and niche-space filling of a common tropical tree, Iriartea deltoidea. *PLoS One*, 6(1).

Andrews, S. (2015). FastQC: A Quality Control tool for High Throughput Sequence Data.

Anisimova, M. and Gascuel, O. (2006). Approximate likelihood-ratio test for branches: A fast, accurate, and powerful alternative. *Syst. Biol.*, 55(4):539–52.

Antonov, A. V., Dietmann, S., and Mewes, H. W. (2008). KEGG spider: interpretation of genomics data in the context of the global gene metabolic network. *Genome Biol.*, 9(12):R179.

Archibald, J. (2005). Jumping Genes and Shrinking Genomes – Probing the Evolution of Eukaryotic Photosynthesis with Genomics. *IUBMB Life (International Union Biochem. Mol. Biol. Life)*, 57(August):539–547.

Archibald, J. (2015). Endosymbiosis and Eukaryotic Cell Evolution. *Curr. Biol.*, 25(19):R911–R921.

Arnaiz, O., Goût, J.-F., Bétermier, M., Bouhouche, K., Cohen, J., Duret, L., Kapusta, A., Meyer, E., and Sperling, L. (2010). Gene expression in a paleopolyploid: a transcriptome resource for the ciliate Paramecium tetraurelia. *BMC Genomics*, 11:547.

Arnaiz, O. and Sperling, L. (2011). ParameciumDB in 2011: New tools and new data for functional and comparative genomics of the model ciliate Paramecium tetraurelia. *Nucleic Acids Res.*, 39(October 2010):632–636.

Aronesty, E. (2013). Comparison of Sequencing Utility Programs. *Open Bioinforma. J.*, 7:1–8.

Ashburner, M., Ball, C. a., Blake, J. a., Botstein, D., Butler, H., Cherry, J. M., Davis, a. P., Dolinski, K., Dwight, S. S., Eppig, J. T., Harris, M. a., Hill, D. P., Issel-Tarver, L., Kasarskis, a., Lewis, S., Matese, J. C., Richardson, J. E., Ringwald, M., Rubin, G. M., and Sherlock, G. (2000). Gene ontology: tool for the unification of biology. *Nat. Genet.*, 25(may):25–29.

Attwood, T. K., Beck, M. E., Bleasby, a. J., and Parry-Smith, D. J. (1994). PRINTS–a database of protein motif fingerprints. *Nucleic Acids Res.*, 22(17):3590–3596.

Aubusson-Fleury, A., Cohen, J., and Lemullois, M. (2015). Chapter 22 - Ciliary heterogeneity within a single cell: The Paramecium model. In Basto, R. and Marshall, W. F., editors, *Methods in Cilia & Flagella*, volume 127 of *Methods in Cell Biology*, pages 457–485. Academic Press.

Auer, P. L. and Doerge, R. W. (2010). Statistical design and analysis of RNA sequencing data. *Genetics*, 185(2):405–16.

Aury, J.-M., Jaillon, O., Duret, L., Noel, B., Jubin, C., Porcel, B. M., Ségurens, B., Daubin, V., Anthouard, V., Aiach, N., Arnaiz, O., Billaut, A., Beisson, J., Blanc, I., Bouhouche, K., Câmara, F., Duharcourt, S., Guigo, R., Gogendeau, D., Katinka, M., Keller, A.-M., Kissmehl, R., Klotz, C., Koll, F., Le Mouël, A., Lepère, G., Malinsky, S., Nowacki, M., Nowak, J. K., Plattner, H., Poulain, J., Ruiz, F., Serrano, V., Zagulski, M., Dessen, P., Bétermier, M., Weissenbach, J., Scarpelli, C., Schächter, V., Sperling, L., Meyer, E., Cohen, J., and Wincker, P. (2006). Global trends of whole-genome duplications revealed by the ciliate Paramecium tetraurelia. *Nature*, 444(7116):171–8.

Bachvaroff, T. R., Handy, S. M., Place, A. R., and Delwiche, C. F. (2011). Alveolate phylogeny inferred using concatenated ribosomal proteins. *J. Eukaryot. Microbiol.*, 58(3):223–33.

Bankevich, A., Nurk, S., Antipov, D., Gurevich, A. a., Dvorkin, M., Kulikov, A. S., Lesin, V. M., Nikolenko, S. I., Pham, S., Prjibelski, A. D., Pyshkin, A. V., Sirotkin, A. V., Vyahhi, N., Tesler, G., Alekseyev, M. a., and Pevzner, P. a. (2012). SPAdes: A New Genome Assembly Algorithm and Its Applications to Single-Cell Sequencing. *J. Comput. Biol.*, 19(5):455–477.

Bannai, H., Tamada, Y., Maruyama, O., Nakai, K., and Miyano, S. (2002). Extensive feature detection of N-terminal protein sorting signals. *Bioinformatics*, 18(2):298–305.

Barker, W. C., Garavelli, J. S., Haft, D. H., Hunt, L. T., Marzec, C. R., Orcutt, B. C., Srinivasarao, G. Y., Yeh, L. S. L., Ledley, R. S., Mewes, H. W., Pfeiffer, F., and Tsugita, a. (1998). The PIR-international Protein Sequence Database. *Nucleic Acids Res.*, 26(1):27–32.

Bashan, Y., Lopez, B. R., Huss, V. a. R., Amavizca, E., and De-Bashan, L. E. (2015). Chlorella sorokiniana (formerly C. vulgaris) UTEX 2714, a non-thermotolerant microalga useful for biotechnological applications and as a reference strain. *J. Appl. Phycol.*

Bateman, a. (2002). The Pfam Protein Families Database. *Nucleic Acids Res.*, 30(1):276–280.

Bengio, Y., Courville, A., and Vincent, P. (2013). Representation learning: A review and new perspectives. *Pattern Anal. ...*, (1993):1–30.

Bengio, Y., Lamblin, P., Popovici, D., and Larochelle, H. (2007). Greedy Layer-Wise Training of Deep Networks. *Adv. Neural Inf. Process. Syst.*, 19(1):153.

Bengtsson, M., Stå hlberg, A., Rorsman, P., and Kubista, M. (2005). Gene expression profiling in single cells from the pancreatic islets of Langerhans reveals lognormal distribution of mRNA levels. pages 1388–1392.

Benson, A. A. and Calvin, M. (1948). The path of carbon in photosynthesis. III. In *Cold Spring Harb. Symp. Quant. Biol.*, volume 13, pages 6–10. Cold Spring Harbor Laboratory Press.

Berger, J. (1980). Feeding Behaviour of Didinium nasutum on Paramecium bursaria with Normal or Apochlorotic Zoochlorellae. *J. Gen. Microbiol.*, 118:397–404.

Berger, J. D. (1986). Autogamy Cell Cycle Stage-specific in Paramecium Commitment to Meiosis. *Exp. Cell Res.*, 166:475–485.

Bergsten, J. (2005). A review of long-branch attraction. 21:163–193.

Bergstra, J. and Bengio, Y. (2012). Random Search for Hyper-Parameter Optimization. *J. ofMachine Learn. Res.*, 13:281–305.

Berk, S. G., Parks, L. H., and Ting, R. S. (1991). Photoadaptation alters the ingestion rate of Paramecium bursaria, a mixotrophic ciliate. *Appl. Environ. Microbiol.*, 57:2312–2316.

Bétermier, M. (2004). Large-scale genome remodelling by the developmentally programmed elimination of germ line sequences in the ciliate Paramecium. *Res. Microbiol.*, 155:399–408.

Bhattacharya, D., Archibald, J. M., Weber, A. P. M., and Reyes-Prieto, A. (2007). How do endosymbionts become organelles? Understanding early events in plastid evolution. *Bioessays*, 29:1239–46.

Bianchi, L. and Díez-Sampedro, A. (2010). A Single Amino Acid Change Converts the Sugar Sensor SGLT3 into a Sugar Transporter. *PLoS One*, 5(4):e10241.

Binga, E. K., Lasken, R. S., and Neufeld, J. D. (2008). Something from (almost) nothing: the impact of multiple displacement amplification on microbial ecology. *ISME J.*, 2:233–241.

Bishop, C. M. (2006). *Pattern Recognition and Machine Learning*. Information Science and Statistics. Springer.

Blainey, P. C. (2013). The future is now: Single-cell genomics of bacteria and archaea. *FEMS Microbiol. Rev.*, 37:407–427.

Blainey, P. C. and Quake, S. R. (2011). Digital MDA for enumeration of total nucleic acid contamination. *Nucleic Acids Res.*, 39(4):1–9.

Blanc, G., Agarkova, I., Grimwood, J., Kuo, A., Brueggeman, A., Dunigan, D. D., Gurnon, J., Ladunga, I., Lindquist, E., Lucas, S., Pangilinan, J., Pröschold, T., Salamov, A., Schmutz, J., Weeks, D., Yamada, T., Lomsadze, A., Borodovsky, M., Claverie, J.-M., Grigoriev, I. V., and Van Etten, J. L. (2012). The genome of the polar eukaryotic microalga Coccomyxa subellipsoidea reveals traits of cold adaptation. *Genome Biol.*, 13(5):R39.

Blanc, G., Duncan, G., Agarkova, I., Borodovsky, M., Gurnon, J., Kuo, A., Lindquist, E., Lucas, S., Pangilinan, J., Polle, J., Salamov, A., Terry, A., Yamada, T., Dunigan, D. D., Grigoriev, I. V., Claverie, J.-M., and Van Etten, J. L. (2010). The Chlorella variabilis NC64A genome reveals adaptation to photosymbiosis, coevolution with viruses, and cryptic sex. *Plant Cell*, 22(9):2943–55.

Boenigk, J., Ereshefsky, M., Hoef-Emden, K., Mallet, J., and Bass, D. (2012). Concepts in protistology: Species definitions and boundaries. *Eur. J. Protistol.*, 48(2):96–102.

Boetius, a., Ravenschlag, K., Schubert, C. J., Rickert, D., Widdel, F., Gieseke, a., Amann, R., Jø rgensen, B. B., Witte, U., and Pfannkuche, O. (2000). A marine microbial consortium apparently mediating anaerobic oxidation of methane. *Nature*, 407(October):623–626.

Bolger, A. M., Lohse, M., and Usadel, B. (2014). Trimmomatic: A Flexible Trimmer for Illumina Sequence Data. *Bioinformatics*, 30(15):2114–2120.

Bonetta, L. (2006). Genome sequencing in the fast lane. *Nat. Methods*, 3(2):141–147.

Boser, B. E., Guyon, I. M., and Vapnik, V. N. (1992). A Training Algorithm for Optimal Margin Classifiers. *Proc. 5th Annu. ACM Work. Comput. Learn. Theory*, pages 144–152.

Bouchard-Côté, A. and Jordan, M. I. (2013). Evolutionary inference via the Poisson Indel Process. *Proc. Natl. Acad. Sci. U. S. A.*, 110(4):1160–6.

Bradley, P. S. and Bradley, P. S. (1998). Refining Initial Points for K-Means Clustering. *Microsoft Res.*, pages 91–99.

Bradski, G. (2000). OpenCV library. *Dr. Dobb's J. Softw. Tools*.

Braslavsky, I., Braslavsky, I., Hebert, B., Hebert, B., Kartalov, E., Kartalov, E., Quake, S. R., and Quake, S. R. (2003). Sequence information can be obtained from single DNA molecules. *Proc. Natl. Acad. Sci. U. S. A.*, 100:3960–4.

Bray, N. L., Pimentel, H., Melsted, P., and Pachter, L. (2015). Near-optimal RNA-Seq quantification. *aRxiv*.

Breiman, L. (2001). Random forests. *Mach. Learn.*, pages 5–32.

Brown, C. T., Howe, A., Zhang, Q., Pyrkosz, A. B., and Brom, T. H. (2012). A Reference-Free Algorithm for Computational Normalization of Shotgun Sequencing Data. *arXiv*, 1203.4802:1–18.

Brown, J. a. and Nielsen, P. J. (1974). Transfer of photosynthetically produced carbohydrate from endosymbiotic chlorellae to Paramecium bursaria. *J. Protozool.*, 21:569–570.

Buchan, D. W. a., Shepherd, A. J., Lee, D., Pearl, F. M. G., Rison, S. C. G., Thornton, J. M., and Orengo, C. a. (2002). Gene3D: structural assignment for whole genes and genomes using the CATH domain structure database. *Genome Res.*, 12:503–14.

Buchfink, B., Xie, C., and Huson, D. H. (2015). Fast and Sensitive Protein Alignment using DIAMOND. *Under Rev.*, 12(1).

Buchheim, M. a., Keller, A., Koetschan, C., Förster, F., Merget, B., and Wolf, M. (2011). Internal transcribed spacer 2 (nu ITS2 rRNA) sequence-structure phylogenetics: towards an automated reconstruction of the green algal tree of life. *PLoS One*, 6(2):e16931.

Burki, F. (2014). The Eukaryotic Tree of Life from a Global Phylogenomic Perspective. *Cold Spring Harb. Perspect. Biol.*, 6(5):1–18.

Camin, J. H. and Sokal, R. R. (1965). A Method for deducing branching sequences in phylogeny. *Evolution (N. Y).*, 19(3):311–326.

Camoni, L., Marra, M., Garufi, A., Visconti, S., and Aducci, P. (2006). The maize root plasma membrane H+-ATPase is regulated by a sugar-induced transduction pathway. *Plant Cell Physiol.*, 47(6):743–747.

Capella-Gutiérrez, S., Silla-Martínez, J. M., and Gabaldón, T. (2009). trimAl: A tool for automated alignment trimming in large-scale phylogenetic analyses. *Bioinformatics*, 25(15):1972–1973.

Carradec, Q., Gotz, U., Arnaiz, O., Pouch, J., Simon, M., Meyer, E., and Marker, S. (2015). Primary and secondary siRNA synthesis triggered by RNAs from food bacteria in the ciliate Paramecium tetraurelia. *Nucleic Acids Res.*, 43(3):1818–1833.

Casadevall, A. and Fang, F. C. (2008). Descriptive Science. *Infect. Immun.*, 76(9):3835–3836.

Caspi, R., Foerster, H., Fulcher, C. a., Kaipa, P., Krummenacker, M., Latendresse, M., Paley, S., Rhee, S. Y., Shearer, a. G., Tissier, C., Walk, T. C., Zhang, P., and Karp, P. D. (2007). The MetaCyc Database of metabolic pathways and enzymes and the BioCyc collection of Pathway/Genome Databases. *Nucleic Acids Res.*, 36(October 2007):D623–D631.

Cavalli-Sforza, L. L. and Edwards, a. W. F. (1967). Phylogenetic analysis. Models and estimation procedures. *Am. J. Hum. Genet.*, 19(012):233–257.

CCAP (2012). NCL Media Recipe.

Chalker, D. L., Meyer, E., and Mochizuki, K. (2013). Epigenetics of ciliates. *Cold Spring Harb. Prespectives Epigenetics*, 5:a017764.

Chang, Z., Li, G., Liu, J., Zhang, Y., Ashby, C., Liu, D., Cramer, C. L., and Huang, X. (2015). Bridger: a new framework for de novo transcriptome assembly using RNA-seq data. *Genome Biol.*, 16:30.

Chen, S., Yao, H., Han, J., Liu, C., Song, J., Shi, L., Zhu, Y., Ma, X., Gao, T., Pang, X., Luo, K., Li, Y., Li, X., Jia, X., Lin, Y., and Leon, C. (2010). Validation of the ITS2 region as a novel DNA barcode for identifying medicinal plant species. *PLoS One*, 5(1):e8613.

Chen, T.-T. (1940). Polyploidy in Paramecium bursaria. *Genentics*, 26:239–240.

Cho, K.-O., Kim, G.-W., and Lee, O.-K. (2011). Wolbachia Bacteria Reside in Host Golgi-Related Vesicles Whose Position Is Regulated by Polarity Proteins. *PLoS One*, 6(7):e22703.

Coleman, A. W. (2003). ITS2 is a double-edged tool for eukaryote evolutionary comparisons. *Trends Genet.*, 19(7):370–375.

Conesa, a., Gotz, S., Garcia-Gomez, J. M., Terol, J., Talon, M., and Robles, M. (2005). Blast2GO: a universal tool for annotation, visualization and analysis in functional genomics research. *Bioinformatics*, 21(18):3674–3676.

Cooper, G. (2013). *The cell : a molecular approach*. Sinauer Associates, Sunderland, MA.

Corduneanu, A. and Bishop, C. M. (2001). Variational Bayesian Model Selection for Mixture Distributions. *Artif. Intell.*, 51:27–34.

Corporation, G. C. (2015). Sequencher® version 4.10.1 sequence analysis software.

Cortes, C. and Vapnik, V. (1995). Support-vector networks. *Mach. Learn.*, 20:273–297.

Crespi, M. and Frugier, F. (2008). De novo organ formation from differentiated cells: root nodule organogenesis. *Sci. Signal.*, 1(49):re11.

Crick, F. (1966). *Of molecules and man*. University of Washington.

Criscuolo, A. (2011). Molecular Phylogenetics and Evolution morePhyML : Improving the phylogenetic tree space exploration with PhyML 3. *Mol. Phylogenet. Evol.*, 61(3):944–948.

Crusoe, M. R., Alameldin, H. F., Awad, S., Boucher, E., Caldwell, A., Cartwright, R., Charbonneau, A., Constantinides, B., Edvenson, G., Fay, S., Fenton, J., Fenzl, T., Fish, J., Garcia-Gutierrez, L., Garland, P., Gluck, J., González, I., Guermond, S., Guo, J., Gupta, A., Herr, J. R., Howe, A., Hyer, A., Härpfer, A., Irber, L., Kidd, R., Lin, D., Lippi, J., Mansour, T., McA'Nulty, P., McDonald, E., Mizzi, J., Murray, K. D., Nahum, J. R., Nanlohy, K., Nederbragt, A. J., Ortiz-Zuazaga, H., Ory, J., Pell, J., Pepe-Ranney, C., Russ, Z. N., Schwarz, E., Scott, C., Seaman, J., Sievert, S., Simpson, J., Skennerton, C. T., Spencer, J., Srinivasan, R., Standage, D., Stapleton, J. a., Steinman, S. R., Stein, J., Taylor, B., Trimble, W., Wiencko, H. L., Wright, M., Wyss, B., Zhang, Q., Zyme, E., and Brown, C. T. (2015). The khmer software package: enabling efficient nucleotide sequence analysis. *F1000Research*, pages 1–9.

Cullis, C. A. (1972). DNA amounts in the nuclei of Paramecium bursaria. *Chromosoma*, 40:127–133.

Curtin, R. R., Cline, J. R., Slagle, N. P., March, W. B., Ram, P., Mehta, N. A., and Gray, A. G. (2013). MLPACK: A Scalable C++ Machine Learning Library. *J. Mach. Learn. Res.*, 14:801–805.

Cuvelier, M. L., Allen, a. E., Monier, a., McCrow, J. P., Messie, M., Tringe, S. G., Woyke, T., Welsh, R. M., Ishoey, T., Lee, J.-H., Binder, B. J., DuPont, C. L., Latasa, M., Guigand, C., Buck, K. R., Hilton, J., Thiagarajan, M., Caler, E., Read, B., Lasken, R. S., Chavez, F. P., and Worden, a. Z. (2010). Targeted metagenomics and ecology of globally important uncultured eukaryotic phytoplankton. *Proc. Natl. Acad. Sci.*, 107(33):14679–14684.

Darriba, D., Taboada, G. L., Doallo, R., and Posada, D. (2011). ProtTest 3: fast selection of best-fit models of protein evolution. *Bioinformatics*, 27(8):1164–5.

Darriba, D., Taboada, G. L., Doallo, R., and Posada, D. (2012). jModelTest 2: more models, new heuristics and parallel computing. *Nat. Methods*, 9(8):772–772.

Dayhoff, M., Schwartz, R., and Orcutt, B. (1978). A Model of Evolutionary Change in Proteins.

de Bary, A. (1869). *Dir Erscheinung der Symbiose*. Verlag von Karl J. Trübner, Strassburg.

De Queiroz, K. (2007). Species concepts and species delimitation. *Syst. Biol.*, 56(6):879–886.

Dillies, M.-a., Rau, a., Aubert, J., Hennequet-Antier, C., Jeanmougin, M., Servant, N., Keime, C., Marot, G., Castel, D., Estelle, J., Guernec, G., Jagla, B., Jouneau, L., Laloe, D., Le Gall, C., Schaeffer, B., Le Crom, S., Guedj, M., and Jaffrezic, F. (2013). A comprehensive evaluation of normalization methods for Illumina high-throughput RNA sequencing data analysis. *Brief. Bioinform.*, 14(6):671–683.

Ding, Y., Zhao, Y., Xipeng Shen, N., Musuvathi, M., and Todd Mytkowicz, M. (2015). Yinyang K-Means: A Drop-In Replacement of the Classic K-Means with Consistent Speedup. 37.

Dohra, H., Fujishima, M., and Ishikawa, H. (1998). Structure and expression of a GroE-homologous operon of a macronucleus-specific symbiont Holospora obtusa of the ciliate Paramecium caudatum. *J. Eukaryot. Microbiol.*, 45:71–79.

Dolan, J. (1992). Mixotrophy in Ciliates: A Review of Chlorella Symbiosis and Chloroplast Retention. *Mar. Microb. Food Webs*, 6(2):115–132.

Döring, A., Weese, D., Rausch, T., and Reinert, K. (2008). SeqAn An efficient, generic C++ library for sequence analysis. *BMC Bioinformatics*, 9:11.

Dorrell, R. G. and Smith, A. G. (2011). Do red and green make brown?: Perspectives on plastid acquisitions within chromalveolates. *Eukaryot. Cell*, 10(7):856–868.

Dougherty, E. R. (2008). On the epistemological crisis in genomics. *Curr. Genomics*, 9:69–79.

Douglas, a. E. H. V. a. R. (1986). On the characteristics and taxonomic position of symbiotic Chlorella. *Arch Microbiol*, 145:80–84.

Dressman, D., Yan, H., Traverso, G., Kinzler, K. W., and Vogelstein, B. (2003). Transforming single DNA molecules into fluorescent magnetic particles for detection and enumeration of genetic variations. *Proc. Natl. Acad. Sci. U. S. A.*, 100(M):8817–8822.

Dröge, J. and Mchardy, A. C. (2012). Taxonomic binning of metagenome samples generated by next-generation sequencing technologies. *Brief. Bioinform.*, 13(6):646–655.

Duret, L., Cohen, J., Jubin, C., Dessen, P., Goût, J.-f., Mousset, S., Jaillon, O., Noël, B., Arnaiz, O., Bétermier, M., Wincker, P., Meyer, E., and Aury, J.-m. (2008). Analysis of sequence variability in the macronuclear DNA of Paramecium tetraurelia : A somatic view of the germline. *Genome Res.*, 18:585–596.

Eck, R. V. and Dayhoff, M. O. (1966). Atlas of Protein Sequence and Structure.

Eckert, K. and Kunkel, T. (1990). High fidelity DNA synthesis by the Thermus aquaticus polymerase. *Biochemistry*, 18(13):3739–3744.

Eddy, S. and R, E. (2011). Accelerated Profile HMM Searches. *PLoS Comput. Biol.*, 7(10):e1002195.

Eddy, S. R. (1995). Multiple alignment using hidden Markov model. *Intell. Syst. Mol. Biol.*, ISMB-95:114–120.

Edgar, R. C. (2004a). MUSCLE : a multiple sequence alignment method with reduced time and space complexity. *BMC Bioinformatics*, 5(113):1–19.

Edgar, R. C. (2004b). MUSCLE: Multiple sequence alignment with high accuracy and high throughput. *Nucleic Acids Res.*, 32(5):1792–1797.

Eggensperger, K., Feurer, M., and Hutter, F. (2013). Towards an empirical foundation for assessing bayesian optimization of hyperparameters. *... Bayesian Optim. ...* , pages 1–5.

Eisen, J. a., Coyne, R. S., Wu, M., Wu, D., Thiagarajan, M., Wortman, J. R., Badger, J. H., Ren, Q., Amedeo, P., Jones, K. M., Tallon, L. J., Delcher, A. L., Salzberg, S. L., Silva, J. C., Haas, B. J., Majoros, W. H., Farzad, M., Carlton, J. M., Smith, R. K., Garg, J., Pearlman, R. E., Karrer, K. M., Sun, L., Manning, G., Elde, N. C., Turkewitz, A. P., Asai, D. J., Wilkes, D. E., Wang, Y., Cai, H., Collins, K., Stewart, B. A., Lee, S. R., Wilamowska, K., Weinberg, Z., Ruzzo, W. L., Wloga, D., Gaertig, J., Frankel, J., Tsao, C. C., Gorovsky, M. a., Keeling, P. J., Waller, R. F., Patron, N. J., Cherry, J. M., Stover, N. a., Krieger, C. J., Del Toro, C., Ryder, H. F., Williamson, S. C., Barbeau, R. a., Hamilton, E. P., and Orias, E. (2006). Macronuclear genome sequence of the ciliate Tetrahymena thermophila, a model eukaryote. *PLoS Biol.*, 4(9):1620–1642.

El Hadidi, M., Ruscheweyh, H.-J., and Huson, D. (2013). Improved metagenome analysis using MEGAN5. In *Jt. 21st Annu. Int. Conf. Intell. Syst. Mol. Biol. 12th Eur. Conf. Comput. Biol. 2013*.

Ellegaard, K. M., Klasson, L., and Andersson, S. G. E. (2013a). Testing the reproducibility of multiple displacement amplification on genomes of clonal endosymbiont populations. *PLoS One*, 8(11):21–25.

Ellegaard, K. M., Klasson, L., Näslund, K., Bourtzis, K., and Andersson, S. G. E. (2013b). Comparative genomics of Wolbachia and the bacterial species concept. *PLoS Genet.*, 9(4):e1003381.

Emanuelsson, O., Brunak, S. r., von Heijne, G., and Nielsen, H. (2007). Locating proteins in the cell using TargetP, SignalP and related tools. *Nat. Protoc.*, 2(4):953–971.

Ester, M., Kriegel, H. P., Sander, J., and Xu, X. (1996). A Density-Based Algorithm for Discovering Clusters in Large Spatial Databases with Noise. In *Proc. 2nd Int. Conf. Knowl. Discov. Data Min.*, pages 226–231.

Fang, F. C. and Casadevall, A. (2011). Reductionistic and holistic science. *Infect. Immun.*, 79(4):1401–1404.

Fayyad, U., Grinstein, G. G., and Wierse, A. (2001). *Information Visualization in Data Mining and Knowledge Discovery*. Morgan Kaufmann Publishers Inc., San Francisco, CA, USA.

Federhen, S. (2012). The NCBI Taxonomy database. *Nucleic Acids Res.*, 40(December 2011):136–143.

Fedurco, M., Romieu, A., Williams, S., Lawrence, I., and Turcatti, G. (2006). BTA, a novel reagent for DNA attachment on glass and efficient generation of solid-phase amplified DNA colonies. *Nucleic Acids Res.*, 34(3).

Feldmesser, E., Rosenwasser, S., Vardi, A., and Ben-Dor, S. (2014). Improving transcriptome construction in non-model organisms: integrating manual and automated gene definition in Emiliania huxleyi. *BMC Genomics*, 15(1):148.

Felsenstein, J. (1978). Society of Systematic Biologists. *Soc. Syst. Biol.*, 27(4):401–410.

Felsenstein, J. (1981). Evolutionary trees from DNA sequences: a maximum likelihood approach. *J. Mol. Evol.*, 17:368–376.

Felsenstein, J. (1985). Confidence Limits on Phylogenies: An Approach Using the Bootstrap. *Evolution (N. Y).*, 39(4):783–791.

Felsenstein, J. (2001). The troubled growth of statistical phylogenetics. *Syst. Biol.*, 50(4):465–467.

Fenchel, T. and Finlay, B. (1992). Production of methane and hydrogen by anaerobic ciliates containing symbiotic .... *Microbiology*, pages 475–480.

Feng, D. F. and Doolittle, R. F. (1987). Progressive sequence alignment as a prerequisite to correct phylogenetic trees. *J. Mol. Evol.*, 25:351–360.

Fernández-Delgado, M., Cernadas, E., Barro, S., and Amorim, D. (2014). Do we Need Hundreds of Classifiers to Solve Real World Classification Problems? *J. Mach. Learn. Res.*, 15:3133–3181.

Fiehn, O. (2002). Metabolomics – the link between genotypes and phenotypes. *Plant Mol. Biol.*, 48:155–171.

Fitch, W. M. and Magoliash, E. (1967). Construction of Phylogenetic Tress. *Science (80-.).*, 155(279).

Fokin, S. I. and Görtz, H.-d. (2009). Diversity of Holospora Bacteria in Paramecium and Their Characterization. In Fujishima, M., editor, *Endosymbionts in Paramecium*, volume 12 of *Microbiology Monographs*, chapter 7, pages 161–199. Springer.

Fokin, S. I., Przyboś, E., Chivilev, S. M., Beier, C. L., Horn, M., Skotarczak, B., Wodecka, B., and Fujishima, M. (2004). Morphological and molecular investigations of Paramecium schewiakoffi sp. nov. (Ciliophora, Oligohymenophorea) and current status of distribution and taxonomy of Paramecium spp. *Eur. J. Protistol.*, 40:225–243.

Forgy, E. W. (1965). Cluster Analysis of Multivariate Data : Efficiency Versus Interpretability of Classifications. *Biometrics*, 21:768–769.

Freund, Y. and Schapire, R. E. (1997). A Decision-Theoretic Generalization of On-Line Learning and an Application to Boosting. *J. Comput. Syst. Sci.*, 55:119–139.

Funfak, A., Fisch, C., Abdel Motaal, H. T., Diener, J., Combettes, L., Baroud, C. N., and Dupuis-Williams, P. (2015). Paramecium swimming and ciliary beating patterns: a study on four RNA interference mutations. *Integr. Biol.*, 7:90–100.

Gabow, H. N. and Tarjan, R. E. (1985). A linear-time algorithm for a special case of disjoint set union. *J. Comput. Syst. Sci.*, 30:209–221.

Gabrielsen, T. M., Minge, M. a., Espelund, M., Tooming-Klunderud, A., Patil, V., Nederbragt, A. J., Otis, C., Turmel, M., Shalchian-Tabrizi, K., Lemieux, C., and Jakobsen, K. S. (2011). Genome evolution of a tertiary dinoflagellate plastid. *PLoS One*, 6(4).

Galvani, A. and Sperling, L. (2002). RNA interference by feeding in Paramecium. *Trends Genet.*, 18(1):11–2.

Garcia-Cuetos, L., Moestrup, O., and Hansen, P. J. (2012). Studies on the genus mesodinium II. Ultrastructural and molecular investigations of five marine species help clarifying the taxonomy. *J. Eukaryot. Microbiol.*, 59(4):374–400.

Gascuel, O. (1997). BIONJ: an improved version of the NJ algorithm based on a simple model of sequence data. *Mol. Biol. Evol.*, 14:685–695.

Gelman, a., Hill, J., and Yajima, M. (2009). Why we (usually) don't have to worry about multiple comparisons. *arXiv:0907.2478 [stat.AP]*, pages 1–25.

Gerhard, D. S., Wagner, L., Feingold, E. a., Shenmen, C. M., Grouse, L. H., Schuler, G., Klein, S. L., Old, S., Rasooly, R., Good, P., Guyer, M., Peck, A. M., Derge, J. G., Lipman, D., Collins, F. S., Jang, W., Sherry, S., Feolo, M., Misquitta, L., Lee, E., Rotmistrovsky, K., Greenhut, S. F., Schaefer, C. F., Buetow, K. H., Bonner, T. I., Haussler, D., Kent, J., Diekhans, M., Furey, T., Brent, M., Prange, C., Schreiber, K., Shapiro, N., Bhat, N. K., Hopkins, R. F., Hsie, F., Driscoll, T., Soares, M. B., Bonaldo, M. F., Casavant, T. L., Scheetz, T. E., Brownstein, M. J., Usdin, T. B., Toshiyuki, S., Carninci, P., Piao, Y., Dudekula, D. B., Ko, M. S. H., Kawakami, K., Suzuki, Y., Sugano, S., Gruber, C. E., Smith, M. R., Simmons, B., Moore, T., Waterman, R., Johnson, S. L., Ruan, Y., Lin Wei, C., Mathavan, S., Gunaratne, P. H., Wu, J., Garcia, A. M., Hulyk, S. W., Fuh, E., Yuan, Y., Sneed, A., Kowis, C., Hodgson, A., Muzny, D. M., McPherson, J., Gibbs, R. a., Fahey, J., Helton, E., Ketteman, M., Madan, A., Rodrigues, S., Sanchez, A., Whiting, M., Madan, A., Young, A. C., Wetherby, K. D., Granite, S. J., Kwong, P. N., Brinkley, C. P., Pearson, R. L., Bouffard, G. G., Blakesly, R. W., Green, E. D., Dickson, M. C., Rodriguez, A. C., Grimwood, J., Schmutz, J., Myers, R. M., Butterfield, Y. S. N., Griffith, M., Griffith, O. L., Krzywinski, M. I., Liao, N., Morrin, R., Palmquist, D., Petrescu, A. S., Skalska, U., Smailus, D. E., Stott, J. M., Schnerch, A., Schein, J. E., Jones, S. J. M., Holt, R. a., Baross, A., Marra, M. a., Clifton, S., Makowski, K. a., Bosak, S., and Malek, J. (2004). The status, quality, and expansion of the NIH full-length cDNA project: The Mammalian Gene Collection (MGC). *Genome Res.*, 14:2121–2127.

Geurts, P., Ernst, D., and Wehenkel, L. (2006). Extremely randomized trees. *Mach. Learn.*, 63(October 2005):3–42.

Gilbert, D. G. (2013). Gene-omes built from mRNA-seq not genome DNA. In *7th Annu. Arthropod Genomics Symp.*, Notre Dame.

Giordano, M. and Raven, J. a. (2014). Nitrogen and sulfur assimilation in plants and algae. *Aquat. Bot.*, 118:45–61.

Glenn, T. C. (2011). Field guide to next-generation DNA sequencers. *Mol. Ecol. Resour.*, 11:759–769.

Gomaa, F., Kosakyan, A., Heger, T. J., Corsaro, D., Mitchell, E. a. D., and Lara, E. (2014). One Alga to Rule them All: Unrelated Mixotrophic Testate Amoebae (Amoebozoa, Rhizaria and Stramenopiles) Share the Same Symbiont (Trebouxiophyceae). *Protist*, 165(2):161–176.

Goodacre, R., Broadhurst, D., Smilde, A. K., Kristal, B. S., Baker, J. D., Beger, R., Bessant, C., Connor, S., Capuani, G., Craig, A., Ebbels, T., Kell, D. B., Manetti, C., Newton, J., Paternostro, G., Somorjai, R., Sjöström, M., Trygg, J., and Wulfert, F. (2007). Proposed minimum reporting standards for data analysis in metabolomics. *Metabolomics*, 3:231–241.

Goodstein, D. M., Shu, S., Howson, R., Neupane, R., Hayes, R. D., Fazo, J., Mitros, T., Dirks, W., Hellsten, U., Putnam, N., and Rokhsar, D. S. (2012). Phytozome: a comparative platform for green plant genomics. *Nucleic Acids Res.*, 40(November 2011):D1178–D1186.

Gortz, H.-d. (1982). Infections of Paramecium Bursaria with Bacteria and Yeasts. *J. Cell Sci.*, 58:445–453.

Görtz, H.-d. and Fokin, S. I. (2009). Diversity of Endosymbiotic Bacteria in Paramecium. In Fujishima, M., editor, *Endosymbionts in Paramecium*, volume 12 of *Microbiology Monographs*, chapter 6, pages 131–160. Springer.

Gough, J. and Chothia, C. (2002). SUPERFAMILY: HMMs representing all proteins of known structure. SCOP sequence searches, alignments and genome assignments. *Nucleic Acids Res.*, 30(1):268–72.

Gouy, M., Guindon, S., and Gascuel, O. (2010). SeaView version 4: A multiplatform graphical user interface for sequence alignment and phylogenetic tree building. *Mol. Biol. Evol.*, 27(2):221–4.

Grabherr, M. G., Haas, B. J., Yassour, M., Levin, J. Z., Thompson, D. a., Amit, I., Adiconis, X., Fan, L., Raychowdhury, R., Zeng, Q., Chen, Z., Mauceli, E., Hacohen, N., Gnirke, A., Rhind, N., di Palma, F., Birren, B. W., Nusbaum, C., Lindblad-Toh, K., Friedman, N., and Regev, A. (2011). Full-length transcriptome assembly from RNA-Seq data without a reference genome. *Nat. Biotechnol.*, 29(7).

Green, B. R. (2011). After the primary endosymbiosis: An update on the chromalveolate hypothesis and the origins of algae with Chl c. *Photosynth. Res.*, 107:103–115.

Gribaldo, S., Poole, A. M., Daubin, V., Forterre, P., and Brochier-Armanet, C. (2010). The origin of eukaryotes and their relationship with the Archaea: are we at a phylogenomic impasse? *Nat. Rev. Microbiol.*, 8(10):743–52.

Gribskov, M., Homyak, M., Edenfield, J., and Eisenberg, D. (1988). Profile scanning for three-dimensional structural patterns in protein sequences.

Grigoriev, I. V., Nordberg, H., Shabalov, I., Aerts, A., Cantor, M., Goodstein, D., Kuo, A., Minovitsky, S., Nikitin, R., Ohm, R. a., Otillar, R., Poliakov, A., Ratnere, I., Riley, R., Smirnova, T., Rokhsar, D., and Dubchak, I. (2011). P@JGI-DOE@The Genome Portal of the Department of Energy Joint Genome Institute. *Nucleic Acids Res.*, 40(November 2011):1–7.

Guarnieri, M. T., Nag, A., Smolinski, S. L., Darzins, A., Seibert, M., and Pienkos, P. T. (2011). Examination of triacylglycerol biosynthetic pathways via de novo transcriptomic and proteomic analyses in an unsequenced microalga. *PLoS One*, 6(10).

Guindon, S. and Gascuel, O. (2003). A Simple, Fast, and Accurate Algorithm to Estimate Large Phylogenies by Maximum Likelihood. *Syst. Biol.*, 52(5):696–704.

Gunderson, J. H., Elwood, H., Ingold, a., Kindle, K., and Sogin, M. L. (1987). Phylogenetic relationships between chlorophytes, chrysophytes, and oomycetes. *Proc Natl Acad Sci U S A*, 84(August):5823–5827.

Gurevich, A., Saveliev, V., Vyahhi, N., and Tesler, G. (2013). QUAST: Quality assessment tool for genome assemblies. *Bioinformatics*, 29(8):1072–1075.

Haas, B. J., Papanicolaou, A., Yassour, M., Grabherr, M., Blood, P. D., Bowden, J., Couger, M. B., Eccles, D., Li, B., Lieber, M., Macmanes, M. D., Ott, M., Orvis, J., Pochet, N., Strozzi, F., Weeks, N., Westerman, R., William, T., Dewey, C. N., Henschel, R., Leduc, R. D., Friedman, N., and Regev, A. (2013). De novo transcript sequence reconstruction from RNA-seq using the Trinity platform for reference generation and analysis. *Nat. Protoc.*, 8(8):1494–512.

Haft, D. H. (2003). The TIGRFAMs database of protein families. *Nucleic Acids Res.*, 31(1):371–373.

Hamel, A., Fisch, C., Combettes, L., Dupuis-Williams, P., and Baroud, C. N. (2011). Transitions between three swimming gaits in Paramecium escape. *Proc. Natl. Acad. Sci. U. S. A.*, 108:7290–7295.

Harris, M. a., Clark, J., Ireland, a., Lomax, J., Ashburner, M., Foulger, R., Eilbeck, K., Lewis, S., Marshall, B., Mungall, C., Richter, J., Rubin, G. M., Blake, J. a., Bult, C., Dolan, M., Drabkin, H., Eppig, J. T., Hill, D. P., Ni, L., Ringwald, M., Balakrishnan, R., Cherry, J. M., Christie, K. R., Costanzo, M. C., Dwight, S. S., Engel, S., Fisk, D. G., Hirschman, J. E., Hong, E. L., Nash, R. S., Sethuraman, a., Theesfeld, C. L., Botstein, D., Dolinski, K., Feierbach, B., Berardini, T., Mundodi, S., Rhee, S. Y., Apweiler, R., Barrell, D., Camon, E., Dimmer, E., Lee, V., Chisholm, R., Gaudet, P., Kibbe, W., Kishore, R., Schwarz, E. M., Sternberg, P., Gwinn, M., Hannick, L., Wortman, J., Berriman, M., Wood, V., de la Cruz, N., Tonellato, P., Jaiswal, P., Seigfried, T., and White, R. (2004). The Gene Ontology (GO) database and informatics resource. *Nucleic Acids Res.*, 32:D258–D261.

Harris, T. D., Buzby, P. R., Babcock, H., Beer, E., Bowers, J., Braslavsky, I., Causey, M., Colonell, J., Dimeo, J., Efcavitch, J. W., Giladi, E., Gill, J., Healy, J., Jarosz, M., Lapen, D., Moulton, K., Quake, S. R., Steinmann, K., Thayer, E., Tyurina, A., Ward, R., Weiss, H., and Xie, Z. (2008). Single-molecule DNA sequencing of a viral genome. *Science*, 320(April):106–109.

Hasegawa, M., Kishino, H., and Yano, T. A. (1985). Dating of the human-ape splitting by a molecular clock of mitochondrial DNA. *J. Mol. Evol.*, 22:160–174.

Hayden, K. J., Garbelotto, M., Knaus, B. J., Cronn, R. C., Rai, H., and Wright, J. W. (2014). Dual RNA-seq of the plant pathogen Phytophthora ramorum and its tanoak host. *Tree Genet. Genomes*, 10:489–502.

He, K., Zhang, X., Ren, S., and Sun, J. (2015). Delving Deep into Rectifiers: Surpassing Human-Level Performance on ImageNet Classification. *arXiv:1502.01852*.

Heeg, J. S. and Wolf, M. (2015). ITS2 and 18S rDNA sequence-structure phylogeny of Chlorella and allies (Chlorophyta, Trebouxiophyceae, Chlorellaceae). *Plant Gene*, 4:20–28.

Henikoff, S. and Henikoff, J. G. (1992). Amino acid substitution matrices from protein blocks. *Proc. Natl. Acad. Sci. U. S. A.*, 89(November):10915–10919.

Henneberger, R., Moissl, C., Amann, T., Rudolph, C., and Huber, R. (2006). New insights into the lifestyle of the cold-loving SM1 euryarchaeon: Natural growth as a monospecies biofilm in the subsurface. *Appl. Environ. Microbiol.*, 72(1):192–199.

Hershkovitz, M. and Lewis, L. A. (1996). Deep-Level Diagnostic Value of the rDNA-ITS Region. *Mol Biol Evol*, 13(9):1276–1295.

Hinton, G. and Salakhutdinov, R. (2006). Reducing the Dimensionality of Data with Neural Networks. *Science (80-.).*, 313(July):504–507.

Hirakawa, Y., Burki, F., and Keeling, P. J. (2012). Genome-based reconstruction of the protein import machinery in the secondary plastid of a chlorarachniophyte alga. *Eukaryot. Cell*, 11:324–333.

Hirsch, A. A. (1992). Developmental biology of legume nodulation. *New Phytol.*, (40):211–237.

Hodges, M. E., Wickstead, B., Gull, K., and Langdale, J. a. (2011). Conservation of ciliary proteins in plants with no cilia. *BMC Plant Biol.*, 11(1):185.

Hoffman, P., Grinstein, G., Marx, K., Grosse, I., and Stanley, E. (1997). DNA visual and analytic data mining.

Hoffmeister, M. and Martin, W. (2003). Interspecific evolution: microbial symbiosis, endosymbiosis and gene transfer. *Environ. Microbiol.*, 5:641–9.

Hori, H., Lim, B. L., and Osawa, S. (1985). Evolution of green plants as deduced from 5S rRNA sequences. *Proc. Natl. Acad. Sci. U. S. A.*, 82(February):820–823.

Hörtnagl, P. H. and Sommaruga, R. (2007). Photo-oxidative stress in symbiotic and aposymbiotic strains of the ciliate Paramecium bursaria. *Photochem. Photobiol. Sci.*, 6(8):842–847.

Horton, P. and Nakai, K. (1997). Better prediction of protein cellular localization sites with the k nearest neighbors classifier. *Proc. Int. Conf. Intell. Syst. Mol. Biol.*, 5:147–152.

Horton, P., Park, K., Obayashi, T., and Nakai, K. (2006). Protein Subcellular Localisation Prediction with WoLF PSORT. *Ser Adv Bioinform*, 3:39–48.

Horton, P., Park, K.-J., Obayashi, T., Fujita, N., Harada, H., Adams-Collier, C., and Nakai, K. (2007). WoLF PSORT: protein localization predictor. *Nucleic Acids Res.*, 35(17):W585–W587.

Hoshina, R. (2012). Photobiont Flexibility in Paramecium bursaria: Double and Triple Photobiont Co-Habitation. *Adv. Microbiol.*, 02(September):227–233.

Hoshina, R. and Fujiwara, Y. (2013). Molecular characterization of Chlorella cultures of the National Institute for Environmental Studies culture collection with description of Micractinium inermum sp. nov., Didymogenes sphaerica sp. nov., and Didymogenes soliella sp. nov. (Chlorellaceae, Tr. *Phycol. Res.*, 61(2):124–132.

Hoshina, R. and Imamura, N. (2008). Multiple Origins of the Symbioses in Paramecium bursaria. *Protist*, 159(January).

Hoshina, R. and Imamura, N. (2009). Origins of Algal Symbionts of Paramecium bursaria. In Fujishima, M., editor, *Endosymbionts in Paramecium*, volume 12 of *Microbiology Monographs 12*, chapter 1, pages 2–29. Springer.

Hoshina, R., Iwataki, M., and Imamura, N. (2010). Chlorella variabilis and Micractinium reisseri sp. nov. (Chlorellaceae, Trebouxiophyceae): Redescription of the endosymbiotic green algae of Paramecium bursaria (Peniculia, Oligohymenophorea) in the 120th year. *Phycol. Res.*, 58(3):188–201.

Hoshina, R., Kamako, S.-I., and Imamura, N. (2004). Phylogenetic position of endosymbiotic green algae in Paramecium bursaria Ehrenberg from Japan. *Plant Biol. (Stuttg).*, 6(4):447–53.

Hosono, S., Faruqi, a. F., Dean, F. B., Du, Y., Sun, Z., Wu, X., Du, J., Kingsmore, S. F., Egholm, M., and Lasken, R. S. (2003). Unbiased whole-genome amplification directly from clinical samples. *Genome Res.*, 13:954–964.

Hosoya, H., Kimura, K., Matsuda, S., Kitaura, M., Takahashi, T., and Kosaka, T. (1995). Symbiotic Algae-free Strains of The Green Paramecium Paramecium bursaria Produced by the Herbicide Paraquat. *Zoolog. Sci.*, 12:807–810.

Hotelling, H. (1933). Analysis of a complex of statistical variables into principal components. *J. Educ. Psychol.*, 24(6):417.

Huber, H., Hohn, M. J., Rachel, R., and Fuchs, T. (2002). A new phylum of Archaea represented by a nanosized hyperthermophilic symbiont. *Nature*, 417(May):63–67.

Huelsenbeck, J. P. and Ronquist, F. (2001). MRBAYES: Bayesian inference of phylogenetic trees. *Bioinformatics*, 17(8):754–5.

Huerta-Cepas, J., Dopazo, J., and Gabaldón, T. (2010). ETE: a python Environment for Tree Exploration. *BMC Bioinformatics*, 11:24.

Huson, D. H., Auch, A. F., Qi, J., and Schuster, S. C. (2007). MEGAN analysis of metagenomic data. *Genome Res.*, 17:377–386.

Huygens, C. (1899). *Œuvres complètes de Christiaan Huygens, Correspondances Volume VII: 1676-1684*. Dutch Society of Sciences, The Hague.

ISO International Standard (2011). ISO/IEC 14882:2011(E) – Programming Language C++.

Iwatsuki, K. and Naitoh, Y. (1988). Behavioural responses to light in Paramecium bursaria in relation to its symbiotic green alga Chlorella. *J. Exp. Biol.*, 60:43–60.

Jahn, C. L. and Klobutcher, L. a. (2002). Genome remodeling in ciliated protozoa. *Annu. Rev. Microbiol.*, 56:489–520.

Jaszczyszyn, Y., Thermes, C., and Dijk, E. L. V. (2014). Ten years of next-generation sequencing technology. *Trends Genet.*, 30(9).

Jennings, H. S. (1939). Genetics of Paramecium Bursaria. I. Mating Types and Groups, Their Interrelations and Distribution; Mating Behavior and Self Sterility. *Genetics*, 24(March):202–233.

Jiggins, C. D., Hirschmann, R. J., Bundey, R. a., Insel, P. a., Crossland, J. P., Pool, J. E., Kassner, V. a., Aquadro, C. F., Carroll, S. B., Swinehart, J., Kingsley, E. P., Jensen, J. D., Hoekstra, H. E., Larson, J. G., Manceau, M., Wiley, C. D., Stephens, M., Duhl, D. M. J., Millar, S. E., Miller, K. a., Barsh, G. S., Hernandez, R. D., Williamson, S. H., Bustamante, C. D., Kim, Y., Hartl, D. L., Parsch, J., Goncalves, G., Chupasko, J., Kay, E., Kingsley, E., Demboski, J., Foundation, S., Agency, P., Fellowship, P., and Commission, P. (2013). Circadian Control of Chloroplast. *Nature*, 339(March):1316–1319.

Johnson, L. S., Eddy, S. R., and Portugaly, E. (2010). Hidden Markov model speed heuristic and iterative HMM search procedure. *BMC Bioinformatics*, 11:431.

Johnson, M. D. (2011). Acquired phototrophy in ciliates: a review of cellular interactions and structural adaptations. *J. Eukaryot. Microbiol.*, 58(3):185–95.

Jones, M., Dry, I. R., Frampton, D., Singh, M., Kanda, R. K., Yee, M. B., Kellam, P., Hollinshead, M., Kinchington, P. R., O'Toole, E. a., and Breuer, J. (2014). RNA-seq Analysis of Host and Viral Gene Expression Highlights Interaction between Varicella Zoster Virus and Keratinocyte Differentiation. *PLoS Pathog.*, 10(1).

Jukes, T. H. and Cantor, C. R. (1969). Evolution of protein molecules. *Mamm. protein Metab.*, 3:21–132.

Kadono, T., Kawano, T., Hosoya, H., and Kosaka, T. (2004). Flow cytometric studies of the host-regulated cell cycle in algae symbiotic with green paramecium. *Protoplasma*, 223:133–141.

Kafsack, B. F. and Llinás, M. (2010). Eating at the Table of Another: Metabolomics of Host-Parasite Interactions. *Cell Host Microbe*, 7:90–99.

Kajitani, R., Toshimoto, K., Noguchi, H., Toyoda, A., Ogura, Y., Okuno, M., Yabana, M., Harada, M., Nagayasu, E., Maruyama, H., Kohara, Y., Fujiyama, A., Hayashi, T., and Itoh, T. (2014). Efficient de novo assembly of highly heterozygous genomes from whole-genome shotgun short reads. *Genome Res.*, 24:1384–1395.

Käll, L., Krogh, A., and Sonnhammer, E. L. L. (2007). Advantages of combined transmembrane topology and signal peptide prediction-the Phobius web server. *Nucleic Acids Res.*, 35:429–432.

Kamako, S.-i., Hoshina, R., Ueno, S., and Imamura, N. (2005). Establishment of axenic endosymbiotic strains of Japanese Paramecium bursaria and the utilization of carbohydrate and nitrogen compounds by the isolated algae. *Eur. J. Protistol.*, 41:193–202.

Kaminuma, E., Kosuge, T., Kodama, Y., Aono, H., Mashima, J., Gojobori, T., Sugawara, H., Ogasawara, O., Takagi, T., Okubo, K., and Nakamura, Y. (2011). DDBJ progress report. *Nucleic Acids Res.*, 39(September 2010):D22–7.

Kandler, O. and Hopf, H. (1982). Oligosaccharides Based on Sucrose (Sucrosyl Oligosaccharides). In Loewus, F. and Tanner, W., editors, *Plant Carbohydrates I SE - 8*, volume 13 / A of *Encyclopedia of Plant Physiology*, pages 348–383. Springer Berlin Heidelberg.

Kanehisa, M., Goto, S., Sato, Y., Kawashima, M., Furumichi, M., and Tanabe, M. (2014). Data, information, knowledge and principle: back to metabolism in KEGG. *Nucleic Acids Res.*, 42(November 2013):D199–D205.

Kapaun, E. and Reisser, W. (1995). A chitin-like glycan in the cell wall of a Chlorella sp. (Chlorococcales, Chlorophyceae). *Planta*, 197:577–582.

Karakashian, S. (1963). Growth of Paramecium bursaria as Influenced by the Presence of Algal Symbionts. *Physiol. Zool.*, 36(1):52–68.

Karkar, S., Facchinelli, F., Price, D. C., Weber, A. P. M., and Bhattacharya, D. (2015). Metabolic connectivity as a driver of host and endosymbiont integration. *Proc. Natl. Acad. Sci. U. S. A.*, page 201421375.

Karp, P. D., Paley, S., and Romero, P. (2002). The Pathway Tools software. *Bioinformatics*, 18 Suppl 1:S225–S232.

Karp, P. D., Paley, S. M., Krummenacker, M., Latendresse, M., Dale, J. M., Lee, T. J., Kaipa, P., Gilham, F., Spaulding, a., Popescu, L., Altman, T., Paulsen, I., Keseler, I. M., and Caspi, R. (2010). Pathway Tools version 13.0: integrated software for pathway/genome informatics and systems biology. *Brief. Bioinform.*, 11(1):40–79.

Karp, R. M. (1972). Reducibility among combinatorial problems. In *Complex. Comput. Comput. Proc. a Symp. Complex. Comput. Comput.*, pages 85–103.

Kato, Y. and Imamura, N. (2008a). Effect of calcium ion on uptake of amino acids by symbiotic Chlorella F36-ZK isolated from Japanese Paramecium bursaria. *Plant Sci.*, 174(1):88–96.

Kato, Y. and Imamura, N. (2008b). Effect of sugars on amino acid transport by symbiotic Chlorella. *Plant Physiol. Biochem.*, 46(10):911–7.

Kato, Y. and Imamura, N. (2009a). Amino acid transport systems of Japanese Paramecium symbiont F36-ZK. *Symbiosis*, pages 99–107.

Kato, Y. and Imamura, N. (2009b). Metabolic Control Between the Symbiotic Chlorella and the Host Paramecium. In Fujishima, M., editor, *Endosymbionts in Paramecium*, volume 12 of *Microbiology Monographs*, chapter 3, pages 57–82. Springer.

Kato, Y., Ueno, S., and Imamura, N. (2006). Studies on the nitrogen utilization of endosymbiotic algae isolated from Japanese Paramecium bursaria. *Plant Sci.*, 170(3):481–486.

Katoh, K., Kuma, K.-i., Toh, H., and Miyata, T. (2005). MAFFT version 5: improvement in accuracy of multiple sequence alignment. *Nucleic Acids Res.*, 33(2):511–518.

Katoh, K., Misawa, K., Kuma, K.-i., and Miyata, T. (2002). MAFFT: a novel method for rapid multiple sequence alignment based on fast Fourier transform. *Nucleic Acids Res.*, 30(14):3059–3066.

Katoh, K. and Standley, D. M. (2013). MAFFT Multiple Sequence Alignment Software Version 7: Improvements in Performance and Usability. *Mol. Biol. Evol.*, 30(4):772–780.

Kaufman, L. and Rousseeuw, P. J. (1987). Clustering by means of medoids. In Dodge, Y., editor, *Stat. Data Anal. Based L 1-Norm Relat. Methods*, pages 405–416.

Kawahara, Y., Oono, Y., Kanamori, H., Matsumoto, T., Itoh, T., and Minami, E. (2012). Simultaneous RNA-seq analysis of a mixed transcriptome of rice and blast fungus interaction. *PLoS One*, 7(11):e49423.

Keeling, P. J. (2010). The endosymbiotic origin, diversification and fate of plastids. *Philos. Trans. R. Soc. Lond. B. Biol. Sci.*, 365:729–748.

Keeling, P. J. (2013). The number, speed, and impact of plastid endosymbioses in eukaryotic evolution. *Annu. Rev. Plant Biol.*, 64:583–607.

Keeling, P. J. and Palmer, J. D. (2008). Horizontal gene transfer in eukaryotic evolution. *Nat. Rev. Genet.*, 9(august):605–618.

Keller, A., Schleicher, T., Förster, F., Ruderisch, B., Dandekar, T., Müller, T., and Wolf, M. (2008). ITS2 data corroborate a monophyletic chlorophycean DO-group (Sphaeropleales). *BMC Evol. Biol.*, 8:218.

Keller, L. C., Romijn, E. P., Zamora, I., Yates, J. R., and Marshall, W. F. (2005). Proteomic Analysis of Isolated Chlamydomonas Centrioles Reveals Orthologs of Ciliary-Disease Genes. *Curr. Biol.*, 15:1090–1098.

Kessler, E. and Huss, V. A. R. (1990). Biochemical Taxonomy of Symbiotic Chlorella Strains from Paramecium and Acanthocystis*. *Bot. Acta*, 103(2):140–142.

Kies, L. and Kremer, B. P. (1979). Function of cyanelles in the thecamoeba Paulinella chromatophora. *Naturwissenschaften*, 66:578–579.

Kim, D., Pertea, G., Trapnell, C., Pimentel, H., Kelley, R., and Salzberg, S. L. (2013). TopHat2: accurate alignment of transcriptomes in the presence of insertions, deletions and gene fusions. *Genome Biol.*, 14(4):R36.

Klukas, C. and Schreiber, F. (2007). Dynamic exploration and editing of KEGG pathway diagrams. *Bioinformatics*, 23(3):344–350.

Knittel, K. and Boetius, A. (2009). Anaerobic oxidation of methane: progress with an unknown process. *Annu. Rev. Microbiol.*, 63:311–334.

Kodama, Y. and Fujishima, M. (2008). Cycloheximide induces synchronous swelling of perialgal vacuoles enclosing symbiotic Chlorella vulgaris and digestion of the algae in the ciliate Paramecium bursaria. *Protist*, 159(May):483–94.

Kodama, Y. and Fujishima, M. (2009). Infection of Paramecium bursaria by Symbiotic Chlorella Species. In Fujishima, M., editor, *Endosymbionts in Paramecium*, volume 12 of *Microbiology Monographs*, chapter 2, pages 31–55. Springer.

Kodama, Y. and Fujishima, M. (2011). Endosymbiosis of Chlorella species to the ciliate Paramecium bursaria alters the distribution of the host's trichocysts beneath the host cell cortex. *Protoplasma*, 248:325–337.

Kodama, Y. and Fujishima, M. (2012). Characteristics of the digestive vacuole membrane of the alga-bearing ciliate Paramecium bursaria. *Protist*, 163(4):658–70.

Kodama, Y. and Fujishima, M. (2014). Symbiotic Chlorella variabilis incubated under constant dark conditions for 24 hours loses the ability to avoid digestion by host lysosomal enzymes in digestive vacuoles of host ciliate Paramecium bursaria. *FEMS Microbiol. Ecol.*, 90:946–955.

Kodama, Y., Nakahara, M., and Fujishima, M. (2007). Symbiotic alga Chlorella vulgaris of the ciliate Paramecium bursaria shows temporary resistance to host lysosomal enzymes during the early infection process. *Protoplasma*, 230(1-2):61–7.

Kodama, Y., Shumway, M., and Leinonen, R. (2012). The sequence read archive: explosive growth of sequencing data. *Nucleic Acids Res.*, 40(October 2011):D54–D56.

Kodama, Y., Suzuki, H., Dohra, H., Sugii, M., Kitazume, T., Yamaguchi, K., Shigenobu, S., and Fujishima, M. (2014). Comparison of gene expression of Paramecium bursaria with and without Chlorella variabilis symbionts. *BMC Genomics*, 15:183.

Koga, R., Tsuchida, T., and Fukatsu, T. (2003). Changing partners in an obligate symbiosis: a facultative endosymbiont can compensate for loss of the essential endosymbiont Buchnera in an aphid. *Proc. Biol. Sci.*, 270(April):2543–2550.

Kolisko, M., Boscaro, V., Burki, F., Lynn, D. H., and Keeling, P. J. (2014). Transcriptomics for Microbial Eukaryotes. *Curr. Biol.*, 24(22):R1081–R1082.

Komer, B., Bergstra, J., and Eliasmith, C. (2014). Hyperopt-Sklearn: Automatic Hyperparameter Configuration for Scikit-Learn. *Proc. 13th Python Sci. Conf.*, (Scipy):33–39.

Kopp, C., Domart-Coulon, I., Escrig, S., Humbel, B. M., Hignette, M., and Meibom, A. (2015). Subcellular investigation of photosynthesis-driven carbon and nitrogen assimilation and utilization in the symbiotic reef coral Pocillopora damicornis. *Submitted*, 6(1):1–9.

Korfhage, C., Fricke, E., and Meier, A. (2015). Whole-Transcriptome Amplification of Single Cells for Next-Generation Sequencing. *Curr. Protoc. Mol. Biol.*, (July):7.20.1–7.20.19.

Krasileva, K. V., Buffalo, V., Bailey, P., Pearce, S., Ayling, S., Tabbita, F., Soria, M., Wang, S., Akhunov, E., Uauy, C., and Dubcovsky, J. (2013). Separating homeologs by phasing in the tetraploid wheat transcriptome. *Genome Biol.*, 14:R66.

Kreutz, M., Stoeck, T., and Foissner, W. (2012). Morphological and Molecular Characterization of Paramecium (Viridoparamecium nov. subgen.) chlorelligerum Kahl, 1935 (Ciliophora). *J. Eukaryot. Microbiol.*, 59(6).

Krogh, a., Larsson, B., von Heijne, G., and Sonnhammer, E. L. (2001). Predicting transmembrane protein topology with a hidden Markov model: application to complete genomes. *J. Mol. Biol.*, 305(3):567–80.

Kruschke, J. K. (2013). Bayesian estimation supersedes the t test. *J. Exp. Psychol. Gen.*, 142(2):573–603.

Kumar, S. (1996). A stepwise algorithm for finding minimum evolution trees. *Mol. Biol. Evol.*, 13(4):584–593.

Küper, U., Meyer, C., Müller, V., Rachel, R., and Huber, H. (2010). Energized outer membrane and spatial separation of metabolic processes in the hyperthermophilic Archaeon Ignicoccus hospitalis. *Proc. Natl. Acad. Sci. U. S. A.*, 107:3152–3156.

Laligne, C., Klotz, C., Garreau de Loubresse, N., Lemullois, M., Hori, M., Laurent, F. X., Papon, J. F., Louis, B., Cohen, J., and Koll, F. (2010). Bug22p, a Conserved Centrosomal/Ciliary Protein Also Present in Higher Plants, Is Required for an Effective Ciliary Stroke in Paramecium. *Eukaryot. Cell*, 9(4):645–655.

Lalonde, S., Boles, E., Hellmann, H., Barker, L., Patrick, J., Frommer, W., and Ward, J. (1999). The dual function of sugar carriers. Transport and sugar sensing. *Plant Cell*, 11(April):707–726.

Lane, N. (2007). Mitochondria: Key to Complexity. In Martin, W. and Müller, M., editors, *Orig. Mitochondria Hydrog. SE - 2*, pages 13–38. Springer Berlin Heidelberg.

Lange, M., Westermann, P., and Ahring, B. K. r. (2005). Archaea in protozoa and metazoa. *Appl. Microbiol. Biotechnol.*, 66:465–474.

Langmead, B. and Salzberg, S. L. (2012). Fast gapped-read alignment with Bowtie 2. *Nat. Methods*, 9(4):357–9.

Lapointe, F.-j., Kirsch, J. A. W., and Bleiwiess, R. (1994). Jackknifing of Weighted Trees: Validation of Phylogenies Reconstructed from Distance Matrices. *Mol. Phylogenet. Evol.*, 3(3):256–267.

Lartillot, N. and Philippe, H. (2004). A Bayesian mixture model for across-site heterogeneities in the amino-acid replacement process. *Mol. Biol. Evol.*, 21(6):1095–1109.

Lasken, R. S. (2007). Single-cell genomic sequencing using Multiple Displacement Amplification. *Curr. Opin. Microbiol.*, 10:510–516.

Lassmann, T., Hayashizaki, Y., and Daub, C. O. (2009). TagDust - A program to eliminate artifacts from next generation sequencing data. *Bioinformatics*, 25(21):2839–2840.

Lassmann, T. and Sonnhammer, E. L. L. (2005). Kalign - an accurate and fast multiple sequence alignment algorithm. *BMC Bioinformatics*, 6(298):1–9.

Le, H. S., Schulz, M. H., Mccauley, B. M., Hinman, V. F., and Bar-Joseph, Z. (2013). Probabilistic error correction for RNA sequencing. *Nucleic Acids Res.*, 41:1–11.

Le, S. Q. and Gascuel, O. (2008). An improved general amino acid replacement matrix. *Mol. Biol. Evol.*, 25(7):1307–1320.

Lee, E., Jung, H., Radivojac, P., Kim, J.-W., and Lee, D. (2009). Analysis of AML genes in dysregulated molecular networks. *BMC Bioinformatics*, 10 Suppl 9:S2.

Legin, A. a., Schintlmeister, A., Jakupec, M. a., Galanski, M., Lichtscheidl, I., Wagner, M., and Keppler, B. K. (2014). NanoSIMS combined with fluorescence microscopy as a tool for subcellular imaging of isotopically labeled platinum-based anticancer drugs. *Chem. Sci.*, 5:3135.

Leinonen, R., Sugawara, H., and Shumway, M. (2011). The Sequence Read Archive. *Nucleic Acids Res.*, 39(November 2010):D19–D21.

Leliaert, F., Smith, D. R., Moreau, H., Herron, M. D., Verbruggen, H., Delwiche, C. F., and De Clerck, O. (2012). Phylogeny and Molecular Evolution of the Green Algae. *CRC. Crit. Rev. Plant Sci.*, 31(1):1–46.

Lepere, G., Nowacki, M., Serrano, V., Gout, J.-F., Guglielmi, G., Duharcourt, S., and Meyer, E. (2009). Silencing-associated and meiosis-specific small RNA pathways in Paramecium tetraurelia. *Nucleic Acids Res.*, 37(3):903–915.

Leung, H., Yiu, S. M., and Chin, F. (2014). IDBA-MTP: A Hybrid MetaTranscriptomic Assembler Based on Protein Information. In Sharan, R., editor, *Res. Comput. Mol. Biol. SE - 12*, volume 8394 of *Lecture Notes in Computer Science*, pages 160–172. Springer International Publishing.

Leung, H. C. M., Yiu, S.-M., Parkinson, J., and Chin, F. Y. L. (2013). IDBA-MT: De Novo Assembler for Metatranscriptomic Data Generated from Next-Generation Sequencing Technology. *J. Comput. Biol.*, 20(7):540–550.

Leung, T. L. F. and Poulin, R. (2008). Parasitism, commensalism, and mutualism: Exploring the many shades of symbioses. *Vie Milieu*, 58(2):107–115.

Li, B., Fillmore, N., Bai, Y., Collins, M., Thomson, J. a., Stewart, R., and Dewey, C. N. (2014). Evaluation of de novo transcriptome assemblies from RNA-Seq data. *Genome Biol.*, 15(553):1–21.

Li, D., Liu, C.-M., Luo, R., Sadakane, K., and Lam, T.-W. (2015). MEGAHIT: An ultra-fast single-node solution for large and complex metagenomics assembly via succinct de Bruijn graph. *Bioinformatics*, 31(January):btv033–.

Li, H. (2015). Seqtk.

Li, H., Handsaker, B., Wysoker, A., Fennell, T., Ruan, J., Homer, N., Marth, G., Abecasis, G., Durbin, R., and Subgroup, . G. P. D. P. (2009). The Sequence Alignment/Map format and SAMtools. *Bioinformatics*, 25(16):2078–2079.

Lima, T., Auchincloss, A. H., Coudert, E., Keller, G., Michoud, K., Rivoire, C., Bulliard, V., de Castro, E., Lachaize, C., Baratin, D., Phan, I., Bougueleret, L., and Bairoch, A. (2009). HAMAP: a database of completely sequenced microbial proteome sets and manually curated microbial protein families in UniProtKB/Swiss-Prot. *Nucleic Acids Res.*, 37(October 2008):D471–8.

Lineberger, R. D. (1980). Cryoprotection by glucose, sucrose, and raffinose to chloroplast thylakoids. *Plant Physiol.*, 65:298–304.

Lipson, D., Raz, T., Kieu, A., Jones, D. R., Giladi, E., Thayer, E., Thompson, J. F., Letovsky, S., Milos, P., and Causey, M. (2009). Quantification of the yeast transcriptome by single-molecule sequencing. *Nat. Biotechnol.*, 27(7):652–658.

Lloyd, S. (1982). Least squares quantization in PCM. *IEEE Trans. Inf. Theory*, 28(2):129–137.

Lowe, E., Swalla, B., and Brown, C. T. (2014). Evaluating a lightweight transcriptome assembly pipeline on two closely related ascidian species. *PeerJ Prepr.*, September:0–10.

Lusk, R. W. (2014). Diverse and widespread contamination evident in the unmapped depths of high throughput sequencing data. *PLoS One*, 9(10).

Maaten, L. V. D. and Hinton, G. (2008). Visualizing Data using t-SNE. *J. Mach. Learn. Res.*, 9:2579–2605.

Macaulay, I. C. and Voet, T. (2014). Single Cell Genomics: Advances and Future Perspectives. *PLoS Genet.*, 10(1).

MacManes, M. D. (2014). On the optimal trimming of high-throughput mRNA sequence data. *Front. Genet.*, 5(January):1–7.

Macmanes, M. D. (2015). Optimizing error correction of RNAseq reads. *bioRxiv Prepr.*, pages 1–4.

Macmanes, M. D. and Eisen, M. B. (2013). Improving transcriptome assembly through error correction of high-throughput sequence reads. *PeerJ*, 1:e113.

Maguire, F., Henriquez, F. L., Leonard, G., Dacks, J. B., Brown, M. W., and Richards, T. a. (2014). Complex patterns of gene fission in the eukaryotic folate biosynthesis pathway. *Genome Biol. Evol.*, 6(10):2709–20.

Maguire, F. and Richards, T. (2014). Organelle Evolution: A Mosaic of 'Mitochondrial' Functions. *Curr. Biol.*, 24(11):R518–R520.

Marçais, G. and Kingsford, C. (2011). A fast, lock-free approach for efficient parallel counting of occurrences of k-mers. *Bioinformatics*, 27(6):764–770.

Mardis, E. R. (2008). Next-generation DNA sequencing methods. *Annu. Rev. Genomics Hum. Genet.*, 9:387–402.

Margulies, M., Egholm, M., Altman, W. E., Attiya, S., Bader, J. S., Bemben, L. a., Berka, J., Braverman, M. S., Chen, Y.-J., Chen, Z., Dewell, S. B., Du, L., Fierro, J. M., Gomes, X. V., Godwin, B. C., He, W., Helgesen, S., Ho, C. H., Irzyk, G. P., Jando, S. C., Alenquer, M. L. I., Jarvie, T. P., Jirage, K. B., Kim, J.-B., Knight, J. R., Lanza, J. R., Leamon, J. H., Lefkowitz, S. M., Lei, M., Li, J., Lohman, K. L., Lu, H., Makhijani, V. B., McDade, K. E., McKenna, M. P., Myers, E. W., Nickerson, E., Nobile, J. R., Plant, R., Puc, B. P., Ronan, M. T., Roth, G. T., Sarkis, G. J., Simons, J. F., Simpson, J. W., Srinivasan, M., Tartaro, K. R., Tomasz, A., Vogt, K. a., Volkmer, G. a., Wang, S. H., Wang, Y., Weiner, M. P., Yu, P., Begley, R. F., and Rothberg, J. M. (2005). Genome Sequencing in Microfabricated High-density Picolitre Reactors. *Nature*, 437(September):376–380.

Markell, D. and Trench, R. (1993). Macromolecules Exuded By Symbiotic Dinoflagellates in Culture: Amino Acid and Sugar Composition1. *J. Phycol.*, 29:64–68.

Marker, S., Carradec, Q., Tanty, V., Arnaiz, O., and Meyer, E. (2014). A forward genetic screen reveals essential and non-essential RNAi factors in Paramecium tetraurelia. *Nucleic Acids Res.*, 42(11):7268–7280.

Martin, W. and Herrmann, R. G. (1998). Gene Transfer from Organelles to the Nucleus: How Much, What Happens, and Why? *Plant Physiol.*, 118(1):9–17.

Martinez, J., Longdon, B., Bauer, S., Chan, Y.-S., Miller, W. J., Bourtzis, K., Teixeira, L., and Jiggins, F. M. (2014). Symbionts commonly provide broad spectrum resistance to viruses in insects: a comparative analysis of Wolbachia strains. *PLoS Pathog.*, In press(9).

Mathews, D. H., Disney, M. D., Childs, J. L., Schroeder, S. J., Zuker, M., and Turner, D. H. (2004). Incorporating chemical modification constraints into a dynamic programming algorithm for prediction of RNA secondary structure. *Proc. Natl. Acad. Sci. U. S. A.*, 101(19):7287–7292.

Mayer, K. M. and Forney, J. D. (1999). A Mutation in the Flanking 5'-TA-3' Dinucleotide Prevents Excision of an Internal Eliminated Sequence From the Paramecium tetraurelia Genome. *Genetics*, 151:597–604.

McAuley, P. (1986). Uptake of Amino Acids by Cultured and Freshly Isolated Symbiotic Chlorella. *New Phytol.*, 104:415–427.

McFadden, G. I. (2014). Origin and evolution of plastids and photosynthesis in eukaryotes. *Cold Spring Harb. Perspect. Biol.*, 6:a016105.

McGrath, C. L., Gout, J.-F., Doak, T. G., Yanagi, A., and Lynch, M. (2014). Insights into three whole-genome duplications gleaned from the Paramecium caudatum genome sequence. *Genetics*, 197(4):1417–28.

Mendes Maia, T., Gogendeau, D., Pennetier, C., Janke, C., and Basto, R. (2014). Bug22 influences cilium morphology and the post-translational modification of ciliary microtubules. *Biol. Open*, 3:138–151.

Meng, D., Cao, M., Oda, T., and Pan, J. (2014). The conserved ciliary protein Bug22 controls planar beating of Chlamydomonas flagella. *J. Cell Sci.*, 127:281–287.

Merkel, D. (2014). Docker: Lightweight Linux Containers for Consistent Development and Deployment. *Linux J.*, 239(March).

Milinkovitch, M. C., Leduc, G., Ada, J., Farnir, F., Georgest, M., and Hasegawa, M. (1996). Effects of Character Weighting and Species Sampling on Phylogeny Reconstruction: A Case Study Based on DNA Sequence Data in Cetaceans. *Genetics*, 144:1817–1833.

Milinkovitch, M. C. and Lyons-Weiler, J. (1998). Finding optimal ingroup topologies and convexities when the choice of outgroups is not obvious. *Mol. Phylogenet. Evol.*, 9(3):348–357.

Miller, R. G. (1974). The Jackknife - A Review.

Minin, V., Abdo, Z., Joyce, P., and Sullivan, J. (2003). Performance-Based Selection of Likelihood Models for Phylogeny Estimation. *Syst. Biol.*, 52(5):674–683.

Mistry, J., Finn, R. D., Eddy, S. R., Bateman, a., and Punta, M. (2013). Challenges in homology search: HMMER3 and convergent evolution of coiled-coil regions. *Nucleic Acids Res.*, 41(12):e121–e121.

Mitchell, T. E. (1997). *Machine Learning*. McGraw Hill.

Miwa, I. (2009). Regulation of Circadian Rhythms of Paramecium bursaria by Symbiotic Chlorella Species. In Fujishima, M., editor, *Endosymbionts in Paramecium*, volume 12 of *Microbiology Monographs*, chapter 4, pages 83–110. Springer.

Mockler, T. C. and Ecker, J. R. (2005). Applications of DNA tiling arrays for whole-genome analysis. *Genomics*, 85:1–15.

Moissl-Eichinger, C. and Huber, H. (2011). Archaeal symbionts and parasites. *Curr. Opin. Microbiol.*, 14:364–370.

Molnar, M. and Ilie, L. (2014). Correcting Illumina data. *Brief. Bioinform.*

Moriya, Y., Itoh, M., Okuda, S., Yoshizawa, a. C., and Kanehisa, M. (2007). KAAS: an automatic genome annotation and pathway reconstruction server. *Nucleic Acids Res.*, 35:W182–W185.

Muñoz Mérida, A., González-Plaza, J. J., Cañada, A., Blanco, A. M., García-López, M. D. C., Rodríguez, J. M., Pedrola, L., Sicardo, M. D., Hernández, M. L., De la Rosa, R., Belaj, A., Gil-Borja, M., Luque, F., Martínez-Rivas, J. M., Pisano, D. G., Trelles, O., Valpuesta, V., and Beuzón, C. R. (2013). De novo assembly and functional annotation of the olive (Olea europaea) transcriptome. *DNA Res.*, 20(January):93–108.

Müller, T., Philippi, N., Dandekar, T., Schultz, J., and Wolf, M. (2007). Distinguishing species. *RNA*, 13:1469–1472.

Murphy, K. P. (2012). *Machine learning: a probabilistic perspective*. MIT Press.

Murray, S. a., Patterson, D. J., and Thessen, A. E. (2012). Transcriptomics and microbial eukaryote diversity: A way forward. *Trends Ecol. Evol.*, 27(12):651–652.

Muscatine, L. (1967). Glycerol Excretion by Symbiotic Algae from Corals and Tridacna and Its Control by the Host. *Science (80-.).*, 156(April):516–519.

Muscatine, L., Karakashian, S. J., and Karakashian, M. W. (1967). Soluble extracellular products of algae symbiotic with a ciliate, a sponge and a mutant hydra. *Comp. Biochem. Physiol.*, 20:1–12.

Nabhan, A. R. and Sarkar, I. N. (2012). The impact of taxon sampling on phylogenetic inference: A review of two decades of controversy. *Brief. Bioinform.*, 13(1):122–134.

Nakai, K. and Horton, P. (1999). PSORT: a program for detecting sorting signals in proteins and predicting their subcellular localization. *Trends Biochem. Sci.*, 24(98):34–35.

Nakai, K. and Kanehisa, M. (1992). A knowledge base for predicting protein localization sites in eukaryotic cells. *Genomics*, 14:897–911.

Nakajima, B. Y. K. and Nakaoka, Y. (1989). Circadian Change of Photosensiuvity in Paramecium Bursaria. *J. Exp. Biol.*, 144:43–51.

Nakao, M., Bono, H., Kawashima, S., Kamiya, T., Sato, K., Goto, S., and Kanehisa, M. (1999). Genome-scale Gene Expression Analysis and Pathway Reconstruction in KEGG. *Genome Inform. Ser. Workshop Genome Inform.*, 10:94–103.

Nakasugi, K., Crowhurst, R., Bally, J., and Waterhouse, P. (2014). Combining Transcriptome Assemblies from Multiple De Novo Assemblers in the Allo-Tetraploid Plant Nicotiana benthamiana. *PLoS One*, 9(3):e91776.

National Center for Biotechnology Information (2011). *SRA Knowledge Base*.

Nederbragt, A. J. (2013). Developments in Next-Generation Sequencing Technologies.

Needleman, S. B. and Wunsch, C. D. (1970). A general method applicable to the search for similarities in the amino acid sequence of two proteins. *J. Mol. Biol.*, 48:443–453.

Nei, M. (1987). The Neighbor-joining Method: A New Method for Reconstructing Phylogenetic Trees'. *Mol Biol Evol*, 4(4):406–425.

Neil, S. T. O. and Emrich, S. J. (2013). Assessing De Novo transcriptome assembly metrics for consistency and utility. *BMC Genomics*.

Neyman, J. (1971). Molecular studies of evolution: a source of novel statistical problems. *Stat. Decis. theory Relat. Top.*, pages 1–27.

Ng, A. Y. and Jordan, M. I. (2002). On discriminative vs. generative classifiers: A comparison of logistic regression and naive bayes. In Dietterich, T., Becker, S., and Ghahramani, Z., editors, *Adv. Neural Inf. Process. Syst. 14 (NIPS 2001)*, pages 841–848. MIT Press.

Nielsen, H., Engelbrecht, J., Brunak, S., and Heijne, G. (1997). Identification of prokaryotic and eukaryotic signal peptides and prediction of their cleavage sites. *Protein Eng.*, 10(1):1–6.

Niess, D., Reisser, W., and Wiessner, W. (1982a). Photobehaviour of Paramecium bursaria infected with different symbiotic and aposymbiotic species of Chlorella. *Planta*, 156:475–480.

Niess, D., Reisser, W., and Wiessner, W. (1982b). Photobehaviour of Paramecium bursaria infected with different symbiotic and aposymbiotic species of Chlorella. *Planta*, 156(5):475–480.

Nikolenko, S. I., Korobeynikov, A. I., and Alekseyev, M. a. (2013). BayesHammer: Bayesian clustering for error correction in single-cell sequencing. *BMC Genomics*, 14 Suppl 1(Suppl 1):S7.

Nordberg, H., Cantor, M., Dusheyko, S., Hua, S., Poliakov, a., Shabalov, I., Smirnova, T., Grigoriev, I. V., and Dubchak, I. (2014). The genome portal of the Department of Energy Joint Genome Institute: 2014 updates. *Nucleic Acids Res.*, 42(November 2013):D26–D31.

Notredame, C., Higgins, D. G., and Heringa, J. (2000). T-Coffee: A novel method for fast and accurate multiple sequence alignment. *J. Mol. Biol.*, 302:205–217.

Novakova, Lenka and Stepankova, O. (2006). Multidimensional clusters in RadViz. *Proc. 6th WSEAS Int. Conf. Simulation, Model. Optim.*, pages 470–475.

Nowack, E. C. M., Vogel, H., Groth, M., Grossman, A. R., Melkonian, M., and Glöckner, G. (2011). Endosymbiotic gene transfer and transcriptional regulation of transferred genes in Paulinella chromatophora. *Mol. Biol. Evol.*, 28(1):407–422.

Nurk, S., Bankevich, A., Antipov, D., Gurevich, A. a., Korobeynikov, A., Lapidus, A., Prjibelski, A. D., Pyshkin, A., Sirotkin, A., Sirotkin, Y., Stepanauskas, R., Clingenpeel, S. R., Woyke, T., McLean, J. S., Lasken, R., Tesler, G., Alekseyev, M. a., and Pevzner, P. a. (2013). Assembling single-cell genomes and mini-metagenomes from chimeric MDA products. *J. Comput. Biol.*, 20(10):714–37.

O'Callaghan, L., Mishra, N., Meyerson, A., Guha, S., and Motwani, R. (2002). Streaming-Data Algorithms for High-Quality Clustering. In *Proc. 18th Int. Conf. Data Eng.*, page 0685. IEEE.

Ogata, H., Goto, S., Sato, K., Fujibuchi, W., Bono, H., Kanehisa, M., Goto, S., Ogata, H., Goto, S., Sato, K., Fujibuchi, W., Bono, H., Kanehisa, M., and Goto, S. (1999). KEGG: Kyoto encyclopedia of genes and genomes. *Nucleic Acids Res.*, 27(1):27–30.

Ohkawa, H., Hashimoto, N., Furukawa, S., Kadono, T., and Kawano, T. (2011). Forced symbiosis between Synechocystis spp. PCC 6803 and apo-symbiotic Paramecium bursaria as an experimental model for evolutionary emergence of primitive photosynthetic eukaryotes. *Plant Signal. Behav.*, 6(July 2015):773–776.

Okuda, S., Yamada, T., Hamajima, M., Itoh, M., Katayama, T., Bork, P., Goto, S., and Kanehisa, M. (2008). KEGG Atlas mapping for global analysis of metabolic pathways. *Nucleic Acids Res.*, 36(May):W423–W426.

Ondov, B. D., Bergman, N. H., and Phillippy, A. M. (2011). Interactive metagenomic visualization in a Web browser. *BMC Bioinformatics*, 12(1):385.

O'Neil, D., Glowatz, H., and Schlumpberger, M. (2013). Ribosomal RNA Depletion for Efficient Use of RNA-Seq Capacity. In *Curr. Protoc. Mol. Biol.*, volume Unit 4.19, chapter 4. John Wiley & Sons, Inc.

Ozsolak, F. and Milos, P. M. (2011). Single-molecule direct RNA sequencing without cDNA synthesis. *Wiley Interdiscip Rev RNA*, 2(4):565–570.

Ozsolak, F., Platt, A. R., Jones, D. R., Reifenberger, J. G., Sass, L. E., McInerney, P., Thompson, J. F., Bowers, J., Jarosz, M., and Milos, P. M. (2009). Direct RNA sequencing. *Nature*, 461(7265):814–818.

O'Malley, M. a. (2015). Molecular organisms. *Biol. Philos.*

Paez, J. G., Lin, M., Beroukhim, R., Lee, J. C., Zhao, X., Richter, D. J., Gabriel, S., Herman, P., Sasaki, H., Altshuler, D., Li, C., Meyerson, M., and Sellers, W. R. (2004). Genome coverage and sequence fidelity of phi29 polymerase-based multiple strand displacement whole genome amplification. *Nucleic Acids Res.*, 32(9):e71.

Parker, R. C. (1926). Symbiosis in Paramecium bursaria. *J. Exp. Zool.*, 46(1):1–12.

Parzen, E. (1962). On Estimation of a Probability Density Function and Mode. *Ann. Math. Stat.*, 33:1065–1076.

Pedregosa, F., Varoquaux, G., Gramfort, A., Michel, V., Thirion, B., Grisel, O., Blondel, M., Prettenhofer, P., Weiss, R., Dubourg, V., Vanderplas, J., Passos, A., Cournapeau, D., Brucher, M., Perrot, M., and Duchesnay, E. (2011). Scikit-learn: Machine Learning in {P}ython. *J. Mach. Learn. Res.*, 12:2825–2830.

Pedrioli, P. G. a., Eng, J. K., Hubley, R., Vogelzang, M., Deutsch, E. W., Raught, B., Pratt, B., Nilsson, E., Angeletti, R. H., Apweiler, R., Cheung, K., Costello, C. E., Hermjakob, H., Huang, S., Julian, R. K., Kapp, E., McComb, M. E., Oliver, S. G., Omenn, G., Paton, N. W., Simpson, R., Smith, R., Taylor, C. F., Zhu, W., and Aebersold, R. (2004). A common open representation of mass spectrometry data and its application to proteomics research. *Nat. Biotechnol.*, 22(11):1459–1466.

Pell, J., Hintze, a., Canino-Koning, R., Howe, a., Tiedje, J. M., and Brown, C. T. (2012). Scaling metagenome sequence assembly with probabilistic de Bruijn graphs. *Proc. Natl. Acad. Sci.*, 109(33):13272–13277.

Peng, Y., Leung, H., Yiu, S. M., and Chin, F. (2010). IDBA – A Practical Iterative de Bruijn Graph De Novo Assembler. In Berger, B., editor, *Res. Comput. Mol. Biol. SE - 28*, volume 6044 of *Lecture Notes in Computer Science*, pages 426–440. Springer Berlin Heidelberg.

Peng, Y., Leung, H. C. M., Yiu, S. M., and Chin, F. Y. L. (2012). IDBA-UD: a de novo assembler for single-cell and metagenomic sequencing data with highly uneven depth. *Bioinformatics*, 28(11):1420–8.

Peng, Y., Leung, H. C. M., Yiu, S.-M., Lv, M.-J., Zhu, X.-G., and Chin, F. Y. L. (2013). IDBA-tran: a more robust de novo de Bruijn graph assembler for transcriptomes with uneven expression levels. *Bioinformatics*, 29:i326–i334.

Peralta, H., Guerrero, G., Aguilar, A., and Mora, J. (2011). Sequence variability of Rhizobiales orthologs and relationship with physico-chemical characteristics of proteins. *Biol. Direct*, 6(1):48.

Pérez, M. T., Dolan, J. R., and Fukai, E. (1997). Planktonic oligotrich ciliates in the NW Mediterranean: growth rates and consumption by copepods. *Mar. Ecol. Prog. Ser.*, 155:89–101.

Perez-Cobas, a. E., Gosalbes, M. J., Friedrichs, a., Knecht, H., Artacho, a., Eismann, K., Otto, W., Rojo, D., Bargiela, R., von Bergen, M., Neulinger, S. C., Daumer, C., Heinsen, F.-a., Latorre, a., Barbas, C., Seifert, J., dos Santos, V. M., Ott, S. J., Ferrer, M., and Moya, a. (2013). Gut microbiota disturbance during antibiotic therapy: a multi-omic approach. *Gut*, 62:1591–1601.

Petersen, T. N., Brunak, S. r., von Heijne, G., and Nielsen, H. (2011). SignalP 4.0: discriminating signal peptides from transmembrane regions. *Nat. Methods*, 8(10):785–6.

Phadke, S. S. and Zufall, R. a. (2009). Rapid diversification of mating systems in ciliates. *Biol. J. Linn. Soc.*, 98:187–197.

Poretsky, R. S., Bano, N., Buchan, A., Kleikemper, J., Pickering, M., Pate, W. M., Moran, M. A., Hollibaugh, J. T., and Lecleir, G. (2005). Analysis of Microbial Gene Transcripts in Environmental Samples. *Appl. Environ. Microbiol.*, 71(7):4121–4126.

Posada, D. (2008). jModelTest: Phylogenetic Model Averaging. *Mol. Biol. Evol.*, 25:1253–1256.

Pound, R. (1893). Symbiosis and Mutualism. *Am. Nat.*, 27:509.

Prell, J. and Poole, P. (2006). Metabolic changes of rhizobia in legume nodules. *Trends Microbiol.*, 14(4):161–168.

Prescott, D. M. (1994). The DNA of ciliated protozoa. *Microbiol. Rev.*, 58(2):233–267.

Preston, C. M., Wu, K. Y., Molinski, T. F., and DeLong, E. F. (1996). A psychrophilic crenarchaeon inhabits a marine sponge: Cenarchaeum symbiosum gen. nov., sp. nov. *Proc. Natl. Acad. Sci. U. S. A.*, 93(June):6241–6246.

Price, D. C., Chan, C. X., Yoon, H. S., Yang, E. C., Qiu, H., Weber, A. P. M., Schwacke, R., Gross, J., Blouin, N. a., and Lane, C. (2012). Cyanophora paradoxa genome elucidates origin of photosynthesis in algae and plants. *Science (80-.).*, 335(March):843–847.

Price, M. N., Dehal, P. S., and Arkin, A. P. (2010). FastTree 2 – approximately maximum-likelihood trees for large alignments. *PLoS One*, 5(3):e9490.

Pruitt, K. D., Tatusova, T., and Maglott, D. R. (2007). NCBI reference sequences (RefSeq): A curated non-redundant sequence database of genomes, transcripts and proteins. *Nucleic Acids Res.*, 35:501–504.

Putt, M. (1990). Abundance, chlorophyll content and photosynthetic rates of ciliates in the Nordic Seas during summer. *Deep. Res.*, 37(11):1713–1731.

Quinlan, A. R. (2014). BEDTools: The Swiss-Army Tool for Genome Feature Analysis. In *Curr. Protoc. Bioinforma.* John Wiley & Sons, Inc.

Quinlan, A. R. and Hall, I. M. (2010). BEDTools: a flexible suite of utilities for comparing genomic features. *Bioinformatics*, 26(6):841–842.

Quinlan, J. R. (1986). Induction of Decision Trees. *Mach. Learn.*, 1(1):81–106.

R Core Team (2015). *R: A Language and Environment for Statistical Computing*. R Foundation for Statistical Computing, Vienna, Austria.

Raikov, I. (1995). Structure and Genetic Organization of the Polyploid Macronucleus of Ciliates: a Comparative Review. *Acta Protozool.*, 34:151–171.

Raj, A. and van Oudenaarden, A. (2008). Nature, Nurture, or Chance: Stochastic Gene Expression and Its Consequences. *Cell*, 135(2):216–226.

Rambaut, A. and Drummond, A. J. (2007). Tracer v1. 4.

Raven, J. (1997). Phagotrophy in phototrophs. *Limnol. Ocean.*, 42(1):198–205.

Redelings, B. D. and Suchard, M. a. (2005). Joint Bayesian estimation of alignment and phylogeny. *Syst. Biol.*, 54(3):401–418.

Rees, T., Larson, T. R., Heldens, J., and Huning, F. (1995). In Situ Glutamine Synthetase Activity in a Marine Unicellular Alga (Development of a Sensitive Colorimetric Assay and the Effects of Nitrogen Status on Enzyme Activity). *Plant Physiol.*, 109(1 995):1405–1410.

Regalado, A. (2014). EmTech: Illumina Says 228,000 Human Genomes Will Be Sequenced This Year. *MIT Technol. Rev.*, (The Year in Review: Health Care).

Reisser, W. (1980). The Metabolic Interactions Between Paramecium bursaria Ehrbg. and Chlorella spec. in the Paramecium bursaria-Symbiosis. *Arch. Microbiol.*, 125:291–293.

Reisser, W., Burbank, D. E., Meints, S. M., Meints, R. H., Becker, B., and Van Etten, J. L. (1988). A comparison of viruses infecting two different Chlorella-like green algae. *Virology*, 167(1):143–149.

Richards, T. a., Soanes, D. M., Foster, P. G., Leonard, G., Thornton, C. R., and Talbot, N. J. (2009). Phylogenomic analysis demonstrates a pattern of rare and ancient horizontal gene transfer between plants and fungi. *Plant Cell*, 21(July):1897–1911.

Ris, H. and Plaut, W. (1962). Ultrastructure of DNA-containing areas in the chloroplast of Chlamydomonas. *J. Cell Biol.*, 13:383–391.

Robertson, G., Schein, J., Chiu, R., Corbett, R., Field, M., Jackman, S. D., Mungall, K., Lee, S., Okada, H. M., Qian, J. Q., Griffith, M., Raymond, A., Thiessen, N., Cezard, T., Butterfield, Y. S., Newsome, R., Chan, S. K., She, R., Varhol, R., Kamoh, B., Prabhu, A.-L., Tam, A., Zhao, Y., Moore, R. a., Hirst, M., Marra, M. a., Jones, S. J. M., Hoodless, P. a., and Birol, I. (2010). De novo assembly and analysis of RNA-seq data. *Nat. Methods*, 7(11):909–912.

Rockwell, N. C., Lagarias, J. C., and Bhattacharya, D. (2014). Primary endosymbiosis and the evolution of light and oxygen sensing in photosynthetic eukaryotes. *Front. Ecol. Evol.*, 2(October):1–13.

Ronquist, F. and Huelsenbeck, J. P. (2003). MrBayes 3: Bayesian phylogenetic inference under mixed models. *Bioinformatics*, 19(12):1572–1574.

Ronquist, F., Teslenko, M., van der Mark, P., Ayres, D. L., Darling, a., Hohna, S., Larget, B., Liu, L., Suchard, M. a., and Huelsenbeck, J. P. (2012). MrBayes 3.2: Efficient Bayesian Phylogenetic Inference and Model Choice Across a Large Model Space. *Syst. Biol.*, 61(3):539–542.

Rosenblatt, M. (1956). Remarks on Some Non-parametric Estimates of a Density Function. *Ann. Math. Stat.*, 27(3):832–837.

Rousseeuw, P. J. (1987). Silhouettes: A graphical aid to the interpretation and validation of cluster analysis. *J. Comput. Appl. Math.*, 20:53–65.

Rowe, J. M., Jeanniard, A., Gurnon, J. R., Xia, Y., Dunigan, D. D., Van Etten, J. L., and Blanc, G. (2014). Global analysis of Chlorella variabilis NC64A mRNA profiles during the early phase of Paramecium bursaria chlorella virus-1 infection. *PLoS One*, 9(3).

Russakovsky, O., Deng, J., Su, H., Krause, J., Satheesh, S., Ma, S., Huang, Z., Karpathy, A., Khosla, A., Bernstein, M., Berg, A. C., and Fei-Fei, L. (2014). Imagenet large scale visual recognition challenge 2010. *arXiv:1409.0575*.

Ruxton, G. D. (2006). The unequal variance t-test is an underused alternative to Student's t-test and the Mann-Whitney U test. *Behav. Ecol.*, 17(May):688–690.

Saier, M. H., Reddy, V. S., Tamang, D. G., and Västermark, A. k. (2014). The transporter classification database. *Nucleic Acids Res.*, 42(November 2013):251–258.

Saier, M. H., Tran, C. V., and Barabote, R. D. (2006). TCDB: the Transporter Classification Database for membrane transport protein analyses and information. *Nucleic Acids Res.*, 34:D181–D186.

Saier, M. H., Yen, M. R., Noto, K., Tamang, D. G., and Elkan, C. (2009). The Transporter Classification Database: recent advances. *Nucleic Acids Res.*, 37(November 2008):D274–D278.

Saitou, N. and Nei, M. (1987). The Neighbor-joining Method: A New Method for Reconstructing Phylogenetic Trees'. *Mol Biol Evol*, 4(4):406–425.

Saji, M. and Oosawa, F. (1974). Mechanism of Photoaccumulation in Paramecium bursaria. *J. Protozool.*, 22(4):57–65.

Salerno, G. L. and Pontis, H. G. (1989). Raffinose Synthesis in Chlorella vulgaris Cultures after a Cold Shock. *Plant Physiol.*, 89:648–51.

Salim, H. M. W., Ring, K. L., and Cavalcanti, a. R. O. (2008). Patterns of Codon Usage in two Ciliates that Reassign the Genetic Code: Tetrahymena thermophila and Paramecium tetraurelia. *Protist*, 159(April):283–298.

Sana, T. R., Roark, J. C., Li, X., Waddell, K., and Fischer, S. M. (2008). Molecular formula and METLIN Personal Metabolite Database matching applied to the identification of compounds generated by LC/TOF-MS. *J. Biomol. Tech.*, 19:258–266.

Sanderson, C. (2010). Conrad Sanderson. Armadillo: An Open Source C++ Linear Algebra Library for Fast Prototyping and Computationally Intensive Experiments. *NICTA*, Technical.

Sanger, F., Air, G. M., Barrell, B. G., Brown, N. L., Coulson, a. R., Fiddes, C. a., Hutchison, C. a., Slocombe, P. M., and Smith, M. (1977a). Nucleotide sequence of bacteriophage phi X174 DNA. *Nature*, 265:687–695.

Sanger, F. and Coulson, A. R. (1975). A rapid method for determining sequences in DNA by primed synthesis with DNA polymerase. *J. Mol. Biol.*, 94:441–448.

Sanger, F., Nicklen, S., and Coulson, a. R. (1977b). DNA sequencing with chain-terminating inhibitors. *Proc. Natl. Acad. Sci. U. S. A.*, 74(12):5463–5467.

Sassera, D., Beninati, T., Bandi, C., Bouman, E. a. P., Sacchi, L., Fabbi, M., and Lo, N. (2006). Candidatus Midichloria mitochondrii', an endosymbiont of the Ixodes ricinus with a unique intramitochondrial lifestyle. *Int. J. Syst. Evol. Microbiol.*, 56:2535–2540.

Sato, S. (2011). The apicomplexan plastid and its evolution. *Cell. Mol. Life Sci.*, 68:1285–1296.

Schrallhammer, M. and Schweikert, M. (2009). The Killer Effect of Paramecium and Its Causative Agents. In Fujishima, M., editor, *Endosymbionts in Paramecium*, volume 12 of *Microbiology Monographs*, chapter 9, pages 227–246. Springer.

Schultz, J., Milpetz, F., Bork, P., and Ponting, C. P. (1998). SMART, a simple modular architecture research tool: identification of signaling domains. *Proc. Natl. Acad. Sci. U. S. A.*, 95(May):5857–5864.

Schultz, J. and Wolf, M. (2009). ITS2 sequence–structure analysis in phylogenetics: A how-to manual for molecular systematics. *Mol. Phylogenet. Evol.*, 52(2):520–523.

Schulz, F. and Horn, M. (2015). Intranuclear bacteria: inside the cellular control center of eukaryotes. *Trends Cell Biol.*, pages 1–8.

Schulz, F., Lagkouvardos, I., Wascher, F., Aistleitner, K., Kostanjšek, R., and Horn, M. (2014). Life in an unusual intracellular niche: a bacterial symbiont infecting the nucleus of amoebae. *ISME J.*, pages 1634–1644.

Schulz, M. H., Zerbino, D. R., Vingron, M., and Birney, E. (2012). Oases: robust de novo RNA-seq assembly across the dynamic range of expression levels. *Bioinformatics*, 28(8):1086–92.

Schussler, a. and Schnepf, E. (1992). Photosynthesis Dependent Acidification of Perialgal Vacuoles in the Paramecium-Bursaria Chlorella Symbiosis - Visualization By Monensin. *Protoplasma*, 166:218–222.

Schwarz, G. (1978). Estimating the dimension of a model. *Ann. Stat.*, 6:461–464.

Scott, D. W. (1979). On optimal and data-based histograms. *Biometrika*, 66(3):605–610.

Servant, F., Bru, C., Carrère, S., Courcelle, E., Gouzy, J., Peyruc, D., and Kahn, D. (2002). ProDom: automated clustering of homologous domains. *Brief. Bioinform.*, 3(3):246–251.

Setter, T. L. and Greenway, H. (1979). Growth and osmoregulation of Chlorella emersonii in NaCl and neutral osmotica. *Plant Physiol.*, 6:47–60.

Shalek, A. K., Satija, R., Adiconis, X., Gertner, R. S., Gaublomme, J. T., Raychowdhury, R., Schwartz, S., Yosef, N., Malboeuf, C., Lu, D., Trombetta, J. J., Gennert, D., Gnirke, A., Goren, A., Hacohen, N., Levin, J. Z., Park, H., and Regev, A. (2013). Single-cell transcriptomics reveals bimodality in expression and splicing in immune cells. *Nature*, 498(7453):236–40.

Shendure, J. and Ji, H. (2008). Next-generation DNA sequencing. *Nat. Biotechnol.*, 26(10):1135–1145.

Shi, D.-Q. (2005). SLOW WALKER1, Essential for Gametogenesis in Arabidopsis, Encodes a WD40 Protein Involved in 18S Ribosomal RNA Biogenesis. *Plant Cell Online*, 17(August):2340–2354.

Shihira, I. and Krauss, R. W. (1965). *Chlorella: physiology and taxonomy of forty-one isolates*. University of Maryland.

Siegel, R. W. (1963). New result on genetics of mating types in Paramecium bursaria. *Genet. Res.*, 4:132–142.

Siegel, R. W. and Karakashian, S. J. (1959). Dissociation and restoration of endocellular symbiosis in Paramecium-Bursaria. In *Anat. Rec.*, volume 134, page 639. WILEY-LISS DIV JOHN WILEY & SONS INC, 605 THIRD AVE, NEW YORK, NY 10158-0012.

Siegel, R. W. and Larison, L. L. (1960). The Genic Control of Mating Types in Paramecium Bursaria. *Proc. Natl. Acad. Sci. U. S. A.*, 46(variety 8):344–349.

Sievers, F., Wilm, A., Dineen, D., Gibson, T. J., Karplus, K., Li, W., Lopez, R., McWilliam, H., Remmert, M., Söding, J., Thompson, J. D., and Higgins, D. G. (2011). Fast, scalable generation of high-quality protein multiple sequence alignments using Clustal Omega. *Mol. Syst. Biol.*, 7(539).

Simmons, M. P. (2003). How Meaningful Are Bayesian Support Values? *Mol. Biol. Evol.*, 21(1):188–199.

Simpson, E. (1951). The Interpretation of Interaction in Contingency Tables. *J. R. Stat. Soc. Ser. B*, 13(2):238–241.

Sims, D., Ilott, N. E., Sansom, S. N., Sudbery, I. M., Johnson, J. S., Fawcett, K. a., Berlanga-Taylor, A. J., Luna-Valero, S., Ponting, C. P., and Heger, A. (2014). CGAT: Computational genomics analysis toolkit. *Bioinformatics*, 30(9):1290–1291.

Smith, C., Elizabeth, J., O'Maille, G., Abagyan, R., and Siuzdak, G. (2006). XCMS: processing mass spectrometry data for metabolite profiling using Nonlinear Peak Alignment,Matching,and Identification. *ACS Publ.*, 78(3):779–787.

Smith, C. A., Maille, G. O., Want, E. J., Qin, C., Trauger, S. A., Brandon, T. R., Custodio, D. E., Abagyan, R., and Siuzdak, G. (2005a). METLIN: A Metabolite Mass Spectral Database. *Ther. Drug Monit.*, 27(6).

Smith, J. C., Northey, J. G. B., Garg, J., Pearlman, R. E., and Siu, K. W. M. (2005b). Robust method for proteome analysis by MS/MS using an entire translated genome: Demonstration on the ciliome of Tetrahymena thermophila. *J. Proteome Res.*, 4:909–919.

Smith, L., Sanders, J., Kaiser, R., Hughes, P., Dodd, C., Connell, C., Heiner, C., Kent, S., and Hood, L. (1986). Fluorescence Detection in Automated DNA Sequence Analysis. *Nature*, 321(June):674–679.

Smith, L. M., Fung, S., Hunkapiller, M. W., Hunkapiller, T. J., and Hood, L. E. (1985). The Synthesis of Oligonucleotides Containing an Alipathic Amino Group at the 5' Terminus: Synthesis of Fluorescent DNA Primers for use in DNA Sequence Analysis. *Nucleic Acids Res.*, 13(7):2399–2412.

Smith, T. and Waterman, M. (1981). Identification of common molecular subsequences. *J. Mol. Biol.*, 147:195–197.

Smith-unna, R., Boursnell, C., Patro, R., Hibberd, J. M., and Kelly, S. (2015). TransRate: reference free quality assessment of de-novo transcriptome assemblies. *bioRxiv Prepr.*, June:1–25.

Sommaruga, R. and Sonntag, B. (2009). Photobiological Aspects of the Mutualistic Association Between Paramecium bursaria and Chlorella. In Fujishima, M., editor, *Endosymbionts in Paramecium*, volume 12 of *Microbiology Monographs*, chapter 5, pages 111–130. Springer.

Sonneborn, T. (1950). Methods in the general biology and genetics of Paramecium aurelia. *J. Exp. Zool.*, 113(1):87–147.

Sonneborn, T. M. (1970). Methods in Paramecium Research. In *Methods Cell Biol.*, volume 4, chapter 12, pages 241–339.

Sonnhammer, E. L., von Heijne, G., and Krogh, A. (1998). A hidden Markov model for predicting transmembrane helices in protein sequences. *Proc. Sixth Int. Conf. Intell. Syst. Mol. Biol.*, 6:175–82.

Spits, C., Le Caignec, C., De Rycke, M., Van Haute, L., Van Steirteghem, A., Liebaers, I., and Sermon, K. (2006). Whole-genome multiple displacement amplification from single cells. *Nat. Protoc.*, 1(4):1965–1970.

Stamatakis, a. (2014). RAxML version 8: a tool for phylogenetic analysis and post-analysis of large phylogenies. *Bioinformatics*, 30(9):1312–1313.

Stamatakis, A., Hoover, P., and Rougemont, J. (2008). A Rapid Bootstrap Algorithm for the RAxML Web Servers. *Syst. Biol.*, 57(5):758–771.

Stiller, J. W., Schreiber, J., Yue, J., Guo, H., Ding, Q., and Huang, J. (2014). The evolution of photosynthesis in chromist algae through serial endosymbioses. *Nat. Commun.*, 5:1–7.

Stocking, C. and Gifford Jr., E. (1959). Incorporation of thymidine into chloroplats of Spirogyra. *Biochem. Biophys. Res. Commun.*, 1(3):159–164.

Stoecker, D. K., Johnson, M. D., De Vargas, C., and Not, F. (2009). Acquired phototrophy in aquatic protists. *Aquat. Microb. Ecol.*, 57(December):279–310.

Stöver, B. C. and Müller, K. F. (2010). TreeGraph 2: Combining and visualizing evidence from different phylogenetic analyses. *BMC Bioinformatics*, 11:7.

Suchard, M. a. and Redelings, B. D. (2006). BAli-Phy: simultaneous Bayesian inference of alignment and phylogeny. *Bioinformatics*, 22(16):2047–8.

Sugiura, N. (1978). Further analysts of the data by akaike's information criterion and the finite corrections: Further analysts of the data by akaike's. *Commun. Stat. Methods*, 7(1):13–26.

Sullivan, J. and Joyce, P. (2005). Model Selection in Phylogenetics. *Annu. Rev. Ecol. Evol. Syst.*, 36(May):445–466.

Summerer, M., Sonntag, B., Hörtnagl, P., and Sommaruga, R. (2009). Symbiotic ciliates receive protection against UV damage from their algae: a test with Paramecium bursaria and Chlorella. *Protist*, 160(2):233–43.

Summerer, M., Sonntag, B., and Sommaruga, R. (2007). An experimental test of the symbiosis specificity between the ciliate Paramecium bursaria and strains of the unicellular green alga Chlorella. *Environ. Microbiol.*, 9(8):2117–22.

Summerer, M., Sonntag, B., and Sommaruga, R. (2008). CILIATE-SYMBIONT SPECIFICITY OF FRESHWATER ENDOSYMBIOTIC CHLORELLA (TREBOUXIOPHYCEAE, CHLOROPHYTA). *J. Phycol.*, 44:77–84.

Sung, W., Tucker, A. E., Doak, T. G., Choi, E., Thomas, W. K., and Lynch, M. (2012). Extraordinary genome stability in the ciliate Paramecium tetraurelia. *Proc. Natl. Acad. Sci. U. S. A.*, 109(47):19339–44.

Suzuki, S., Kakuta, M., Ishida, T., and Akiyama, Y. (2014). GHOSTX: an improved sequence homology search algorithm using a query suffix array and a database suffix array. *PLoS One*, 9(8):e103833.

Suzuki, S., Kakuta, M., Ishida, T., and Akiyama, Y. (2015). Faster sequence homology searches by clustering subsequences. *Bioinformatics*, 31(November 2014):1183–1190.

Swart, E. C., Bracht, J. R., Magrini, V., Minx, P., Chen, X., Zhou, Y., Khurana, J. S., Goldman, A. D., Nowacki, M., Schotanus, K., Jung, S., Fulton, R. S., Ly, A., McGrath, S., Haub, K., Wiggins, J. L., Storton, D., Matese, J. C., Parsons, L., Chang, W. J., Bowen, M. S., Stover, N. a., Jones, T. a., Eddy, S. R., Herrick, G. a., Doak, T. G., Wilson, R. K., Mardis, E. R., and Landweber, L. F. (2013). The Oxytricha trifallax Macronuclear Genome: A Complex Eukaryotic Genome with 16,000 Tiny Chromosomes. *PLoS Biol.*, 11(1).

Takahashi, T., Shirai, Y., Kosaka, T., and Hosoya, H. (2007). Arrest of cytoplasmic streaming induces algal proliferation in green paramecia. *PLoS One*, 2(12):e1352.

Talavera, G. and Castresana, J. (2007). Improvement of phylogenies after removing divergent and ambiguously aligned blocks from protein sequence alignments. *Syst. Biol.*, 56(4):564–577.

Tanaka, M., Murata-Hori, M., Kadono, T., Yamada, T., Kawano, T., Kosaka, T., and Hosoya, H. (2002). Complete elimination of endosymbiotic algae from Paramecium bursaria and its confirmation by diagnostic PCR. *Acta Protozool.*, 41:255–261.

Tange, O. (2011). GNU Parallel - The Command-Line Power Tool. *;login USENIX Mag.*, 36(1):42–47.

Tanner, W., Haass, D., Decker, M., Loos, E., Komor, B., and Komor, E. (1974). Active Hexose Transport in Chlorella vulgaris. In Zimmermann, U. and Dainty, J., editors, *Membr. Transp. Plants SE - 28*, pages 202–208. Springer Berlin Heidelberg.

Tateno, Y., Imanishi, T., Miyazaki, S., Fukami-Kobayashi, K., Saitou, N., Sugawara, H., and Gojobori, T. (2002). DNA Data Bank of Japan (DDBJ) for genome scale research in life science. *Nucleic Acids Res.*, 30(1):27–30.

Tautenhahn, R., Bottcher, C., and Neumann, S. (2008). Highly sensitive feature detection for high resolution LC/MS. *BMC Bioinformatics*, 9:504.

Tautenhahn, R., Cho, K., Uritboonthai, W., Zhu, Z., Patti, G. J., and Siuzdak, G. (2012a). An accelerated workflow for untargeted metabolomics using the METLIN database. *Nat Biotechnol*, 30(9):826–828.

Tautenhahn, R., Patti, G. J., Rinehart, D., and Siuzdak, G. (2012b). XCMS Online: a web-based platform to process untargeted metabolomic data. *Anal. Chem.*, 84:5035–9.

Tavare, S. (1986). Some probabilistic and statistical problems in the analysis of DNA sequences.

Thomas, P. D. (2003). PANTHER: a browsable database of gene products organized by biological function, using curated protein family and subfamily classification. *Nucleic Acids Res.*, 31(1):334–341.

Thompson, J. D., Higgins, D. G., and Gibson, T. J. (1994). CLUSTAL W: improving the sensitivity of progressive multiple sequence alignment through sequence weighting, position-specific gap penalties and weight matrix choice. *Nucleic Acids Res.*, 22(22):4673–4680.

Thompson, J. D., Linard, B., Lecompte, O., and Poch, O. (2011). A Comprehensive Benchmark Study of Multiple Sequence Alignment Methods: Current Challenges and Future Perspectives. *PLoS One*, 6(3):e18093.

Thorne, J. L., Kishino, H., and Felsenstein, J. (1991). An evolutionary model for maximum likelihood alignment of DNA sequences. *J. Mol. Evol.*, 33:114–124.

Tierney, L., Linde, J., Müller, S., Brunke, S., Molina, J. C., Hube, B., Schöck, U., Guthke, R., and Kuchler, K. (2012). An interspecies regulatory network inferred from simultaneous RNA-seq of Candida albicans invading innate immune cells. *Front. Microbiol.*, 3(March):1–14.

Timmis, J. N., Ayliffe, M. a., Huang, C. Y., and Martin, W. (2004). Endosymbiotic gene transfer: organelle genomes forge eukaryotic chromosomes. *Nat. Rev. Genet.*, 5(February):123–135.

Tindall, K. and Kunkel, T. (1988). Fidelity of DNA Synthesis by the Thermus aquaticus DNA Polymerase. *Biochemistry*, 27:6008–6013.

Tonooka, Y. and Watanabe, T. (2002). A natural strain of Paramecium bursaria lacking symbiotic algae. *Eur. J. Protistol.*, 38:55–58.

Torgerson, W. (1952). Multidimensional Scaling: I Theory and Method. *Psychometrika*, 17(4):401–419.

Trapnell, C., Williams, B. a., Pertea, G., Mortazavi, A., Kwan, G., van Baren, M. J., Salzberg, S. L., Wold, B. J., and Pachter, L. (2011). Transcript assembly and abundance estimation from RNA-Seq reveals thousands of new transcripts and switching among isoforms. *Nat. Biotechnol.*, 28(5):511–515.

Tsiatis, A. C., Norris-Kirby, A., Rich, R. G., Hafez, M. J., Gocke, C. D., Eshleman, J. R., and Murphy, K. M. (2010). Comparison of Sanger sequencing, pyrosequencing, and melting curve analysis for the detection of KRAS mutations: diagnostic and clinical implications. *J. Mol. Diagn.*, 12(4):425–432.

Van Etten, J. L., Burbank, D. E., Kuczmarski, D., and Meints, R. H. (1983). Virus Infection of Culturable Chlorella-Like Algae and Dlevelopment of a Plaque Assay. *Science (80-.).*, 219:994–996.

van Gorkom, H. J. (1974). Identification of the reduced primary electron acceptor of Photosystem II as a bound semiquinone anion. *Biochim. Biophys. Acta - Bioenerg.*, 347:439–442.

Vapnik, V. and Lerner, a. (1963). Pattern recognition using generalized portrait method. *Autom. Remote Control*, 24:774–780.

Vapnik, V. N. and Kotz, S. (1982). *Estimation of dependences based on empirical data*, volume 41. Springer-Verlag New York.

Vert, J.-P. (2002). A tree kernel to analyse phylogenetic profiles. *Bioinformatics*, 18 Suppl 1:S276–S284.

Vijay, N., Poelstra, J. W., Künstner, A., and Wolf, J. B. W. (2013). Challenges and strategies in transcriptome assembly and differential gene expression quantification. A comprehensive in silico assessment of RNA-seq experiments. *Mol. Ecol.*, 22:620–634.

Vitter, J. S. (1985). Random Sampling with a Reservoir. *ACM Trans. Math. Softw.*, 11(1):37–57.

Vogt, G. (1992). Enclosure of bacteria by the rough endoplasmic reticulum of shrimp hepatopancreas cells. *Protoplasma*, 171:89–96.

von Dohlen, C. D., Kohler, S., Alsop, S. T., and McManus, W. R. (2001). Mealybug β-proteobacterial endosymbionts contain γ-proteobacterial symbionts. *Nature*, 412(July):433–436.

von Heijne, G. (2006). Membrane-protein topology. *Nat. Rev. Mol. Cell Biol.*, 7(December):909–918.

Vorobyev, K., Andronov, E., Skoblo, I., Migunova, A., and Kvitko, K. (2009). An atypical Chlorella symbiont from Paramecium bursaria. *Protistology*, 6(1):39–44.

Wang, L. and Jiang, T. (1994). On the complexity of multiple sequence alignment. *J. Comput. Biol.*, 1:337–348.

Wang, Z., Gerstein, M., and Snyder, M. (2009). RNA-Seq: a revolutionary tool for transcriptomics. *Nat. Rev. Genet.*, 10:57–63.

Waskom, M., Botvinnik, O., Hobson, P., Warmenhoven, J., Cole, J. B., Halchenko, Y., Vanderplas, J., Hoyer, S., Villalba, S., Quintero, E., Miles, A., Augspurger, T., Yarkoni, T., Evans, C., Wehner, D., Rocher, L., Megies, T., Coelho, L. P., Ziegler, E., Hoppe, T., Seabold, S., Pascual, S., Cloud, P., Koskinen, M., Hausler, C., Kjemmett, Milajevs, D., Qalieh, A., Allan, D., and Meyer, K. (2015). seaborn: v0.6.0 (June 2015).

Watnick, P. and Kolter, R. (2000). Biofilm, city of microbes. *J. Bacteriol.*, 182(10):2675–2679.

Weiberg, A., Bellinger, M., and Jin, H. (2015). Conversations between kingdoms: small RNAs. *Curr. Opin. Biotechnol.*, 32C:207–215.

Weis, D. S. (1984). The Effect of Accumulated Time of Separate Cultivation on the Frequency of Infection of Aposymbiotic Ciliates by Symbiotic Algae in Paramebium bursaria. *J. Protozool.*, 31(4):A13—-A14.

Weis, D. S. and Ayala, A. (1976). Effect of Exposure Period and Algal Concentration on the Frequency of Infection of Aposymbiotic Ciliates by Symbiotic Algae from Paramecium bursaria. *J. Protozool.*, 26(2):245–248.

Welch, B. (1947). The Generalisation of the 'Student's' Problem when Several Different Population Variances are Involved. *Biometrika*, 34(1/2):28–35.

Wernegreen, J. J. (2012). Endosymbiosis. *Curr. Biol.*, 22:555–561.

Westermann, A. J., Gorski, S. a., and Vogel, J. (2012). Dual RNA-seq of pathogen and host. *Nat. Rev. Microbiol.*, 10(9):618–630.

White, T. J., Bruns, T., Lee, S., Taylor, J. W., and Others (1990). Amplification and direct sequencing of fungal ribosomal RNA genes for phylogenetics. *PCR Protoc. a Guid. to methods Appl.*, 18:315–322.

Wichterman, R. (1946). TIME RELATIONSHIPS OF THE NUCLEAR BEHAVIOR IN THE CONJUGATION OF GREEN AND COLORLESS PARAMECIUM-BURSARIA. In *Anat. Rec.*, volume 94, pages 381–382. WILEY-LISS DIV JOHN WILEY & SONS INC, 605 THIRD AVE, NEW YORK, NY 10158-0012.

Wichterman, R. (1948). The Biological Effects of X-Rays on Mating Types and Conjugation of Paramecium Bursaria. *Biol. Bull.*, 94(2):113–127.

Wickham, H. (2009). *ggplot2: elegant graphics for data analysis*. Springer New York.

Wickham, H. and Francois, R. (2014). *dplyr: A Grammar of Data Manipulation*.

Wilcox, L. W. (1986). Prokaryotic endosymbionts in the chloroplast stroma of the dinoflagellate Woloszynskia pascheri. *Protoplasma*, 135:71–79.

Wilhelm, B. T. and Landry, J.-R. (2009). RNA-Seq—quantitative measurement of expression through massively parallel RNA-sequencing. *Methods*, 48(3):249–257.

Williams, T., Kelley, C., and others, M. (2010). Gnuplot 4.4: an interactive plotting program. http://gnuplot.sourceforge.net/.

Winnepenninckx, B., Backeljau, T., and De Wachter, R. (1993). Extraction of high molecular weight DNA from molluscs. *Trends Genet.*, 9(127):407.

Wolpert, D. and Macready, W. G. (1995). No free lunch theorems for search. *Tech. Rep. SFI-TR-95-02-010*, pages 1–38.

Wolpert, D. H. (1996). The Existence of A Priori Distinctions Between Learning Algorithms. *Neural Comput.*, 8(7):1391–1420.

Wolpert, D. H. and Macready, W. G. (1997). No free lunch theorems for optimization. *IEEE Trans. Evol. Comput.*, 1(1):67–82.

Wrede, C., Dreier, A., Kokoschka, S., and Hoppert, M. (2012). Archaea in symbioses. *Archaea*, 2012:596846.

Wu, A. R., Neff, N. F., Kalisky, T., Dalerba, P., Treutlein, B., Rothenberg, M. E., Mburu, F. M., Mantalas, G. L., Sim, S., Clarke, M. F., and Quake, S. R. (2014). Quantitative assessment of single-cell RNA-sequencing methods. *Nat. Methods*, 11(1):41–6.

Wu, R., Shengen, Y., Shan, Y., Dang, Q., and Sun, G. (2015). Deep Image: Scaling up Image Recognition. *arXiv:1501.02876*.

Xiang, T., Nelson, W., Rodriguez, J., Tolleter, D., and Grossman, A. R. (2015). Symbiodinium transcriptome and global responses of cells to immediate changes in light intensity when grown under autotrophic or mixotrophic conditions. *Plant J.*, 82:67–80.

Xie, Y., Wu, G., Tang, J., Luo, R., Patterson, J., Liu, S., Huang, W., He, G., Gu, S., Li, S., Zhou, X., Lam, T. W., Li, Y., Xu, X., Wong, G. K. S., and Wang, J. (2014). SOAPdenovo-Trans: De novo transcriptome assembly with short RNA-Seq reads. *Bioinformatics*, 30(12):1660–1666.

Yanagi, A. (2004). Autogamy is induced in Paramecium bursaria by methyl cellulose. *Eur. J. Protistol.*, 40:313–315.

Yang, X., Chockalingam, S. P., and Aluru, S. (2013). A survey of error-correction methods for next-generation sequencing. *Brief. Bioinform.*, 14(1):56–66.

Yang, Z. (1993). Maximum-likelihood estimation of phylogeny from DNA sequences when substitution rates differ over sites. *Mol. Biol. Evol.*, 10(6):1396–1401.

Yang, Z. (1994). Maximum likelihood phylogenetic estimation from DNA sequences with variable rates over sites: approximate methods. *J. Mol. Evol.*, 39:306–314.

Yang, Z. (1996). Among-site rate variation and its impact on phylogenetic analyses. *TREE*, 11(9):367–372.

Yang, Z. and Rannala, B. (2012). Molecular phylogenetics: principles and practice. *Nat. Rev. Genet.*, 13(May):303–314.

Yashchenko, V. V., Gavrilova, O. V., Rautian, M. S., and Jakobsen, K. S. (2012). Association of Paramecium bursaria Chlorella viruses with Paramecium bursaria cells: ultrastructural studies. *Eur. J. Protistol.*, 48(2):149–59.

Yule, G. (1903). Notes on the theory of association of attributes in statistics. *Biometrika*, 2(2):121–134.

Zdobnov, E. M. and Apweiler, R. (2001). signature-recognition methods in InterPro. 17(9):847–848.

Zerbino, D. R. and Birney, E. (2008). Velvet: algorithms for de novo short read assembly using de Bruijn graphs. *Genome Res.*, 18:821–9.

Zhang, Q., Awad, S., and Brown, C. (2015). Crossing the streams : a framework for streaming analysis of short DNA sequencing reads PrePrints analysis of short DNA sequencing reads PrePrints. pages 0–27.

Zhang, Q., Pell, J., Canino-Koning, R., Howe, A. C., and Brown, C. T. (2014). These Are Not the K-mers You Are Looking For: Efficient Online K-mer Counting Using a Probabilistic Data Structure. *PLoS One*, 9(7):e101271.

Zhang, T., Ramakrishnan, R., and Livny, M. (1996). BIRCH: An Efficient Data Clustering Databases Method for Very Large. *ACM SIGMOD Int. Conf. Manag. Data*, 1:103–114.

Zhou, C., Mao, F., Yin, Y., Huang, J., Gogarten, J. P., and Xu, Y. (2014). AST: An automated sequence-sampling method for improving the taxonomic diversity of gene phylogenetic trees. *PLoS One*, 9(6):2–10.

Zhou, Y., Brinkmann, H., Rodrigue, N., Lartillot, N., and Philippe, H. (2010). A dirichlet process covarion mixture model and its assessments using posterior predictive discrepancy tests. *Mol. Biol. Evol.*, 27(2):371–384.

Ziesenisz, E., Reisser, W., and Wiessner, W. (1981). Evidence of de novo synthesis of maltose excreted by the endosymbiotic Chlorella from Paramecium bursaria. *Planta*, 153:481–485.

Zwickl, D. J. and Hillis, D. M. (2002). Increased taxon sampling greatly reduces phylogenetic error. *Syst. Biol.*, 51(4):588–598.

Appendices

A

Appendix 1

A.1 Arboretum classifier comparison

A.1.1 Genomes Used

Genomes used in transcript binning
Arabidopsis thaliana
Chlamydomonas reinhardtii
Ostreococcus tauri
Micromonas pusilla CCMP1545
Chlorella variabilis NC64A
Chlorella vulgaris C-169
Physcomitrella patens
Saccharomyces cerevisiae S288C
Neurospora crassa OR74A
Homo sapiens
Mus musculus
Dictyostelium discoideum
Paramecium caudatum
Paramecium tetraurelia
Tetrahymena thermophila macronucleus
Oxytricha trifallax
Toxoplasma gondii
Guillardia theta
Bigelowiella natans
Emiliania huxleyi CCMP1516
Aureococcus anophagefferens
Ectocarpus siliculosus
Schizosaccharomyces pombe
Bacillus cereus ATCC 14579
Escherichia coli str. K-12 substr. MG1655
Escherichia coli O157 H7 str. Sakai
Salmonella enterica subsp. enterica serovar Typhi str. CT18
Amycolatopsis mediterranei U32
Aquifex aeolicus VF5
Borrelia burgdorferi B31
Chlamydophila pneumoniae CWL029
Chlorobium tepidum TLS
Deinococcus radiodurans R2
Caulobacter crescentus CB15
Sulfolobus islandicus M.14.25
Nanoarchaeum equitans Kin4-M
Haloferax mediterranei ATCC 33500
Methanococcus maripaludis S2
Cenarchaeum symbiosum A

Table A.1.1: Table of genomes using in transcript binning pipeline. Genomes were chosen to be a representative of the sampled diversity of the eukaryotic tree of life as possible